Accounting For Environmental Co-variables in Loblolly Pine *(Pinus taeda L.)* Diameter Distributions in the Western Gulf Physiographic Region of the United States

by

Gabriel de Oliveira Pontes Maciel

(Under the Direction of Bronson P. Bullock)

Abstract

Diameter distribution modeling in loblolly pine (*Pinus taeda L.*) plantations was conducted using the percentile estimation technique and the parameter recovery approach to evaluate the effects of silvicultural management intensity (fertilization and vegetation control) and environmental co-variables (precipitation, temperature, and water deficit) on the three-parameter Weibull distribution estimation. Data from the Plantation Management Research Cooperative in the Western Gulf Cultural Density trial established across three physiographic regions included five initial planting densities and two management regimes was used in this thesis. The results showed that with higher intensity of silvicultural management the predicted percentiles were higher, and Weibull parameter was affected according to the level of silvicultural intensity and planting density, demonstrating their combined influence on stand structure. Incorporating environmental co-variables into the models influenced the Weibull three-parameter (location, shape, scale) and improved both model fit and the precision of parameter estimates compared to models without environmental co-variables.

Index words: Diameter distributions, Weibull function, percentile estimation, parameter recovery, environmental co-variables, loblolly pine

Accounting For Environmental Co-variables in Loblolly Pine *(Pinus taeda L.)* Diameter Distributions in the Western Gulf Physiographic Region of the United States

by

Gabriel de Oliveira Pontes Maciel

B.S.F., College of Social and Agricultural Sciences of Itapeva, São Paulo, Brazil 2020

A Thesis Submitted to the Graduate Faculty

of The University of Georgia in Partial Fulfillment

of the

Requirements for the Degree

Master of Science

Athens, Georgia

2025

Accounting For Environmental Co-variables in Loblolly Pine *(Pinus taeda L.)* Diameter Distributions in the Western Gulf Physiographic Region of the United States

by

Gabriel de Oliveira Pontes Maciel

Approved:

Major Professor: Bronson P. Bullock

Committee: Stephen M. Kinane
Bruno Kanieski da Silva

Electronic Version Approved:

Ron Walcott
Dean of the Graduate School
The University of Georgia
December 2025

Dedication

To my Savior, Jesus Christ, for His faithfulness, goodness, forgiveness, mercy, and love.

Acknowledgments

My deepest gratitude, first of all, to God, for granting me this incredible opportunity — something that once seemed impossible to me — and for giving me the strength and knowledge to face the challenges throughout this master's program.

I would like to express my sincere appreciation to the Warnell School of Forestry and Natural Resources at the University of Georgia and to the Plantation Management Research Cooperative (PMRC), along with its member companies, for providing the essential financial support that made the completion of this program possible — an invaluable contribution.

My sincere thank you to my major advisor, Dr. Bronson Bullock, for giving me the opportunity to pursue this master's degree, for believing in my potential, and for his constant encouragement throughout this journey; for his suggestions, ideas, and patience; and for sharing his valuable knowledge in forest biometrics, which was fundamental to the completion of this research. I would like to thank Dr. Stephen Kinane for his guidance and for all the support during this master's program. His patience, advice, and encouragement — both academically and professionally — are things I will always remember, as well as our conversations and laughter. I would also like to thank Dr. Bruno da Silva for being part of my committee and for contributing his valuable insights to my project.

A huge thank you to Dr. Simon Sandoval, visiting researcher at the PMRC Biometrics Lab, for all his help, support, suggestions, and advice during the development of the chapter II. His knowledge was significantly important in guiding me through the research process, as well as for the insightful morning conversations we often shared. I would like to thank the PMRC team, especially the PMRC researchers and Mr. Clayton David, PMRC's field crew leader, for all the support provided in obtaining the data used in this research.

My sincere thanks to Ms. Kate deDufour, graduate program administrator at the Warnell School, for all her help and support even before I began my program. Her patience and dedication were essential in making this opportunity a reality.

My gratitude to Mr. Jacob “Jake” Knox, writing instructor at the Warnell School for his help and great patience in reviewing this entire thesis. I truly appreciate his willingness to assist me throughout this process — his feedback, suggestions, and friendship were fundamental to improving the grammar and writing quality of this work and were greatly valued during this journey.

I would like to thank all the PMRC graduate students and PMRC alumni, especially to the future Dr. Noah Shephard (my boy), for his advice, suggestions, help and patience in always listening to my complaints — I will always be grateful for our friendship. To Dr. Angel Adhikari and Mr. Caddis Fulford, thank you for all the help in classes and with the questions I had throughout this period.

Lastly, I would like to thank the Oliveira Fontanini Maciel family for believing in me and for their constant support. Special thanks to my mother, Lourdes Fontanini de Oliveira, for her prayers, for always doing everything within her reach to provide what I needed back home, and above all, for always emphasizing the importance of education and learning.

Table of Contents

List of Figures

List of Tables

Chapter 1

Introduction and literature review

1.1 Introdution

Forest biometricians have worked for more than a century to develop growth and yield models to provide information about forests (e.g., tree growth, site quality, diameter increment, yield) (Schenck, 1905). Growth and yield (G&Y) models are used to help forest managers make management decision (e.g., thinning, fertilization, vegetation control, site preparation). Growth refers to the increase in size of one or more trees over a given period (i.e., volume growth in ft^3 ac^{-1} y^{-1}). Yield represents the final amount available for harvest at the end of that period (i.e., volume ft^3 ac^{-1}) (Vanclay, 1994). These models can provide important information about a forest, such as prediction of future yield, tree stocking, and silviculture management response. Additionally, G&Y models support decisions related to timberland acquisitions, and forecast resource needs. These models also play a key role in estimating future timber values used in appraisals (Robinson and Monserud, 2003; Henderson et al., 2013; **?**). Loblolly pine (*Pinus taeda L.*) plantations are one of the most common species uses in G&Y models. The species loblloly pine is the major commercial softwood species in the Southern United States, with a planting area expected to increase to more than 54 million acres by 2040 (Sabatia and Burkhart, 2014).

Studies on loblolly pine have focused on different ways to improve stand productivity and model predictability for stand dynamics. Many of these studies focus on modeling diameter distribution, which has been emphasized in forestry due to its effectiveness in representing stand and stock tables based on tree by diameter class (Burkhart and Tomé, 2012). Tree per acre by diameter class can be easily obtained using various distribution functions. The

Weibull function is one of the ways to describe diameter distributions, and it has been commonly employed in the past due to its flexibility in represent various diameter distributions (Bailey and Dell, 1973).

Diameter distribution models are a powerful tool for characterizing forest structure and providing valuable information (e.g., volume per diameter class, mortality, ingrowth, silviculture management response). However, despite extensive research on diameter distributions, a knowledge gap remains regarding the influence of different co-variables in these models. For example, environmental co-variables (e.g., temperature, precipitation, potential evapotranspiration, soil) have a significant correlation with yield and are expected to directly impact tree growth (Ford, 1983). There is a strong need to incorporate environmental co-variables into diameter distribution models, to obtain accuracy and precision information of forest structure. By understanding forest behavior when these variables are included, more accurate results can be obtained, leading to better-informed decision-making.

1.2 Thesis Structure

This thesis is structured into three chapters. The first chapter provides a general introduction to the study, including a literature review based on the project framework (study design), and a description of the dataset. The subsequent chapter addresses modeling diameter distributions based on two silvicultural managements regimes. The third chapter focuses on incorporating environmental co-variables into a diameter distribution modeling process, for that reason the environmental co-variable review is not included the in the first chapter.

1.3 Literature Review

Planting density

Planting density (i.e., trees per acre) is one of the most important decisions for a forest manager to make during the establishment of a plantation stand. Trees per acre (TPA) is associated with stand density, and the information is used to generate yield tables for planted stands. Spacing and TPA can influence tree height, diameter at breast height (DBH), crown size, and survival in a pine plantation stand (Sharma et al., 2002).

Past studies have shown conflicting results on how dominant height can be affected by TPA. Initial investigation on TPA on southern pine plantations and concluded that TPA does not significantly affect average dominant height (Ware and Stahelin, 1948). Another study concluded that the initial spacing did not significantly affect the average and dominant heights at the end of the stand's rotation in a plantation of loblolly pine in Brazil (Cardoso et al., 2013). Another study showed that, within traditional levels of initial planting density (600–900 TPA), no significant differences were found in average tree height. However, the same study reported significant differences between extremely high initial planting density ($>$ 1490 TPA) and extremely low initial planting density ($\approx$300 TPA) after age 10 in loblolly pine plantations (Zhao et al., 2020).

A study developed in southeastern Oklahoma showed that higher the TPA, the lower the average dominant height (Hennessey et al., 2004). Another study has shown that higher initial planting densities can affect dominant height at mid-rotation, resulting in lower site index values under higher density conditions due to competition (MacFarlane et al., 2000). In contrast, for diameter, studies have shown a consensus that TPA and spacing have effects on diameter increment. The average DBH in wider spacings is uniformly higher than at closer spacings (Harms et al., 2000; Weng et al., 2024). Sharma et al. (2002) affirms that spacing has a meaningful effect on mean DBH, and the effect is due to the TPA.

Another study examined how different planting densities and age categories impact the diameter and height of pine trees in East Texas plantations. In this study the researchers divided the planting densities into five groups: $\leq$ 400, 500, 600, 700, and $\geq$ 800. They also categorized the trees into four age groups: 5, 10, 15, and $\geq$ 20 years old. The findings revealed that at 5 years of age, there were no significant differences in diameter between the five planting densities. However, by the time the trees reached 15 years of age, those planted at densities of 400 and 500 TPA exhibited significantly greater diameters compared to those planted at 600, 700, and 800 TPA. As the trees aged to 20 years, the diameter decreased with increasing TPA (Lee and Lenhart, 1998). This implies that while initial planting density may not affect diameter during the early growing years, it becomes a factor as the trees mature, with denser plantations resulting in smaller diameters at older ages.

The planting density should be accounted for in diameter distributions models, since past studies have shown that diameter is directly affected by TPA. It is important that diameter distribution information is accurate, because it is used to estimate timber product classes and, ultimately, guide forest management decisions.

Thinning as a silviculture treatment

Thinning is a silvicultural treatment to improve a forest's performance, and as a treatment can directly affect forest productivity. A fundamental tool in driving management objectives such as management stand density, controlling tree growth, improving wood quality, and preventing insect attacks. Traditionally, forest professionals have acknowledged five different methods of thinning (Ford Robertson, 1970; Daniel et al., 1979; Smith, 1986; Helms, 1998; Nyland, 2016; Smith, 1997):

- The low thinning method (i.e., from below) eliminates trees with the lowest crowns and smallest size generates few gaps.
- The crown method (i.e., thinning from above) removes selected dominant and co-dominant trees—typically those of lower vigor or poorer form—to favor the growth of

higher-quality or more vigorous dominants and co-dominants with greater potential to develop in the stand.

- The selection method (i.e., diameter-limit thinning) removes trees with diameters larger than a given size limit, which is applied in a stand to favor trees with smaller diameters and great potential of growth.

- Mechanical thinning (i.e., geometric thinning) eliminates trees with a fixed spacing between trees, which removes trees by row.

- Free thinning method (crop tree release), which favors only crop tree.

Several studies have examined the effects of thinning on height-diameter. The height-diameter relationship between tree in a stand is associated with tree volume. This relationship will be different in stands that received thinning treatment compared to non-thinned stands (Zhang et al., 1997). A study in southeastern Oklahoma founded that plots that received two thinning treatments at age 9 and 24 had an average diameter that was greater than unthinned plots (Hennessey et al., 2004). Other studies have shown that heavier thinning has a considerable effect on diameter increment in different species. Heavy thinning where the residual stocking is well below the 60 - 70% in general will increase the diameter increment (Allen et al., 1970). Hilt (1979) concluded in a study developed for oaks (*Quercus*) that the heavier the thinning the better the response in diameter growth. Heavy thinning increased the rate of diameter growth crown-thinned plots when compared to unthinned plots in oak (*Quercus petraea and Quercus robur*) species (Kerr, 1996). For Norway spruce (*Picea abies L. Karst*) species, thinning does not affect the total volume growth increment, but it does affect diameter increment (Mäkinen and Isomäki, 2004).

A study in 2017 examined the impact of post-thinning density and fertilization on a loblolly pine plantation. The authors found a significant positive relationship between low density and diameter growth, indicating that trees in low-density environments exhibited faster growth rates and larger diameters compared to those in higher density (Albaugh et al., 2017).

Applying thinning treatments can offer several benefits for a forest stand, as mentioned above. Diameter incremental growth is one of the benefits that thinning can provide. Incorporating a variable for thinning in a diameter distribution model may improve predictability, while providing additional insight for foresters on how this treatment can affect the diameter distribution. With this information, foresters can develop accurate yield tables that will help with forest management decisions, including thinning triggers to obtain more trees per unit area for a specific diameter class.

Fertilization

The development of silvicultural management for loblolly pine plantation is typically merged with the goal of increasing productivity. Fertilization has become a common technique in pine plantations in the United States to improve tree growth and forest productivity (Bolstad and Allen, 1987; Allen, 2001; Fox et al., 2007a; Shephard et al., 2021). Forest biometricians have been developed several models for including this treatment to understand the tree and stand level responses with fertilization applications (Zhao et al., 2011; Cardoso et al., 2013).

Fertilization (F) has been shown to be a crucial tool for increasing soil nutrients, addressing soil nutritional deficiencies (i.e., poor yield, chlorosis, lowered defenses), and to improving forest productivity (i.e., volume growth). Tree characteristics are significantly affected by F in loblolly pine plantations (Matziris and Zobel, 1976a; Rahman et al., 2006). Annual F applications can increase early growth and tree development (Colbert et al., 1990). Stands that receive F have a greater increase in diameter, height, and volume compared to stands with no F application (Matziris and Zobel, 1976b). The application of nitrogen (N) and Phosphorus (P) are commonly used for mid-rotation site manipulation to achieve a higher site quality. The common elemental rates are 200 lb ac^{-1} and 50 lb ac^{-1}, respectively (Fox et al., 2007b). The combination of N and P increase DBH, height, total volume and merchantable volume growth (Bolstad and Allen, 1987; Williams and Farrish, 2000; Liechty and Fristoe, 2013).

Studies with F treatment in loblolly pine plantations have concluded that this treatment has a strong affect in forest structure. Application of F in a study in North Louisiana resulted in increases of 27, 44, and 43% in DBH, total volume, and merchantable volume, respectively, six years after treatment (Williams and Farrish, 2000).

Mid-rotation F affects the diameter distribution parameters, making them slightly flattened and shifted to the right (Carlson et al., 2008). Tree diameter changes by F application need to be considered in diameter distribution modeling, since individual diameter increment affects the allocation to different diameter class (Allen et al., 1983). By considering F in diameter modeling, more accurate TPA estimation by diameter class can be obtained.

Vegetation Control

Silvicultural manipulation to increase forest productivity is known as intensive management, includes but is not limited to site preparation, fertilizer applications, vegetation or competition control, thinning, and pest control (e.g., tip moth) (Allen, 2008). These techniques are applied with the objective of improving the development and increasing the growth and subsequent value of loblolly pine plantations.

Vegetation control (VC) plays an important role in intensive management, especially in reallocating two essential factors – nutrients and water resources – by eliminating any non-target plant species that may be competing for these factors in the same environment (Allen and Albaugh, 2000; Fox, 2000; Allen, 2008).

Pine plantations benefit in several ways from the implementation of VC, such as an increase in stand growth. In other words, VC has a direct effect on tree height, DBH, above-ground biomass, and total biomass (Zutter et al., 1986; Fox, 2000). However, VC can alter the nutrient stock in the soil when soil properties and the composition of plant groups are affected by this manipulation (Gurlevik et al., 2004). As a result of this negative effect, the composition of the plant community and the quality of forest soil may be modified (Gurlevik et al., 2003).

To avoid damage that could affect tree development, the combination of VC and F has become a common technique during mid-rotation in loblolly pine plantations, with the main goal of addressing any deficiency that could delay tree growth. The combination of herbicide and F can lead to strong positive growth increments in loblolly pine characteristics (e.g., height, DBH, volume per tree), and stand productivity during the initial growing seasons (Miller et al., 1991; Haywood et al., 1997; Sword et al., 1998; Borders and Bailey, 2001).

The combination of VC and F, in addition to promoting increased growth of pine plantations, affects the structure (e.g., diameter distribution) of a managed forest, increasing the proportion of higher-value timber products, such as sawtimber, in a shorter period (Jokela et al., 2004).

Diameter distributions

Diameter at breast height (DBH) classes are a common metric employed across various studies to assess the dynamics of tree stands. DBH is measured at a point 4.5 feet above ground level from the uphill side of the stem (Burkhart et al., 2018). DBH is used in diameter distribution models to provide estimations of TPA by diameter classes (Frazier, 1981). Diameter is associated with other crucial variables such as volume yield, products classes, forest value, and forest management decisions (Bailey and Dell, 1973).

The distributional diameter classes provide stand table projections on mortality, ingrowth, stand yield, and future stocking. Such information directly influences management decision-making within a stand and the evaluation of forest development. By utilizing stand tables derived from diameter distributions, managers can make informed and optimal decisions, ultimately facilitating effective forest management practices. For example, implementing thinning treatments can effectively mitigate mortality risks and promote diameter growth in a specific class (Powers et al., 2010; Saarinen et al., 2020; Erkan et al., 2023; Tavankar et al., 2025). Additionally, decisions based on those projections are relative to financial considerations, as forest managers can use stand table information to determine the optimal timing for thinning or harvesting. This helps prevent overstocking and self-thinning while providing early income to landowners though precommercial thinning treatments (Schaedel et al., 2017; Tanger et al., 2021).

Diameter distributions can be characterized by two methods: the first is related to a mathematical approach, which means a characterization of the whole distribution curve, and the second is related to a mathematical or biological approach, in this case, the characterization of a specific attribute of the curve (Nelson, 1964). In typical applications, age, quadric mean diameter (D_q), tree height, and TPA are needed as input to obtain distributional information. These models have been used extensively to estimate and project a forest's current and future growth over decades.

The oldest example of a diameter distribution model is the geometric progression created by De Liocourt in 1898, for uneven-aged forests (Meyer, 1952). Meyer and Stevenson (1943) used the De Liocourt geometric progression modeling technique in structure and growth for virgin beech-birch maple. Later, Meyer (1952) presented a new approach in an unmanaged forest using calculation of percentage of the number of trees in different diameters classes and applied the exponential probability density function for uneven-aged stands. The same approach was used by Schmelz and Lindsey (1965) to characterize old-growth hardwood forests with size-class structure in Indiana.

The Gamma distribution was used to investigate the cubic foot growth for even-aged forest stand in a loblolly pine plantation (Nelson, 1964). Osborne and Schumacher (1935) developed red gum *(Eucalyptus camaldulensis)* tables by applying the Pearl-Reed (growth curve) population growth shape to cumulative frequency distribution by DBH, concluding that this modeling approach performed well for an even-aged loblolly pine stand (Equation 1.1).

$$\ln\left\{\frac{100-\mathrm{y}}{\mathrm{y}}\right\} = \mathrm{a} + \beta_1\mathrm{x} + \beta_2\mathrm{x}^2 + \beta_3\mathrm{x}^3 \tag{1.1}$$

Where, y: is the cumulative frequency to the upper limit of any diameter; x is the corresponding upper limit itself; and $\ln(\cdot)$ is the natural logarithm.

Diameter distributions for even-aged stands are unimodal and slightly skewed; the curves can be modeled for distributions with many mathematical functions, such as beta, Weibull, Gamma, Johnson S_b, and Lognormal distributions (Burkhart and Tomé, 2012).

Hafley and Schreuder (1977) compared five distributions (Weibull, Gamma, Johnson S_b, Lognormal, and Generalized normal) to investigate their flexibility in the skewness squared and kurtosis plane for southern pines, concluding that the Johnson S_b model demonstrated consistent stability across a range of datasets. A similar study conducted by Kudus et al. (2000) on *Acacia mangium* even-aged and uneven-aged mixed species stands, shows that Johnson S_b is the most consistent performer for an empirical dataset, which they concluded that the Johnson S_b approach showed a certain level of stability across the dataset. Johnson S_b also shows a good fit in data for diameter distributions for Araucária *(Araucaria angustifolia)* (Hentz et al., 2016).

There are four different parameters included in the Johnson S_b distribution function: the lower limit, the higher limit, ϵ, and the range, λ, respectively which can be expressed as follows:

$$f(\mathrm{x}) = \frac{\delta}{\sqrt{2\pi}} \cdot \frac{\lambda}{(\mathrm{x}-\epsilon)(\epsilon+\lambda-x)} \exp\left\{-\frac{1}{2}\left[\gamma + \delta\ln\left(\frac{\mathrm{x}-\epsilon}{\epsilon+\lambda-\mathrm{x}}\right)\right]^2\right\}$$

$$\epsilon < \mathrm{x} < \epsilon+\lambda, \quad \delta > 0, \quad -\infty < \gamma < \infty, \quad \lambda > 0,$$

$$\lambda + \delta\ln\left(\frac{\mathrm{x}-\epsilon}{\epsilon+\lambda-\mathrm{x}}\right) = \mathrm{Z_x} \approx \mathrm{N}(0,1) \tag{1.2}$$

where λ is scale parameter; λ, δ is the shape parameter; x is the random variable; and $\ln(\cdot)$ is the natural logarithm.

A popular approach for diameter distributions is the Weibull distribution. Bailey and Dell (1973) introduced the Weibull distribution function in their research, offering exceptional estimations for diameter distributions in even-aged stands. Diameter distributions is often use the Weibull probability function with two parameters or three parameters. The probability density function (PDF) for the two-parameter for Weibull distribution of a random variable, x, can be written as:

$$f(\mathrm{x}) = \frac{\gamma}{\beta}\left(\frac{\mathrm{x}}{\beta}\right)^{\gamma-1} \exp\left[-\left(\frac{x}{\beta}\right)^{\gamma}\right] \tag{1.3}$$

Weibull function with three parameters (Equation 1.4) includes α as the location parameter. The location parameter, $\alpha \geq 0$, in the case of forest diameter distributions refers to the minimum diameter. When the location parameter in the function is equal or presumed to be 0, the function with three parameters is converted to a two-parameters function (Equation 1.3) by using the relationship $\mathrm{x} = \mathrm{y} + \alpha$.

$$f(\mathrm{x}) = \frac{\gamma}{\beta}\left(\frac{\mathrm{x}-\alpha}{\beta}\right)^{\gamma-1} \exp\left[-\left(\frac{\mathrm{x}-\alpha}{\beta}\right)^{\gamma}\right] \tag{1.4}$$

When the variable technique is changed in the Weibull PDF, the cumulative distribution function (CDF) is created (Equation 1.5).

$$\mathrm{F}(\mathrm{x}) = 1 - \exp\left[-\left(\frac{\mathrm{x}-\alpha}{\beta}\right)^{\gamma}\right] \tag{1.5}$$

Where, α is the location parameter; β is the scale parameter; γ is the shape parameter; x is the random variable; $\exp[\cdot]$ is the exponential function (the base of the natural logarithm).

When $\gamma < 1$, the curve exhibits a reversed J-shaped. However, when $\gamma = 1$, the outcome follows an exponential distribution. For $\gamma < 3.6$, the outcome is positive, and the curve is mound shaped. In rare cases, the Rayleigh distribution occurs when $\gamma = 2$. When γ is approximately 3.6, the Weibull distribution approximates a normal distribution. When the value for γ increases above 3.6, the results are a more negatively skewed distribution (Bailey and Dell, 1973).

The Weibull function has been used extensively for diameter distributions because it is flexible and allows for different unimodal shapes and curves (Yatich, 2009). For example, Burk and Burkhart (1984) used the Weibull function for a natural stand of loblolly pine, and Lenhart (1988) applied the same techniques to create a yield prediction system for unthinned loblolly and slash pine plantations. Bullock and Burkhart (2005) used the Weibull function with two parameters in a juvenile loblolly pine plantation, including age, basal area per acre, and TPA as independent variables and Cao and McCarty (2006) performed Weibull distribution to predict future diameter distributions from the current plot conditions. Lou et al. (2021) improved the Weibull density function for loblolly pine plantations in the Western Gulf Coastal Plain, concluding that the model is a preferred method for predicting growth and yield information in that region.

Over decades, many studies have been developed for diameter distributions around the world to provide information based on stand tables. The importance of stand and stock table information has resulted in many studies that have focused on modeling diameter distributions for even-age plantations. Using the PDF, it is possible to estimate the frequency of trees by diameter class.

As mentioned previously, the Weibull function is commonly employed for diameter distributions because of its flexibility in accommodating various shapes and its simplicity in parameter estimation. Despite the considerable amount of research that has been conducted in the past on diameter distributions, there still exists a gap in utilizing the Weibull function that incorporates environmental co-variables. Incorporating environmental co-variables, such as soil moisture, temperature, soil composition, precipitation, and evapotranspiration, could offer additional information and for diameter distribution behaviors and, therefore, improve model predictability.

1.4 Rationale and significance

Forest biometricians and quantitative silviculturists have studied forest dynamics over the last six decades, using various models to understand forest dynamic and structure. Many approaches have been developed to clarify how tree growth is influenced by different silvicultural treatments (e.g., fertilization, thinning, vegetation control, site preparation) to improve predictions. Besides the common silvicultural variables, environmental co-variables became an important variable in forest and ecology models with the goal of understanding how environmental factors affect forest development and productivity. Accounting for environmental co-variables in diameter distribution models can provide an improvement in forest productivity predictions and can be used to create yield tables with merchantable product.

Managers can adjust G&Y models based on diameter distribution to optimize planning and decision-making processes, including the implementation of thinning treatments, fertilization, and other management strategies. Furthermore, given changing climate conditions, this research will offer a better understanding of how environmental factors influence loblolly pine growth and, consequently, plantation productivity.

The purpose of the project is to examine, derive, and estimate diameter distributions for loblolly pine plantations in the Western Gulf physiographic region of the southeastern United States. This will also include exploring the effects of environmental co-variables on estimating loblolly pine diameter distribution parameters. Additionally, the study will assess the impact of planting density and silvicultural management on diameter distributions.

1.5 Goal, Objectives, and Hypotheses

1.5.1 Overall goal

Utilize environmental co-variables to improve estimates of the three-parameter Weibull distribution for characterizing loblolly pine plantation diameter distributions.

1.5.2 Study objectives

1. Analyze two different silviculture management intensity levels on diameter distributions in the Western Gulf physiographic region in the southeastern United States.

   (a) Hypothesis: Three-parameter Weibull distribution estimation has no difference between different levels of silviculture management intensity.

2. Study the effects of environmental co-variables on loblolly pine plantation diameter distributions in the Western Gulf physiographic region in the southeastern United States.

   (a) Hypothesis: No effect of the environmental co-variables on the estimation of the three parameter Weibull distribution parameters.

1.6 Study Site

For the propose of this study, we used the Western Gulf Culture Density Study (WGCDS) from the Plantation Management Research Cooperative (PMRC) at the University of Georgia (Figure 1.1). The study plantings were established in 2001, 2002, and 2003 in three regions of the Western Gulf (Arkansas, Louisiana, Texas, and Mississippi) in the Upper Coastal Plain, Lower Coastal Plain, and the Interior Flatwoods in Arkansas (Table 1.1). The WGCDS was initially managed by Texas A&M University until the responsibility was transferred to the University of Georgia in 2008. From when PMRC took over all responsibility for treatments, measurements, and study maintenance.

Study design

The design for WGCDS is split plot, with initial planting density (PLTPA) as main plots and silvicultural management (MAN) as the subplot. WGCDS contain 18 installations, each installation contains a unique combination of five PLTPA (Table 1.2), two MAN intensive and maximum, and two levels of thinning (thin to 200 and 450).

Each installation has 16 plots, for this study 10 of 16 plots did not have a thinning treatment imposed on them, while 6 of the 16 plot per installation include thinning as a treatment.

The five levels of PLTPA are:

- 200 (15.6 feet x 14 feet spacing).
- 450 (9.7 feet x 10 feet spacing).
- 700 (6.2 feet x 10 feet spacing).
- 950 (5.7 feet x 8 feet spacing).
- 1200 (4.5 feet x 8 feet spacing) TPA.

The Western Gulf physiographic region of United States contains different soil types (Table 1.3). The WGCDS soil group is based on drainage class and depth to subsurface restrictive layers, where it is classified as:

- A and B: poorly – somewhat poorly drained.
- C and D: moderately well – well drained.

Installations 1, 8, and 16 contain soil A, installations 5, 6, 7, 10, 11, and 12 contain soil B, installations 2, 14, 15, and 17 contain soil C, and installations 3, 4, 9, 13, and 18 contain soil D. The silviculture management intensive (INT) includes mechanical site preparation for specific soil group:

- Group A bedding and ripping.
- Group B bedding only.
- Group C ripping only.
- Group D none.

Additional treatments included tip moth *Rhyacionia frustrana* control during the first two growing seasons, competition control in the first year, and fertilization during the first and tenth growing seasons. The maximum (MAX) management includes the same site preparation as the INT silvicultural management. However, herbicide control was also implemented in years 2 and 3 with complete control and fertilization in years 2, 4, and 6.

The mechanical thinning method took place in six plots at each installation. The 450 PLTPA received one thinning to 200 TPA, and two plots of 700 PLTPA were separately thinned to 450 and 200 TPA. The thinning treatment was conducted at age 10 in 700 PLTPA for INT regime and 450 or 700 PLTPA for MAX regime. The other treatment had to meet suitable conditions to receive thinning at age 12. The criterion to apply the thinning was based on the site density index (SDI), when SDI reaches 55% of the maximum (450 TPA for loblolly pine) which means that plots were thinned at different ages when they tit this thinning trigger point.

Measurements

Tree height and DBH were measured on trees at least 4.5 feet (ft) tall at ages 2 – 20. Height of all trees greater than 4.5 ft was measured through age 6. At age 8 and afterward, height was measured on all trees for the 200 PLTPA, every other tree for the 450 PLTPA, and every third tree for the 700, 950, and 1200 PLTPA. After the 8^{th} growing season, height to the base of the live crown was measured on all trees that were measured for total height, and conarium presence on the stem was recorded for all trees. Since the WGCDS research project is an ongoing project the trees measurement is scheduled for other very three years.

Imputing Missing Tree Heights

Missing tree heights were estimated using a regression model with parameters estimated for each plot at every age (Equation 1.6).

$$\mathrm{HT} = \beta_0 + \beta_1 \mathrm{DBH}^{-1} + \epsilon \tag{1.6}$$

Where, β_0, β_1 are the coefficients to be estimate; HT is total Height (ft); DBH is diameter at breast Height (inches).

Dominant tree height classification

The dominant tree classification was based on PMRC analytical procedures, where trees with a DBH greater than the plot's arithmetic mean were classified as dominant trees.

Basal area

The basal area is the estimated total of the cross-sectional surface area at breast height of the trees in a sample plot, and it expands to reference all the trees in a stand, expressed as square feet per acre. It is correlated with stand stem volume, and can provide information to describe stand density and stocking levels.

Quadratic mean diameter

The $\overline{\mathrm{D}}_{\mathrm{q}}$ is obtain from basal area and TPA. For diameter distribution based on percentile method the $\overline{\mathrm{D}}_{\mathrm{q}}$ is the most crucial independent variable (Lee, 2006). The following equation was used to obtain the $\overline{\mathrm{D}}_{\mathrm{q}}$.

$$\overline{\mathrm{D}}_{\mathrm{q}} = \sqrt{\frac{\left(\frac{\mathrm{BA}}{\mathrm{TPA}}\right)}{0.0054542}} \tag{1.7}$$

Where, BA is the basal area ($\mathrm{ft}^2/\mathrm{ac}^{-1}$); TPA is tree per acre.

1.7 Dataset Summary

Average quadratic mean diameter

As expected, smaller PLTPA had higher average $\overline{\mathrm{D}}_{\mathrm{q}}$ values. PLTPA 450 that received thinning, reducing TPA to 200, outperformed plots of PLTPA 450 that did not receive thinning. The same occurred for PLTPA 700 that received thinning to 450 and 200. For all five PLTPA, across all years, and for those that received thinning to 450 or 200, MAX management obtained the highest average $\overline{\mathrm{D}}_{\mathrm{q}}$ (Figure 1.2).

Average basal area per acre

The MAX management showed higher average BA per acre for all PLTPA without thinning. PLTPA 200 and 450 under MAX management had the highest average BA until age 18. At age 21, INT management had the highest BA per acre. This difference is due to mortality in the MAX management. A similar result was observed for PLTPA 700, 950, and 1200; however, MAX management had higher BA until age 15, and at ages 18 and 21, INT management had the highest BA per acre.

For PLTPA that received thinning treatment and reduced TPA to 200, the MAX management had the highest BA per acre, and this result continued after thinning at age 21. For PLTPA 700 that received thinning to 200, the result was similar. Before thinning at age 8, INT management had the highest BA per acre, and after thinning, MAX management returned to being the one with the highest BA per acre up to age 21. For PLTPA 700 that received thinning to 450, MAX management had the highest BA per acre, and this result continued after thinning until age 18. At age 21, INT management surpassed MAX in BA per acre. Thinning that reduced PLTPA 700 to 450 TPA helped recover BA per acre, with MAX management values becoming very close to INT management values for PLTPA 700 without thinning (Figure 1.3).

Average dominant height

Average dominant height did not show any difference between the two management levels (MAN) in PLTPA 200, 450, and 700. In PLTPA 950 and 1200, a small difference between the two management levels is noticeable. As expected, dominant height increases over time, but there is no significant difference in height among the five PLTPA. For the plots that received thinning treatment, HD did not show an increase compared to PLTPA 450 and 700 that did not receive thinning treatment (Figure 1.4).

Average tree per acre

As expected, lower PLTPA values showed lower mortality rates over the years. For PLTPA 200, only at age 21 was there significant mortality, and MAX management had a higher percentage of mortality than INT management. For PLTPA 450 without thinning, mortality increased over the years, with the highest levels occurring between ages 15 and 21. As with PLTPA 200, MAX management showed higher mortality than INT.

For PLTPA 450 that received thinning and reduced density to 200 TPA, MAX management had higher mortality, and this difference between management types remained until age 21. For PLTPA 700, the difference in mortality between the two management levels was visible from age 6 and remained until age 12; between ages 15 and 21, MAX management showed a higher level of mortality. For PLTPA 700 that received thinning to reduce TPA to 450, MAX management had higher mortality both before and after the thinning treatment. On the other hand, for PLTPA 700 that received thinning reducing TPA to 200, after treatment, INT management showed higher mortality. For both PLTPA 950 and 1200, MAX management showed higher levels of mortality, with this level being noticeable from age 6 through age 21 (Figure 1.5).

Overall, based on average TPA and PLTPA, MAX management showed higher mortality (%) than INT management in plots without thinning, and in plots with thinning applied to reduce TPA to 200 and 450 (Table 1.4).

Thesis dataset

The data used in this thesis focus on tree-level information. For the purposes of analysis and modeling, the dataset was re-formatted to align with the modeling objectives; further details are provided in the respective chapters of this thesis. Due to certain factors, such as self-thinning and other operational constraints (e.g., presence of overhead power lines), some measurements were excluded. The measurements for non-thinning represents 69.26%; thinning to 200 TPA represents 11.79%; and thinning to 450 represent 10.10%. As a result, the dataset used in this thesis represents 91.15% of the total data.

1.8 References

Albaugh, T. J., Fox, T. R., Rubilar, R. A., Cook, R. L., Amateis, R. L., and Burkhart, H. E. (2017). Post-thinning density and fertilization affect pinus taeda stand and individual tree growth. *Forest Ecology and Management*, 396:207–216.

Allen, H. (2008). *Silvicultural Treatments to Enhance Productivity*, pages 129 – 139.

Allen, H. and Albaugh, T. (2000). Understanding the interactions between vegetation control and fertilization in young plantations: Southern pine plantations in the southeast usa.

Allen, H. L. (2001). Silvicultural treatments to enhance productivity. *The Forests Handbook: Applying Forest Science for Sustainable Management*, 2:129–139.

Allen, H. L., Duzan, D., Ballard, R., and Gessel, S. (1983). Nutritional management of loblolly pine stands: A status report of the north carolina state forest fertilization cooperative. *Forest site and continuous productivity*, pages 379–384.

Allen, R., Marquis, D., Northeastern Forest Experiment Station (Radnor, P., and Service, U. S. F. (1970). *Effect of Thinning on Height and Diameter Growth of Oak & Yellow-poplar Saplings*. USDA Forest Service research paper NE. Northeastern Forest Experiment Station, Forest Service, U.S. Department of Agriculture.

Bailey, R. L. and Dell, T. (1973). Quantifying diameter distributions with the weibull function. *forest science*, 19(2):97–104.

Bolstad, P. V. and Allen, H. L. (1987). Height and diameter growth response in loblolly pine stands following fertilization. *Forest science*, 33(3):644–653.

Borders, B. E. and Bailey, R. L. (2001). Loblolly pine—pushing the limits of growth. *Southern Journal of Applied Forestry*, 25(2):69–74.

Bullock, B. P. and Burkhart, H. E. (2005). Juvenile diameter distributions of loblolly pine characterized by the two-parameter weibull function. *New Forests*, 29:233–244.

Burk, T. E. and Burkhart, H. E. (1984). Diameter distributions and yields of natural stands of loblolly pine. *Virginia Tech. Division of Forestry and Wildlife Resources.*

Burkhart, H. E., Brooks, E. B., Dinon-Aldridge, H., Sabatia, C. O., Gyawali, N., Wynne, R. H., and Thomas, V. A. (2018). Regional simulations of loblolly pine productivity with co2 enrichment and changing climate scenarios. *Forest Science*, 64(4):349–357.

Burkhart, H. E. and Tomé, M. (2012). *Modeling forest trees and stands.* Springer Science & Business Media.

Cao, Q. V. and McCarty, S. M. (2006). New methods for estimating parameters of weibull functions to characterize future diameter distributions in forest stands. In *13th Biennial Southern Silvicultural Research Conference*, page 338.

Cardoso, D. J., Lacerda, A. E. B., Rosot, M. A. D., Garrastazú, M. C., and Lima, R. T. (2013). Influence of spacing regimes on the development of loblolly pine (pinus taeda l.) in southern brazil. *Forest Ecology and management*, 310:761–769.

Carlson, C. A., Burkhart, H. E., Allen, H. L., and Fox, T. R. (2008). Absolute and relative changes in tree growth rates and changes to the stand diameter distribution of pinus taeda as a result of midrotation fertilizer applications. *Canadian Journal of Forest Research*, 38(7):2063–2071.

Colbert, S. R., Jokela, E. J., and Neary, D. G. (1990). Effects of annual fertilization and sustained weed control on dry matter partitioning, leaf area, and growth efficiency of juvenile loblolly and slash pine. *Forest Science*, 36(4):995–1014.

Daniel, T. W., Helms, J. A., and Baker, F. S. (1979). *Principles of silviculture.* No. Ed. 2. McGraw-Hill Book Company.

Erkan, N., Güner, Ş. T., and Aydın, A. C. (2023). Thinning effects on stand growth, carbon stocks, and soil properties in brutia pine plantations. *Carbon Balance and Management*, 18(1):6.

Ford, D. (1983). What do we need to know about forest productivity and how can we measure it. In *IUFRO Symposium on Forest Site and Continuous Productivity. USDA Forest Service, General Technical Report, PNW-163*, pages 2–12.

Ford Robertson, F. C. (1970). Terminology of forest science, technology, practice and products. english-language version.

Fox, T. R. (2000). Sustained productivity in intensively managed forest plantations. *Forest Ecology and Management*, 138(1):187–202.

Fox, T. R., Lee Allen, H., Albaugh, T. J., Rubilar, R., and Carlson, C. A. (2007a). Tree nutrition and forest fertilization of pine plantations in the southern united states. *Southern Journal of Applied Forestry*, 31(1):5–11.

Fox, T. R., Lee Allen, H., Albaugh, T. J., Rubilar, R., and Carlson, C. A. (2007b). Tree nutrition and forest fertilization of pine plantations in the southern united states. *Southern Journal of Applied Forestry*, 31(1):5–11.

Frazier, J. R. (1981). Compatible whole-stand and diameter distribution models for loblolly pine plantations. *Virginia Polytechnic Institute and State University.*

Gurlevik, N., Kelting, D. L., and Allen, H. L. (2003). The effects of vegetation control and fertilization on net nutrient release from decomposing loblolly pine needles. *Canadian Journal of Forest Research*, 33(12):2491–2502.

Gurlevik, N., Kelting, D. L., and Allen, H. L. (2004). Nitrogen mineralization following vegetation control and fertilization in a 14-year-old loblolly pine plantation. *Soil Science Society of America Journal*, 68(1):272–281.

Hafley, W. and Schreuder, H. (1977). Statistical distributions for fitting diameter and height data in even-aged stands. *Canadian Journal of Forest Research*, 7(3):481–487.

Harms, W. R., Whitesell, C. D., and DeBell, D. S. (2000). Growth and development of loblolly pine in a spacing trial planted in hawaii. *Forest Ecology and Management*, 126(1):13–24.

Haywood, J. D., Tiarks, A. E., and Sword, M. a. (1997). Fertilization, weed control, and pine litter influence loblolly pine stem productivity and root development. *New Forests*, 14:233–249.

Helms, J. A. (1998). *The dictionary of forestry.* Society of American Foresters.

Henderson, J. E., Roberts, S. D., Grebner, D. L., and Munn, I. A. (2013). A graphical comparison of loblolly pine growth-and-yield models. *Southern Journal of Applied Forestry*, 37(3):169–176.

Hennessey, T., Dougherty, P., Lynch, T., Wittwer, R., and Lorenzi, E. (2004). Long-term growth and ecophysiological responses of a southeastern oklahoma loblolly pine plantation to early rotation thinning. *Forest Ecology and Management*, 192(1):97–116.

Hentz, Â. M. K., Pasa, D. L., Talgatti, M., Ferreira, A. d. R. C., and de Mello Filho, J. A. (2016). Distribuição diamétrica e determinação da altura em plantio de araucaria angustifolia (bertol.) kuntze na região central do rio grande do sul. *Scientia Plena*, 12(1).

Hilt, D. E. (1979). *Diameter growth of upland oaks after thinning*, volume 437. Department of Agriculture, Forest Service, Northeastern Forest Experiment ....

Jokela, E. J., Dougherty, P. M., and Martin, T. A. (2004). Production dynamics of intensively managed loblolly pine stands in the southern united states: a synthesis of seven long-term experiments. *Forest ecology and management*, 192(1):117–130.

Kerr, G. (1996). The effect of heavy or ‘free growth’thinning on oak (quercus petraea and q. robur). *Forestry: An International Journal of Forest Research*, 69(4):303–317.

Kudus, K. A., Ahmad, M., and Yahya, A. Z. (2000). Modelling diameter distribution in even-aged and uneven-aged forest stands. *Journal of Tropical Forest Science*, pages 669–681.

Lee, Y.-J. and Lenhart, J. D. (1998). Influence of planting density on diameter and height in east texas pine plantations. *Southern Journal of Applied Forestry*, 22(4):241–244.

Lenhart, J. D. (1988). Diameter-distribution yield-prediction system for unthinned loblolly and slash pine plantations on non-old-fields in east texas. *Southern Journal of Applied Forestry*, 12(4):239–242.

Liechty, H. O. and Fristoe, C. (2013). Response of midrotation pine stands to fertilizer and herbicide application in the western gulf coastal plain. *Southern Journal of Applied Forestry*, 37(2):69–74.

Lou, X., Weng, Y., Fang, L., and Grogan, J. (2021). Modeling diameter distributions of loblolly pine plantations in western gulf coastal plain. *Journal of Forestry*, 119(2):152–163.

MacFarlane, D. W., Green, E. J., and Burkhart, H. E. (2000). Population density influences assessment and application of site index. *Canadian Journal of Forest Research*, 30(9):1472–1475.

Mäkinen, H. and Isomäki, A. (2004). Thinning intensity and growth of norway spruce stands in finland. *Forestry*, 77(4):349–364.

Matziris, D. I. and Zobel, B. J. (1976a). Effect of fertilization on growth and quality characteristics of loblolly pine. *Forest Ecology and Management*, 1:21–30.

Matziris, D. I. and Zobel, B. J. (1976b). Effect of fertilization on growth and quality characteristics of loblolly pine. *Forest Ecology and Management*, 1:21–30.

Meyer, H. A. (1952). Structure, growth, and drain in balanced uneven-aged forests. *Journal of forestry*, 50(2):85–92.

Meyer, H. A. and Stevenson, D. D. (1943). The structure and growth of virgin beech-birch-maple-hemlock forests in northern. *Journal of Agricultural Research*, 67:465.

Miller, J. H., Zutter, B. R., Zedaker, S. M., Edwards, M. B., Haywood, J. D., and Newbold, R. A. (1991). A regional study on the influence of woody and herbaceous competition on early loblolly pine growth. *Southern Journal of Applied Forestry*, 15(4):169–179.

Nelson, T. C. (1964). Diameter distribution and growth of loblolly pine. *Forest Science*, 10(1):105–114.

Nyland, R. D. (2016). *Silviculture: concepts and applications*. Waveland Press.

Osborne, J. G. and Schumacher, F. X. (1935). The construction of normal yield and stand tables for even-aged timber stands. *J. Agric. Res. 51:547-564.*

Powers, M. D., Palik, B. J., Bradford, J. B., Fraver, S., and Webster, C. R. (2010). Thinning method and intensity influence long-term mortality trends in a red pine forest. *Forest Ecology and Management*, 260(7):1138–1148.

Rahman, M. S., Messina, M. G., and Fisher, R. F. (2006). Intensive forest management affects loblolly pine (pinus taeda l.) growth and survival on poorly drained sites in southern arkansas. *Society of American Foresters*, 30:79–85.

Robinson, A. P. and Monserud, R. A. (2003). Criteria for comparing the adaptability of forest growth models. *Forest Ecology and Management*, 172(1):53–67.

Saarinen, N., Kankare, V., Yrttimaa, T., Viljanen, N., Honkavaara, E., Holopainen, M., Hyyppä, J., Huuskonen, S., Hynynen, J., and Vastaranta, M. (2020). Assessing the effects of thinning on stem growth allocation of individual scots pine trees. *Forest Ecology and Management*, 474:118344.

Sabatia, C. O. and Burkhart, H. E. (2014). Predicting site index of plantation loblolly pine from biophysical variables. *Forest Ecology and Management*, 326:142–156.

Schaedel, M. S., Larson, A. J., Affleck, D. L., Belote, R. T., Goodburn, J. M., Wright, D. K., and Sutherland, E. K. (2017). Long-term precommercial thinning effects on larix occidentalis (western larch) tree and stand characteristics. *Canadian Journal of Forest Research*, 47(7):861–874.

Schenck, C. A. (1905). *Forest mensuration*. The University Press.

Schmelz, D. V. and Lindsey, A. A. (1965). Size-class structure of old-growth forests in indiana. *Forest Science*, 11(3):258–264.

Sharma, M., Burkhart, H. E., and Amateis, R. L. (2002). Modeling the effect of density on the growth of loblolly pine trees. *Southern Journal of Applied Forestry*, 26(3):124–133.

Shephard, N. T., Joshi, O., Meek, C. R., and Will, R. E. (2021). Long-term growth effects of simulated-drought, mid-rotation fertilization, and thinning on a loblolly pine plantation in southeastern oklahoma, usa. *Forest Ecology and Management*, 494:119323.

Smith, D. M. (1986). *The practice of silviculture.* J. Wiley and Sons Inc., New York.

Smith, D. M., L. B. C. K. M. J. . A. P. M. S. (1997). *The practice of silviculture.* J. Wiley and Sons Inc., New York.

Sword, M. A., Tiarks, A. E., and Haywood, J. D. (1998). Establishment treatments affect the relationships among nutrition, productivity and competing vegetation of loblolly pine saplings on a gulf coastal plain site. *Forest Ecology and Management*, 105(1-3):175–188.

Tanger, S., Blazier, M., Holley, A., McConnell, T., Vanderschaaf, C., Clason, T., and Kc, D. (2021). Financial performance of diverse levels of early competition suppression and pre-commercial thinning on loblolly pine stand development. *New Forests*, 52(2):217–235.

Tavankar, F., Picchio, R., Nikooy, M., Marian, B. K., Venanzi, R., and Lo Monaco, A. (2025). Impact of loblolly pine (pinus taeda l.) plantation management on biomass, carbon sequestration rates and storage. *Sustainability*, 17(3):888.

Vanclay, J. (1994). *Modelling Forest Growth and Yield: Applications to Mixed Tropical Forests*. CAB International.

Ware, L. M. and Stahelin, R. (1948). Growth of southern pine plantations at various spacings. *Journal of Forestry*, 46(4):267–274.

Weng, Y., Coble, D., Grogan, J., Ding, C., and Lou, X. (2024). Evaluating stand density measures for regulating mid-rotation loblolly pine plantation density in the western gulf, usa. *Sustainability*, 16(21):9452.

Williams, R. A. and Farrish, K. W. (2000). Response of loblolly pine plantations to late-rotation fertilization and herbicide applications in north louisiana. *Southern Journal of Applied Forestry*, 24(3):166–175.

Yatich, A. K. (2009). Diameter distribution prediction models for thinned slash and loblolly pine plantations in the southeast. *University of Georgia*, (IR).

Zhang, S., Burkhart, H. E., and Amateis, R. L. (1997). The influence of thinning on tree height and diameter relationships in loblolly pine plantations. *Southern Journal of Applied Forestry*, 21(4):199–205.

Zhao, D., Bullock, B. P., Montes, C. R., Wang, M., Westfall, J., and Coulston, J. W. (2020). Long-term dynamics of loblolly pine crown structure and aboveground net primary production as affected by site quality, planting density and cultural intensity. *Forest Ecology and Management*, 472:118259.

Zhao, D., Kane, M., and Borders, B. E. (2011). Growth responses to planting density and management intensity in loblolly pine plantations in the southeastern usa lower coastal plain. *Annals of Forest Science*, 68(3):625–635.

Zutter, B. R., Gjerstad, D. H., and Glover, G. R. (1986). Effects of interfering vegetation on biomass, fascicle morphology and leaf area of loblolly pine seedlings. *Forest science*, 32(4):1016–1031.

1.9 Tables and Figures

Table 1.1: WGCDS Summary Information.

Installation	Year Established	Soil Group	County	State	Region
1	2001	A	Jasper	TX	LCP
2	2001	C	Nacogdoches	TX	UCP
3	2001	D	Newton	TX	LCP
4	2001	D	Vernon	LA	UCP
5	2001	B	Vernon	LA	UCP
6	2001	B	Bradley	AR	IF
7	2001	B	Ashley	LA	IF
8	2001	A	Livingston	MS	LCP
9	2001	D	Lamar	LA	UCP
10	2002	B	Vernon	AR	LCP
11	2002	B	Bradley	AR	IF
12	2002	B	Ashley	AR	IF
13	2002	D	Howard	TX	UCP
14	2003	C	San Augustine	LA	UCP
15	2003	C	Sabine	AR	UCP
16	2003	A	Calhoun	AR	IF
17	2003	C	Union	AR	UCP
18	2003	D	Garland	RA	UCP

Table 1.2: WGCDS five planting densities and associated tree spacing and plot attributes.

Planting Density (TPA)	Spacing ft x ft	Trees per Measurement Plot	Measurement Plot Size Acres	Gross Treatment Plot Size Acres
1200	4.5 x 8	120	0.1 15 trees x 8 rows	0.23 23 trees x 12 rows
950	5.7 x 8	96	0.1 12 trees x 8 rows	0.25 20 trees x 12 rows
700	6.2 x 10	72	0.1 9 trees x 8 rows	0.26 15 trees x 8 rows
450	9.7 x 10	48	0.1 6 trees x 8 rows	0.27 10 trees x 12 rows
200	15.6 x 14	42	0.2 7 trees x 6 rows	0.55 11 trees x 10 rows

Table 1.3: WGCDS soil groups based on drainage class and depth to subsurface restrictive layer.

WGCDS Soil Group	Drainage Class	Depth to Subsurface Restrictive Layer
A	Poorly - somewhat poorly	< 20
B	Poorly - somewhat poorly	> 20
C	Moderately well - well	< 20
D	Moderately well - well	> 20

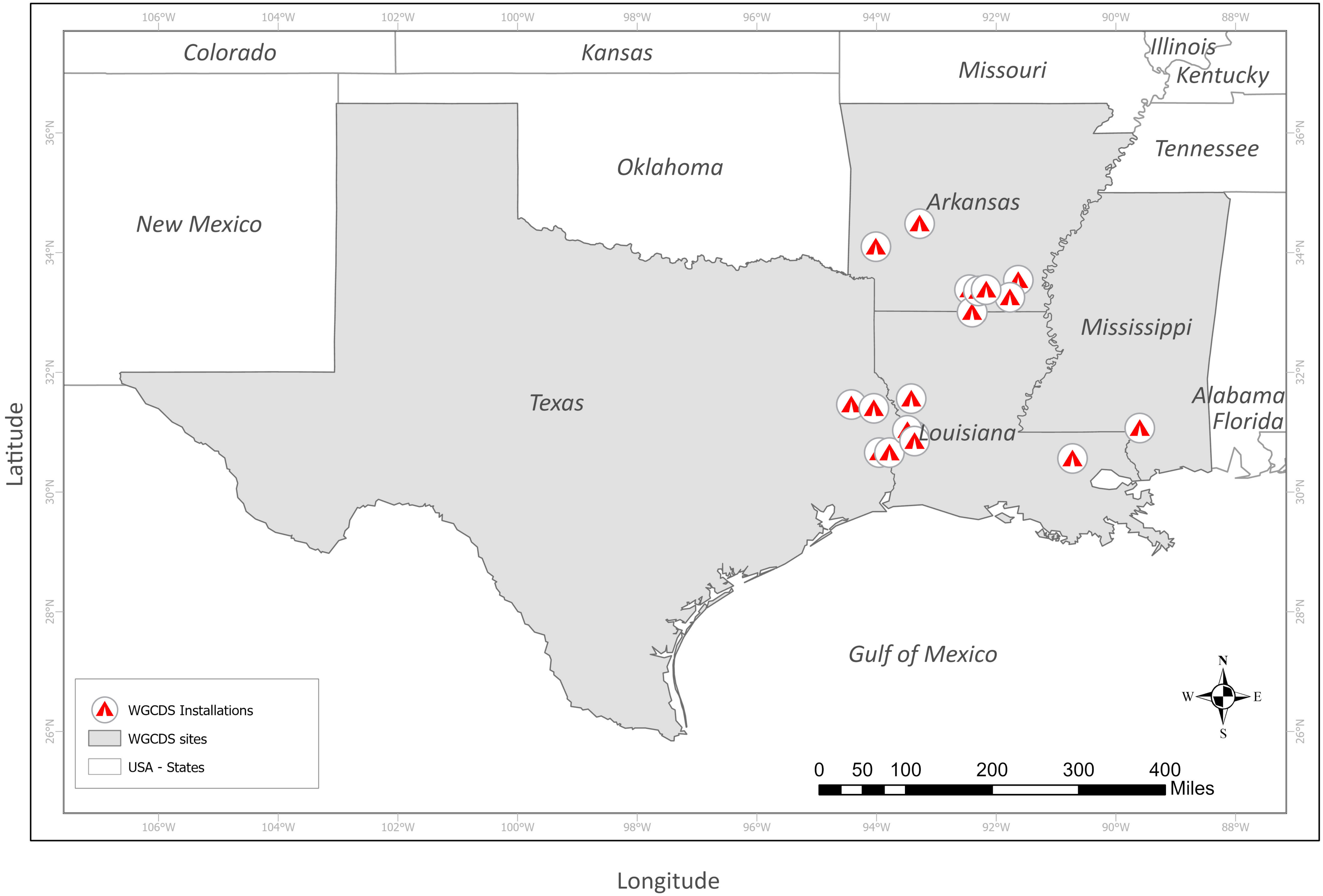

Figure 1.1: Western Gulf Culture Density Study installations for the Plantation Management Research Cooperative used in this thesis.

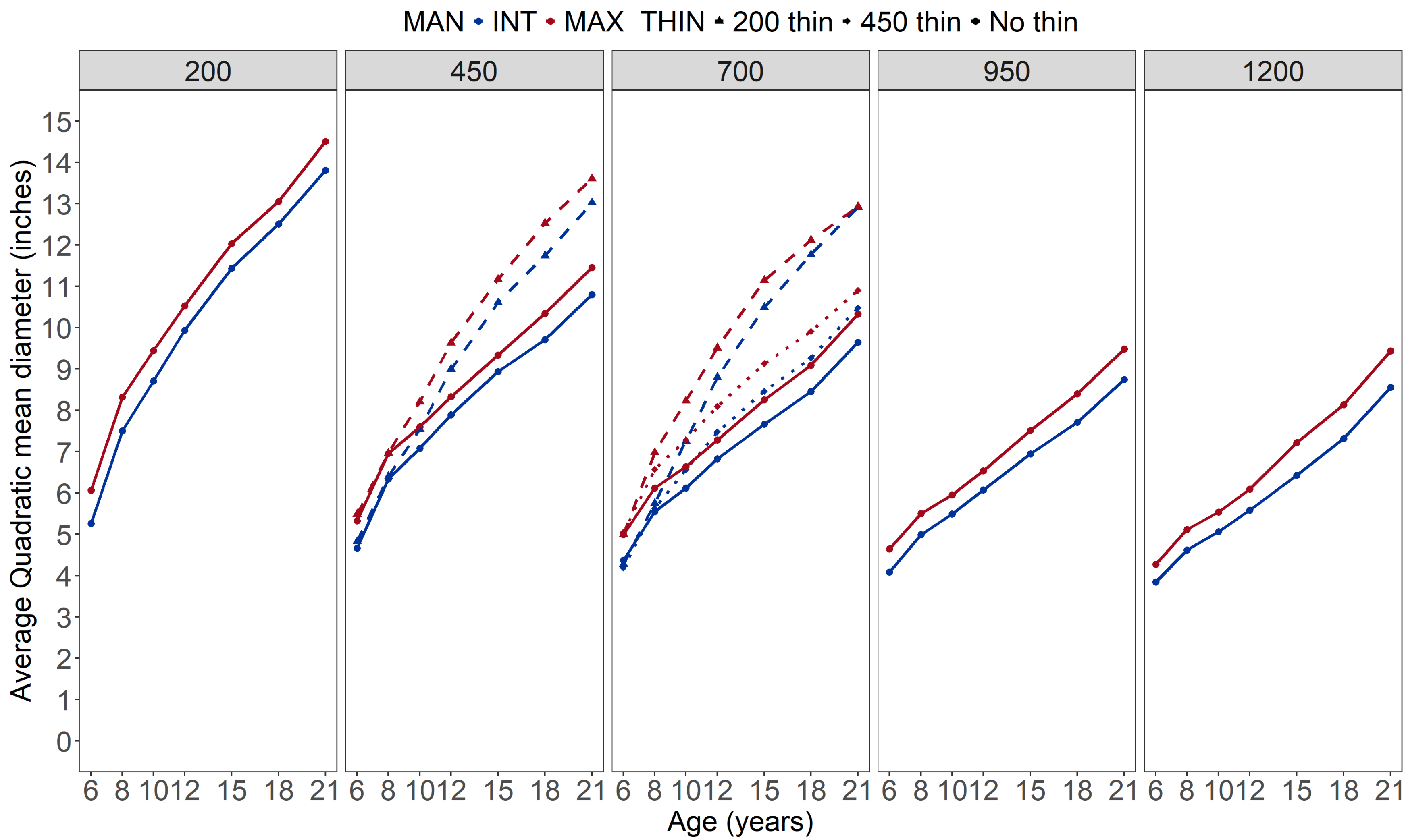

Figure 1.2: WGCDS average quadratic mean diameter ($\overline{\mathrm{D}}_\mathrm{q}$) across all five planting densities, two silvicultural management levels, and two thinning treatments. Blue lines represent intensive (INT) management intensity, and red lines represent maximum (MAX) management intensity. The dashed line indicates thinning to 200 TPA, and the dotted line indicates thinning to 450 TPA.

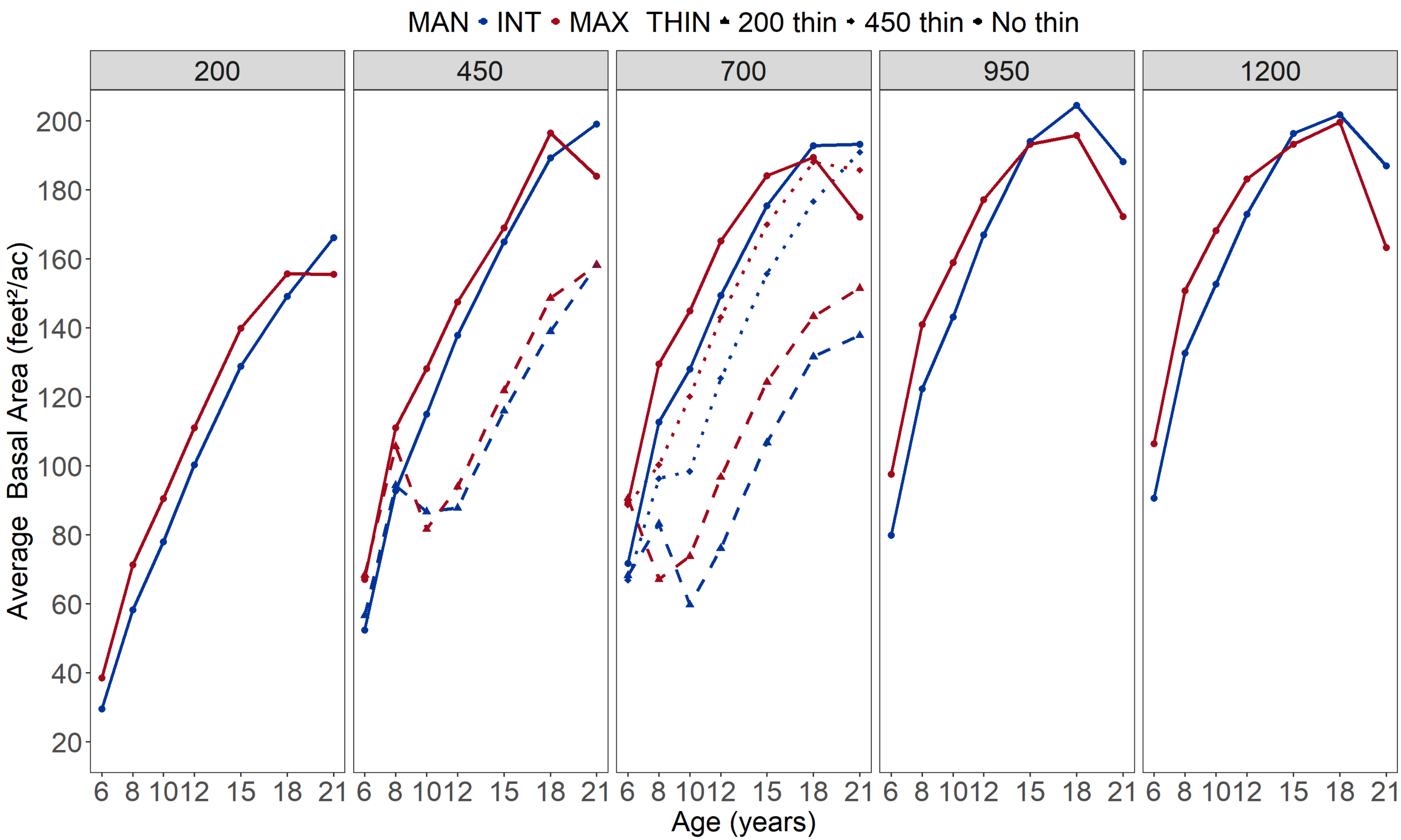

Figure 1.3: WGCDS average basal area (BA/ft^2 ac^{-1})per acre across all five planting densities, two silvicultural management levels, and two thinning treatments. Blue lines represent intensive (INT) management intensity, and red lines represent maximum (MAX) management intensity. The dashed line indicates thinning to 200 TPA, and the dotted line indicates thinning to 450 TPA.

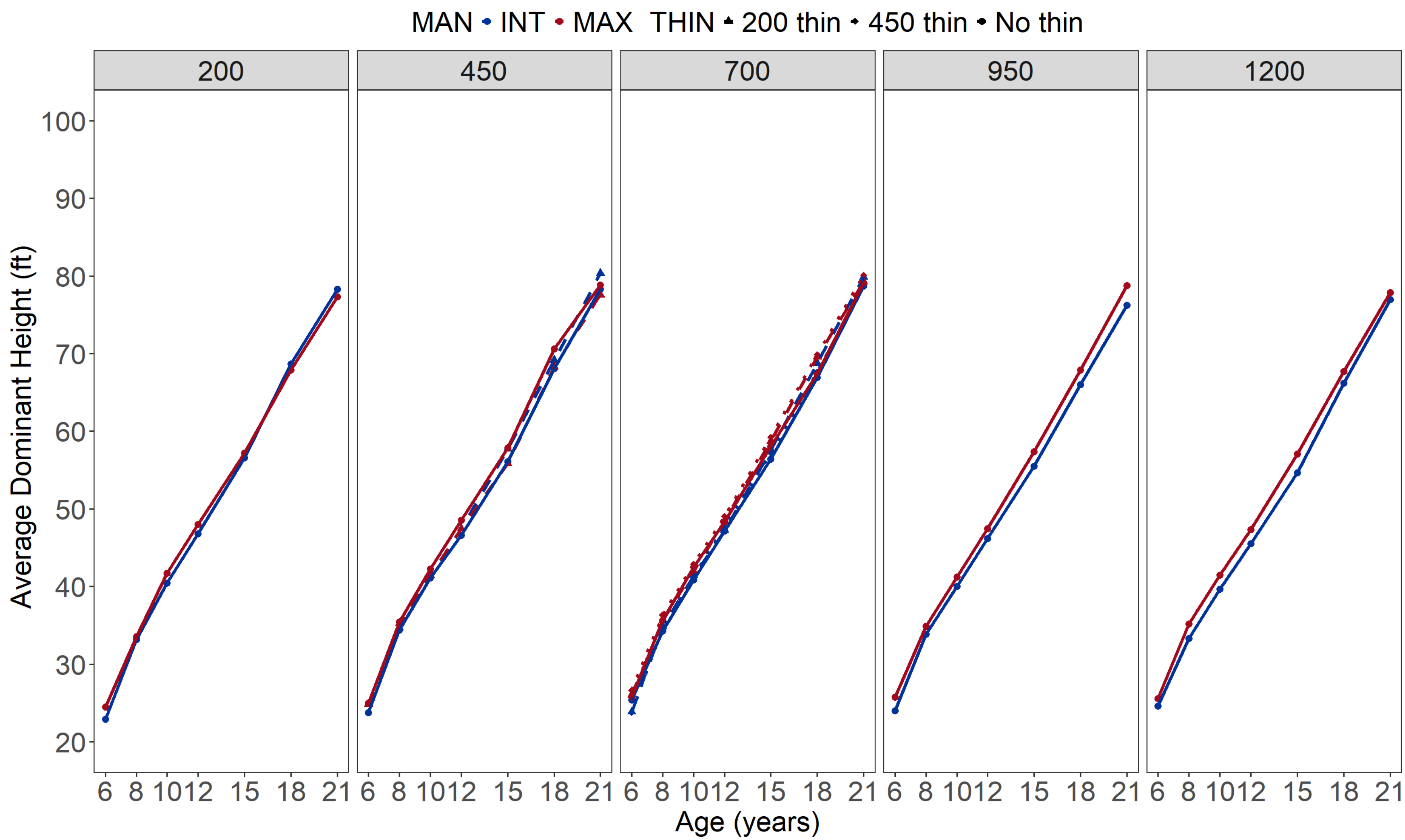

Figure 1.4: WGCDS average dominant height (HD) across all five planting densities, two silvicultural management levels, and two thinning treatments. Blue lines represent intensive (INT) management intensity, and red lines represent maximum (MAX) management intensity. The dashed line indicates thinning to 200 TPA, and the dotted line indicates thinning to 450 TPA.

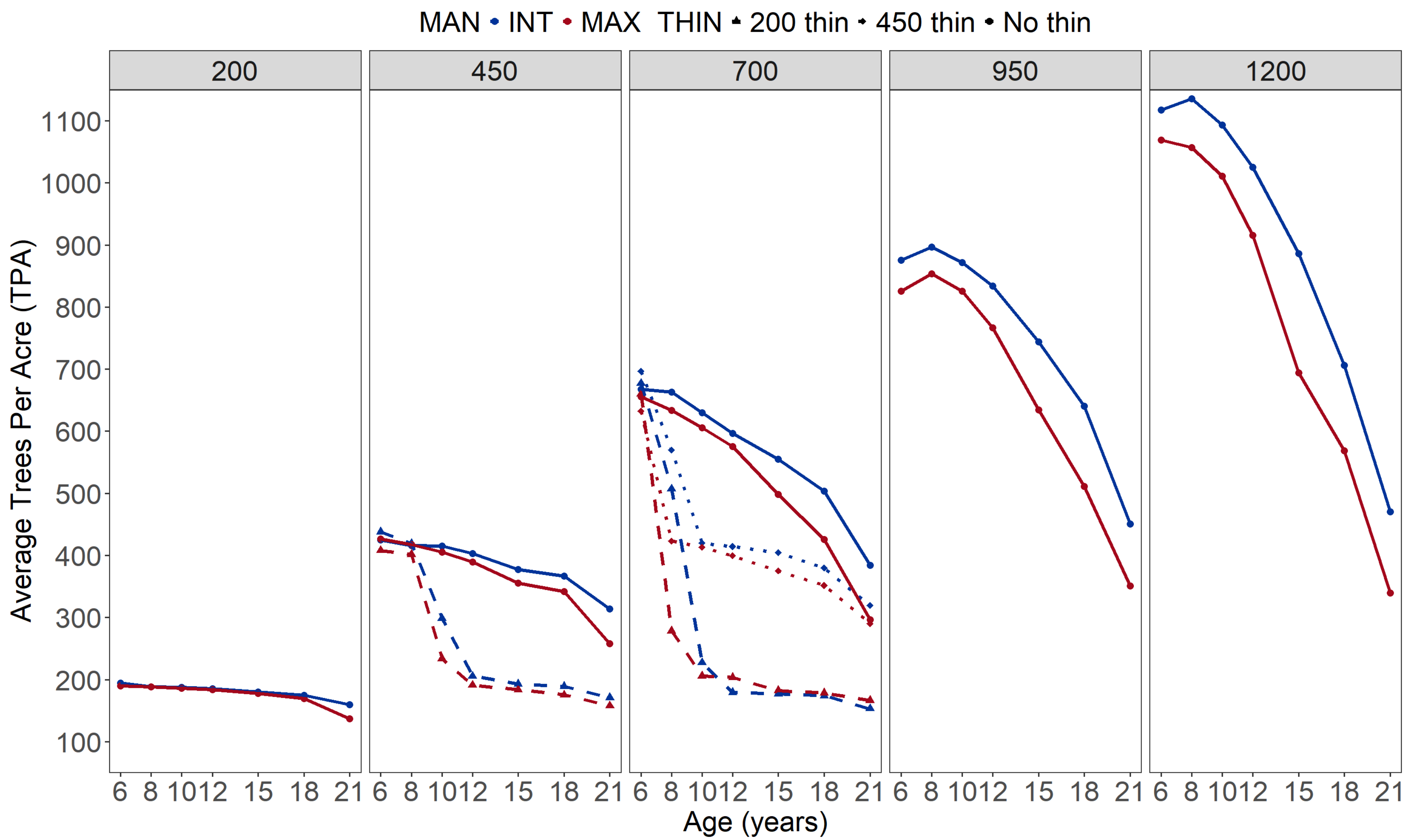

Figure 1.5: WGCDS trees per acre (TPA) across all five planting densities, two silvicultural management levels, and two thinning treatments. Blue lines represent intensive (INT) management intensity, and red lines represent maximum (MAX) management intensity. The dashed line indicates thinning to 200 TPA, and the dotted line indicates thinning to 450 TPA.

Table 1.4: Mortality (%) by age, planting density (PLTPA), and thinning regime (THIN) under two silvicultural managements (MAN) level.

AGE	MAN	THIN	PLTPA				
			200	450	700	950	1200
6	INT	No-thin	2.65	5.78	6.20	7.18	9.83
	MAX		5.02	5.89	6.94	8.00	10.97
	INT	200	–	2.70	3.26	–	–
	MAX		–	9.35	5.76	–	–
	INT	450	–	–	0.47	–	–
	MAX		–	–	9.67	–	–
8	INT	No-thin	12.56	20.20	5.61	7.59	7.82
	MAX		15.41	31.57	5.20	7.15	9.96
	INT	200	–	6.83	27.55	–	–
	MAX		–	10.72	60.21	–	–
	INT	450	–	–	18.60	–	–
	MAX		–	–	39.52	–	–
10	INT	No-thin	10.51	16.15	18.58	30.19	4.65
	MAX		13.50	21.08	24.08	42.60	6.32
	INT	200	–	33.67	67.51	–	–
	MAX		–	48.10	70.59	–	–
	INT	450	–	–	40.01	–	–
	MAX		–	–	41.00	–	–
12	INT	No-thin	5.26	10.06	14.82	20.67	28.08
	MAX		9.47	13.42	17.77	28.77	39.14
	INT	200	–	54.34	74.41	–	–
	MAX		–	57.55	70.90	–	–
	INT	450	–	–	40.79	–	–
	MAX		–	–	42.93	–	–
15	INT	No-thin	45.07	7.83	5.61	8.24	12.20
	MAX		57.66	13.06	10.15	13.13	19.30
	INT	200	–	57.07	74.70	–	–
	MAX		–	59.18	73.94	–	–
	INT	450	–	–	42.21	–	–
	MAX		–	–	46.39	–	–
18	INT	No-thin	21.72	32.60	52.54	6.90	5.39
	MAX		33.20	46.16	63.09	10.93	11.94
	INT	200	–	57.92	75.14	–	–
	MAX		–	61.07	74.46	–	–
	INT	450	–	–	45.73	–	–
	MAX		–	–	49.75	–	–
21	INT	No-thin	8.87	14.59	26.16	41.12	60.82
	MAX		15.79	23.69	42.13	52.58	71.73
	INT	200	–	62.04	78.12	–	–
	MAX		–	64.92	76.19	–	–
	INT	450	–	–	54.35	–	–
	MAX		–	–	58.56	–	–

Chapter 2

Diameter distributions for two silvicultural management levels in loblolly pine (*Pinus taeda L.*) plantations in the Western Gulf physiographic region of the Southeastern United States[1]

[1]Maciel, G.O.P., B. P. Bullock, S.M. Kinane, and S. Sandoval. To be submitted to *Forest Science*.

2.1 Abstract

Diameter distribution models are one of the many forest models that integrate the forest growth and yield system. The growth and yield system provides valuable quantitative forest information to guide and support forest management decisions. This study evaluated the diameter distribution of loblolly pine plantations in the Western Gulf physiographic region of the United States under two levels of management intensity, across five initial planting densities and seven measurement ages. The intensive regime included site preparation specific to each site type, tip-mound application, vegetation control during the first year, and fertilization in the first and tenth growing seasons. The maximum regime included the same treatments as the intensive regime; however, vegetation control was applied during the first, second, and third years, and fertilization occurred in the second, fourth, and sixth years. The parameter recovery approach was performed using the percentile estimation technique to compute the three-parameter Weibull distribution. With the three-parameter Weibull distribution the cumulative density function is obtained and used to calculate the frequency of trees per acre by diameter class. A two-sample t-test with one-tailed was used to compare the basal area per acre estimation between the two management intensities. Results revealed that maximum regime intensity had statistically higher mean basal area per acre in young age and mid-rotation age for all five initial planting densities compared to intensive regime intensity. The results of this study support the effect of these treatments on loblolly pine growth and provide a broader understanding of how different management intensity levels affect loblolly pine plantation growth and production.

2.2 Introduction

Silvicultural practices have evolved significantly over the years in pursuit of better forest management. Treatments such as fertilization, site preparation, vegetation control, thinning or their combination are effective means to optimize growth and yield (G&Y) (Matziris and Zobel, 1976; Haywood, 2005; Ferreira et al., 2020). Forest fertilization, and vegetation control for example, has become a standard techniques to manipulate forests and increase tree growth and subsequent forest value. The major goal of fertilization application and vegetation control in forest management, especially in loblolly pine plantations, is to increase stand productivity and forest value. Several studies have shown that these techniques have an important role in forest management, especially tree development (Haywood et al., 2003; Gyawali and Burkhart, 2015). Diameter at breast height (DBH), tree height, basal area, and leaf area are some of the tree characteristics affected positively by fertilization, vegetation control or their combination (Jokela et al., 1989; Windsor and Reines, 1973). The application of nitrogen (N) in pine plantations, for example, has a direct effect on DBH increment, and phosphorus (P) is used to increase soil nutrients used in tree development (Shafii et al., 1990; Albaugh et al., 2017).

The effect of fertilization and vegetation control is not limited just to tree improvement; it also has economic impact, adding value in pine plantations (Albaugh et al., 2009; de Souza Kulmann et al., 2023). Because these treatments increase individual tree DBH, forests can achieve higher concentrations of trees per acre (TPA) in large diameter class and increased wood for higher value sawtimber products (Albaugh et al., 2018; Consalter et al., 2021). As previously mentioned, the goal of silvicultural management is to increase forest productivity. In other words, it involves making interventions (e.g., fertilization, vegetation control, thinning, site preparation) to grow trees with larger diameters, thereby maximizing the TPA within the diameter classes suitable for the sawtimber market. To estimate the TPA across different diameter classes, diameter distribution modeling is commonly used. Diameter distribution modeling enables the creation of distribution curves that reflect the structural composition of a forest. Furthermore, diameter distribution is used to estimate the TPA within each diameter class and to provide information about forest yield.

As previously mentioned, P, N application or their combination plays an important role in DBH growth. This impact is reflected in the diameter distribution curve, which becomes slightly flattened and shifted to the right, indicating a greater concentration of TPA in larger diameters (Allen, 1987; Carlson et al., 2008). Changes in forest structure resulting from silvicultural management (e.g., fertilization) should be considered in diameter distribution modeling, as individual diameter increment influences the allocation of trees across different diameter classes (Allen et al., 1983).

Despite much research demonstrating the benefits of intensive management on tree growth, there is still room to analyze how fertilizer and vegetation control affects forest structure. One way to examine this effect is by understanding how these treatments influences the structural distribution of a loblolly pine plantation. Few researchers, have conducted how fertilization, and vegetation control treatment affect the parameter estimates for the three-parameter (location, scale, and shape) Weibull distribution (Bailey et al., 1989; Cardoso et al., 2013). However, these studies focus only on the common rate and timing of fertilization and vegetation control.

The objective of this study is to analyze, investigate, and compare two levels of silvicultural management, including the application of fertilization and vegetation control, in terms of the estimated diameter distribution parameters. The study considered five initial planting densities (PLTPA) at the ages of 6, 8, 10, 12, 15, 18, and 21 years. The Weibull distribution approach was used to estimate the three parameters and generate diameter distribution curves. The comparison of the Weibull parameters was performed by averaging the parameters between the two silvicultural management (MAN) levels, intensive management (INT) and maximum management (MAX). Additionally, a comparison of basal area per acre estimated from Weibull distribution was conducted as a complementary analysis for parameter estimation between the two silviculture managements levels.

This work should add to and provide useful in providing a deeper understanding of how different management levels intensity affect pine loblolly plantation diameter distribution and stand characteristics. By understanding how different management intensities influence diameter growth and, consequently, the diameter distribution, it will be possible to identify differences in forest structure and determine whether a particular silvicultural management level is more effective in promoting a higher concentration of tree per acre and volume in larger diameter classes, thus adding value to the forest.

2.3 Literature Review

2.3.1 Parameter estimation

As mentioned in chapter I, over time several approaches have been created to represent diameter distributions (e.g., the Weibull distribution has been used).

Parameter estimation techniques have been developed to represent statistical distributions. These methods can be classified as:

- Graphical methods
- Statistical methods
- Combination of the Graphical and Statistical

In graphical methods, estimates are derived by plotting the data. A model needs to be selected before plotting the data, and each process must be performed individually. One major drawback of graphical methods is the limited statistical theory available to assess their performance in small-sample or asymptotic scenarios. Although, they are convenient to provide an initial estimate for statistical methods of estimation.

Statistical methods, however, are broader and more flexible for different types of models and data. In this methodology the estimators of asymptotic properties are well understood (Murthy et al., 2004).

In forestry, the estimation of the Weibull three-parameter for probability density function (PDF) can be classified in two methods, known as parameter prediction method and parameter recovery method. Historically, the parameter prediction method faced challenges in modeling diameter distribution by computing the PDF directly from regressions based on stand characteristics (e.g., site index, age, basal area). The results of parameters failed to represent accurate stand characteristics (Borders et al., 1987). This approach has been shown to be disadvantageous in terms of parameter estimation, with inconsistency between the estimated and observed stand characteristics (Fonseca et al., 2009). The parameter prediction method is an approach of predicting the future parameters of a PDF in a certain diameter distribution directly from the observed data (Hyink and Moser, 1983; Poudel and Cao, 2013).

Parameter recovery emerged as an alternative approach to obtain more realistic estimates of stand characteristics. The parameter recovery method is a relationship between a distribution parameter and stand characteristics, the most common approach for parameter recovery method is the method of moments (e.g., mean and quadratic diameter mean) and percentile method (e.g., median). By using the parameter recovery method, the regression considers stand characteristics (Poudel and Cao, 2013). The variables can be any stand characteristics (e.g., site index, age, basal area, number of tree per acre) that can be mathematically obtained from the distribution (Siipilehto and Mehtätalo, 2013). Parameter recovery predicts distributional parameters, where they are "recovered" from the stand attributes, and is expressed in terms of the DBH distribution (Burk and Burkhart, 1984). In this method one major advantage is that diameter distribution characteristics (e.g., mean, quadratic mean diameter, diameter percentiles) are highly correlated with stand characteristics, enabling a better parameter estimation (Knowe et al., 1997).

2.3.2 Parameter estimation techniques

Maximum likelihood

The most common Weibull parameter estimation techniques are moment estimator, percentile estimator and maximum likelihood estimator. Maximum likelihood (ML) estimates parameters by maximizing the natural logarithm of the likelihood function (Maltamo et al., 2000). The ML method has the greatest relevance to obtain an efficient parameter estimator with Gaussian asymptotic distribution (Mahdi and Ashkar, 2004). Additionally, this method adapts easily for different type of data (e.g., complete, censored), this method is commonly used due to its asymptotic characteristics (Cooray, 2015). However, ML requires highly iterative computations, since the Weibull's three parameters (location, scale and shape) are obtained by solving several iterative equations (Mahdi and Ashkar, 2004; Zarnoch and Dell, 1985; Gu et al., 2024). Other disadvantages are related to sample size, bias in maximum likelihood due to small sample size, and issues with regularity. The main problem is because the distribution has a parameter-dependent lower bound (Hirose, 1991; Teimouri et al., 2013). The complete data are classified when values are available for each observation in a dataset (Murthy et al., 2004). The likelihood function for complete data can be expressed as follows:

$$\mathrm{L}(\alpha,\beta,\gamma)=\frac{\gamma^{\mathrm{n}}}{\beta^{\gamma\mathrm{n}}}\left[\prod_{\mathrm{i}=1}^{\mathrm{n}}(\mathrm{t_i}-\alpha)^{\gamma-1}\right]\exp\left[-\frac{1}{\beta^{\gamma}}\sum_{\mathrm{i}=1}^{\mathrm{n}}(\mathrm{t_i}-\alpha)^{\gamma}\right] \tag{2.1}$$

Maximum likelihood estimates are obtained by solving the three equations below to set the partial derivatives to zero:

$$\hat{\beta}^{\hat{\gamma}}-\frac{1}{\mathrm{n}}\sum_{\mathrm{i}=1}^{\mathrm{n}}(\mathrm{t_i}-\hat{\alpha})^{\hat{\gamma}}=0 \tag{2.2}$$

$$\frac{\sum_{\mathrm{i}=1}^{\mathrm{rn}}(\mathrm{t_i}-\hat{\alpha})^{\hat{\gamma}}\ln(\mathrm{t_i}-\hat{\alpha})}{\sum_{\mathrm{i}=1}^{\mathrm{n}}(\mathrm{t_i}-\hat{\alpha})^{\hat{\gamma}}}-\frac{1}{\hat{\gamma}}-\frac{1}{\mathrm{n}}\sum_{\mathrm{i}=1}^{\mathrm{n}}\ln(\mathrm{t_i}-\hat{\alpha})=0 \tag{2.3}$$

$$(\hat{\gamma} - 1)\sum_{i=1}^{n}(t_i - \hat{\alpha})^{-1} - \hat{\gamma}\hat{\beta}^{-\hat{\gamma}}\sum_{i=1}^{n}(t_i - \hat{\alpha})^{\hat{\gamma}-1} = 0 \tag{2.4}$$

In contrast to complete data, the censored data is defined when partial or all values are not available in a dataset. The ML estimate for censored data can be obtained in a similar approach as the standard Weibull model. When censored data have t_1 ... t_2 ... t_k, the log-likelihood can be express by (Murthy et al., 2004):

$$L(\alpha, \beta, \gamma) = \ln\frac{n!}{(n - k)!} + k(\ln\gamma - \gamma\ln(\beta)) + (\gamma - 1)\sum_{i=1}^{k}(t_i - \alpha) \quad - \beta^{-\gamma}\left[\sum_{i=1}^{k}(t_i - \alpha)^{\gamma} - (n - k)(t_k - \alpha)^{\gamma}\right] \tag{2.5}$$

The maximum likelihood estimates can be expressed as follows:

$$\hat{\beta} = \left[\frac{\sum_{i=1}^{k}(t_i - \hat{\alpha})^{\gamma} - (n - k)(t_k - \hat{\alpha})^{\gamma}}{k}\right]^{\frac{1}{\hat{\gamma}}} \tag{2.6}$$

with $\hat{\gamma}$ and $\hat{\alpha}$ obtained from the following two equations:

$$\hat{\gamma}k = \frac{\sum_{i=1}^{k}(t_i - \hat{\alpha})^{\hat{\gamma}-1} + (n - k)(t_k - \hat{\alpha})^{\hat{\gamma}-1}}{k} \Bigg/ \frac{\sum_{i=1}^{k}(t_i - \hat{\alpha})^{\hat{\gamma}} + (n - k)(t_k - \hat{\alpha})^{\hat{\gamma}}}{k}$$
$$- (\hat{\gamma} - 1)\sum_{i=1}^{k}(t_i - \hat{\alpha})^{-1} = 0 \tag{2.7}$$

$$\left[\frac{k}{\hat{\gamma}} + \sum_{i=1}^{k}\ln(t_i - \hat{\alpha})\right] \cdot \left[\sum_{i=1}^{k}(t_i - \alpha)^{\hat{\gamma}} + (n - k)(t_k - \alpha)^{\hat{\gamma}}\right]$$
$$- k\left[\sum_{i=1}^{k}(t_i - \hat{\alpha})^{\hat{\gamma}}\ln(t_i - \hat{\alpha}) + (n - k)(t_k - \alpha)^{\hat{\gamma}}\ln(t_k - \hat{\alpha})\right] = 0 \tag{2.8}$$

Where, $L(\cdot)$ is the likelihood function; n is the sample size; t is time; $k = [100(1 - \delta/2)]$ $\ln(\cdot)$ is the logarithm function; then α, β, and γ are the location, scale, and shape parameters of the distribution, respectively.

Method of moments

The method of moments (MOM) uses the mean, the variance, and the third central moment to estimate the three parameters of the Weibull distribution(Murthy et al., 2004). For diameter distributions in MOM, the parameters can be obtained from the first, second, and third moments (i.e. diameter mean, diameter variance, and skewness) (Weiskittel et al., 2011; Merganič and Sterba, 2006; Alkan et al., 2025). This method describes the relationship between stand characteristics (e.g., age, site index, density) and the moments (e.g., mean diameter and mean square diameter) (Liu et al., 2004). The stand-level mean, and standard deviation of DBH are the two most common characteristics and are associated to the first and second moments (Rijal and Sharma, 2023). MOM is considered the best method for parameter estimation because it uses simple methods and provides accurate results (Merganič and Sterba, 2006; Alkan et al., 2025). This method is often used in growth and yield models because it usually requires few equations to obtain numeric compatibility (Weiskittel et al., 2011). Although, some researchers prefer to use MOM only for comparing between other methodologies (e.g., percentile, maximum likelihood) (Merganič and Sterba, 2006). The Weibull's three parameters are obtained by simultaneously solving the equations for the mean (Equation 2.9), the variance (Equation 2.10), and the third central moment (Equation 2.11). This approach is exclusively used for complete data period, For this method, the parameters are not expressed directly as a function of the moments (Murthy et al., 2004).

$$\mu = \mathrm{E(T)} = \alpha + \beta\Gamma\left(1 + \frac{2}{\gamma}\right) \tag{2.9}$$

$$\sigma^2 = \beta^2\left[\Gamma\left(1 + \frac{2}{\gamma}\right) - \left[\Gamma\left(1 + \frac{1}{\gamma}\right)\right]^2\right] \tag{2.10}$$

$$\mu_3 = \beta^3\left\{\Gamma\left(\frac{1+3}{\gamma}\right) - 3\Gamma\left(\frac{1+1}{\gamma}\right)\Gamma\left(\frac{1+2}{\gamma}\right) + 2\left[\Gamma\left(\frac{1+1}{\gamma}\right)\right]^3\right\} \tag{2.11}$$

Where, μ, σ^2, and μ_3 are the mean, variance, and third moment respectively; E[·] is the expectation of the random variable; (T) is the random variable; Γ is the gamma function; and α, β, and γ are the location, scale, and shape parameters of the distribution, respectively.

Percentiles

For the percentiles estimator, the dataset is put through the empirical distribution function to derive specific percentiles. The first step of the percentile method (PCT) is obtaining the expression for the percentile in terms of the model parameters (Murthy et al., 2004).

Zanakis (1979) recommended the following equations for percentile estimator procedure:

$$\hat{\alpha} = \frac{\mathrm{X_1X_n - X_2^2}}{\mathrm{X_1 + X_n - 2X_2}} \tag{2.12}$$

if $\mathrm{X_2}$ is closer to $\mathrm{X_1}$ to $\mathrm{X_n}$, $= \mathrm{X_1} =$ otherwise,

Where, $\mathrm{X_i}$ is the estimate of the location parameter; n is sample size; and $\hat{\alpha}$ is estimate of the location parameter.

$$\hat{\beta} = -\hat{\beta} + \mathrm{X}_{[0.63_\mathrm{n}]} \tag{2.13}$$

Where, $\hat{\beta}$ is the estimate of the scale parameter; [·] is the estimate of the scale parameter.

$$\hat{\gamma} = \frac{\ln\frac{\ln(1-\mathrm{p_k})}{\ln(1-\mathrm{p_i})}}{\ln\frac{\mathrm{X[np_k]}-\hat{\beta}}{\mathrm{X_{[np_i]}}-\hat{\beta}}} \tag{2.14}$$

Where, $\mathrm{p_i} = 0.16731$; $\mathrm{p_k}= 0.97366$; and $\hat{\gamma}$ is the estimate of the shape parameter.

For diameter distribution the PCT method shows a strong correlation with the stand characteristic similar to MOM (Liu et al., 2004). This method is very responsive to the shape and skew of the data due to the use of a specific percentiles range (Alkan et al., 2025). The first percentile based on recovery parameters for diameter distribution was created by using a percentile model to predict the 0^{th}, 25^{th}, 50^{th}, 95^{th} (Da Silva, 1969). The PCT method can use multiple percentiles of the diameter distribution to recover the parameters (Weiskittel et al., 2011). Zanakis (1979) suggested several relatively simple percentile estimators of the Weibull parameter and obtained a better estimation for small sample size when $c < 2$ was compared to the ML method (Zarnoch and Dell, 1985). Cao and Burkhart (1984) used five percentile points (0^{th}, 25^{th}, 50^{th}, 75^{th}, and 100^{th}) to define the segmentation of a cumulative distribution function. Borders et al. (1987) modeled 12 systems to obtain specific percentiles and found that this system had high flexibility to provide multimodal stand tables by using simple noniterative mathematics computation. Bailey et al. (1989) applied the percentile method using quadratic mean diameter, minimum diameter (D_0), and the 25^{th} (D_{25}), 50^{th} (D_{50}), and 95^{th} (D_{95}) DBH percentiles to obtain the Weibull three parameters. The percentile method provides benefits compared to other methods, such as easy computation and proficiency to better parameter estimation (Erişoğlu et al., 2020).

2.4 Methods

2.4.1 Data analysis

Data structure

The database described in Chapter I was formatted for use in this chapter, and Chapter III. For this chapter, all analysis and modeling are considering the dataset without thinning. The tree-level dataset was grouped by variables: installation (INST), age (AGE), initial planting density (PLTPA), silvicultural management (MAN) to obtain the dataset for the level analysis. Due to certain factors, such as self-thinning and other operational constraints (e.g., presence of overhead power lines), certain combinations of variables are missing in specific years for some installations (Table 2.1).

Considering the five PLTPA, two-level MAN and seven ages of tree measurements (6, 8, 10, 12, 15, 18, 21), we obtained 970 plot-level observations for the analysis and modeling in this chapter.

2.4.2 Hypothesis test

Analysis of variance (ANOVA) was performed for all plots for each combination of treatments by year. Basal area per acre (BA), quadratic mean diameter ($\overline{\mathrm{D}}_{\mathrm{q}}$), and dominant tree height (HD) were used to test if the five PLTPA, the two MAN levels, and the interaction between PLTPA and MAN have an effect on those stand characteristics (i.e., BA, $\overline{\mathrm{D}}_{\mathrm{q}}$, HD). The Tukey's honestly significant difference (HSD) test was performed to analyze directly all pairwise comparisons at the 95% family-wise confidence level. All statistical analyses were conducted at a 5% significance level ($\alpha = 0.05$) and were performed using R software (Microsoft R Core Team 2005).

The PLTPA variable and the MAN were considered as fixed effects and installations as random effects; the following hypotheses were created:

$$\mathrm{H}_0^{(1)} : \alpha_{\mathrm{BA}_{\mathrm{MAX}}} = \alpha_{\mathrm{BA}_{\mathrm{INT}}}$$
$$\mathrm{H}_0^{(2)} : \alpha_{\mathrm{Dq}_{\mathrm{MAX}}} = \alpha_{\mathrm{Dq}_{\mathrm{INT}}}$$
$$\mathrm{H}_0^{(3)} : \alpha_{\mathrm{HD}_{\mathrm{MAX}}} = \alpha_{\mathrm{HD}_{\mathrm{INT}}}$$

1. *The null hypothesis states that there is no effect of silvicultural treatment on basal area.*

2. *The null hypothesis states that there is no effect of silvicultural treatment on quadratic mean diameter.*

3. *The null hypothesis states that there is no effect of silvicultural treatment on dominant height.*

$$
\begin{aligned}
\mathrm{H}_0^{(1)} &: \beta_{\mathrm{BA}_1} = \beta_{\mathrm{BA}_2} = \beta_{\mathrm{BA}_3} = \beta_{\mathrm{BA}_4} = \beta_{\mathrm{BA}_5} = 0 \\
\mathrm{H}_0^{(2)} &: \beta_{\mathrm{Dq}_1} = \beta_{\mathrm{Dq}_2} = \beta_{\mathrm{Dq}_3} = \beta_{\mathrm{Dq}_4} = \beta_{\mathrm{Dq}_5} = 0 \\
\mathrm{H}_0^{(3)} &: \beta_{\mathrm{HD}_1} = \beta_{\mathrm{HD}_2} = \beta_{\mathrm{HD}_3} = \beta_{\mathrm{HD}_4} = \beta_{\mathrm{HD}_5} = 0
\end{aligned}
$$

1. *The null hypothesis states that there is no effect of initial planting density on basal area.*
2. *The null hypothesis states that there is no effect of initial planting density on quadratic mean diameter.*
3. *The null hypothesis states that there is no effect of initial planting density on dominant height.*

$$
\begin{aligned}
\mathrm{H}_0^{(1)} &: \alpha\beta_{\mathrm{BA}_{1\mathrm{INT}}} = \alpha\beta_{\mathrm{BA}_{1\mathrm{MAX}}} = \cdots = \alpha\beta_{\mathrm{BA}_{5\mathrm{INT}}} = \alpha\beta_{\mathrm{BA}_{5\mathrm{MAX}}} = 0 \\
\mathrm{H}_0^{(2)} &: \alpha\beta_{\mathrm{Dq}_{1\mathrm{INT}}} = \alpha\beta_{\mathrm{Dq}_{1\mathrm{MAX}}} = \cdots = \alpha\beta_{\mathrm{Dq}_{5\mathrm{INT}}} = \alpha\beta_{\mathrm{Dq}_{5\mathrm{MAX}}} = 0 \\
\mathrm{H}_0^{(3)} &: \alpha\beta_{\mathrm{HD}_{1\mathrm{INT}}} = \alpha\beta_{\mathrm{HD}_{1\mathrm{MAX}}} = \cdots = \alpha\beta_{\mathrm{HD}_{5\mathrm{INT}}} = \alpha\beta_{\mathrm{HD}_{5\mathrm{MAX}}} = 0
\end{aligned}
$$

1. *The null hypothesis states that there is no effect of any interaction between silvicultural treatment levels and initial planting density on quadratic mean diameter.*
2. *The null hypothesis states that there is no effect of any interaction between silvicultural treatment levels and initial planting density on basal area.*
3. *The null hypothesis states that there is no effect of any interaction between silvicultural treatment levels and initial planting density on dominant height.*

The model for ANOVA can be expressed as:

$$y_{ijk} = \mu + \alpha_j + \beta_k + (\alpha\beta_{jk}) + \gamma_i + \epsilon_{ijk} \tag{2.15}$$

Where, y_{ijk} is the response variable (BA, $\overline{D}_q$, and HD); μ is the overall mean; α is the fixed effect of the j^{th} level of MAN; β is the fixed effect of the k^{th} level of PLTPA; $(\alpha\beta_{jk})$ is the interaction effect between MAN and PLTPA; γ_i is the random effect i^{th} Region; and ϵ_{ijk} is the residual error.

2.4.3 Diameter Distribution Modeling

Percentile Method

The percentiles or quantiles characterize a distribution. For any value $0 < p < 1$, the quantile of order p for a random variable X is a value ξ p is a value ξ such that:

- $P(X < \xi_p) \leq p$, and
- $P(X \geq \xi_p) \geq p$.

This value ξ_p is also referred to as the $(100_p)^{th}$ percentile of X. The median is the second quartile and is considered the quartile $\xi_{1/2}$; it splits the probability distribution in two equal halves of 50%. The first quartile ($q_1 = \xi_{1/4}$) and the third quartile ($q_3 = \xi_{3/4}$) further divide the lower and upper halves into quarters. Collectively, these three quartiles are labeled q_1, q_2 (the median), and q_3. The interquartile range (IQR) is defined as the difference between the third and first quartiles:

$$IQR = q_3 - q_1$$

It serves as a measure of the spread or dispersion of the distribution. While the median is commonly used to describe the central tendency (center) of the distribution, the interquartile range provides insight into the variability or spread of the data (Hogg et al., 2019).

The models (Equations 2.16 – 2.19) used to predict the percentiles were developed by Jiang and Brooks (2009a), using the D_0, D_{25}, D_{50}, D_{95} from the dataset.

$$D_0 = \exp\left[\beta_{10} + \beta_{11}\ln(D_q) + \beta_{12}\ln(AGE) + \beta_{13}\ln\left(\frac{1}{HD}\right)\right] + \epsilon_1 \tag{2.16}$$

$$D_{25} = \exp\left[\beta_{20} + \beta_{21}ln(D_{50}) + \beta_{22}\ln(AGE)\right] + \epsilon_2 \tag{2.17}$$

$$D_{50} = \exp\left[\beta_{30} + \beta_{31}\ln(D_q)\right] + \epsilon_3 \tag{2.18}$$

$$D_{95} = \exp\left[\beta_{40} + \beta_{41}\ln(D_{50}) + \beta_{42}\ln(AGE) + \beta_{43}\ln\left(\frac{1}{HD}\right)\right] + \epsilon_4 \tag{2.19}$$

The regressions were adapted to the WGCDS dataset, considering the PLTPA as a continuous variable, and the MAN as a factor variable. With that the modified regressions can be written as:

$$D_0 = \exp\left[\beta_{10} + \beta_{11}\ln(D_q) + \beta_{12}\ln(AGE) + \beta_{13}\ln\left(\frac{1}{HD}\right) + \beta_{14}PLTPA + \beta_{15}MAN\right] + \epsilon_1 \tag{2.20}$$

$$D_{25} = \exp\left[\beta_{20} + \beta_{21}\ln(D_{50}) + \beta_{22}\ln(AGE) + \beta_{23}PLTPA + \beta_{24}MAN\right] + \epsilon_2 \tag{2.21}$$

$$D_{50} = \exp\left[\beta_{30} + \beta_{31}ln(D_q) + \beta_{32}PLTPA + \beta_{33}MAN\right] + \epsilon_3 \tag{2.22}$$

$$D_{95} = \exp\left[\beta_{40} + \beta_{41}\ln(D_{50}) + \beta_{42}\ln(AGE) + \beta_{43}\ln\left(\frac{1}{HD}\right) + \beta_{44}PLTPA + \beta_{45}MAN\right] + \epsilon_4 \tag{2.23}$$

Where the response variables, D_0, D_{25}, D_{50}, and D_{95}, are the percentiles diameter at breast height in inches: $\overline{D}_q$ is the quadratic mean diameter in inches from the dataset; AGE is age in years, HD the dominant tree height in feet; β_{ij} are the coefficients to be estimates ($i = 1\ldots,4, j = 0,\ldots,3$); the D_{50} is the 50^{th} DBH percentile from the dataset; $\ln(\cdot)$ is the natural logarithm; ϵ_i is the random error ($i = 1,\ldots,4$) PLTPA is the initial planning density; MAN is then the two silviculture regimes.

The correlation matrix method was used to test the correlation between the variables used in the four regressions (Equations 2.20 – 2.23).

Seemingly Unrelated Regression

Created by Zellner (1962) and used to develop a system of equations in forest stands by Borders (1989), the seemingly unrelated regression (SUR) approach was used to avoid the correlation of errors between the four models (Equations 2.20 – 2.23). SUR was developed to improve the estimated coefficients, at least asymptotically by applying Aitken's generalized least-squares to all systems of equations simultaneously (Zellner, 1962). When the residuals from these equations are correlated, estimating them independently using ordinary least squares (OLS) yields unbiased but inefficient coefficients and incorrect standard errors. Additionally, the simultaneously equations may have the errors correlation due the fact of one independent variable is present in multiple equation (Oliveira and Teixeira-Pinto, 2015; Beasley, 2008). The SUR model addresses this issue by allowing the residuals across equations to share a nonzero covariance structure, thus improving estimation efficiency through the use of generalized least squares (GLS) (Beasley, 2008).

Weibull probability density function estimates

This study used the Weibull three parameter distribution and the percentile estimator, using the parameter recovery approach for all plots. This method was developed by Bailey et al.

(1989), where uses D_q predicted (Equation 2.25), and the predicted percentiles D_0, D_{25}, D_{50}, D_{95} (Equations 2.20 – 2.23). The model to predict quadratic mean diameter (Equation 2.24) was developed by Cao (2004).

$$y = \exp\left[\beta_1 + \beta_2 \ln(RS) + \beta_3 \ln(N) + \beta_4 \ln(HD) + \frac{\beta_5}{AGE}\right] + \epsilon \tag{2.24}$$

The regression above was adapted to the WGCDS dataset, considering the MAN as factor variable. With that the modified regressions can be written as:

$$D_q = \exp\left[\beta_1 + \beta_2 \ln(RS) + \beta_3 \ln(N) + \beta_4 \ln(HD) + \frac{\beta_5}{AGE} + \beta_5 MAN\right] + \epsilon \tag{2.25}$$

Where the y (D_q) is the quadric mean diameter; RS the relative spacing; N is number of trees per acre, HD is dominant tree height; AGE is standing age in years; MAN is then the two-silviculture management; β_i are the coefficients to be estimated $\ln(\cdot)$ is the natural logarithm; ϵ is the random error.

To enhance clarity, the nomenclature used for the three-parameter Weibull distribution were modified as follows: $\hat{\alpha} = \hat{a}; \hat{\beta} = \hat{b}; \hat{\gamma} = \hat{c}$.

Considering the initial assumption that the c parameter value is 3.0, the location parameter estimation was obtained (Equation 2.26) by using the number of trees per plot, the minimum DBH percentile predicted, and the median percentile in the plot.

$$\hat{a} = \frac{n^{1/3} - \hat{D}_0 - \hat{D}_{50}}{n^{1/3} - 1} \tag{2.26}$$

The shape parameter was estimated (Equation 2.27) using the $\hat{a}$, the D_{25}, and D_{95} percentiles predicted.

$$\hat{c} = \frac{\ln\big(-\ln(1 - 0.95)\big) - \ln\big(-\ln(1 - 0.25)\big)}{\ln(\hat{D}_{95} - \hat{a}) - \ln(\hat{D}_{25} - \hat{a})} \tag{2.27}$$

The second moment of the Weibull distribution is computing the scale parameter, by $\hat{a}$ and $\hat{c}$ parameters estimated the scale parameter (Equation 2.30) by using the predict $\mathrm{D_q}$ (Equation 2.25), and the gamma function (Equations 2.28 – 2.29). The gamma function was computed before calculating the scale parameter.

$$\Gamma_1 = \Gamma\left(1 + \frac{1}{\hat{c}}\right) \tag{2.28}$$

$$\Gamma_2 = \Gamma\left(2 + \frac{1}{\hat{c}}\right) \tag{2.29}$$

$$\hat{b} = \frac{-\hat{a}\Gamma_1}{\Gamma_2} + \sqrt{\left(\frac{\hat{a}}{\Gamma_2}\right)^2 (\Gamma_1^2 - \Gamma_2) + \frac{\hat{\mathrm{D}}_\mathrm{q}^2}{\Gamma_2}} \tag{2.30}$$

Where $\hat{a}$ is the estimated location parameter; $\hat{b}$ is the estimated scale parameter; $\hat{c}$ is the estimated shape parameter; $\hat{\mathrm{D}}_0$, $\hat{\mathrm{D}}_{25}$, $\hat{\mathrm{D}}_{50}$, $\hat{\mathrm{D}}_{95}$ are predicted diameters percentiles; $\hat{\mathrm{D}}_\mathrm{q}$ is the predicted quadratic mean diameter; n is the number of tree measurement plot; Γ_1,Γ_2 are gamma function; and $\ln(\cdot)$ is the natural logarithm.

Cumulative density function

The cumulative density function or cumulative distribution function (CDF) are described by Hogg et al. (2019) when X is a random variable, the CDF is defined by Fx (x), where:

$$\mathrm{FX} = \mathrm{PX}([-\infty, \mathrm{x}]) = \mathrm{P}(\mathrm{c} \in \mathrm{C} : \mathrm{X}(\mathrm{c}) \leq \mathrm{x})$$

To simplify the equation, the expression $\mathrm{P}(\mathrm{c} \in \mathrm{C}\text{: } \mathrm{X}(\mathrm{c}) \leq \mathrm{x})$ is modified to $\mathrm{P}(\mathrm{X} \leq \mathrm{x})$, and the Fx(x) is the simple distribution function (df). The cumulative modifier is used as Fx(x) accumulates the probabilities less than or equal to variable x.

The three parameters estimated were used to compute the CDF for Weibull three parameter for all plots (Equation 1.5).

2.4.4 Trees Per Acre & Basal Area Prediction

The proportion of TPA for a specific diameter class was calculated using the CDF for all plots by subtracting the value of the Weibull CDF at the lower diameter class limit from the upper diameter class limit (Equation 2.31). One-inch classes classification (Table 2.34) was used in the proportion of trees calculation.

$$\mathrm{P(x)} = \left[1 - \exp\left(-\left(\frac{\mathrm{x_{upper}} - \hat{a}}{\hat{b}}\right)^{\hat{c}}\right)\right] - \left[1 - \exp\left(-\left(\frac{\mathrm{x_{lower}} - \hat{a}}{\hat{b}}\right)^{\hat{c}}\right)\right] \tag{2.31}$$

Where P(x) is the proportion of trees in a specific diameter class; $\mathrm{x_{upper}}$ is the upper CDF and $\mathrm{x_{lower}}$ is the lower CDF; $\hat{a}$ $\hat{b}$, $\hat{c}$ are the parameters estimated for Weibull PDF.

The process to estimate TPA by diameter class involved multiplying the proportion of trees of a specific DBH class by the number of surviving trees. This calculation continued across all DBH classes until the sum of the proportions for all diameter classes in the plot equaled 1, and the total estimated TPA matched the number of surviving trees in the plot (Burkhart et al., 2018). The basal area per acre across all DBH classes was obtained by multiplying the basal area per tree for a specific class by the TPA estimated for that DBH class (Jiang and Brooks, 2009b).

2.4.5 T-test

The two sample t-test with one-tailed was performed across all ages and all PLTPA to test if there was a difference between the means of basal area per acre predicted based on Weibull

CDF estimate for the MAN groups. With the assumption that basal area per acre estimated had a normal distribution and the variances are equal. A null hypothesis was created:

$$H_0 : \mu_{\hat{\mathrm{BA}}_{\mathrm{MAX}}} \leq \mu_{\hat{\mathrm{BA}}_{\mathrm{INT}}}$$

2.4.6 Goodness of fit test

The error index (EI) was performed to test the goodness-of-fit of the model based on parameter recovery using the percentile estimator. The EI is a common goodness-of-fit test for diameter distribution; the principle of this method developed by Reynolds et al. (1988) is based on weighted sum of the absolute difference between predicted and observed number of TPA in each diameter class. Mehtätalo (2004) proposed a modification in the EI test by incorporating the basal area as a weight factor for each diametric class. Sandoval et al. (2012) expressed the EI test (Equation 2.32) based on the Mehtätalo (2004) to indicate the precision that can be applied to compare the diameter distribution for different classes.

The root mean square error (RMSE) (Equation 2.33) was used to compute the precision of each PDF estimated for the MAN across the five PLTPA overall years.

$$\mathrm{EI} = \sum_{\mathrm{i}=1}^{\mathrm{n}} \frac{\mathrm{BA_i}}{\mathrm{BA}} \left| \mathrm{F}(\mathrm{x_i}) - \hat{\mathrm{F}}(\mathrm{x_i}) \right| \tag{2.32}$$

$$\mathrm{RMSE} = \sqrt{\frac{1}{\mathrm{n}} \sum_{\mathrm{i}=1}^{\mathrm{n}} \left(\mathrm{F}(\mathrm{x_i}) - \hat{\mathrm{F}}(\mathrm{x_i}) \right)^2} \tag{2.33}$$

Where $\mathrm{F}(\mathrm{x_i})$ and $\hat{\mathrm{F}}$ $(\mathrm{x_i})$ are the TPA observed and estimated based on CDF: $\mathrm{BA_i}$ is the basal area estimated based on CDF for each diameter class; BA is the basal area per acre from the observed data; n is the number of diameter class with TPA.

2.5 Results & Discussion

Hypothesis test

The ANOVA for basal area per acre (Table 2.2 – 2.8) indicated that, at ages 8 and 10, the two MAN groups showed statistically significant differences. However, at age 6, the INT and MAX management groups were not significant, and this result was also observed for ages 12, 15, 18, and 21. On the other hand, as expected, the PLTPA was statistically significant (with $\alpha < 0.05$) from ages 6, 8, 10, 12, 15, and 18. At age 21, however, PLTPA was not statistically significant for basal area per acre differences. The interaction between the MAN and the five PLTPA was not significant at any of the evaluated ages.

Based on these ANOVA results, it was observed that at age 6 and ages 12, 15, 18, and 21, the null hypothesis—that there is no difference in mean basal area per acre between the two silvicultural management groups—was failed to rejected. In contrast, at ages 8 and 10, the null hypothesis was rejected in favor of the alternative hypothesis, which suggests a significant difference between the two management groups. Regarding PLTPA, from ages 6, 8, 10, 12, 15, and 18, the null hypothesis—that there is no effect of PLTPA on basal area per acre—was rejected in favor of the alternative hypothesis that at least one density level has a significant effect on basal area per acre. The opposite occurred at age 21; we failed to reject the null hypothesis, indicating no significant effect of PLTPA at that age. For the interaction between MAN and PLTPA, results indicated no statistical significance at any age, thus maintaining the null hypothesis of no interactive effect throughout the entire evaluation period.

Different results from basal area analysis were observed in the analysis of variance for quadratic mean diameter (Table 2.9 – 2.15). The MAN groups were statistically significant at ages 6, 8, 10, 12, and 15 but not significant at ages 18 and 21. On the other hand, a similar pattern to that observed for basal area per acre was noted for PLTPA, which was significant at all ages evaluated for quadratic mean diameter. The interaction between MAN and the five PLTPA was not significant at any age. Considering these results, it is observed that at ages 6, 8, 10, 12, and 15, the null hypothesis—that there is no difference in the mean quadratic diameter between the MAN groups—was rejected in favor of the alternative hypothesis, indicating a significant difference between them. At ages 18 and 21, we failed to reject the null hypothesis, indicating no significant effect of MAN on this variable. For PLTPA, we failed to reject the null at all ages, confirming that at least one density level significantly influences quadratic mean diameter. Regarding the interaction between MAN and PLTPA, no statistical significance was observed at any age, reinforcing the conclusion that there is no interactive effect between these variables on quadratic mean diameter. The analysis of variance for dominant height showed (Table 2.16 – 2.22) that neither MAN, nor PLPTA, nor their interaction were statistically significant. Therefore, we failed to reject the null hypotheses that there is no difference in mean dominant height between the two MAN groups, that there is no effect of PLTPA on this variable, and that there is no significant interaction between MAN and PLTPA. These results were consistent across all evaluated ages.

Tukey test

Based on ANOVA results the Tukey's honestly significant difference (HSD) test was performed. As previously mentioned in the ANOVA results (Table 2.16 - 2.22), the Tukey test was not performed to HD due to neither MAN nor PLTPA having shown any significance in HD variable.

The Tukey test indicated that the only statistically significant differences in basal area per acre between the two MAN types occurred at ages 8 and 10 (Table 2.23). For quadratic mean diameter, significant differences between the two MAN were observed from ages 6 to 15, with p-values less than 0.05 (Table 2.24).

When comparing the five PLTPA levels for basal area per acre, the results varied by age (Table 2.25). At age 6, significant differences were found between PLTPA 200 and 450, 200 and 700, 200 and 950, 200 and 1200, 450 and 950, and 450 and 1200. At age 8, no significant differences were found only between PLTPA 700 and 950, and 950 and 1200. A similar pattern was observed at ages 10 and 12, where no significant differences were found between PLTPA 450 and 700, 700 and 950, and 950 and 1200. At age 15, no significant differences were observed among PLTPA 450 and 700, 700 and 950, 700 and 1200, and 950 and 1200. At age 18, significant differences were found only between PLTPA 200 and 450, 200 and 700, 200 and 950, and 200 and 1200. At age 21, no comparisons among PLTPA showed significant differences in basal area per acre.

The Tukey analysis for D_q showed that from ages 8 to 15, all PLTPA comparisons revealed significant differences, except between PLTPA 950 and 1200. At ages 18 and 21, a similar trend was observed, with no significant differences found between PLTPA 700 and 950, and 950 and 1200. At age 6, four out of ten comparisons showed significant differences: 200 and 700, 200 and 950, 200 and 1200, and 450 and 1200 (Table 2.26)

Correlation

The correlation matrix test was conducted to examine the correlation among the variables used in the four regression models (Equation 2.20 - 2.23). However, no variable was removed from the models, even if it showed a high or low degree of correlation (Figure 2.1). The decision to retain all variables was based on the fact that strong correlation does not imply causality. A high positive or negative value of the sample correlation coefficient r does not mean that changes in x directly cause changes in y. The appropriate conclusion is that there may be a linear relationship between x and y (Mendenhall et al., 2003).

Percentile Seemingly Unrelated Regression

Considering the combination of PLTPA, age, and MAN in the independent regressions for D_0, D_{25}, D_{50}, and D_{95} percentiles, a positive relationship can be observed between the predicted percentiles and age for all five PLTPA (Figure 2.2). Younger stands present lower percentile values, and over time, the percentiles gradually increase, following the dynamics of a managed loblolly pine plantation.

When comparing the percentiles across the five different PLTPA, it becomes evident that stands with lower planting densities exhibit higher percentile values, reinforcing the effect of planting density on tree diameter growth and average DBH (Will et al., 2005; Roth et al., 2007; Antony et al., 2012)

When comparing the MAN, it was observed that the MAX management consistently presented higher percentile values than the INT management. This result was consistent across all percentiles, ages, and PLTPA. For PLTPA 200, the D_{25} percentile under the MAX was close to the D_{50} percentile under the INT management at ages 6, 8, 10, and 12. A similar result was observed for the other densities: at PLTPA of 450, the D_{25} percentile in the MAX was close to the D_{50} in the INT at ages 6 and 8, and the same pattern occurred at PLTPA 700. For PLTPA 950, the D_{25} percentile under the MAX was close to the D_{50} percentile under the INT at age 6.

The positive relationship between the average percentile and age is also reflected in the relationship between the average percentile and average dominant height, where stands with shorter dominant trees exhibit lower percentiles (Figure 2.3), while taller dominant trees correspond to higher percentiles. The relationship between PLTPA and percentiles is also clear: stands with lower planting densities showed higher diameter percentiles, whereas higher planting densities resulted in lower diameter percentile values.

Weibull three-parameter estimation

A clear temporal trend was observed in the a parameter, which exhibited a consistent increase over the time (Figure 2.4). In contrast, the c parameter showed a decreasing tendency over time (Figure 2.6). The behavior of decrease in c suggests that over time the distribution become less positively skewed (Carlson et al., 2008) and indicates a change in the diameter distribution characteristics. The b parameter presented distinct behavior across different

PLTPA. For higher densities (950 and 1200 TPA), an increasing trend in the b parameter was evident throughout the study period. However, for lower densities (200, 450, and 700 TPA), the parameter did not follow a consistent upward trajectory (Figure 2.5).

The average three-parameters Weibull estimates (Table 2.32) were used to create figures 2.7 – 2.11 to represent the density of the distribution for the five PLTPA, MAN across over all ages.

We can observe that, for all PLTPA values and across all ages, the curves for the MAX management shift to the right. This behavior occurs because the start of the curves is directly related to the a parameter, the average of this parameter in MAX management is higher than in INT management.

For PLTPA 200, there is little visual difference at ages of 8, 10, 12, 15, and 18. However, at ages 6 and 21, a more noticeable difference between the MAN can be observed (Figure 2.7). For PLTPA 450, the difference in the curve is more easily observed at ages 6, 10, 12, 15, 18, and 21, but not at age 8 (Figure 2.8). For PLTPA 700, the difference is visible at ages 8, 10, 12, 15, and 21 (Figure 2.9). A similar result is seen for PLTPA 950, with more evident differences at ages 6, 10, 12, 15, 18, and 21 (Figure 2.10).

In PLTPA 1200, a difference in the curve between MAX and INT management is noticeable at all ages. Across all five PLTPA levels, the distributions flattened over time for both MAN. The MAX management showed slightly more flattened compared to INT management. This indicates that MAX management had a greater concentration of TPA in larger DBH classes at certain years and the PLTPA levels, which influences the c parameter as well as the b parameter, which is related to the distribution range (Figure 2.11).

The average of a parameter showed (Figure 2.12) a consistent pattern over the years for all five PLTPA. This parameter was the most influenced by the two levels of MAN, as expected, since the MAX management presents higher values for the minimum DBH. Lower a parameter values were observed in younger stands, and higher values were observed in older stands; this trend was consistent across all PLTPA. Stands with lower PLTPA presented higher values for the a parameter, while stands with higher PLTPA had lower values. The a parameter under the MAX management was higher at all ages and PLTPA when compared to the INT management. A decrease of TPA by mortality is a factor with potential to increase this parameter; however, the relationship with age is more realistic, as over time, an increase in DBH is expected and, consequently, an increase in the a parameter, since it is directly correlated with the minimum DBH. On the other hand, the analysis of the b parameter indicates that it is more influenced by TPA than by the MAN level (Figure 2.13). As mortality occurs over the years, an increase in the b value is observed for higher PLTPA, such as 700, 950, and 1200. In contrast, at lower PLTPA, such as 200 and 450, the b parameter did not show significant difference between the two MAN levels, suggesting that MAN does not have a significant effect on this parameter under these conditions. Furthermore, mortality in these lower PLTPA plots is lower over time, which prevents drastic changes in density that could affect the b parameter. The opposite can be observed in higher PLTPA, with higher percentage of mortality over time, and more difference in b parameter.

Similar to Bailey et al. (1989); Carlson et al. (2008), the c parameters showed a decreasing trend over time, and this behavior was for all PLTPA (Figure 2.14). The c parameter was shown to be affected by the MAN level; however, the difference between the values of the two MAN levels were small. The MAX management presented the lowest values for this parameter, indicating that the curve is flatter. This flattening may be related to mortality or the presence of trees with larger diameters. PLTPA did not appear to be the main factor responsible for this difference in parameters. It was observed that the difference between the c values remains constant over the years, indicating that, even with mortality, this parameter is not significantly affected. This reinforces the idea that the observed difference between the two parameter values were related to the level of silvicultural management.

Two sample t-test - one-tailed

The results of the two-sample t-test with one-tailed at the $\alpha = 0.05$ significance level can be found in figures 2.15 - 2.29. At age 6, for all PLTPA, the p-values indicate no evidence that the mean of basal area per acre for the MAX management is greater than that INT management. On the other hand, at age 8, the t-test results showed that in four out of five densities (450, 700, 950, and 1200), the mean of the MAX management is significantly higher than that of the INT management, with p-values less than $\alpha < 0.05$. A similar result was observed at age 10; however, in this case, all densities analyzed indicate that the mean of the MAX silvicultural management is higher than that of the INT management, also with p-values less than $\alpha < 0.05$

At age 12, the MAX management showed a higher mean than the INT management across all PLTPA, with p-values below $\alpha < 0.05$. At age 15, for PLTPA 200, 700, 950, and 1200, the MAX management also showed a higher mean basal area compared to the INT management. Only in PLTPA 450 was no significant difference observed between the means of the two groups. At age 18, only PLTPA 450 and 1200 indicated that the mean basal area for the MAX management is significantly higher than that of the INT management ($\alpha < 0.05$). For the remaining PLTPA, there is no indication that the MAX management mean is higher than the INT management.

Finally, at age 21, none of the PLTPA analyzed showed a significant difference, with p-values greater than $\alpha = 0.05$, indicating no evidence that the MAX management has a higher mean than the INT management. For PLTPA 200, the null hypothesis was rejected in favor of the alternative hypothesis, indicating that the mean basal area per acre under the silvicultural management MAX was significantly greater than the INT management at ages 10, 12, and 15. For the PLTPA of 450, the null hypothesis was also rejected at ages 8, 10, 12, and 18, because the MAX management resulted in a higher mean basal area per acre compared to the INT management. At 700 PLTPA, this pattern persisted, with statistically significant differences observed at ages 8, 10, 12, and 15 in favor alternative hypotheses. Similar results were found for PLTPA 950 and 1200 at the same ages (Table 2.33).

Goodness-of-fit test

Error index

Although the error index is used to evaluate the goodness-of-fit of a model, in this study it was applied to compare the performance of the INT and MAX management datasets using a common model. The MAX management showed the lowest error index for all five PLTPA levels at ages 10, 12, and 15. At ages 8 and 18, the INT management had the lowest error index for the 200 PLTPA, whereas the MAX management exhibited lower values for the other densities. At age 6, the INT management presented the lowest error index for the 450 PLTPA, while the MAX management showed lower values for 200, 700, 950, and 1200 PLTPA. Finally, at age 21, the MAX management achieved the lowest error index for most densities, except for 700 PLTPA (Table 2.35).

RMSE

As mentioned previously, the RMSE analysis is used to test the precision of the Weibull estimated PDF from different models. However, in this study, it was used as a tool to assess the precision of the Weibull estimates obtained from the same model but using two different datasets — INT and MAX — to evaluate the adjustment for each management regime. The RMSE results showed a pattern similar to that observed with the error index. The MAX management presented the lowest RMSE values for all PLTPA densities at ages 10, 15, and 21. As also observed with the error index, the INT management showed the lowest RMSE for the 200 PLTPA at ages 8 and 18. At age 6, the INT management had the lowest RMSE at 450 PLTPA, whereas at age 12, its lowest value occurred at 700 PLTPA (Table 2.35).

2.6 Conclusion

The work presented here shows that diameter distribution modeling for loblolly pine plantations in the WGCDS is influenced by the two levels of MAN and TPA. The location parameter of the Weibull distribution is the most affected, and results showed that this parameter exhibits a relatively larger difference between MAN compared to the shape parameter, which is also influenced by the MAN level, but with less noticeable differences. Mortality was identified as the main reason for the observed difference in the scale parameter between the two MAN levels.

It is important to emphasize that the percentile-based approach is highly correlated with DBH, as it makes predictions based on DBH percentiles. It is also worth noting that higher concentrations of fertilization, vegetation control contribute to increased diameter growth. This explains the results between the two MAN levels, considering that the MAX management achieves higher DBH values.

The MAX management presented higher estimates of TPA in diameter classes for both non-sawtimber and sawtimber, confirming that this regime results in greater volume within commercially relevant diameter classes. Additionally, MAX showed higher estimates of basal area at mid-rotation compared to the INT management. However, a financial and cost analysis should be conducted to determine whether the MAX of management is economically viable to apply, despite its demonstrated optimization of TPA in the target diameter classes.

Overall, based on the error index and RMSE, the MAX management achieved lower values, indicating that the estimated Weibull three-parameter for this regime are better adjusted to the observed data, due to the higher concentration of TPA in the larger DBH classes.

2.7 References

Albaugh, T., Allen, H. L., Fox, T. R., Carlson, C. A., and Rubilar, R. A. (2009). Opportunities for fertilization of loblolly pine in the sandhills of the southeastern united states. *Southern Journal of Applied Forestry*, 33(3):129–136.

Albaugh, T. J., Fox, T. R., Cook, R. L., Raymond, J. E., Rubilar, R. A., and Campoe, O. C. (2018). Forest fertilizer applications in the southeastern united states from 1969 to 2016. *Forest Science*, 65(3):355–362.

Albaugh, T. J., Fox, T. R., Rubilar, R. A., Cook, R. L., Amateis, R. L., and Burkhart, H. E. (2017). Post-thinning density and fertilization affect pinus taeda stand and individual tree growth. *Forest Ecology and Management*, 396:207–216.

Alkan, O., Cao, Q. V., and Özçelik, R. (2025). Characterizing diameter distribution of pinus nigra stands in türkiye with a weibull distribution. *Canadian Journal of Forest Research*, 55:1–12.

Allen, H. (1987). Nutrient amendment, stand productivity, and environmental impact. *J. For*, 85:37–46.

Allen, H. L., Duzan, D., Ballard, R., and Gessel, S. (1983). Nutritional management of loblolly pine stands: A status report of the north carolina state forest fertilization cooperative. *Forest site and continuous productivity*, pages 379–384.

Antony, F., Schimleck, L. R., Jordan, L., Daniels, R. F., and Clark, A. (2012). Modeling the effect of initial planting density on within tree variation of stiffness in loblolly pine. *Annals of forest science*, 69:641–650.

Bailey, R. L., Burgan, T. M., and Jokela, E. J. (1989). Fertilized midrotation-aged slash pine plantations—stand structure and yield prediction models. *Southern Journal of Applied Forestry*, 13(2):76–80.

Beasley, T. M. (2008). Seemingly unrelated regression (sur) models as a solution to path analytic models with correlated errors. *General Linear Model Journal*, 34.

Borders, B. E. (1989). Systems of equations in forest stand modeling. *Forest Science*, 35(2):548–556.

Borders, B. E., Souter, R. A., Bailey, R. L., and Ware, K. D. (1987). Percentile-based distributions characterize forest stand tables. *Forest Science*, 33(2):570–576.

Burk, T. E. and Burkhart, H. E. (1984). Diameter distributions and yields of natural stands of loblolly pine. *Virginia Tech. Division of Forestry and Wildlife Resources.*

Burkhart, H. E., Avery, T. E., and Bullock, B. P. (2018). *Forest measurements.* Sixth Ed. Long Grove, IL: Waveland Press, 343-376 p.

Cao, Q. and Burkhart, H. (1984). A segmented distribution approach for modeling diameter frequency data. *Forest Science*, 30:129–137.

Cao, Q. V. (2004). Predicting parameters of a weibull function for modeling diameter distribution. *Forest Science*, 50(5):682–685.

Cardoso, D. J., Lacerda, A. E. B., Rosot, M. A. D., Garrastazú, M. C., and Lima, R. T. (2013). Influence of spacing regimes on the development of loblolly pine (pinus taeda l.) in southern brazil. *Forest Ecology and management*, 310:761–769.

Carlson, C. A., Burkhart, H. E., Allen, H. L., and Fox, T. R. (2008). Absolute and relative changes in tree growth rates and changes to the stand diameter distribution of pinus taeda as a result of midrotation fertilizer applications. *Canadian Journal of Forest Research*, 38(7):2063–2071.

Consalter, R., Motta, A. C. V., Barbosa, J. Z., Vezzani, F. M., Rubilar, R. A., Prior, S. A., Nisgoski, S., and Bassaco, M. V. M. (2021). Fertilization of pinus taeda l. on an acidic oxisol in southern brazil: growth, litter accumulation, and root exploration. *European Journal of Forest Research*, 140(5):1095–1112.

Cooray, K. (2015). A study of moments and likelihood estimators of the odd weibull distribution. *Statistical Methodology*, 26:72–83.

de Souza Kulmann, M. S., Deliberali, I., Schumacher, M. V., Stahl, J., Figura, M. A., Ludvichak, A. A., and Stape, J. L. (2023). Can fertilization and stand uniformity affect the growth and biomass production in a pinus taeda plantation in southern brazil. *Forest Ecology and Management*, 541:121075.

Erişoğlu, Ü., Erisoglu, M., and Servi, T. (2020). Increasing the efficiency of percentile parameter estimation method for weibull distribution. *Adıyaman University Journal of Science*, 10(2):483–493.

Ferreira, G. W., Rau, B. M., and Aubrey, D. P. (2020). Herbicide, fertilization, and planting density effects on intensively managed loblolly pine early stand development. *Forest Ecology and Management*, 472:118206.

Fonseca, T. F., Marques, C. P., and Parresol, B. R. (2009). Describing maritime pine diameter distributions with johnson's sb distribution using a new all-parameter recovery approach. *Forest Science*, 55(4):367–373.

Gu, J., Kong, X., Guo, J., Qi, H., and Wang, Z. (2024). Parameter estimation of three-parameter weibull distribution by hybrid gray genetic algorithm with modified maximum likelihood method with small samples. *Journal of Mechanical Science and Technology*, 38(10):5363–5379.

Gyawali, N. and Burkhart, H. E. (2015). General response functions to silvicultural treatments in loblolly pine plantations. *Canadian Journal of Forest Research*, 45(3):252–265.

Haywood, J. D. (2005). Influence of precommercial thinning and fertilization on total stem volume and lower stem form of loblolly pine. *Southern Journal of Applied Forestry*, 29(4):215–220.

Haywood, J. D., Goelz, J. C., Sayer, M. A. S., and Tiarks, A. E. (2003). Influence of fertilization, weed control, and pine litter on loblolly pine growth and productivity and understory plant development through 12 growing seasons. *Canadian Journal of Forest Research*, 33(10):1974–1982.

Hirose, H. (1991). Percentile point estimation in the three parameter weibull distribution by the extended maximum likelihood estimate. *Computational statistics & data analysis*, 11(3):309–331.

Hogg, R. V., McKean, J., and Craig, A. (2019). *Introduction to Mathematical Statistics*. Eighth Ed. Boston, MA: Pearson, 51 p.

Hyink, D. M. and Moser, J. W. (1983). A generalized framework for projecting forest yield and stand structure using diameter distributions. *Forest Science*, 29(1):85–95.

Jiang, L. and Brooks, J. R. (2009a). Predicting diameter distributions for young longleaf pine plantations in southwest georgia. *Southern Journal of Applied Forestry*, 33(1):25–28.

Jiang, L. and Brooks, J. R. (2009b). Predicting diameter distributions for young longleaf pine plantations in southwest georgia. *Southern Journal of Applied Forestry*, 33(1):25–28.

Jokela, E., Harding, R., and Nowak, C. (1989). Long-term effects of fertilization on stem form, growth relations, and yield estimates of slash pine. *Forest science*, 35(3):832–842.

Knowe, S. A., Ahrens, G. R., and DeBell, D. S. (1997). Comparison of diameter-distribution-prediction, stand-table-projection, and individual-tree-growth modeling approaches for young red alder plantations. *Forest Ecology and Management*, 98(1):49–60.

Liu, C., Zhang, S., Lei, Y., Newton, P. F., and Zhang, L. (2004). Evaluation of three methods for predicting diameter distributions of black spruce (picea mariana) plantations in central canada. *Canadian Journal of Forest Research*, 34(12):2424–2432.

Mahdi, S. and Ashkar, F. (2004). Exploring generalized probability weighted moments, generalized moments and maximum likelihood estimating methods in two-parameter weibull model. *Journal of Hydrology*, 285(1-4):62–75.

Maltamo, M., Kangas, A., Uuttera, J., Torniainen, T., and Saramäki, J. (2000). Comparison of percentile based prediction methods and the weibull distribution in describing the diameter distribution of heterogeneous scots pine stands. *Forest Ecology and Management*, 133(3):263–274.

Matziris, D. I. and Zobel, B. J. (1976). Effect of fertilization on growth and quality characteristics of loblolly pine. *Forest Ecology and Management*, 1:21–30.

Mehtätalo, L. (2004). An algorithm for ensuring compatibility between estimated percentiles of diameter distribution and measured stand variables. *Forest Science*, 50(1):20–32.

Mendenhall, W., Sincich, T., and Boudreau, N. S. (2003). *A second course in statistics: Regression analysis*, volume 6. Prentice Hall Upper Saddle River, NJ.

Merganič, J. and Sterba, H. (2006). Characterisation of diameter distribution using the weibull function: method of moments. *European Journal of Forest Research*, 125:427–439.

Murthy, D. P., Xie, M., and Jiang, R. (2004). *Weibull models*. Hoboken, NJ: John Wiley 'I&' Sons , 58-101 p.

Oliveira, R. and Teixeira-Pinto, A. (2015). Analyzing multiple outcomes: is it really worth the use of multivariate linear regression? = *Journal of Biometrics Biostatistics*.

Poudel, K. P. and Cao, Q. V. (2013). Evaluation of methods to predict weibull parameters for characterizing diameter distributions. *Forest Science*, 59(2):243–252.

Reynolds, M. R., Burk, T. E., and Huang, W.-C. (1988). Goodness-of-fit tests and model selection procedures for diameter distribution models. *Forest science*, 34(2):373–399.

Rijal, B. and Sharma, M. (2023). Modelling diameter at breast height distribution of jack pine and black spruce natural stands in eastern canada. *Canadian Journal of Forest Research*, 54(5):554–568.

Roth, B. E., Li, X., Huber, D. A., and Peter, G. F. (2007). Effects of management intensity, genetics and planting density on wood stiffness in a plantation of juvenile loblolly pine in the southeastern usa. *Forest Ecology and Management*, 246(2-3):155–162.

Sandoval, S., Cancino, J., Rubilar, R., Esquivel, E., Acuna, E., Munoz, F., and Espinosa, M. (2012). Probability distributions in high-density dendroenergy plantations. *Forest Science*, 58(6):663–672.

Shafii, B., Moore, J. A., and Newberry, J. D. (1990). Individual-tree diameter growth models for quantifying within-stand response to nitrogen fertilization. *Canadian Journal of Forest Research*, 20(8):1149–1155.

Siipilehto, J. and Mehtätalo, L. (2013). Parameter recovery vs. parameter prediction for the weibull distribution validated for scots pine stands in finland. *Finnish Society of Forest Science*.

Teimouri, M., Hoseini, S. M., and Nadarajah, S. (2013). Comparison of estimation methods for the weibull distribution. *Statistics*, 47(1):93–109.

Weiskittel, A. R., Hann, D. W., Kershaw Jr, J. A., and Vanclay, J. K. (2011). *Forest growth and yield modeling*. Hoboken, NJ: John Wiley 'I&' Sons, 169-172 p.

Will, R. E., Narahari, N. V., Shiver, B. D., and Teskey, R. O. (2005). Effects of planting density on canopy dynamics and stem growth for intensively managed loblolly pine stands. *Forest Ecology and Management*, 205(1-3):29–41.

Windsor, C. L. and Reines, M. (1973). Diameter growth in loblolly pine after fertilization. *Journal of Forestry*, 71(10):659–661.

Zanakis, S. H. (1979). A simulation study of some simple estimators for the three-parameter weibull distribution. *Journal of Statistical Computation and Simulation*, 9(2):101–116.

Zarnoch, S. J. and Dell, T. R. (1985). An evaluation of percentile and maximum likelihood estimators of weibull parameters. *Forest Science*, 31(1):260–268.

Zellner, A. (1962). An efficient method of estimating seemingly unrelated regressions and tests for aggregation bias. *Journal of the American statistical Association*, 57(298):348–368.

2.8 Tables and Figures

Table 2.1: Measurement plot data removed from analysis due to certain factors, such as self-thinning and other operational constraints (i.e., presence of overhead power lines)

AGE	PLTPA	MAN	INST
6	All	INT/MAX	1, 2, 3, 4, 5, 6, 7, 8, 9, 10, 11, 12, 13
8	200	INT	5
	450	MAX	5
10	200	INT	5
	450	INT	9
	450	MAX	5, 9
12	200	INT	5
	450	INT	9
	450	MAX	5, 9
15	450	INT	9, 11, 13
	450	MAX	5, 9, 11
	700	INT/MAX	11, 13
	950	INT/MAX	11
	1200	INT/MAX	11
18	200	INT	5, 6, 11, 18
	200	MAX	6, 11, 18
	450	INT	6, 9, 11, 13, 18
	450	MAX	3, 5, 6, 9, 11, 18
	700	INT/MAX	6, 11, 13, 18
	950	INT/MAX	6, 11, 18
	1200	INT/MAX	6, 11, 18
21	200	INT/MAX	3, 5, 6, 11, 14, 15, 16, 17, 18
	450	INT	3, 5, 6, 9, 11, 13, 14, 15, 16, 17, 18
	450	MAX	3, 5, 6, 9, 11, 14, 15, 16, 17, 18
	700	INT/MAX	3, 5, 6, 11, 13, 14, 15, 16, 17, 18
	950	INT/MAX	3, 5, 6, 11, 14, 15, 16, 17, 18
	1200	INT/MAX	3, 5, 6, 11, 14, 15, 16, 17, 18

Table 2.2: Parameter estimates from the ANOVA model, 6 year basal area per acre.

	Estimate	Std. Error	t value	Pr(> $\|t\|$)
(Intercept)	29.5420	5.8413	5.0574	0.0000
MANMAX	9.0160	8.2609	1.0914	0.2818
PLTPA450	22.8780	8.2609	2.7694	0.0086
PLTPA700	42.1060	8.2609	5.0970	0.0000
PLTPA950	50.3540	8.2609	6.0955	0.0000
PLTPA1200	61.1060	8.2609	7.3971	0.0000
MANMAX:PLTPA450	5.5677	11.6826	0.4766	0.6363
MANMAX:PLTPA700	8.5753	11.6826	0.7340	0.4673
MANMAX:PLTPA950	8.5695	11.6826	0.7335	0.4676
MANMAX:PLTPA1200	6.7087	11.6826	0.5742	0.5691

Table 2.3: Parameter estimates from the ANOVA model, 8 year basal area per acre.

	Estimate	Std. Error	t value	Pr(> $\|t\|$)
(Intercept)	58.3497	4.7692	12.2346	0.0000
MANMAX	13.2202	6.1920	2.1351	0.0342
PLTPA450	34.6154	6.1920	5.5904	0.0000
PLTPA700	54.5737	6.1920	8.8136	0.0000
PLTPA950	64.1654	6.1920	10.3627	0.0000
PLTPA1200	74.5037	6.1920	12.0323	0.0000
MANMAX:PLTPA450	4.9497	8.7572	0.5652	0.5727
MANMAX:PLTPA700	3.5800	8.6938	0.4118	0.6810
MANMAX:PLTPA950	5.4068	8.6938	0.6219	0.5349
MANMAX:PLTPA1200	4.8611	8.6938	0.5592	0.5768

Table 2.4: Parameter estimates from the ANOVA model, 10 year basal area per acre.

	Estimate	Std. Error	t value	Pr(> $\|t\|$)
(Intercept)	78.1160	5.6104	13.9236	0.0000
MANMAX	12.6134	6.2292	2.0249	0.0445
PLTPA450	37.1112	6.3170	5.8748	0.0000
PLTPA700	50.2238	6.2292	8.0627	0.0000
PLTPA950	65.3282	6.2292	10.4875	0.0000
PLTPA1200	74.8766	6.2292	12.0203	0.0000
MANMAX:PLTPA450	0.3937	8.9429	0.0440	0.9649
MANMAX:PLTPA700	4.2336	8.7459	0.4841	0.6290
MANMAX:PLTPA950	3.1550	8.7459	0.3607	0.7188
MANMAX:PLTPA1200	2.9434	8.7459	0.3365	0.7369

Table 2.5: Parameter estimates from the ANOVA model, 12 year basal area per acre.

	Estimate	Std. Error	t value	Pr(> $\|t\|$)
(Intercept)	100.2952	6.3609	15.7675	0.0000
MANMAX	10.8184	6.9612	1.5541	0.1221
PLTPA450	37.5324	7.0594	5.3166	0.0000
PLTPA700	49.2023	6.9612	7.0680	0.0000
PLTPA950	66.7506	6.9612	9.5889	0.0000
PLTPA1200	72.7690	6.9612	10.4535	0.0000
MANMAX:PLTPA450	-1.3375	9.9939	-0.1338	0.8937
MANMAX:PLTPA700	4.8960	9.7737	0.5009	0.6171
MANMAX:PLTPA950	-0.6395	9.7737	-0.0654	0.9479
MANMAX:PLTPA1200	-0.7003	9.7737	-0.0717	0.9430

Table 2.6: Parameter estimates from the ANOVA model, 15 year basal area per acre.

	Estimate	Std. Error	t value	Pr(> $\|t\|$)
(Intercept)	129.0871	9.5444	13.5249	0.0000
MANMAX	11.1365	8.8207	1.2625	0.2087
PLTPA450	36.0338	9.1015	3.9591	0.0001
PLTPA700	46.6113	8.9526	5.2065	0.0000
PLTPA950	65.2749	8.8207	7.4002	0.0000
PLTPA1200	67.5861	8.8207	7.6623	0.0000
MANMAX:PLTPA450	-7.1007	12.7787	-0.5557	0.5793
MANMAX:PLTPA700	-2.5386	12.5679	-0.2020	0.8402
MANMAX:PLTPA950	-11.9939	12.3789	-0.9689	0.3341
MANMAX:PLTPA1200	-14.2693	12.3789	-1.1527	0.2509

Table 2.7: Parameter estimates from the ANOVA model, 18 year basal area per acre.

	Estimate	Std. Error	t value	Pr(> $\|t\|$)
(Intercept)	148.9413	9.1324	16.3091	0.0000
MANMAX	6.3245	8.6929	0.7275	0.4682
PLTPA450	40.5014	9.0101	4.4951	0.0000
PLTPA700	43.7186	8.8406	4.9452	0.0000
PLTPA950	55.1228	8.6929	6.3411	0.0000
PLTPA1200	52.5261	8.6929	6.0424	0.0000
MANMAX:PLTPA450	-0.1234	12.7774	-0.0097	0.9923
MANMAX:PLTPA700	-9.7917	12.3985	-0.7898	0.4311
MANMAX:PLTPA950	-14.9872	12.1865	-1.2298	0.2210
MANMAX:PLTPA1200	-8.5263	12.1865	-0.6997	0.4854

Table 2.8: Parameter estimates from the ANOVA model, 21 year basal area per acre.

	Estimate	Std. Error	t value	Pr(> $\|t\|$)
(Intercept)	168.4277	19.0625	8.8355	0.0000
MANMAX	-10.5290	17.0049	-0.6192	0.5377
PLTPA450	34.3372	18.2205	1.8845	0.0635
PLTPA700	27.7006	17.5365	1.5796	0.1185
PLTPA950	22.0789	17.0049	1.2984	0.1982
PLTPA1200	20.8211	17.0049	1.2244	0.2247
MANMAX:PLTPA450	-5.3916	25.2625	-0.2134	0.8316
MANMAX:PLTPA700	-10.5555	24.7887	-0.4258	0.6715
MANMAX:PLTPA950	-5.4029	24.0486	-0.2247	0.8229
MANMAX:PLTPA1200	-13.0475	24.0486	-0.5425	0.5891

Table 2.9: Parameter estimates from the ANOVA model, 6 year quadratic mean diameter.

	Estimate	Std. Error	t value	Pr(> $\|t\|$)
(Intercept)	5.2664	0.1572	33.5062	0.0000
MANMAX	0.8000	0.2223	3.5991	0.0009
PLTPA450	-0.5985	0.2223	-2.6925	0.0104
PLTPA700	-0.8923	0.2223	-4.0142	0.0003
PLTPA950	-1.1852	0.2223	-5.3320	0.0000
PLTPA1200	-1.4145	0.2223	-6.3637	0.0000
MANMAX:PLTPA450	-0.1422	0.3144	-0.4525	0.6534
MANMAX:PLTPA700	-0.1832	0.3144	-0.5828	0.5634
MANMAX:PLTPA950	-0.2373	0.3144	-0.7548	0.4549
MANMAX:PLTPA1200	-0.3790	0.3144	-1.2056	0.2352

Table 2.10: Parameter estimates from the ANOVA model, 8 year quadratic mean diameter.

	Estimate	Std. Error	t value	Pr(> $\|t\|$)
(Intercept)	7.5007	0.1230	60.9765	0.0000
MANMAX	0.8237	0.1715	4.8019	0.0000
PLTPA450	-1.1603	0.1715	-6.7647	0.0000
PLTPA700	-1.9522	0.1715	-11.3810	0.0000
PLTPA950	-2.5120	0.1715	-14.6450	0.0000
PLTPA1200	-2.8820	0.1715	-16.8017	0.0000
MANMAX:PLTPA450	-0.2089	0.2426	-0.8612	0.3904
MANMAX:PLTPA700	-0.2477	0.2408	-1.0284	0.3052
MANMAX:PLTPA950	-0.3067	0.2408	-1.2736	0.2046
MANMAX:PLTPA1200	-0.3250	0.2408	-1.3495	0.1790

Table 2.11: Parameter estimates from the ANOVA model, 10 year quadratic mean diameter.

	Estimate	Std. Error	t value	$Pr(>\|t\|)$
(Intercept)	8.7098	0.1263	68.9395	0.0000
MANMAX	0.7337	0.1762	4.1647	0.0001
PLTPA450	-1.6230	0.1787	-9.0838	0.0000
PLTPA700	-2.5880	0.1762	-14.6903	0.0000
PLTPA950	-3.2208	0.1762	-18.2821	0.0000
PLTPA1200	-3.6474	0.1762	-20.7035	0.0000
MANMAX:PLTPA450	-0.2181	0.2529	-0.8622	0.3898
MANMAX:PLTPA700	-0.2212	0.2474	-0.8943	0.3725
MANMAX:PLTPA950	-0.2679	0.2474	-1.0830	0.2804
MANMAX:PLTPA1200	-0.2582	0.2474	-1.0439	0.2981

Table 2.12: Parameter estimates from the ANOVA model, 12 year quadratic mean diameter.

	Estimate	Std. Error	t value	$Pr(>\|t\|)$
(Intercept)	9.9233	0.1661	59.7594	0.0000
MANMAX	0.5913	0.1916	3.0855	0.0024
PLTPA450	-2.0429	0.1943	-10.5120	0.0000
PLTPA700	-3.1126	0.1916	-16.2418	0.0000
PLTPA950	-3.8626	0.1916	-20.1558	0.0000
PLTPA1200	-4.3578	0.1916	-22.7395	0.0000
MANMAX:PLTPA450	-0.1562	0.2751	-0.5676	0.5711
MANMAX:PLTPA700	-0.1341	0.2691	-0.4986	0.6188
MANMAX:PLTPA950	-0.1285	0.2691	-0.4775	0.6336
MANMAX:PLTPA1200	-0.0838	0.2691	-0.3116	0.7558

Table 2.13: Parameter estimates from the ANOVA model, 15 year quadratic mean diameter.

	Estimate	Std. Error	t value	$Pr(>\|t\|)$
(Intercept)	11.4340	0.2373	48.1869	0.0000
MANMAX	0.6029	0.2516	2.3962	0.0178
PLTPA450	-2.4992	0.2596	-9.6270	0.0000
PLTPA700	-3.7694	0.2554	-14.7615	0.0000
PLTPA950	-4.4911	0.2516	-17.8508	0.0000
PLTPA1200	-5.0098	0.2516	-19.9126	0.0000
MANMAX:PLTPA450	-0.2016	0.3645	-0.5532	0.5809
MANMAX:PLTPA700	-0.0187	0.3585	-0.0522	0.9584
MANMAX:PLTPA950	-0.0391	0.3531	-0.1107	0.9120
MANMAX:PLTPA1200	0.1856	0.3531	0.5257	0.5999

Table 2.14: Parameter estimates from the ANOVA model, 18 year quadratic mean diameter.

	Estimate	Std. Error	t value	Pr(> |t|)
(Intercept)	12.5497	0.3163	39.6728	0.0000
MANMAX	0.5494	0.3123	1.7594	0.0809
PLTPA450	-2.7969	0.3237	-8.6409	0.0000
PLTPA700	-4.0564	0.3176	-12.7727	0.0000
PLTPA950	-4.7965	0.3123	-15.3597	0.0000
PLTPA1200	-5.1889	0.3123	-16.6161	0.0000
MANMAX:PLTPA450	0.0632	0.4590	0.1377	0.8907
MANMAX:PLTPA700	0.0934	0.4454	0.2096	0.8343
MANMAX:PLTPA950	0.1375	0.4378	0.3142	0.7539
MANMAX:PLTPA1200	0.2696	0.4378	0.6159	0.5390

Table 2.15: Parameter estimates from the ANOVA model, 21 year quadratic mean diameter.

	Estimate	Std. Error	t value	Pr(> |t|)
(Intercept)	13.8537	0.2869	48.2851	0.0000
MANMAX	0.6991	0.3614	1.9343	0.0569
PLTPA450	-3.0522	0.3871	-7.8858	0.0000
PLTPA700	-4.1856	0.3727	-11.2313	0.0000
PLTPA950	-5.0629	0.3614	-14.0084	0.0000
PLTPA1200	-5.2558	0.3614	-14.5420	0.0000
MANMAX:PLTPA450	-0.0166	0.5369	-0.0309	0.9754
MANMAX:PLTPA700	-0.0112	0.5269	-0.0213	0.9831
MANMAX:PLTPA950	0.0346	0.5111	0.0676	0.9463
MANMAX:PLTPA1200	0.1836	0.5111	0.3591	0.7205

Table 2.16: Parameter estimates from the ANOVA model, 6 years dominant tree height.

	Estimate	Std. Error	t value	Pr(> |t|)
(Intercept)	22.2811	1.4279	15.6045	0.0000
MANMAX	1.5500	1.2410	1.2490	0.2191
PLTPA450	0.8260	1.2410	0.6656	0.5096
PLTPA700	2.4320	1.2410	1.9598	0.0572
PLTPA950	1.0840	1.2410	0.8735	0.3877
PLTPA1200	1.6580	1.2410	1.3361	0.1893
MANMAX:PLTPA450	-0.3520	1.7550	-0.2006	0.8421
MANMAX:PLTPA700	-1.1460	1.7550	-0.6530	0.5176
MANMAX:PLTPA950	0.1800	1.7550	0.1026	0.9188
MANMAX:PLTPA1200	-0.5840	1.7550	-0.3328	0.7411

Table 2.17: Parameter estimates from the ANOVA model, 8 years dominant tree height.

	Estimate	Std. Error	t value	$Pr(>\|t\|)$
(Intercept)	33.2141	1.3015	25.5203	0.0000
MANMAX	0.3563	1.0129	0.3517	0.7255
PLTPA450	1.1841	1.0129	1.1689	0.2441
PLTPA700	1.0863	1.0129	1.0724	0.2851
PLTPA950	0.6713	1.0129	0.6627	0.5084
PLTPA1200	0.1063	1.0129	0.1049	0.9166
MANMAX:PLTPA450	0.7191	1.4326	0.5019	0.6164
MANMAX:PLTPA700	1.0437	1.4222	0.7339	0.4641
MANMAX:PLTPA950	0.6515	1.4222	0.4581	0.6475
MANMAX:PLTPA1200	1.5320	1.4222	1.0772	0.2829

Table 2.18: Parameter estimates from the ANOVA model, 10 years dominant tree height.

	Estimate	Std. Error	t value	$Pr(>\|t\|)$
(Intercept)	40.5678	1.3169	30.8066	0.0000
MANMAX	1.2455	1.3128	0.9487	0.3441
PLTPA450	0.6335	1.3313	0.4759	0.6348
PLTPA700	0.4122	1.3128	0.3140	0.7539
PLTPA950	-0.4311	1.3128	-0.3284	0.7430
PLTPA1200	-0.8128	1.3128	-0.6191	0.5367
MANMAX:PLTPA450	-0.0628	1.8848	-0.0333	0.9735
MANMAX:PLTPA700	0.3711	1.8432	0.2013	0.8407
MANMAX:PLTPA950	-0.0261	1.8432	-0.0142	0.9887
MANMAX:PLTPA1200	0.5878	1.8432	0.3189	0.7502

Table 2.19: Parameter estimates from the ANOVA model, 12 years dominant tree height.

	Estimate	Std. Error	t value	$Pr(>\|t\|)$
(Intercept)	46.8928	1.3859	33.8345	0.0000
MANMAX	1.1723	1.3913	0.8426	0.4007
PLTPA450	-0.1888	1.4110	-0.1338	0.8937
PLTPA700	0.3518	1.3913	0.2528	0.8007
PLTPA950	-0.5982	1.3913	-0.4300	0.6678
PLTPA1200	-1.2610	1.3913	-0.9063	0.3661
MANMAX:PLTPA450	0.7383	1.9975	0.3696	0.7122
MANMAX:PLTPA700	0.0466	1.9535	0.0238	0.9810
MANMAX:PLTPA950	0.0577	1.9535	0.0295	0.9765
MANMAX:PLTPA1200	0.6310	1.9535	0.3230	0.7471

Table 2.20: Parameter estimates from the ANOVA model, 15 years dominant tree height.

	Estimate	Std. Error	t value	Pr(> $\|t\|$)
(Intercept)	56.5196	1.5397	36.7071	0.0000
MANMAX	0.6292	1.8952	0.3320	0.7404
PLTPA450	-0.4491	1.9555	-0.2297	0.8187
PLTPA700	-0.1369	1.9235	-0.0712	0.9434
PLTPA950	-1.1114	1.8952	-0.5864	0.5585
PLTPA1200	-1.9020	1.8952	-1.0036	0.3172
MANMAX:PLTPA450	1.1388	2.7456	0.4148	0.6789
MANMAX:PLTPA700	0.9896	2.7003	0.3665	0.7145
MANMAX:PLTPA950	1.2885	2.6597	0.4844	0.6288
MANMAX:PLTPA1200	1.7361	2.6597	0.6528	0.5149

Table 2.21: Parameter estimates from the ANOVA model, 18 years dominant tree height.

	Estimate	Std. Error	t value	Pr(> $\|t\|$)
(Intercept)	68.5884	1.7836	38.4540	0.0000
MANMAX	-0.7918	2.4101	-0.3285	0.7430
PLTPA450	-0.5818	2.4981	-0.2329	0.8162
PLTPA700	-1.7329	2.4512	-0.7069	0.4809
PLTPA950	-2.6691	2.4101	-1.1075	0.2701
PLTPA1200	-2.5011	2.4101	-1.0378	0.3013
MANMAX:PLTPA450	3.3530	3.5425	0.9465	0.3457
MANMAX:PLTPA700	1.2668	3.4376	0.3685	0.7131
MANMAX:PLTPA950	2.6738	3.3789	0.7913	0.4302
MANMAX:PLTPA1200	2.3165	3.3789	0.6856	0.4942

Table 2.22: Parameter estimates from the ANOVA model, 21 years dominant tree height.

	Estimate	Std. Error	t value	Pr(> $\|t\|$)
(Intercept)	77.9039	2.2041	35.3456	0.0000
MANMAX	-0.9144	1.9910	-0.4593	0.6474
PLTPA450	0.0159	2.1333	0.0075	0.9941
PLTPA700	0.4151	2.0532	0.2022	0.8404
PLTPA950	-2.0133	1.9910	-1.0112	0.3152
PLTPA1200	-1.3044	1.9910	-0.6552	0.5144
MANMAX:PLTPA450	1.4386	2.9578	0.4864	0.6281
MANMAX:PLTPA700	1.3382	2.9023	0.4611	0.6461
MANMAX:PLTPA950	3.4589	2.8157	1.2285	0.2232
MANMAX:PLTPA1200	1.8522	2.8157	0.6578	0.5127

Table 2.23: Tukey multiple comparison of means at the 95% family-wise confidence level for basal area per acre between MAN at ages 6, 8, 10, 12, 15, 18, and 21. Significant p-values are shown in bold

MAX - INT	
YEAR	Pr(> |z|)
6	0.2750
8	**0.0328**
10	**0.0429**
12	0.1200
15	0.2070
18	0.4670
21	0.5360

Table 2.24: Tukey multiple comparison of means at the 95% family-wise confidence level for quadratic mean diameter between MAN at ages 6, 8, 10, 12, 15, 18, and 21. Significant p-values are shown in bold

MAX - INT	
YEAR	Pr(> |z|)
6	**0.0003**
8	**0.0000**
10	**0.0000**
12	**0.0020**
15	**0.0166**
18	0.0785
21	0.0531

Table 2.25: Tukey multiple comparison of means at the 95% family-wise confidence level for basal area per acre between PLTPA at ages 6, 8, 10, 12, 15, 18, and 21. Significant p-values are shown in bold.

YEAR 6

Comparison PLTPA	Pr(> |z|)
450 - 200	**0.0445**
700 - 200	< **0.001**
950 - 200	< **0.001**
1200 - 200	< **0.001**
700 - 450	0.1362
950 - 450	**0.0079**
1200 - 450	< **0.001**
950 - 700	0.8562
1200 - 700	0.1448
1200 - 950	0.6903

YEAR 8

Comparison PLTPA	Pr(> |z|)
450 - 200	< **0.001**
700 - 200	< **0.001**
950 - 200	< **0.001**
1200 - 200	< **0.001**
700 - 450	**0.0095**
950 - 450	< **0.001**
1200 - 450	< **0.001**
950 - 700	0.5156
1200 - 700	**0.0096**
1200 - 950	0.4375

YEAR 10

Comparison PLTPA	Pr(> $\|z\|$)
450 - 200	< **0.001**
700 - 200	< **0.001**
950 - 200	< **0.001**
1200 - 200	< **0.001**
700 - 450	0.2177
950 - 450	< **0.001**
1200 - 450	< **0.001**
950 - 700	0.0999
1200 - 700	< **0.001**
1200 - 950	0.5263

YEAR 12

Comparison PLTPA	Pr(> $\|z\|$)
450 - 200	< **0.001**
700 - 200	< **0.001**
950 - 200	< **0.001**
1200 - 200	< **0.001**
700 - 450	0.4486
950 - 450	< **0.001**
1200 - 450	< **0.001**
950 - 700	0.0783
1200 - 700	**0.0053**
1200 - 950	0.9054

YEAR 15

Comparison PLTPA	Pr(> $\|z\|$)
450 - 200	< **0.001**
700 - 200	< **0.001**
950 - 200	< **0.001**
1200 - 200	< **0.001**
700 - 450	0.7729
950 - 450	**0.0098**
1200 - 450	**0.0040**
950 - 700	0.2132
1200 - 700	0.1213
1200 - 950	0.9989

YEAR 18

Comparison PLTPA	Pr(> $\|z\|$)
450 - 200	**0.000**
700 - 200	**0.000**
950 - 200	**0.000**
1200 - 200	**0.000**
700 - 450	0.997
950 - 450	0.466
1200 - 450	0.656
950 - 700	0.684
1200 - 700	0.849
1200 - 950	0.998

YEAR 21

Comparison PLTPA	Pr(> $\|z\|$)
450 - 200	0.3250
700 - 200	0.5100
950 - 200	0.6920
1200 - 200	0.7370
700 - 450	0.9970
950 - 450	0.9620
1200 - 450	0.9470
950 - 700	0.9980
1200 - 700	0.9950
1200 - 950	1.0000

Table 2.26: Tukey multiple comparison of means at the 95% family-wise confidence level for quadratic mean diameter between PLTPA at ages 6, 8, 10, 12, 15, 18, and 21. Significant p-values are shown in bold

YEAR 6

Comparison PLTPA	Pr(> |z|)
450 - 200	0.0551
700 - 200	< **0.001**
950 - 200	< **0.001**
1200 - 200	< **0.001**
700 - 450	0.6777
950 - 450	0.0635
1200 - 450	**0.0022**
950 - 700	0.6802
1200 - 700	0.1295
1200 - 950	0.8407

YEAR 8

Comparison PLTPA	Pr(> |z|)
450 - 200	< **0.001**
700 - 200	< **0.001**
950 - 200	< **0.001**
1200 - 200	< **0.001**
700 - 450	< **0.001**
950 - 450	< **0.001**
1200 - 450	< **0.001**
950 - 700	**0.0082**
1200 - 700	< **0.001**
1200 - 950	0.1841

YEAR 10

Comparison PLTPA	Pr(> |z|)
450 - 200	< **0.001**
700 - 200	< **0.001**
950 - 200	< **0.001**
1200 - 200	< **0.001**
700 - 450	< **0.001**
950 - 450	< **0.001**
1200 - 450	< **0.001**
950 - 700	**0.0024**
1200 - 700	< **0.001**
1200 - 950	0.1007

YEAR 12

Comparison PLTPA	Pr(> |z|)
450 - 200	< **0.001**
700 - 200	< **0.001**
950 - 200	< **0.001**
1200 - 200	< **0.001**
700 - 450	< **0.001**
950 - 450	< **0.001**
1200 - 450	< **0.001**
950 - 700	< **0.001**
1200 - 700	< **0.001**
1200 - 950	0.0664

YEAR 15

Comparison PLTPA	Pr(> $\|z\|$)
450 - 200	< **0.001**
700 - 200	< **0.001**
950 - 200	< **0.001**
1200 - 200	< **0.001**
700 - 450	< **0.001**
950 - 450	< **0.001**
1200 - 450	< **0.001**
950 - 700	**0.0336**
1200 - 700	< **0.001**
1200 - 950	0.2225

YEAR 18

Comparison PLTPA	Pr(> $\|z\|$)
450 - 200	**0.0001**
700 - 200	**0.0001**
950 - 200	**0.0001**
1200 - 200	**0.0001**
700 - 450	**0.0010**
950 - 450	**0.0001**
1200 - 450	**0.0001**
950 - 700	0.1234
1200 - 700	**0.0026**
1200 - 950	0.7042

YEAR 21

Comparison PLTPA	Pr(> $\|z\|$)
450 - 200	**0.0001**
700 - 200	**0.0001**
950 - 200	**0.0001**
1200 - 200	**0.0001**
700 - 450	**0.0350**
950 - 450	**0.0001**
1200 - 450	**0.0001**
950 - 700	0.1280
1200 - 700	**0.0333**
1200 - 950	0.9839

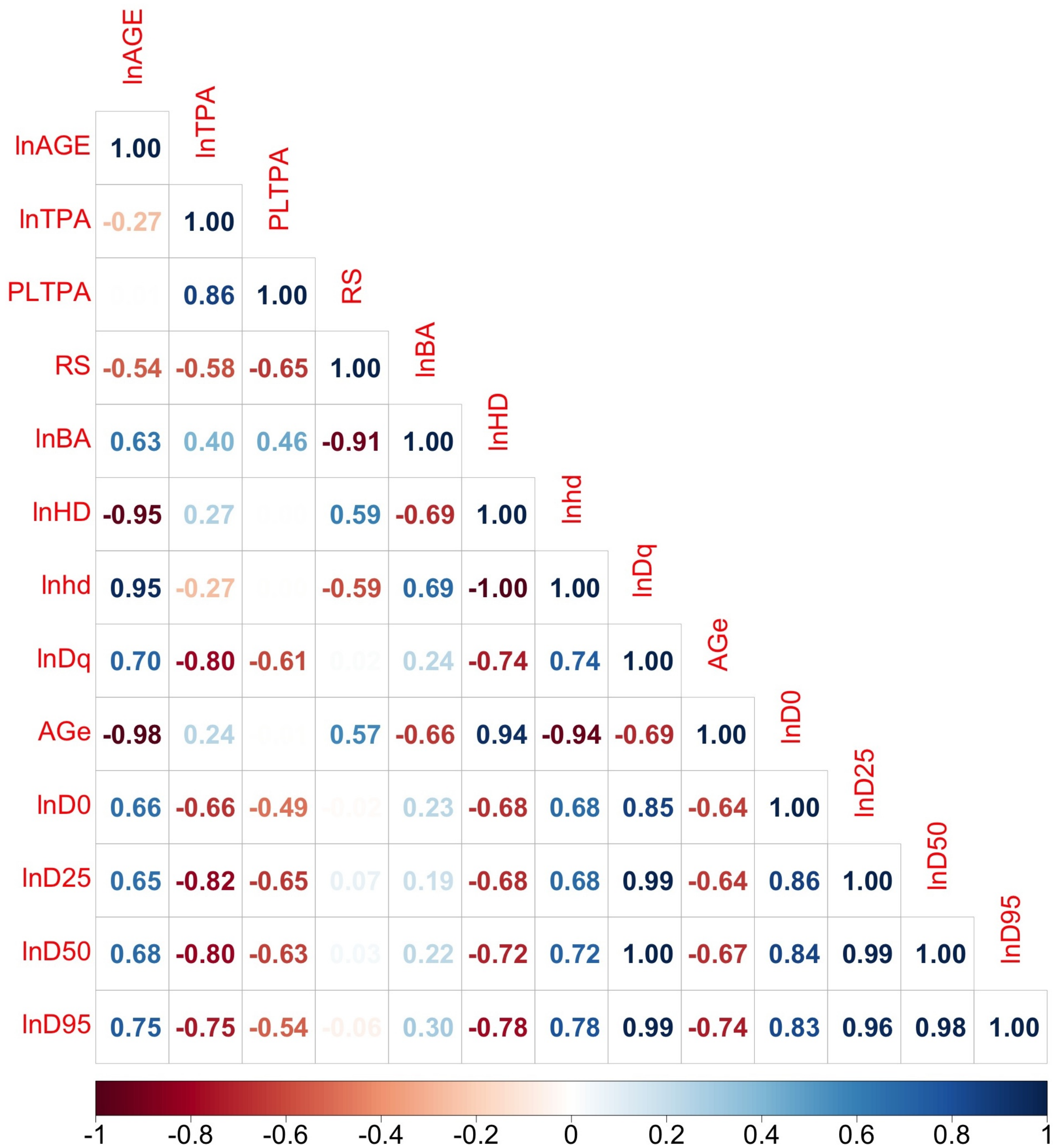

Figure 2.1: Correlation matrix for 13 variables. Variables include log of age (lnAGE); log of tree per acre (lnTPA), initial planting density (PLTPA); relative space (RS) log of basal area per acre (lnBA); log of dominant tree height (lnHD); log of $\frac{1}{\text{HD}}$ (lnhd); log of quadric mean diameter (lnDq); log of $\frac{1}{\text{AGE}}$ AGe; log of minimum diameter (lnD0); log of percentile 25 of diameter(lnD25); log of percentile 50 of diameter (lnD50); log of percentile 95 of diameter (lnD95). Blank cells indicate the absence of correlation between the variables, whereas cells with lighter colors represent correlations of low magnitude. As color intensity increases, the strength of the correlation between the variables becomes more pronounced, corresponding to higher correlation values.

Table 2.27: Coefficients estimates from the regression D_0 percentile.

	Estimate	Std. Error	t value	Pr(> $|t|$)
(Intercept)	-2.0790	0.1665	-12.4880	0.0000
lnDq	1.2692	0.1076	11.7961	0.0000
lnAGE	0.1105	0.0818	1.3519	0.1767
lnHD	-0.1818	0.1050	-1.7307	0.0838
PLTPA	-0.0001	0.0001	-2.0305	0.0426
MANMAX	0.0229	0.0195	1.1758	0.2400

Table 2.28: Coefficients estimates from the regression D_{25} percentile.

	Estimate	Std. Error	t value	Pr(> $|t|$)
(Intercept)	-0.1385	0.0168	-8.2646	0.0000
lnD50	1.0378	0.0138	75.3178	0.0000
lnAGE	-0.0100	0.0087	-1.1576	0.2473
PLTPA	0.0000	0.0000	-5.2378	0.0000
MANMAX	-0.0048	0.0031	-1.5551	0.1203

Table 2.29: Coefficients estimates from the regression D_{50} percentile.

	Estimate	Std. Error	t value	Pr(> $|t|$)
(Intercept)	0.0562	0.0066	8.5297	0.0000
lnDq	0.9771	0.0028	351.8575	0.0000
PLTPA	0.0000	0.0000	-9.8694	0.0000
MANMAX	0.0036	0.0013	2.7975	0.0053

Table 2.30: Coefficients estimates from the regression D_{95} percentile.

	Estimate	Std. Error	t value	Pr(> $|t|$)
(Intercept)	0.0891	0.0214	4.1551	0.0000
LnD50	0.9485	0.0137	69.3950	0.0000
LnAGE	0.0124	0.0100	1.2432	0.2141
LnHD	-0.0370	0.0113	-3.2744	0.0011
PLTPA	0.0001	0.0000	8.3562	0.0000
MANMAX	-0.0006	0.0030	-0.2085	0.8349

Table 2.31: Coefficients estimates from the regression D_q.

	Estimate	Std. Error	t value	$Pr(>\|t\|)$
(Intercept)	4.590017	0.207855	22.083	0.0000
RS	-1.271080	0.093842	-13.545	0.0000
N	-0.462589	0.012434	-37.203	0.0000
LnHD	0.146495	0.030786	4.759	0.0000
AGE	-0.591623	0.207771	-2.847	0.0045
MANMAX	0.036864	0.004454	8.276	0.0000

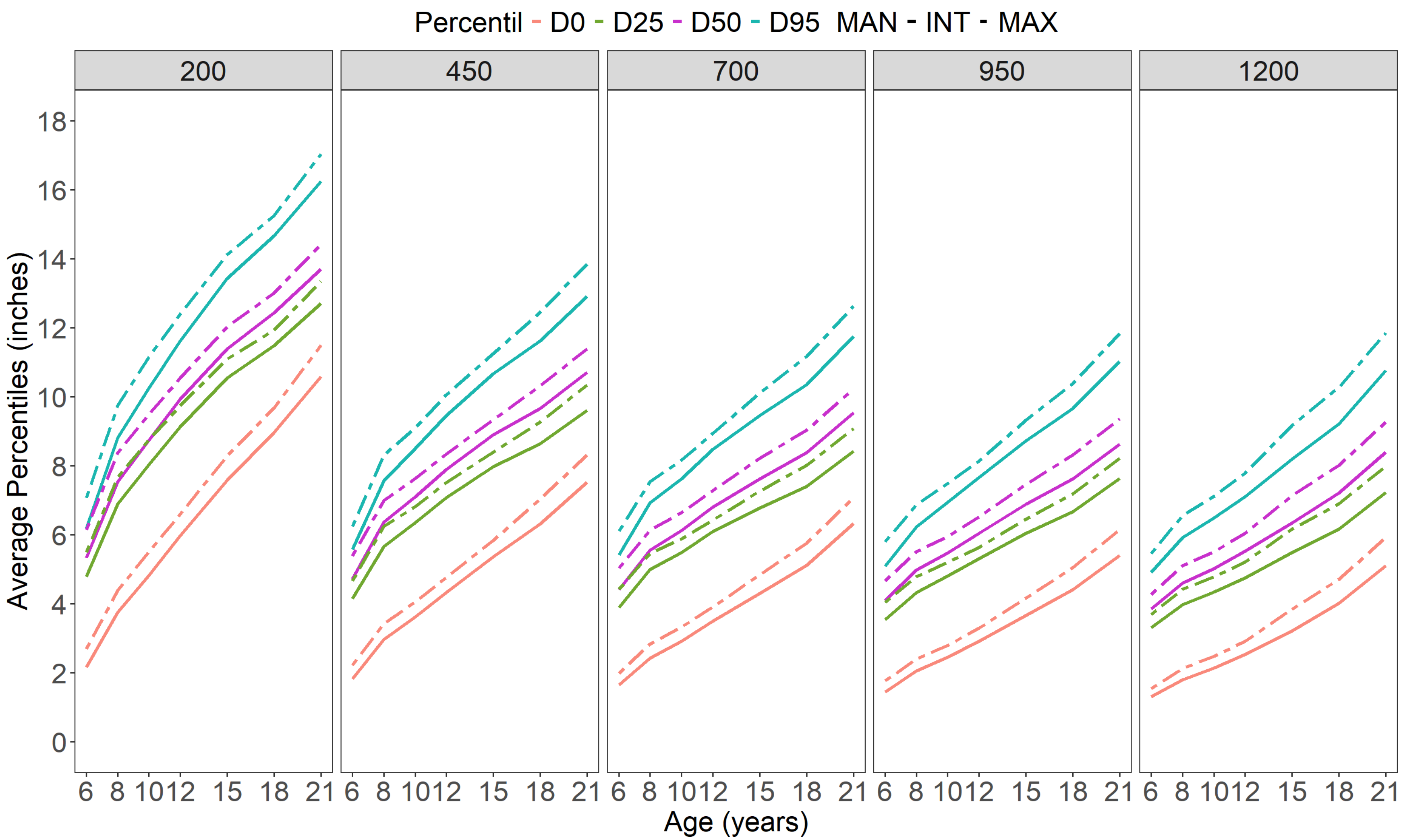

Figure 2.2: Average percentiles across all five planting densities under two silvicultural management levels. The solid line represents intensive (INT) management intensity, and the dashed line represents maximum (MAX) management intensity. Percentiles D_0, D_{25}, D_{50}, and D_{95} are represented by orange, green, purple, and blue, respectively.

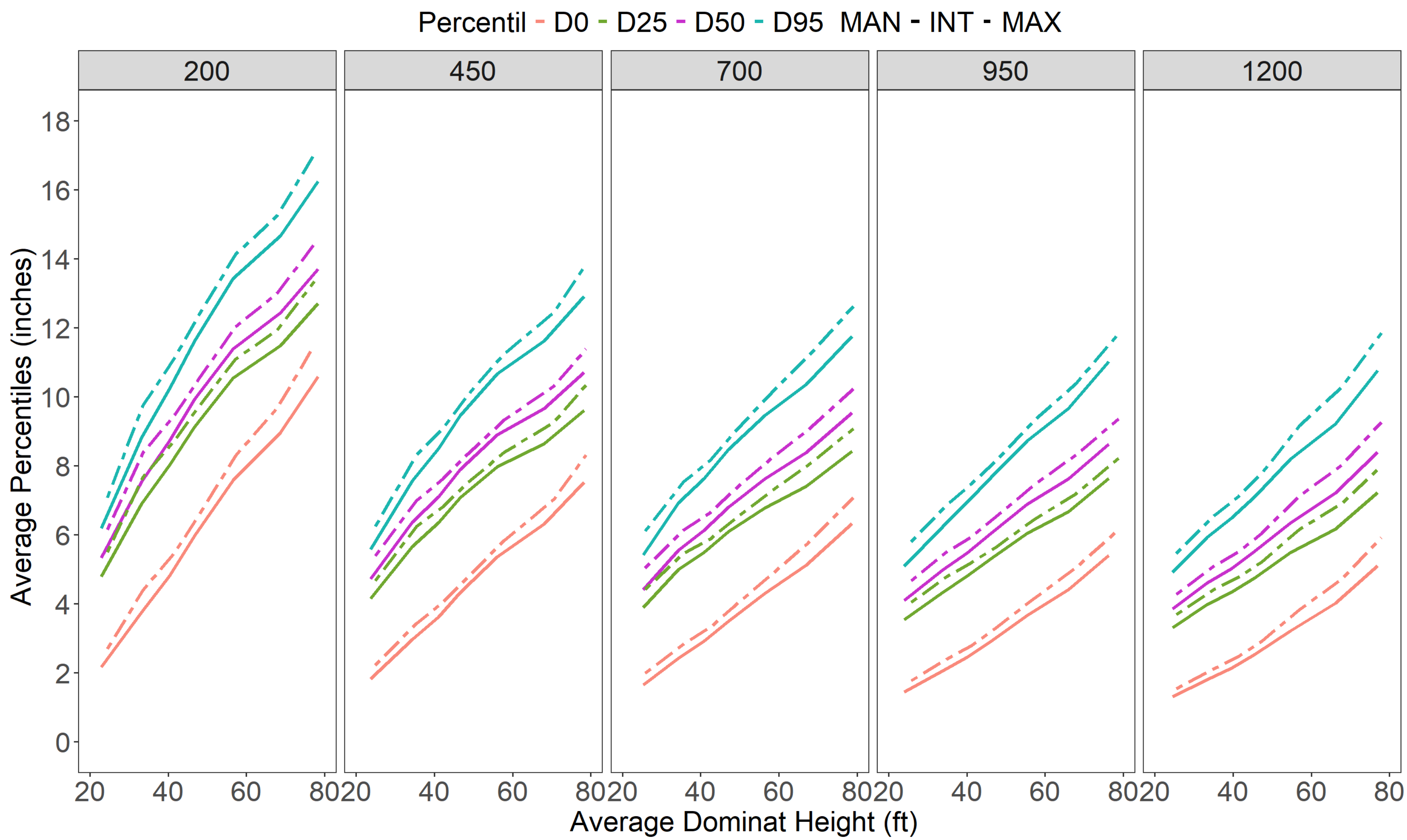

Figure 2.3: Average percentiles across all five planting densities under two silvicultural management levels for dominant tree height (HD). The solid line represents intensive (INT) management intensity, and the dashed line represents maximum (MAX) management intensity. Percentiles D_0, D_{25}, D_{50}, and D_{95} are represented by orange, green, purple, and blue, respectively.

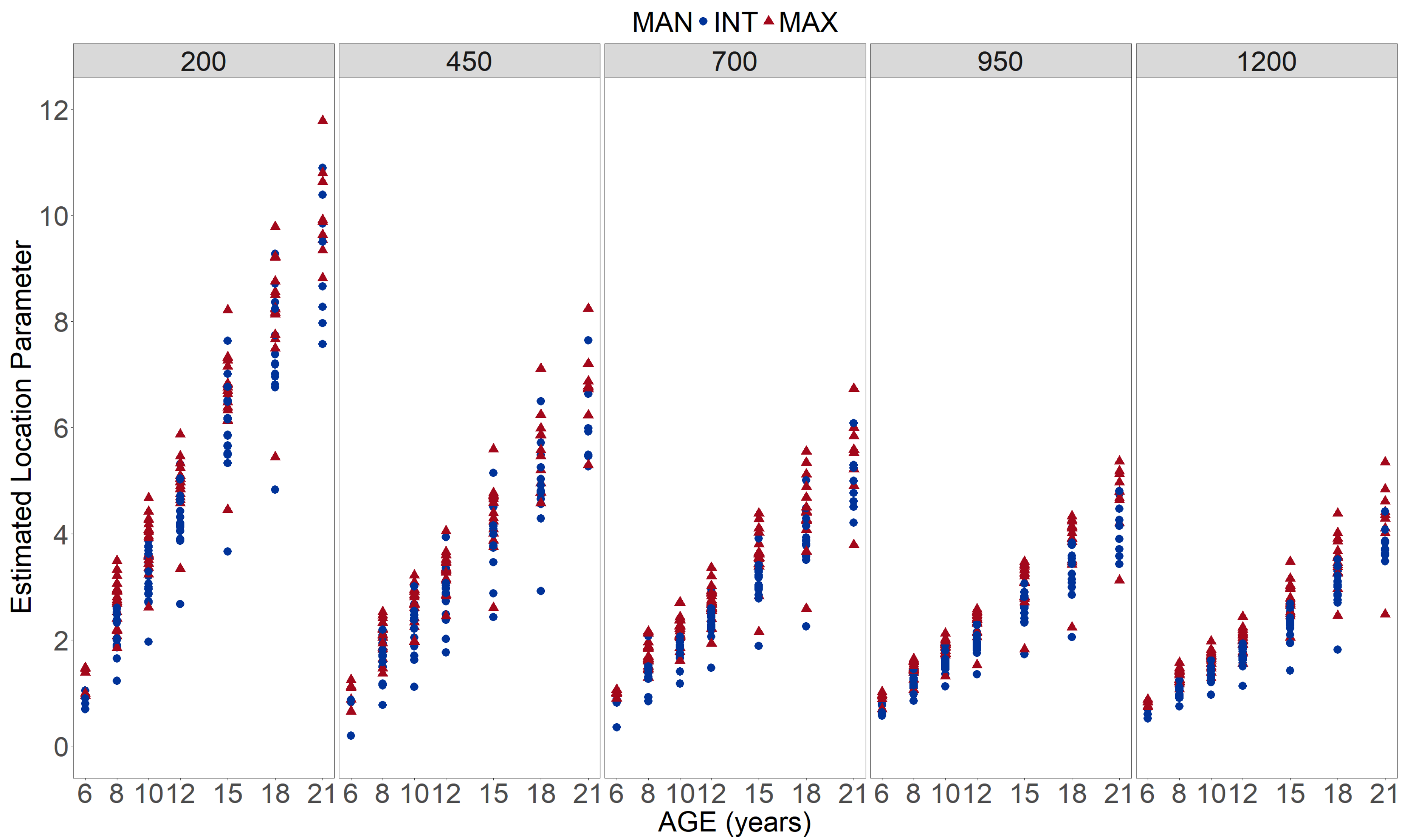

Figure 2.4: The location parameters of the diameter distribution across all five planting densities and two silvicultural management levels. Blue dots represent intensive (INT) management intensity, and red triangles represent maximum (MAX) management intensity.

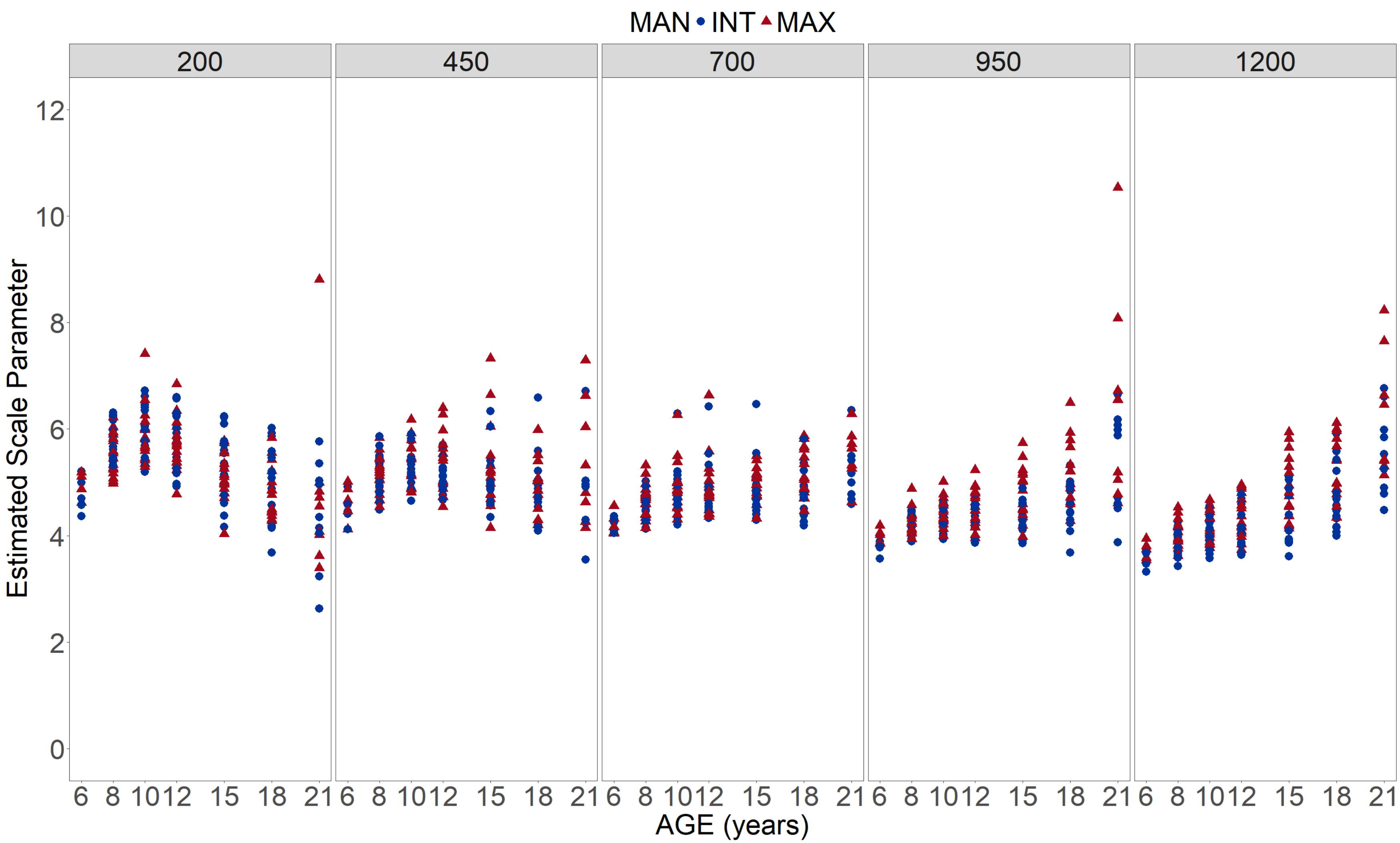

Figure 2.5: The scale parameters of the diameter distribution across all five planting densities and two silvicultural management levels. Blue dots represent intensive (INT) management intensity, and red triangles represent maximum (MAX) management intensity.

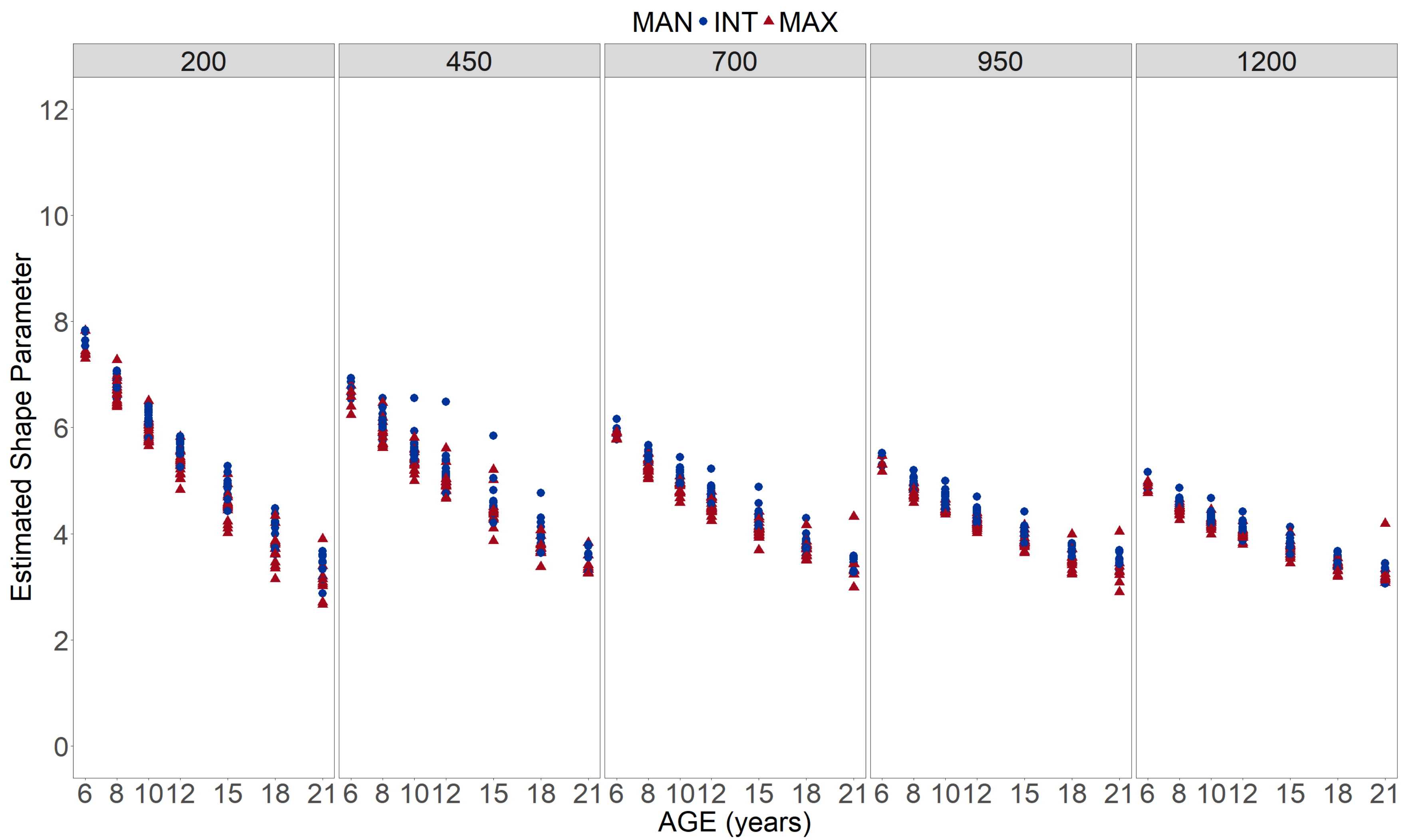

Figure 2.6: The shape parameters of the diameter distribution across all five planting densities and two silvicultural management levels. Blue dots represent intensive (INT) management intensity, and red triangles represent maximum (MAX) management intensity.

Table 2.32: Estimated average parameter values for thee three-parameter Weibull distribution across all five planting densities and two silvicultural management levels.

AGE	PLTPA	INT			MAX		
		location ($\hat{a}$)	scale ($\hat{b}$)	shape ($\hat{c}$)	location ($\hat{a}$)	scale ($\hat{b}$)	shape ($\hat{c}$)
6	200	0.87	4.73	7.67	1.25	4.92	7.47
	450	0.72	4.50	6.74	1.00	4.62	6.54
	700	0.74	4.20	5.94	0.99	4.22	5.84
	950	0.67	3.80	5.41	0.90	3.99	5.31
	1200	0.64	3.59	4.96	0.81	3.73	4.89
8	200	2.18	5.68	6.89	2.73	5.47	6.68
	450	1.63	5.10	6.08	2.03	5.07	5.88
	700	1.40	4.50	5.46	1.72	4.60	5.27
	950	1.21	4.13	4.92	1.47	4.22	4.81
	1200	1.07	3.84	4.57	1.32	4.01	4.47
10	200	3.19	5.93	6.21	3.82	5.83	5.94
	450	2.24	5.22	5.60	2.64	5.28	5.36
	700	1.82	4.77	5.09	2.17	4.85	4.87
	950	1.56	4.28	4.64	1.85	4.40	4.50
	1200	1.37	4.01	4.31	1.64	4.20	4.20
12	200	4.31	5.74	5.60	4.94	5.66	5.32
	450	2.89	5.14	5.21	3.31	5.32	4.97
	700	2.34	4.84	4.76	2.71	4.89	4.54
	950	1.98	4.33	4.37	2.29	4.53	4.19
	1200	1.71	4.12	4.08	2.01	4.39	3.98
15	200	5.95	5.33	4.82	6.68	5.14	4.49
	450	3.88	5.08	4.63	4.33	5.33	4.42
	700	3.09	4.84	4.31	3.58	5.00	4.09
	950	2.65	4.41	4.01	3.05	4.83	3.84
	1200	2.29	4.32	3.80	2.76	4.89	3.70
18	200	7.48	5.05	4.01	8.19	4.90	3.70
	450	4.89	4.89	4.02	5.62	4.97	3.74
	700	3.89	4.85	3.86	4.43	5.23	3.72
	950	3.33	4.63	3.67	3.83	5.23	3.50
	1200	2.96	4.75	3.49	3.52	5.25	3.38
21	200	9.19	4.49	3.39	10.04	4.97	3.13
	450	6.06	4.88	3.57	6.76	5.50	3.42
	700	4.96	5.23	3.48	5.45	6.56	3.43
	950	4.12	5.47	3.48	4.67	6.55	3.33
	1200	3.81	5.64	3.29	4.27	7.30	3.30

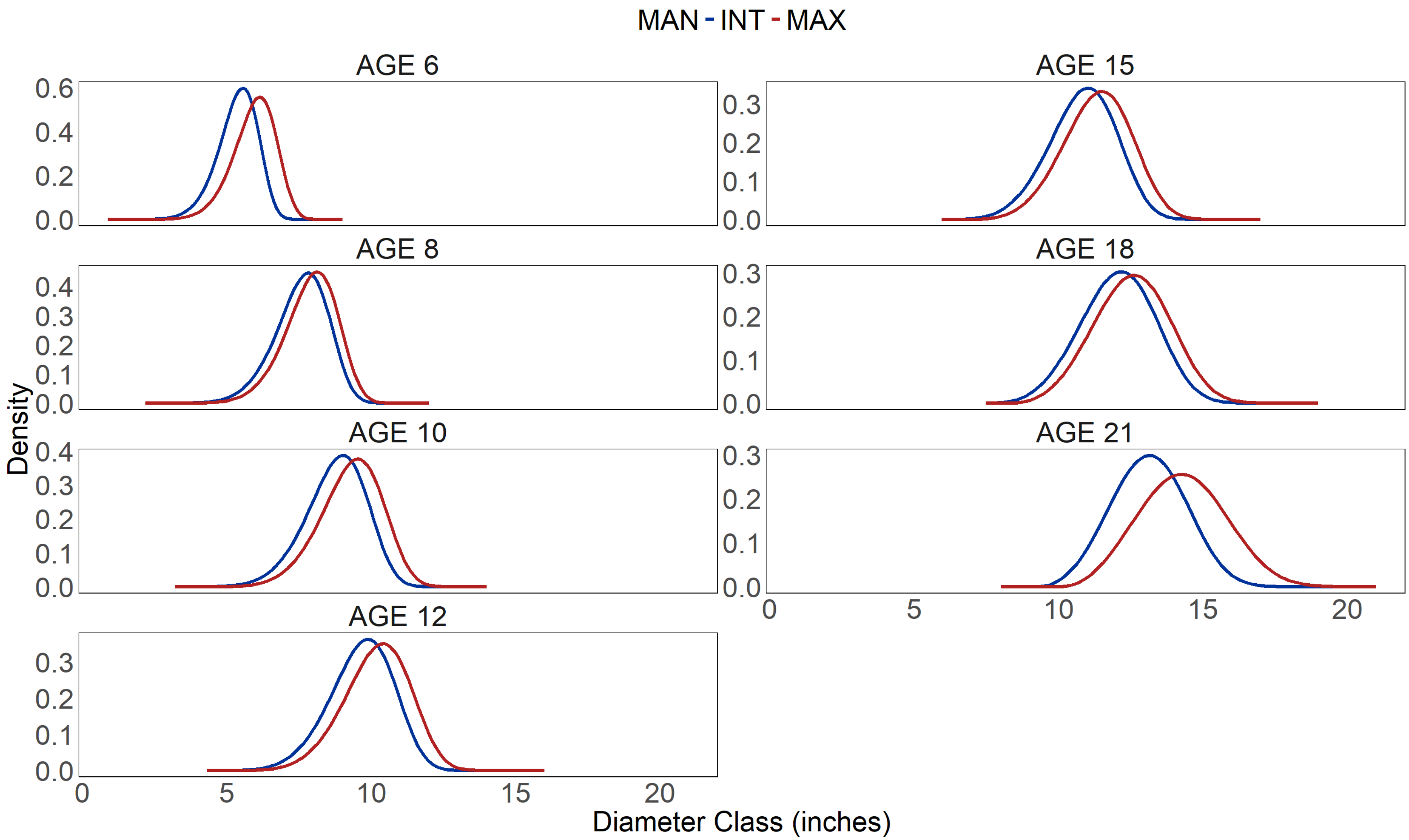

Figure 2.7: The Weibull density curve based on the estimated average three-parameter for breast height diameter for initial planting density (PLTPA) 200 tree per acre, over all ages, and two silvicultural management levels. Blue curves represent intensive (INT) management intensity, and red curves represent maximum (MAX) management intensity.

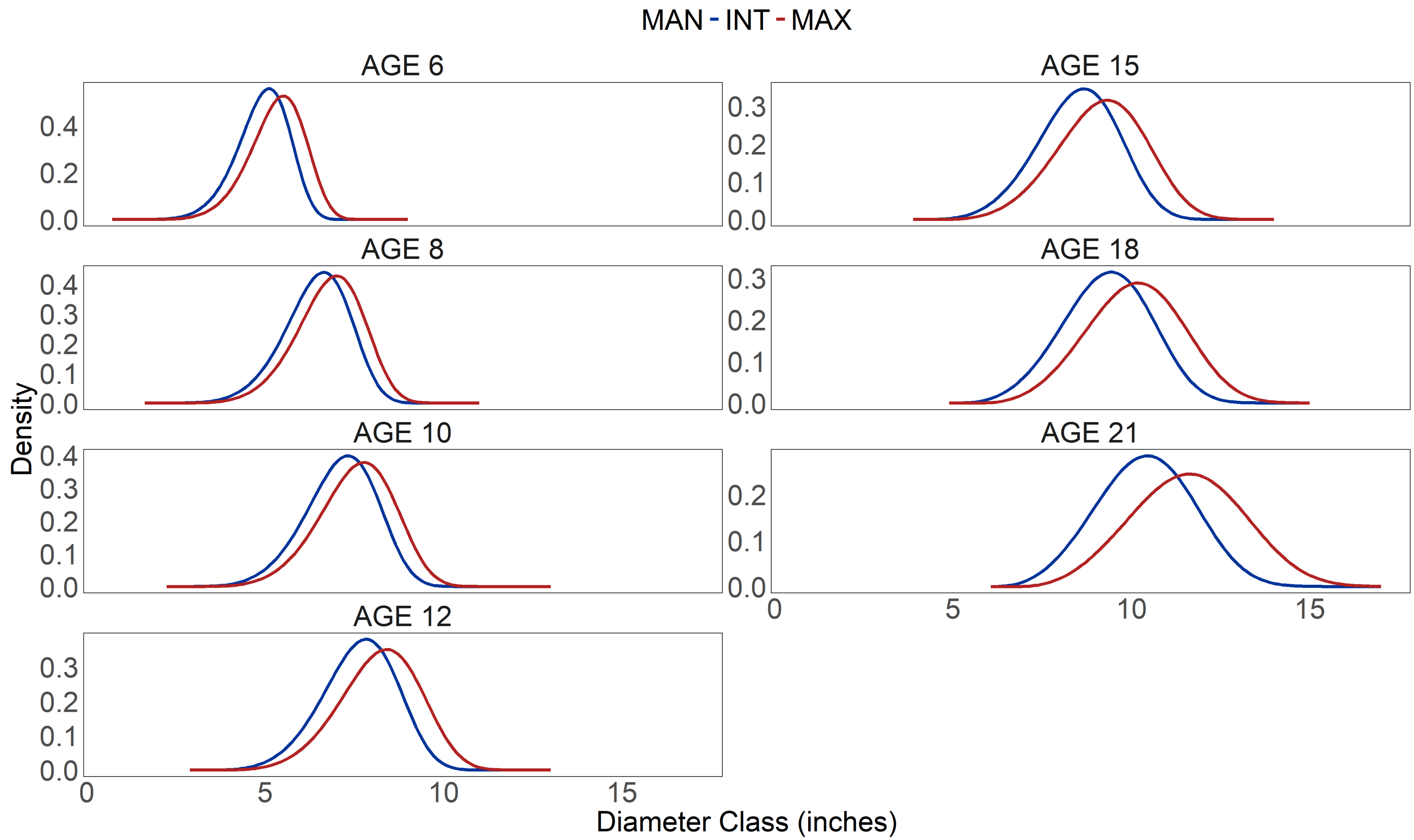

Figure 2.8: The Weibull density curve based on the estimated average three-parameter for breast height diameter for initial planting density (PLTPA) 450 tree per acre, over all ages, and two silvicultural management levels. Blue curves represent intensive (INT) management intensity, and red curves represent maximum (MAX) management intensity.

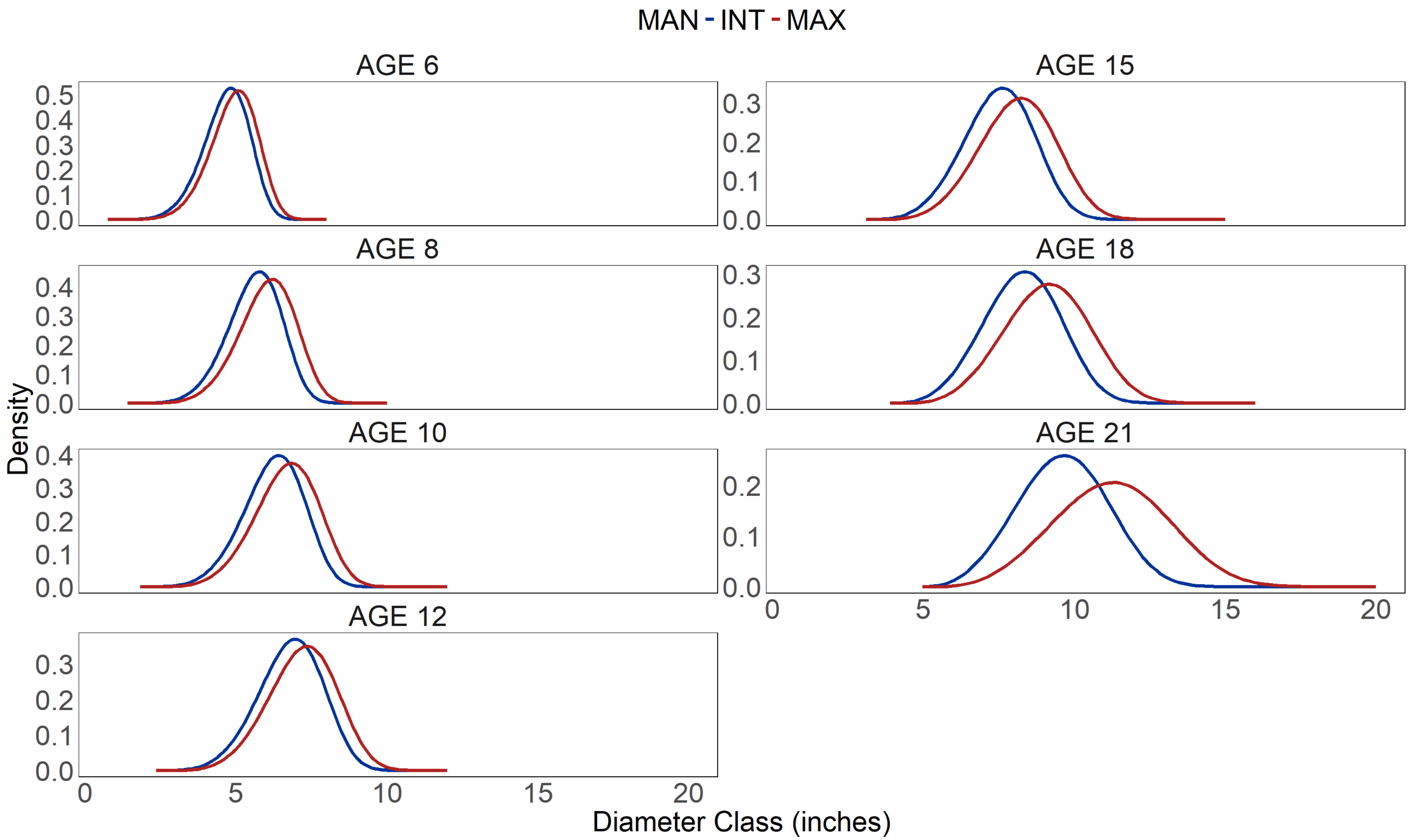

Figure 2.9: The Weibull density curve based on the estimated average three-parameter for breast height diameter for initial planting density (PLTPA) 700 tree per acre, over all ages, and two silvicultural management levels. Blue curves represent intensive (INT) management intensity, and red curves represent maximum (MAX) management intensity.

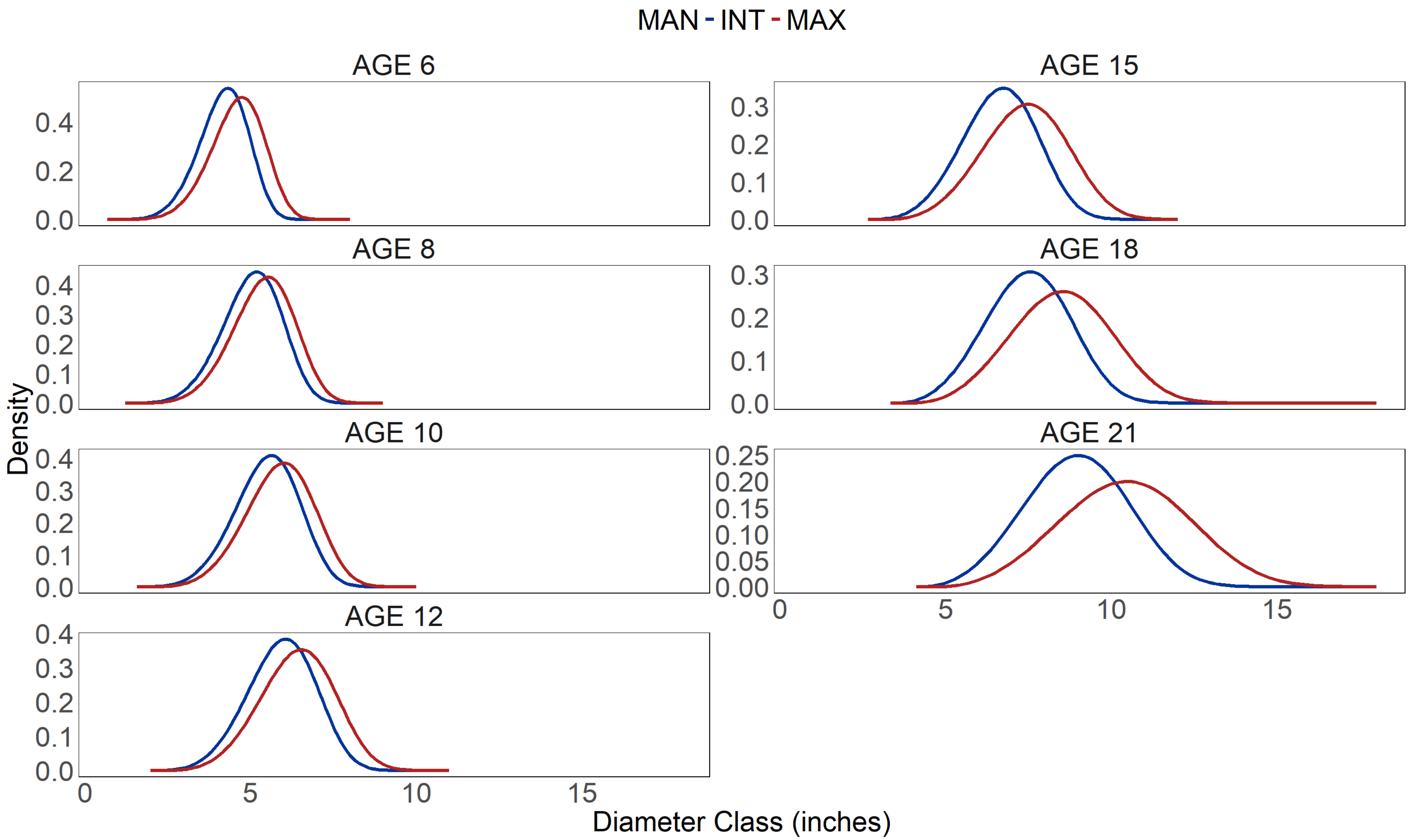

Figure 2.10: The Weibull density curve based on the estimated average three-parameter for breast height diameter for initial planting density (PLTPA) 950 tree per acre, over all ages, and two silvicultural management levels. Blue curves represent intensive (INT) management intensity, and red curves represent maximum (MAX) management intensity.

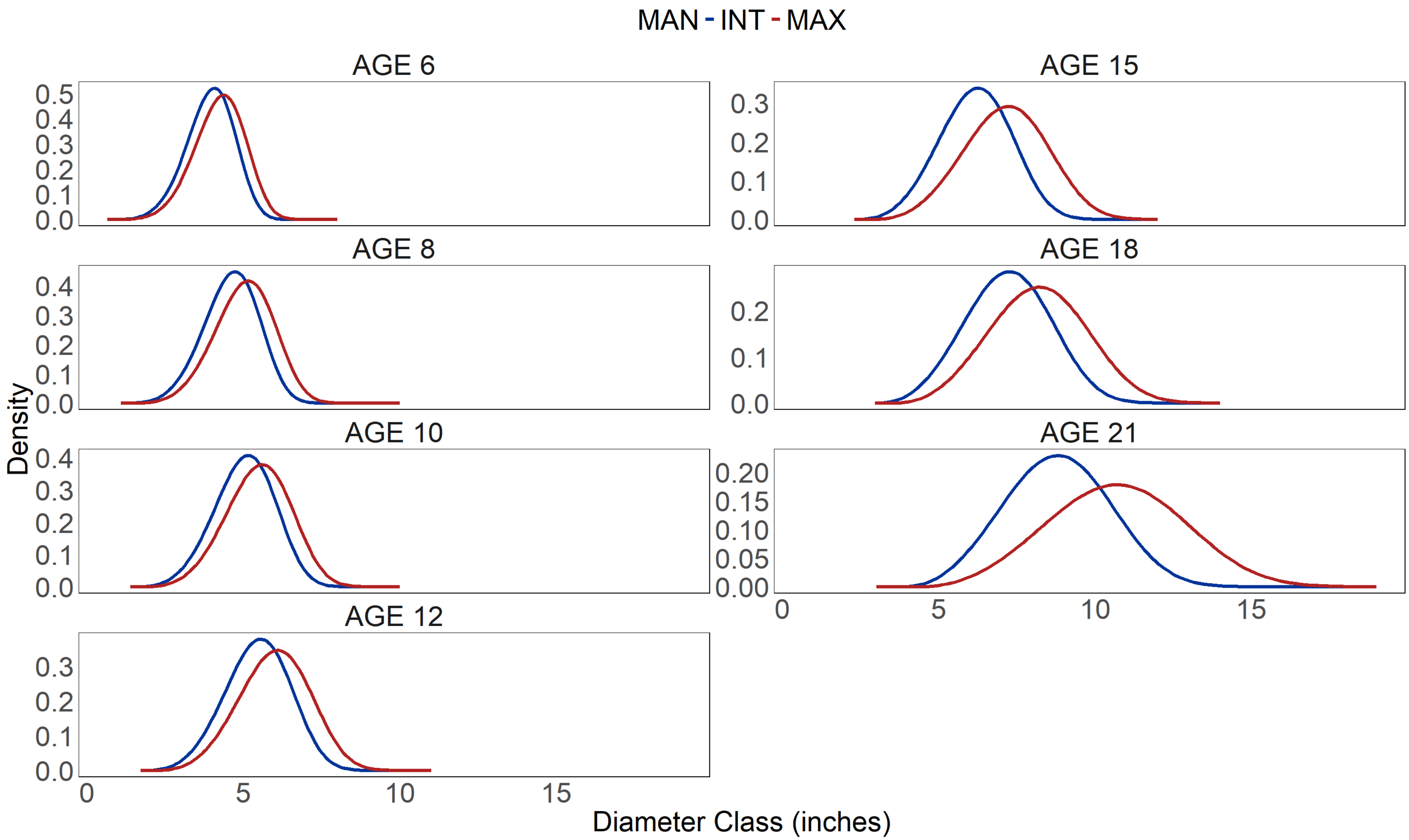

Figure 2.11: The Weibull density curve based on the estimated average three-parameter for breast height diameter for initial planting density (PLTPA) 1200 tree per acre, over all ages, and two silvicultural management levels. Blue curves represent intensive (INT) management intensity, and red curves represent maximum (MAX) management intensity.

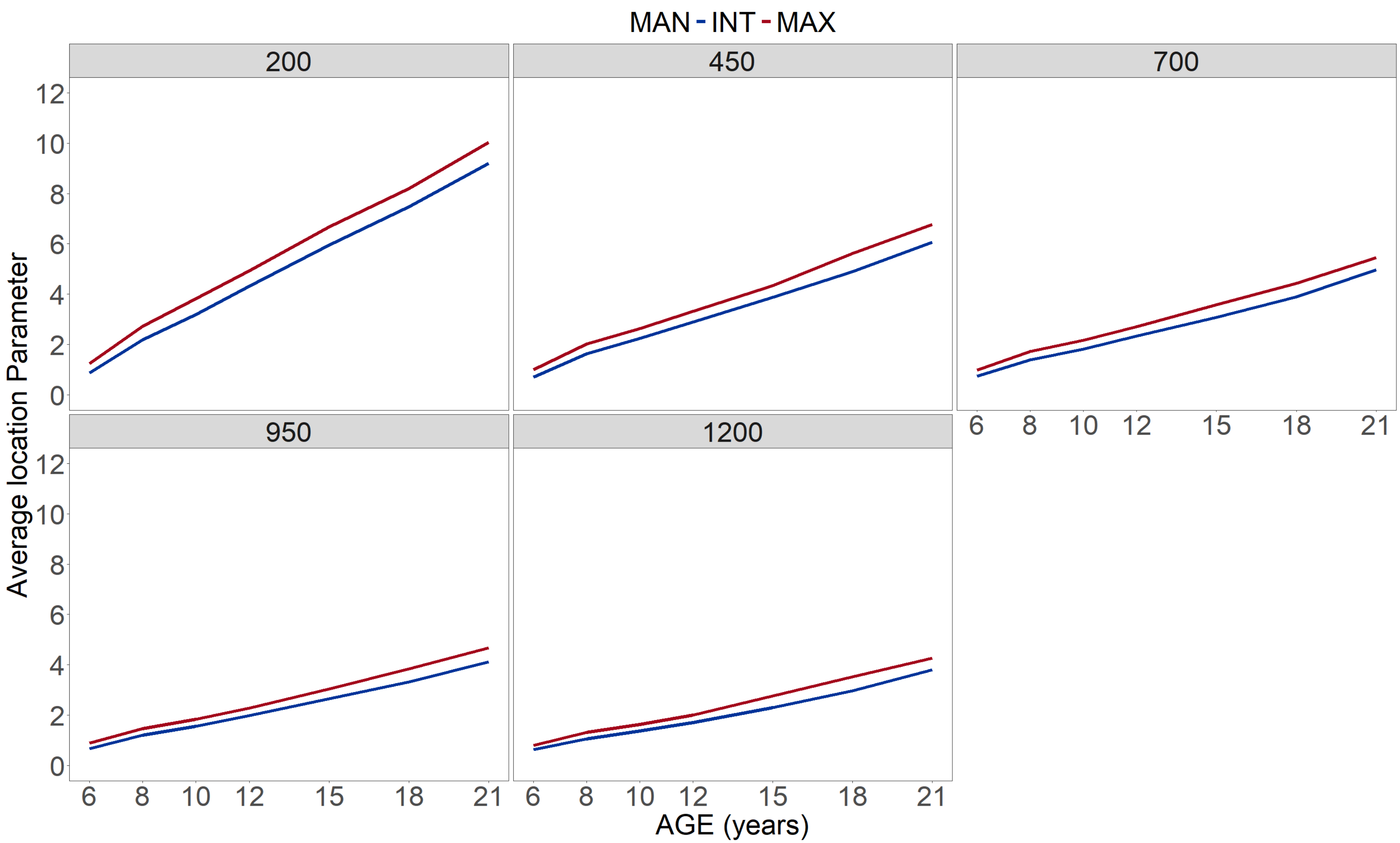

Figure 2.12: The estimated average location parameter across all five planting densities and two silvicultural management levels. Blue lines represent intensive (INT) management intensity, and red lines represent maximum (MAX) management intensity.

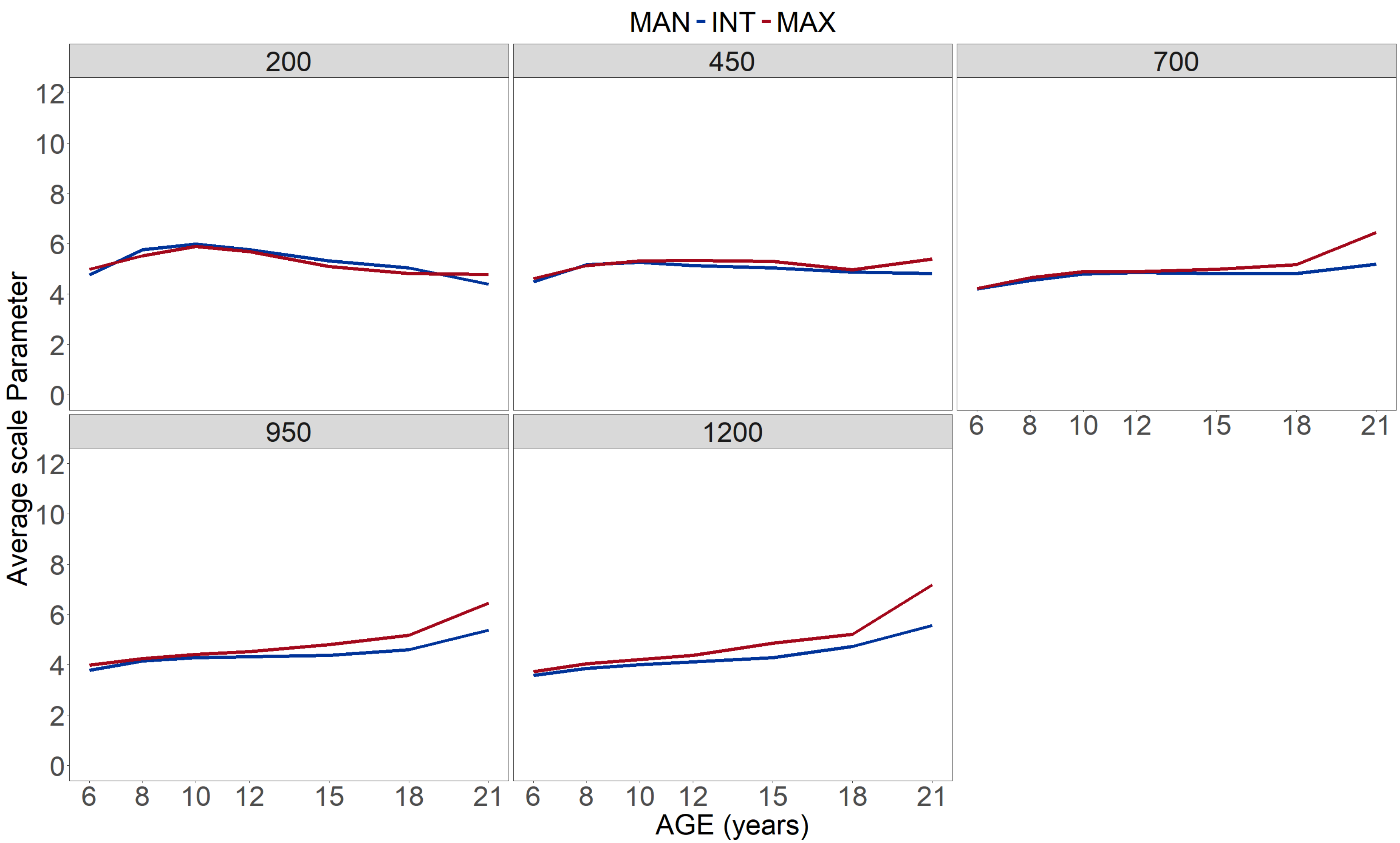

Figure 2.13: The estimated average scale parameter across all five planting densities and two silvicultural management levels. Blue lines represent intensive (INT) management intensity, and red lines represent maximum (MAX) management intensity

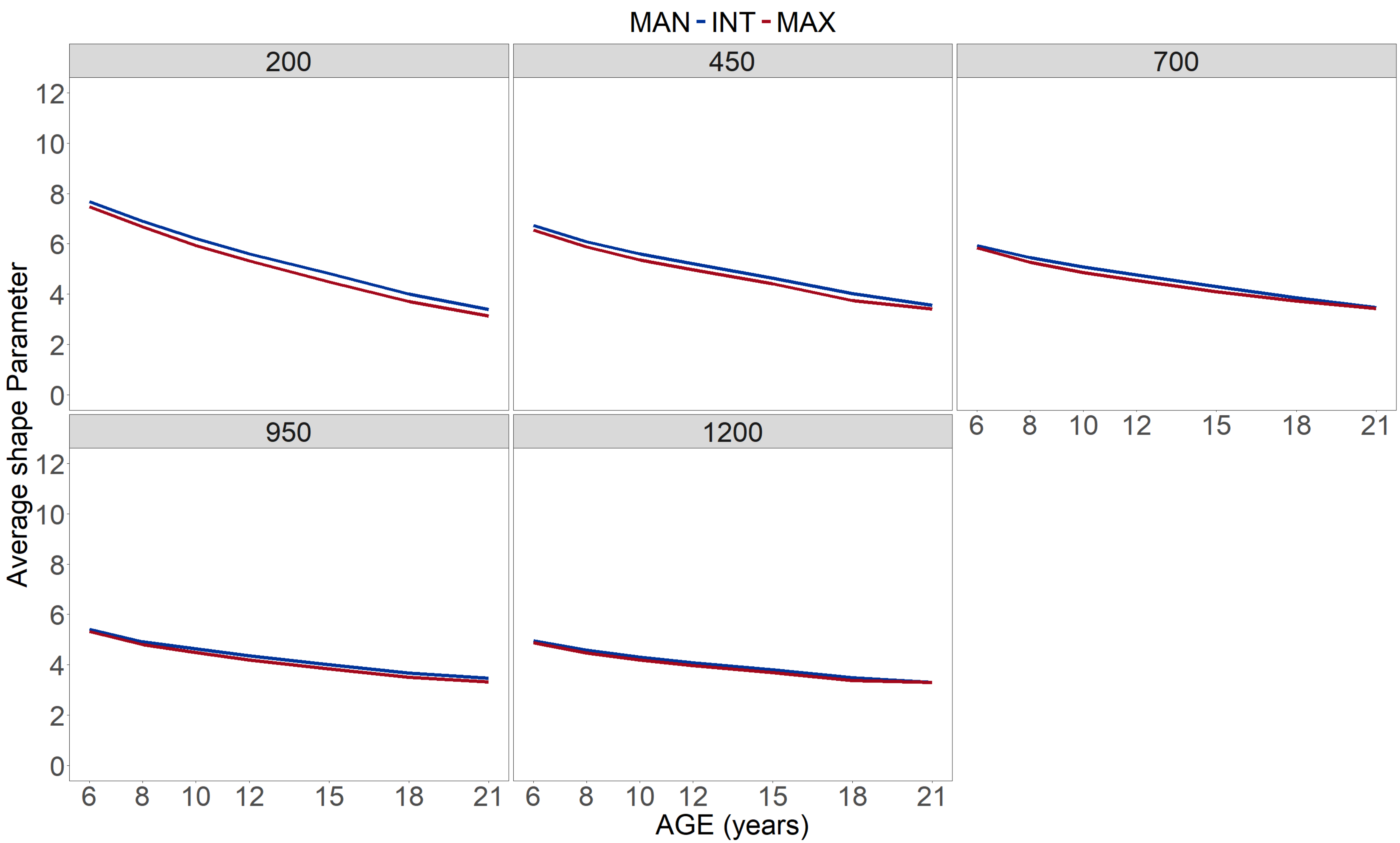

Figure 2.14: The estimated average shape parameter across all five planting densities and two silvicultural management levels. Blue lines represent intensive (INT) management intensity, and red lines represent maximum (MAX) management intensity

Table 2.33: P-values from the two-sample t-tests ($\alpha = 0.05$) of basal area per acre estimated based on Weibull CDF for two silvicultural management, initial planting density (PLTPA), and year in age (Year) combination. Degrees of freedom (DF) for each test. Significant p-value at the $\alpha = 0.05$ significance level are shown in bold.

PLTPA - 200

YEAR	DF	p-value
6	8	0.0971
8	33	0.0514
10	33	**0.0096**
12	33	**0.0031**
15	31	**0.0076**
18	27	0.0703
21	16	0.6271

PLTPA - 450

YEAR	DF	p-value
6	8	0.1483
8	33	**0.0182**
10	31	**0.0323**
12	31	**0.0214**
15	28	0.0821
18	23	**0.0117**
21	13	0.2323

PLTPA - 700

YEAR	DF	p-value
6	8	0.1378
8	34	**0.0034**
10	34	**0.0010**
12	34	**0.0012**
15	30	**0.0134**
18	26	0.0568
21	14	0.6243

PLTPA - 950

YEAR	DF	p-value
6	8	0.0873
8	34	**0.0028**
10	34	**0.0014**
12	34	**0.0005**
15	32	**0.0099**
18	28	0.0643
21	16	0.3061

PLTPA - 1200

YEAR	DF	p-value
6	8	0.1079
8	34	**0.0003**
10	34	**0.0005**
12	34	**0.0017**
15	32	**0.0481**
18	28	**0.0123**
21	16	0.7155

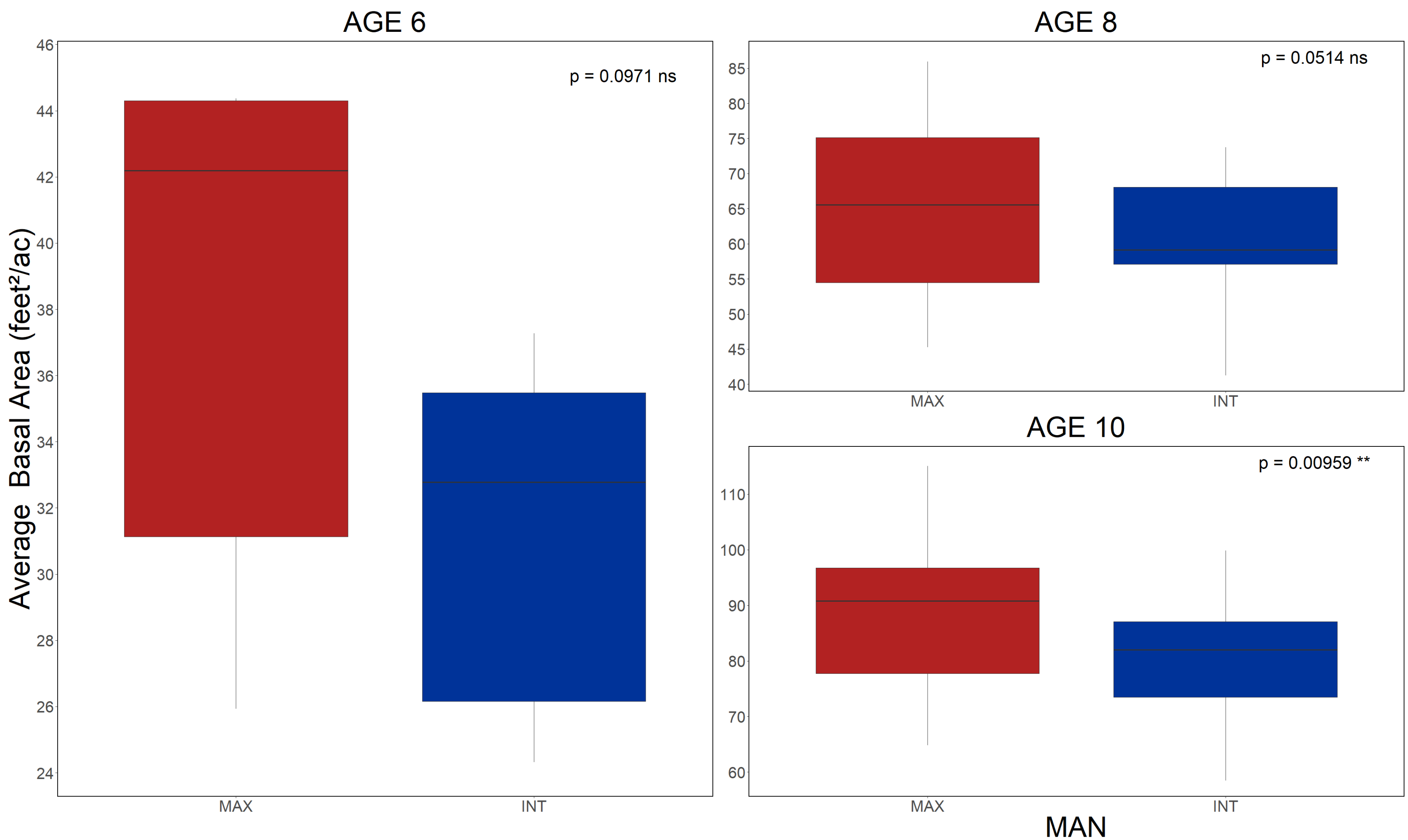

Figure 2.15: Box-plot of two-sample t-test for basal area per acre estimated at age 6, 8, and 10, based on Weibull CDF, comparing maximum (MAX) management and intensive (INT) management intensity at an initial planting density (PLTPA) of 200 trees per acre. Significance is based on p-values with $\alpha = 0.05$: **(ns)** not significant, **(*)** significant, **(**)** very significant, and **(***)** highly significant.

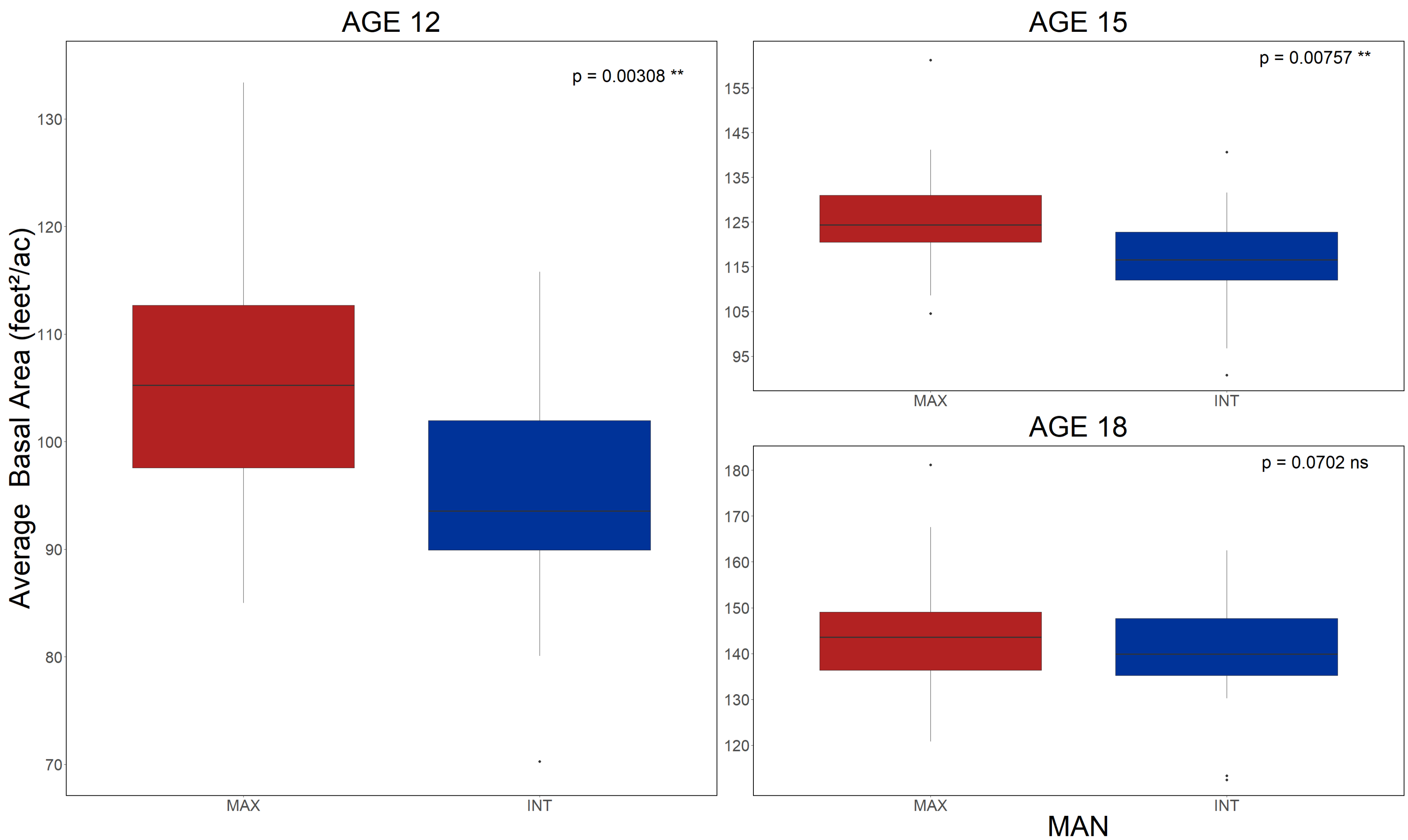

Figure 2.16: Box-plot of two-sample t-test for basal area per acre estimated at age 12, 15, and 18, based on Weibull CDF, comparing maximum (MAX) management and intensive (INT) management intensity at an initial planting density (PLTPA) of 200 trees per acre. Significance is based on p-values with $\alpha = 0.05$: **(ns)** not significant, **(*)** significant, **(**)** very significant, and **(***)** highly significant.

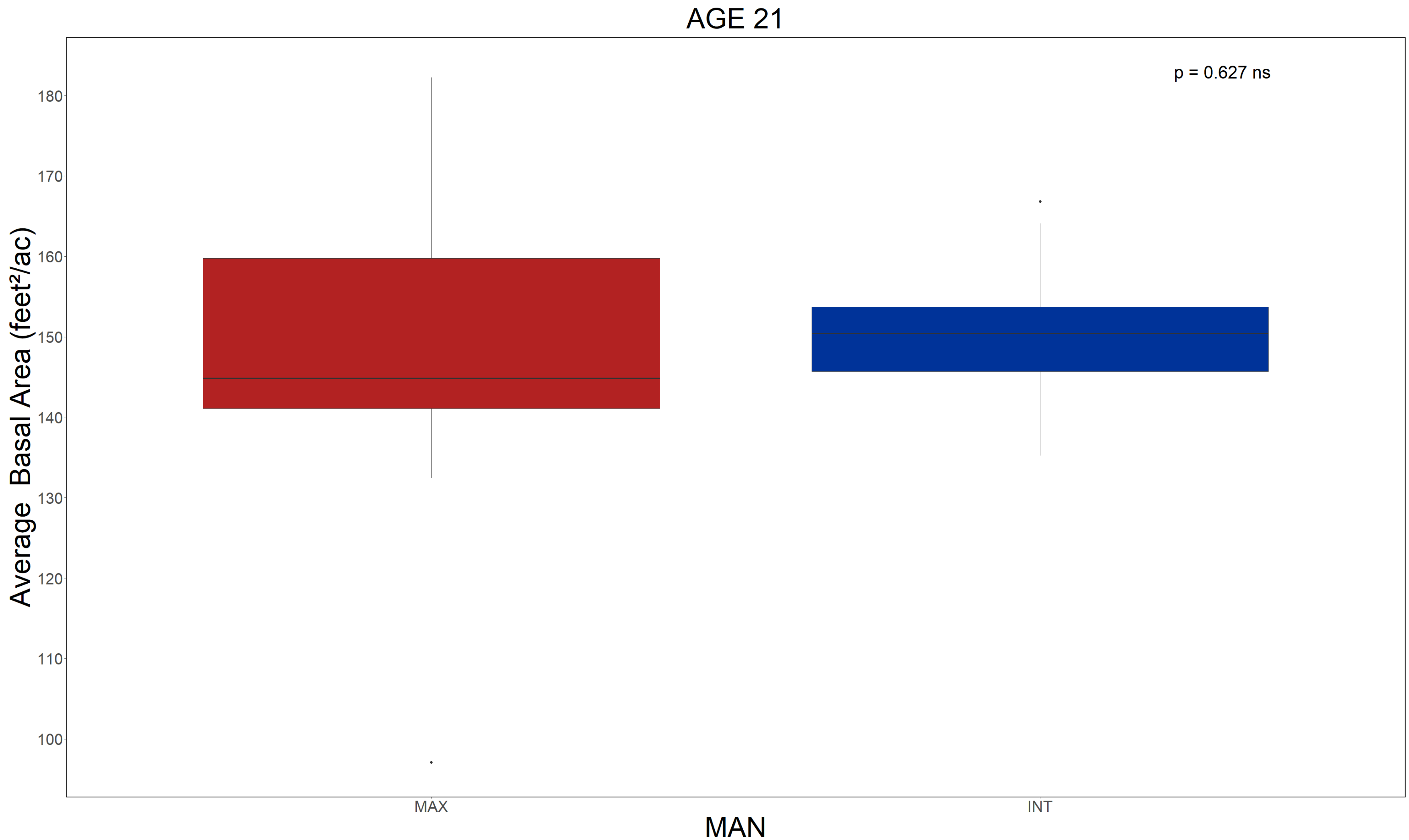

Figure 2.17: Box-plot of two-sample t-test for basal area per acre estimated at age 21, based on Weibull CDF, comparing maximum (MAX) management and intensive (INT) management intensity at an initial planting density (PLTPA) of 200 trees per acre. Significance is based on p-values with $\alpha = 0.05$: **(ns)** not significant, **(*)** significant, **(**)** very significant, and **(***)** highly significant.

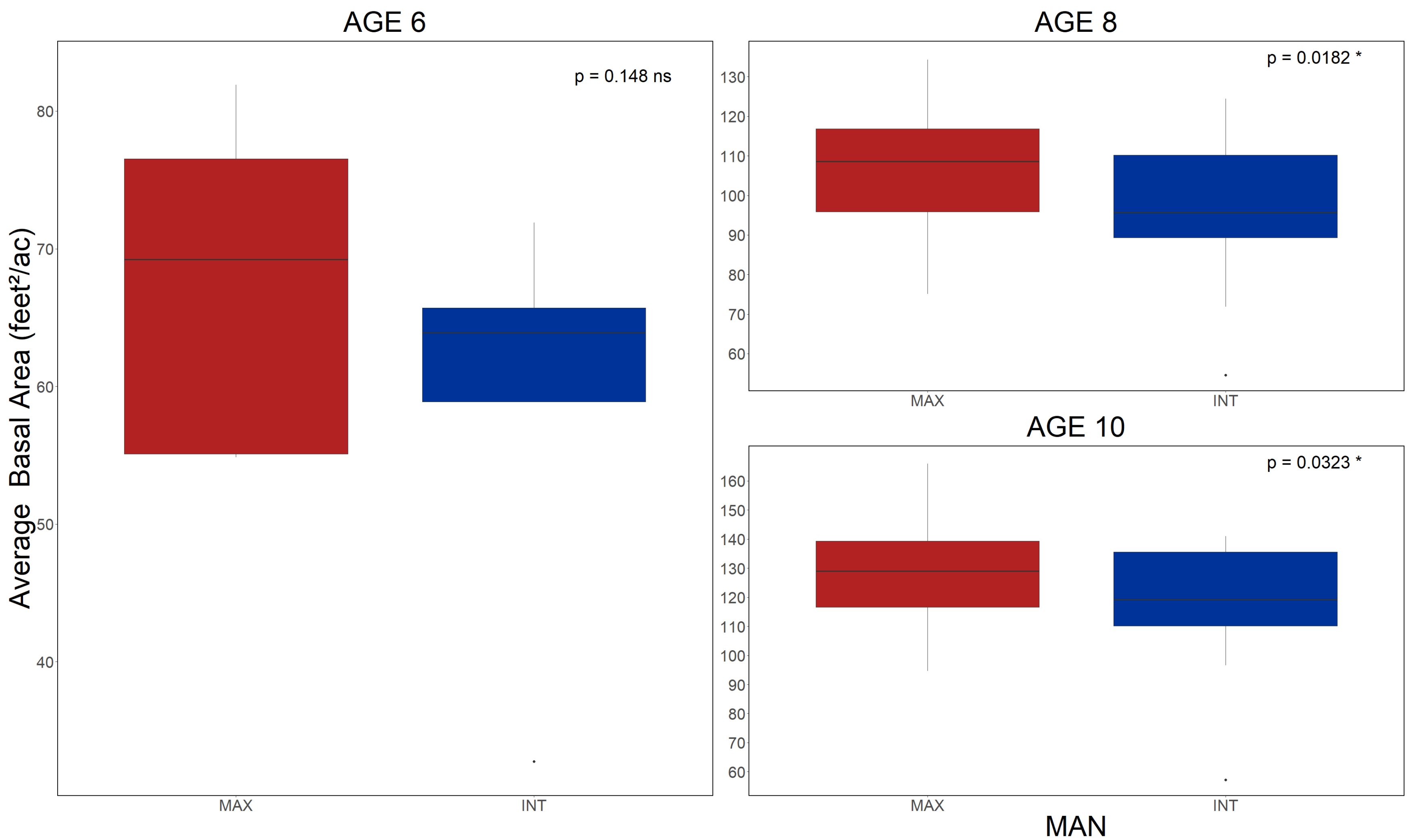

Figure 2.18: Box-plot of two-sample t-test for basal area per acre estimated at age 6, 8, and 10, based on Weibull CDF, comparing maximum (MAX) management and intensive (INT) management intensity at an initial planting density (PLTPA) of 450 trees per acre. Significance is based on p-values with $\alpha = 0.05$: **(ns)** not significant, **(*)** significant, **(**)** very significant, and **(***)** highly significant.

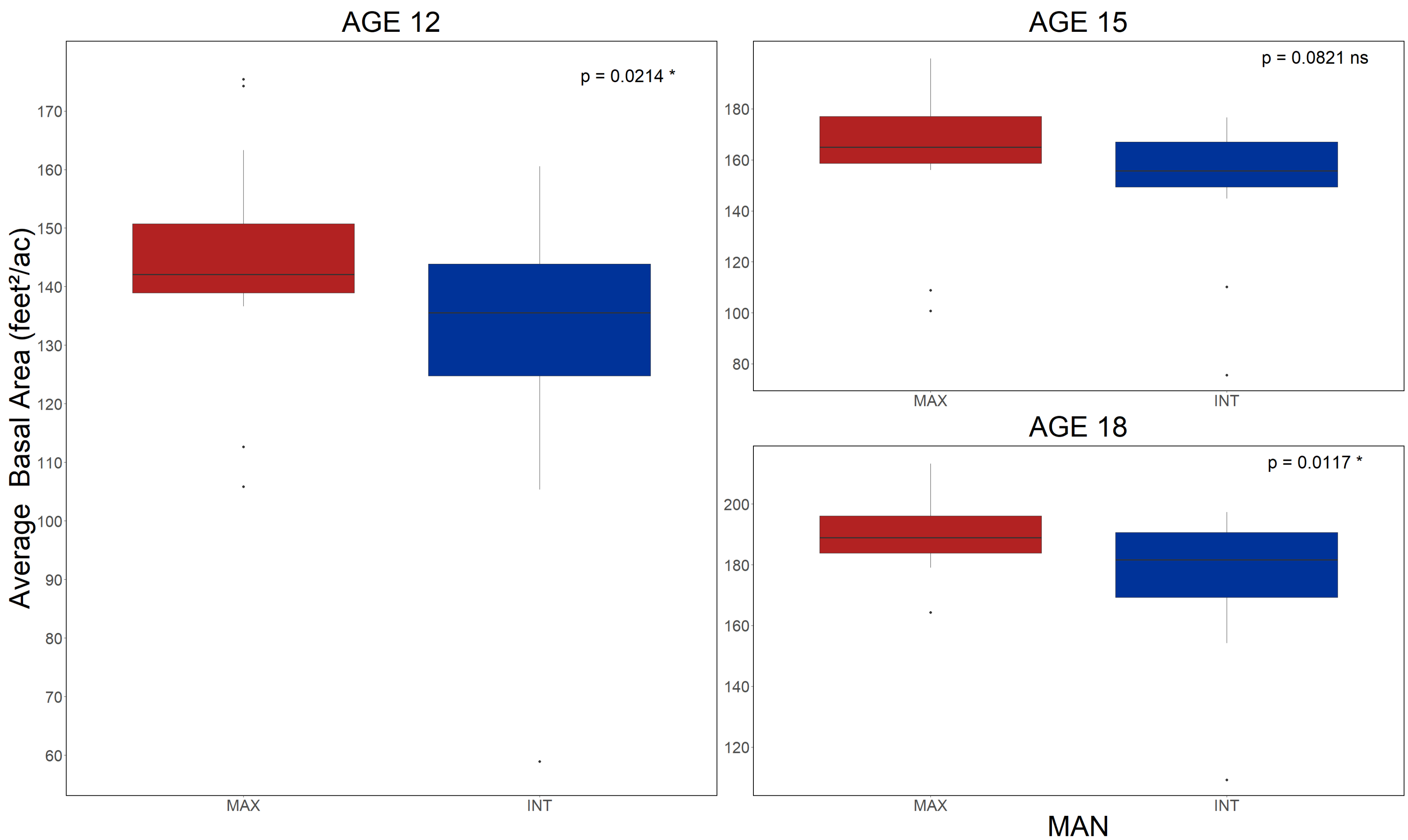

Figure 2.19: Box-plot of two-sample t-test for basal area per acre estimated at age 12, 15, and 18, based on Weibull CDF, comparing maximum (MAX) management and intensive (INT) management intensity at an initial planting density (PLTPA) of 450 trees per acre. Significance is based on p-values with $\alpha = 0.05$: **(ns)** not significant, **(*)** significant, **(**)** very significant, and **(***)** highly significant.

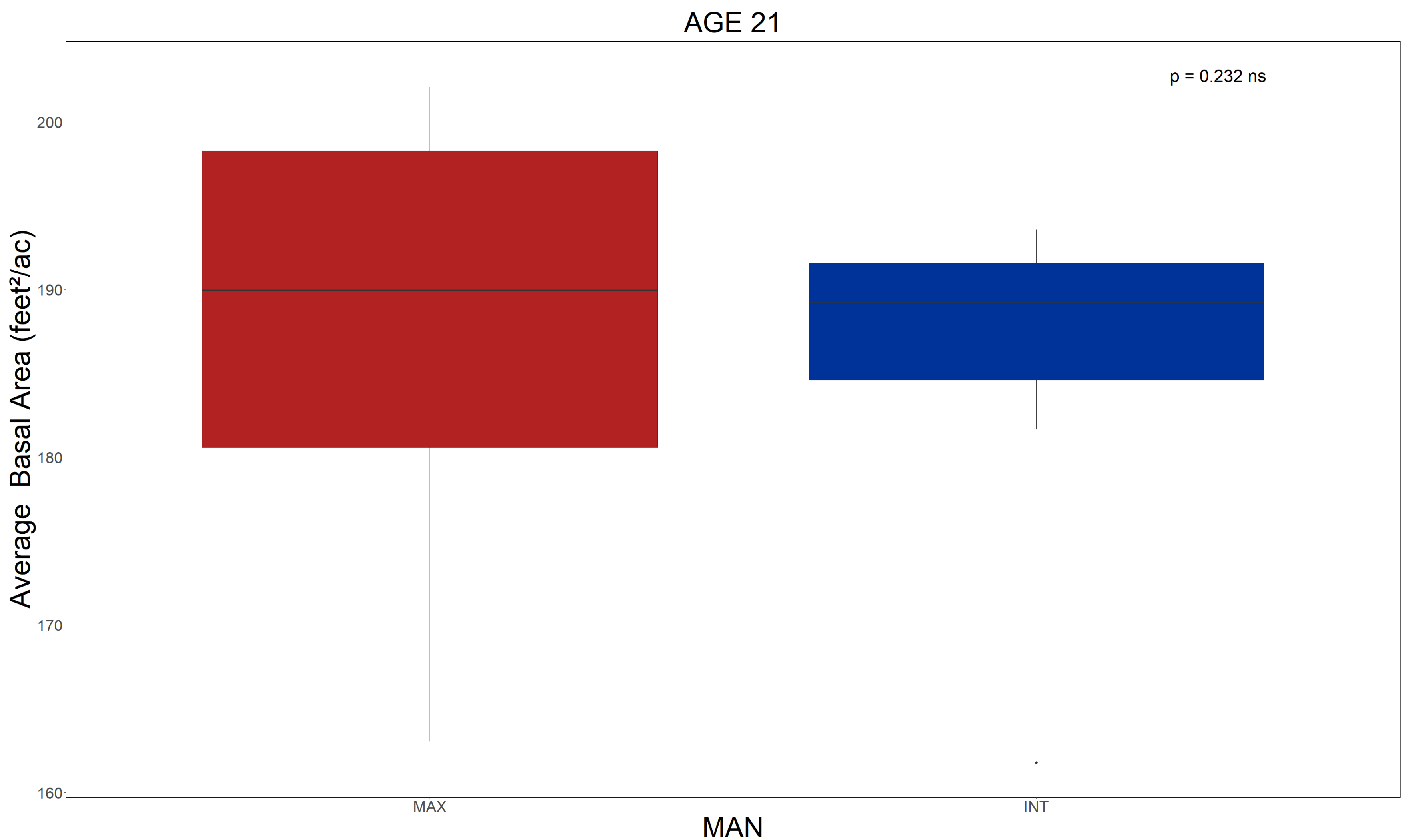

Figure 2.20: Box-plot of two-sample t-test for basal area per acre estimated at age 21, based on Weibull CDF, comparing maximum (MAX) management and intensive (INT) management intensity at an initial planting density (PLTPA) of 450 trees per acre. Significance is based on p-values with $\alpha = 0.05$: **(ns)** not significant, **(*)** significant, **(**)** very significant, and **(***)** highly significant.

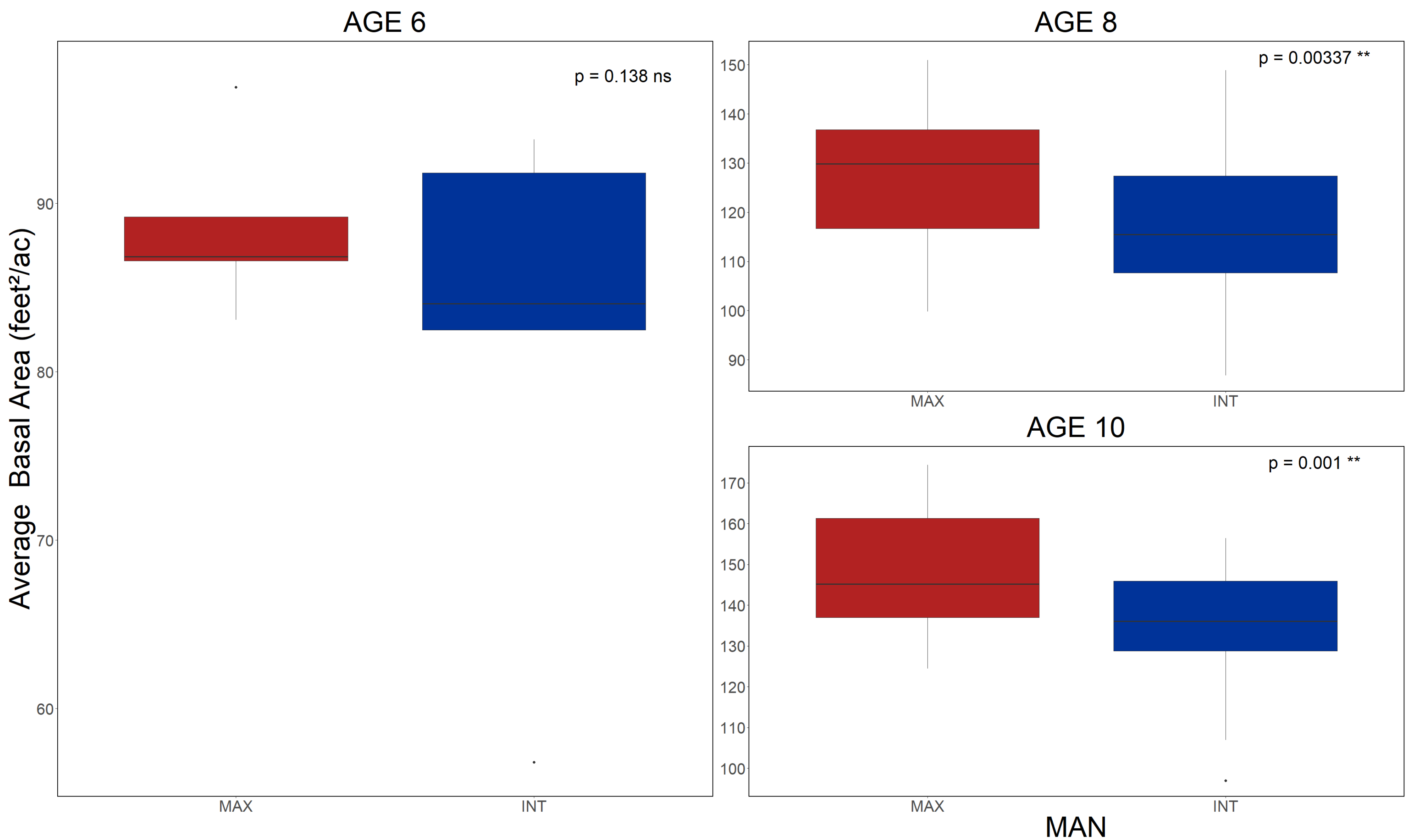

Figure 2.21: Box-plot of two-sample t-test for basal area per acre estimated at age 6, 8, and 10, based on Weibull CDF, comparing maximum (MAX) management and intensive (INT) management intensity at an initial planting density (PLTPA) of 700 trees per acre. Significance is based on p-values with $\alpha = 0.05$: **(ns)** not significant, **(*)** significant, **(**)** very significant, and **(***)** highly significant.

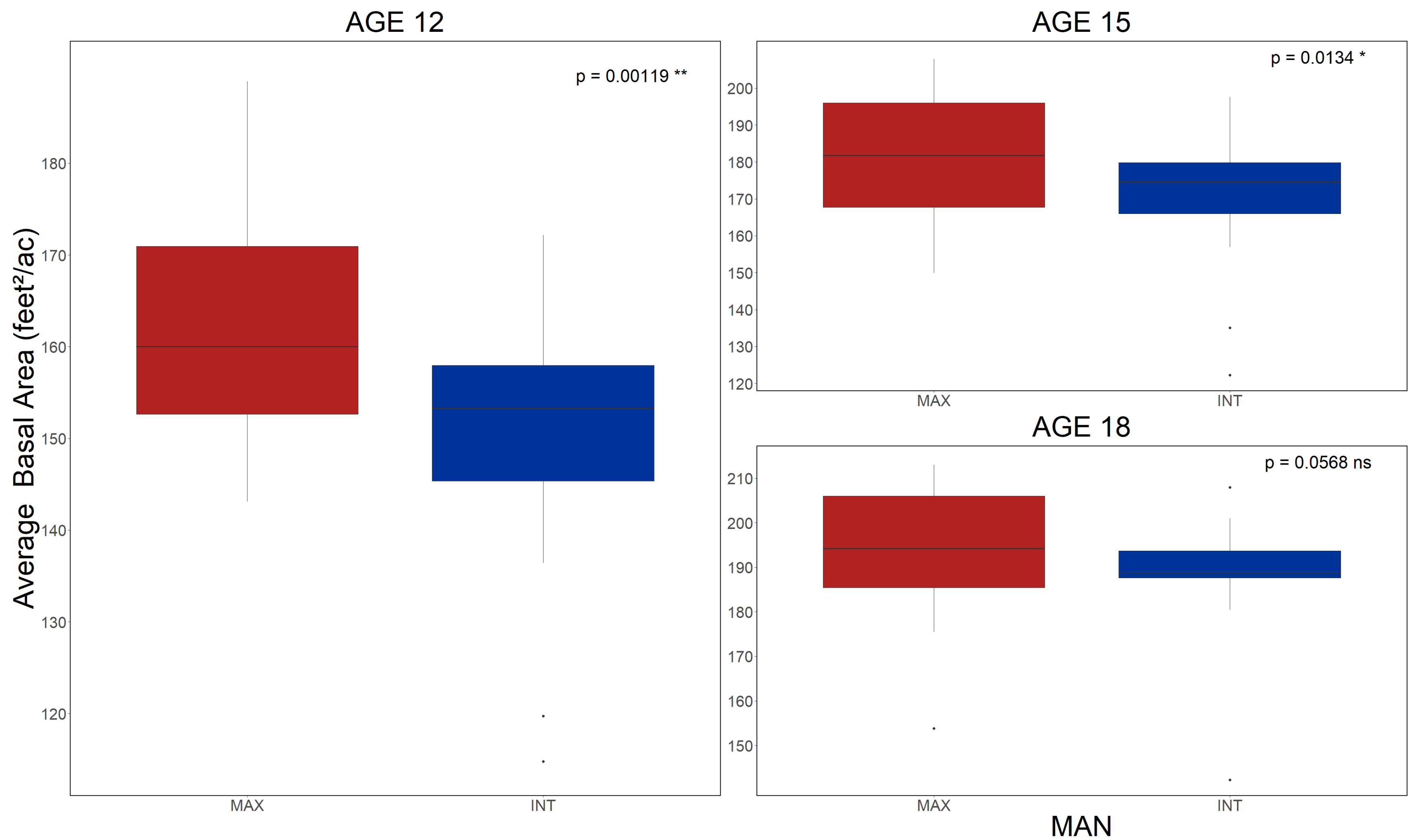

Figure 2.22: Box-plot of two-sample t-test for basal area per acre estimated at age 12, 15, and 18, based on Weibull CDF, maximum (MAX) management and intensive (INT) management intensity at an initial planting density (PLTPA) of 700 trees per acre. Significance is based on p-values with $\alpha = 0.05$: **(ns)** not significant, **(*)** significant, **(**)** very significant, and **(***)** highly significant.

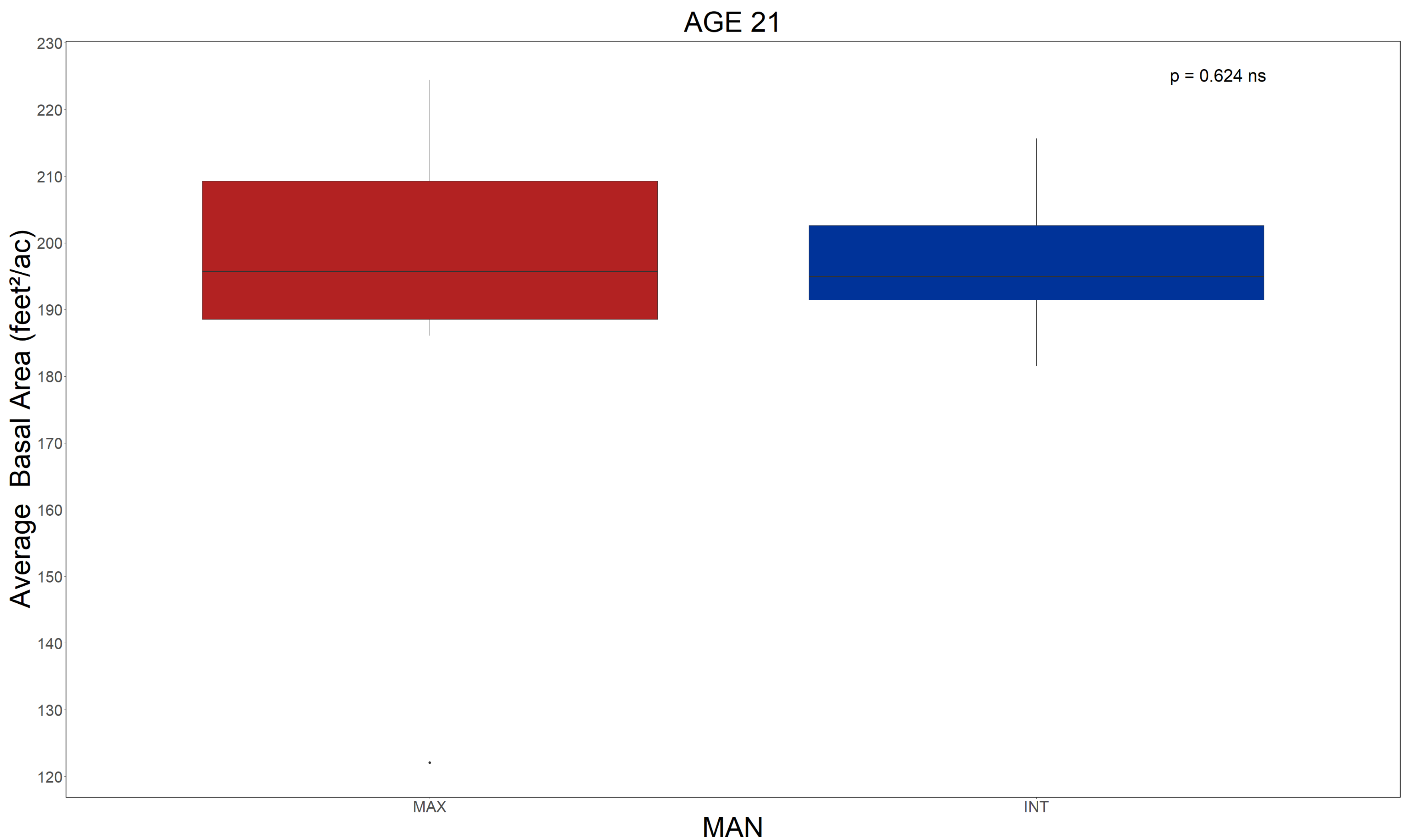

Figure 2.23: Box-plot of two-sample t-test for basal area per acre estimated at age 21, based on Weibull CDF, maximum (MAX) management and intensive (INT) management intensity at an initial planting density (PLTPA) of 700 trees per acre. Significance is based on p-values with $\alpha = 0.05$: **(ns)** not significant, **(*)** significant, **(**)** very significant, and **(***)** highly significant.

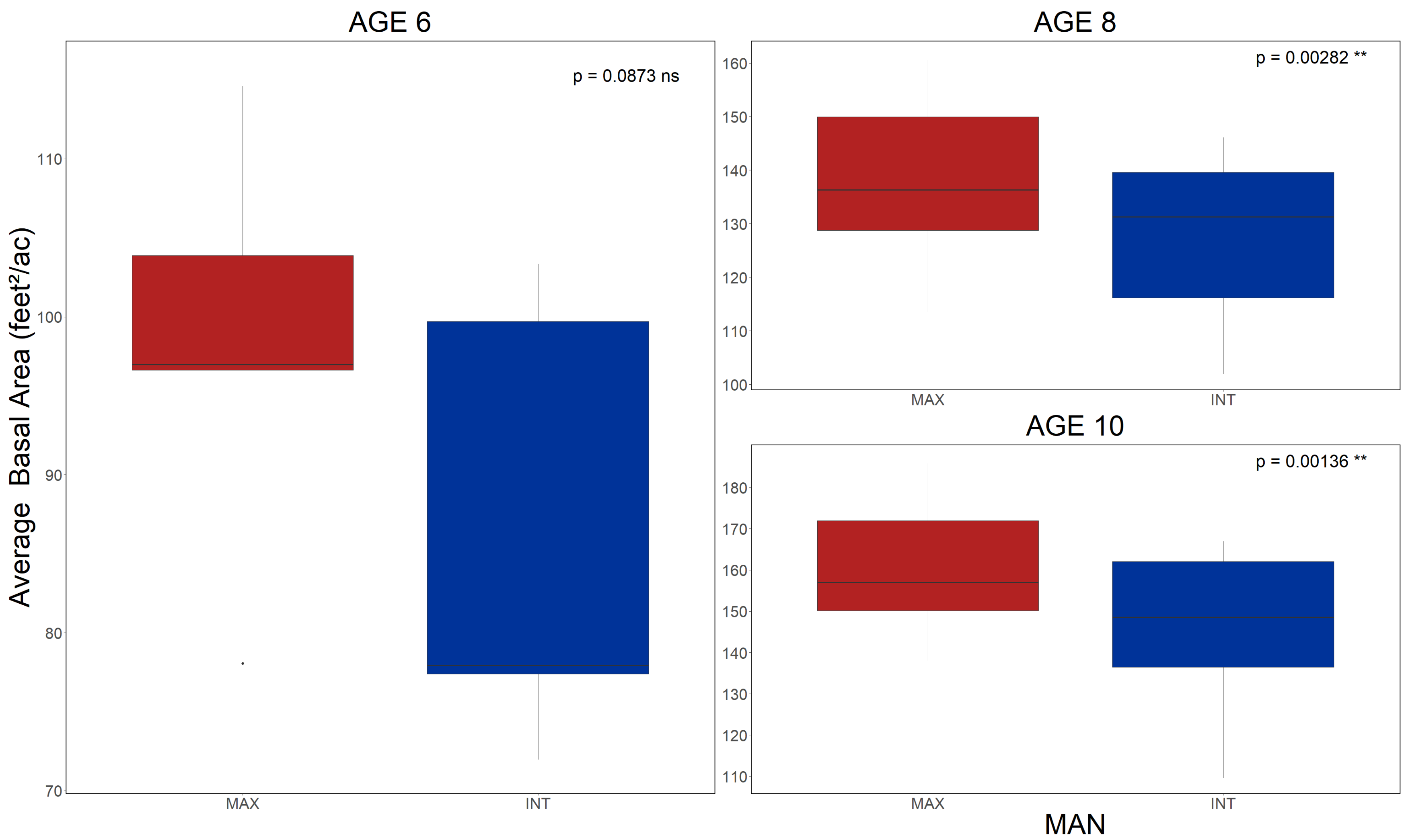

Figure 2.24: Box-plot of two-sample t-test for basal area per acre estimated at age 6, 8, and 10, based on Weibull CDF, comparing maximum (MAX) management and intensive (INT) management intensity at an initial planting density (PLTPA) of 950 trees per acre. Significance is based on p-values with $\alpha = 0.05$: **(ns)** not significant, **(*)** significant, **(**)** very significant, and **(***)** highly significant.

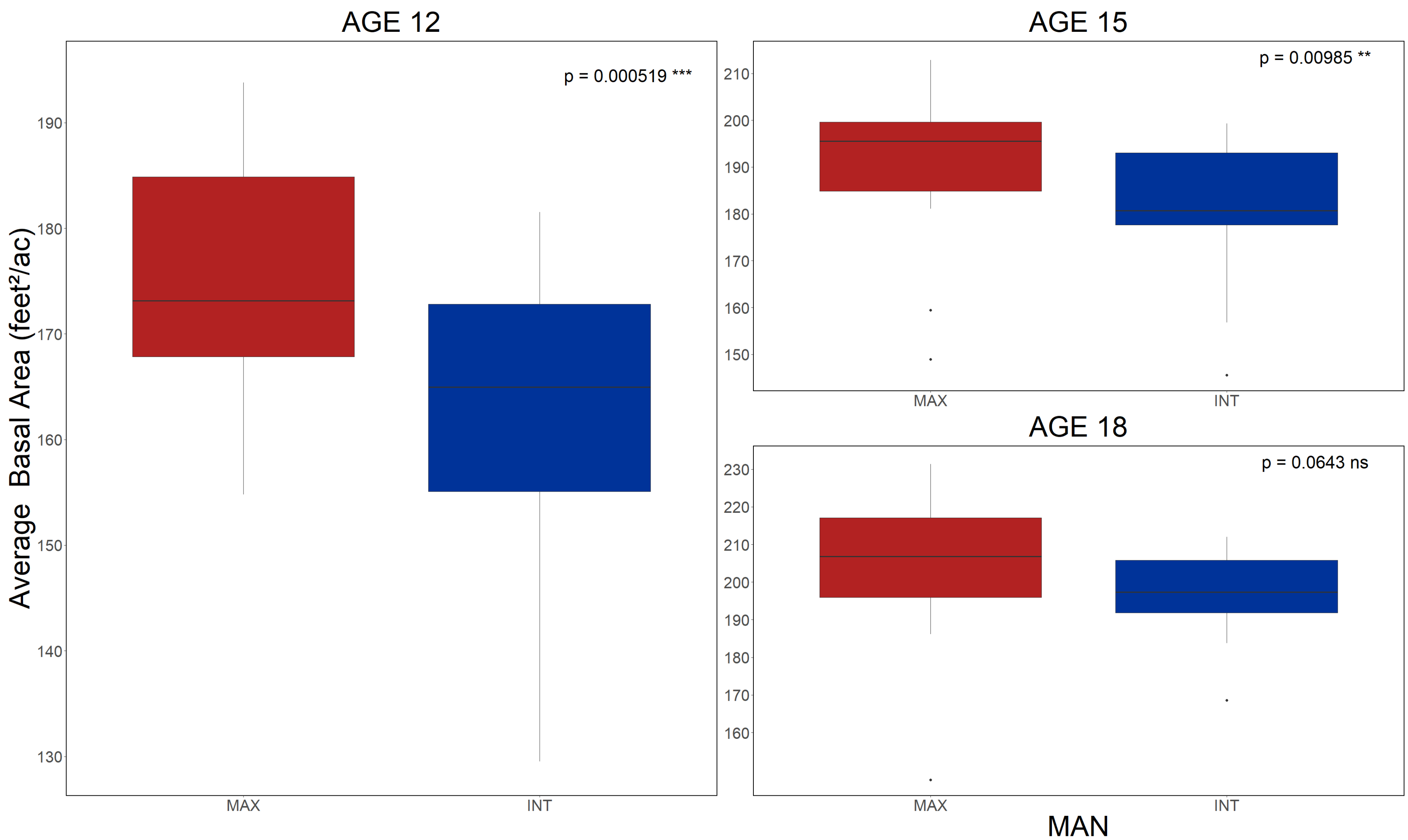

Figure 2.25: Box-plot of two-sample t-test for basal area per acre estimated at age 12, 15, and 18, based on Weibull CDF, comparing maximum (MAX) management and intensive (INT) management intensity at an initial planting density (PLTPA) of 950 trees per acre. Significance is based on p-values with $\alpha = 0.05$: **(ns)** not significant, **(*)** significant, **(**)** very significant, and **(***)** highly significant.

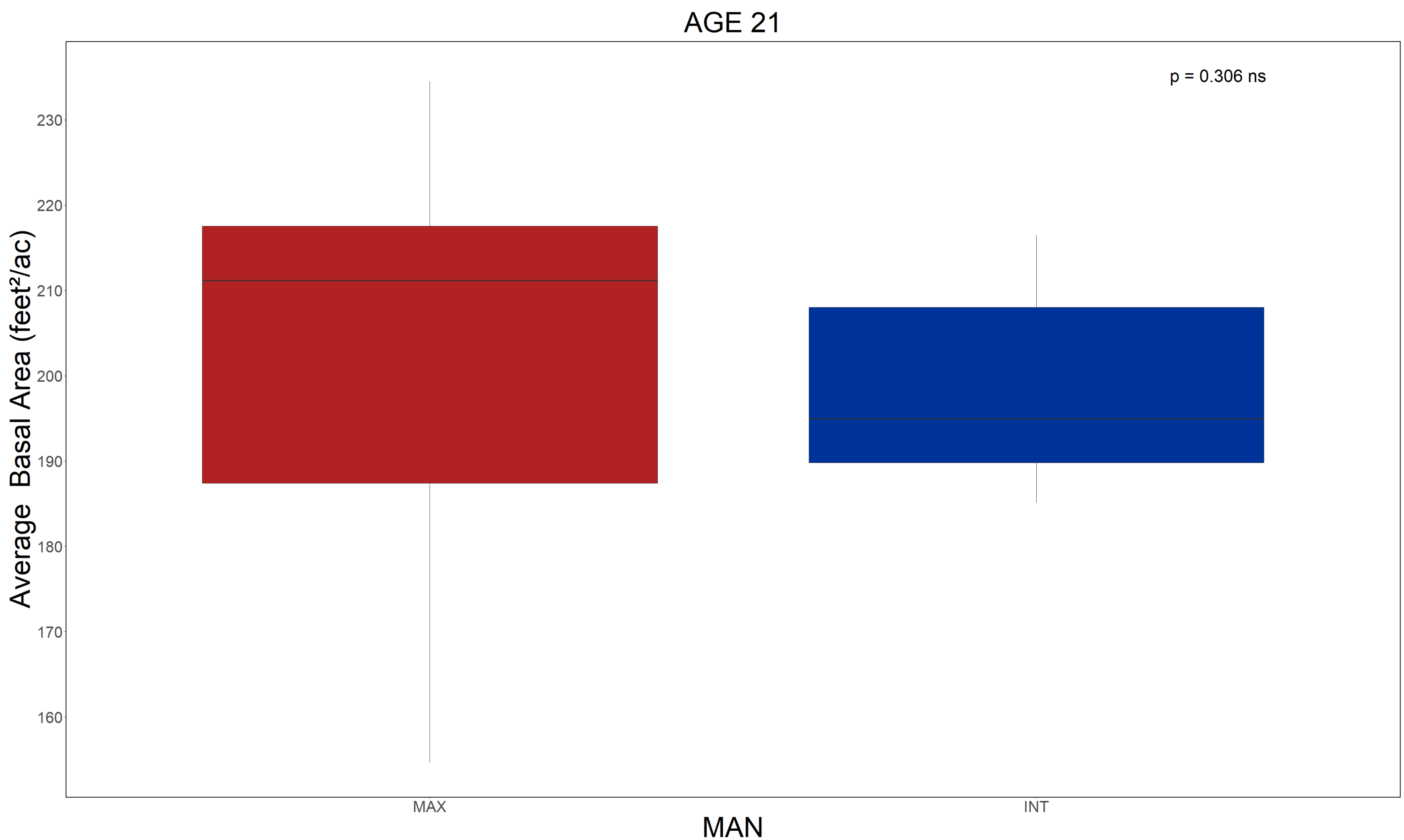

Figure 2.26: Box-plot of two-sample t-test for basal area per acre estimated at age 21, based on Weibull CDF, comparing maximum (MAX) management and intensive (INT) management intensity at an initial planting density (PLTPA) of 950 trees per acre. Significance is based on p-values with $\alpha = 0.05$: **(ns)** not significant, **(*)** significant, **(**)** very significant, and **(***)** highly significant.

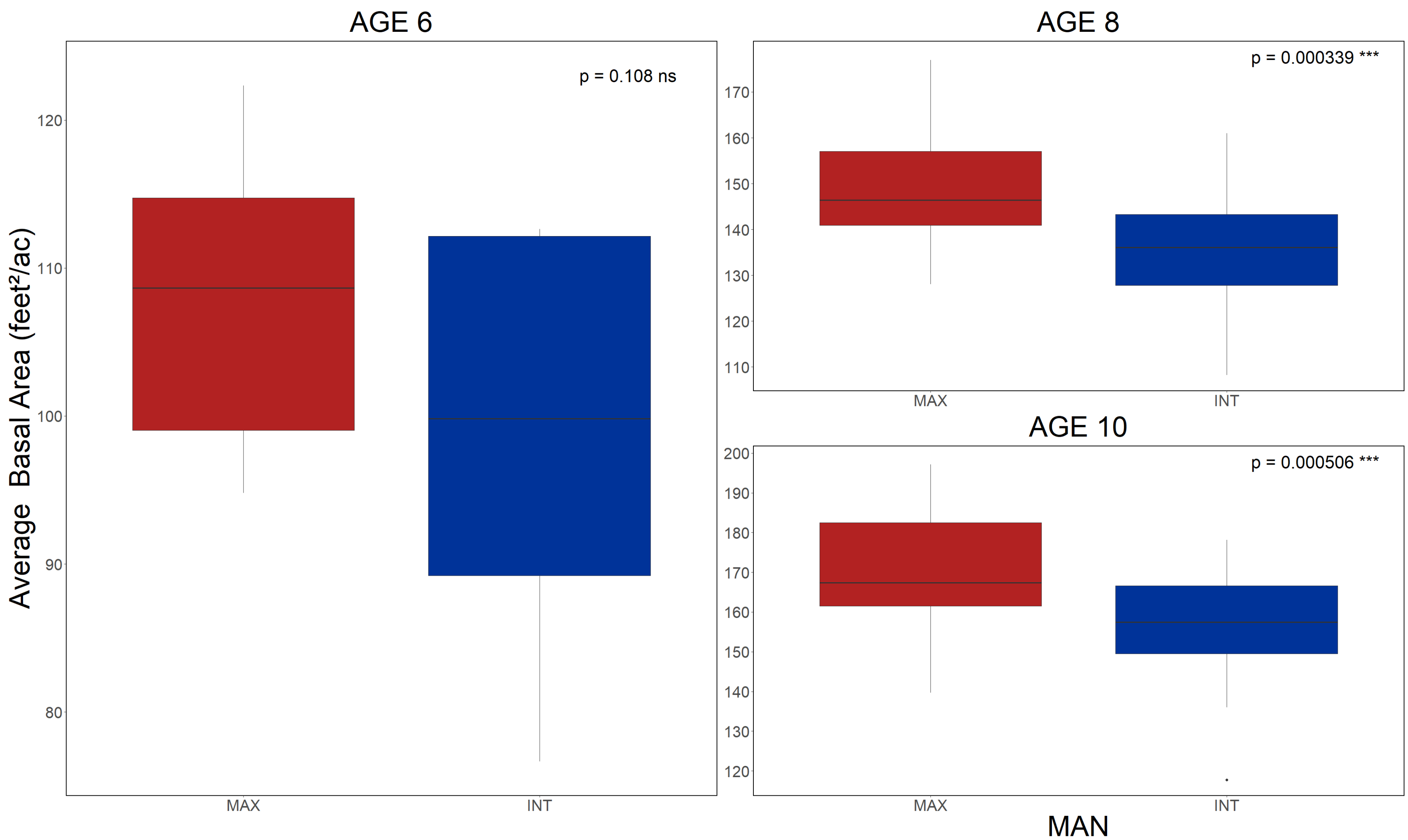

Figure 2.27: Box-plot of two-sample t-test for basal area per acre estimated at age 6, 8, and 10, based on Weibull CDF, comparing maximum (MAX) management and intensive (INT) management intensity at an initial planting density (PLTPA) of 1200 trees per acre. Significance is based on p-values with $\alpha = 0.05$: **(ns)** not significant, **(*)** significant, **(**)** very significant, and **(***)** highly significant.

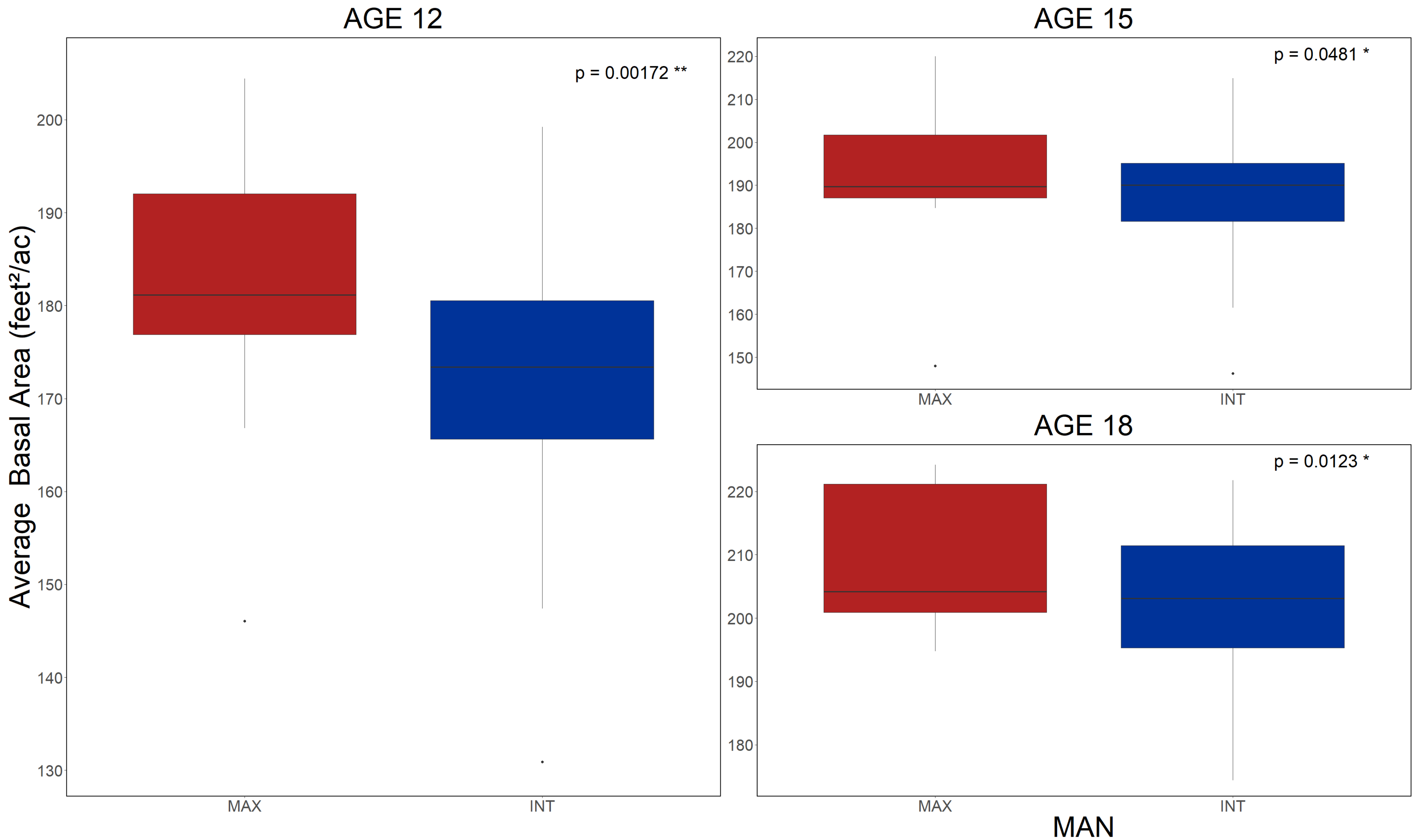

Figure 2.28: Box-plot of two-sample t-test for basal area per acre estimated at age 12, 15, and 18, based on Weibull CDF, comparing maximum (MAX) management and intensive (INT) management intensity at an initial planting density (PLTPA) of 1200 trees per acre. Significance is based on p-values with $\alpha = 0.05$: **(ns)** not significant, **(*)** significant, **(**)** very significant, and **(***)** highly significant.

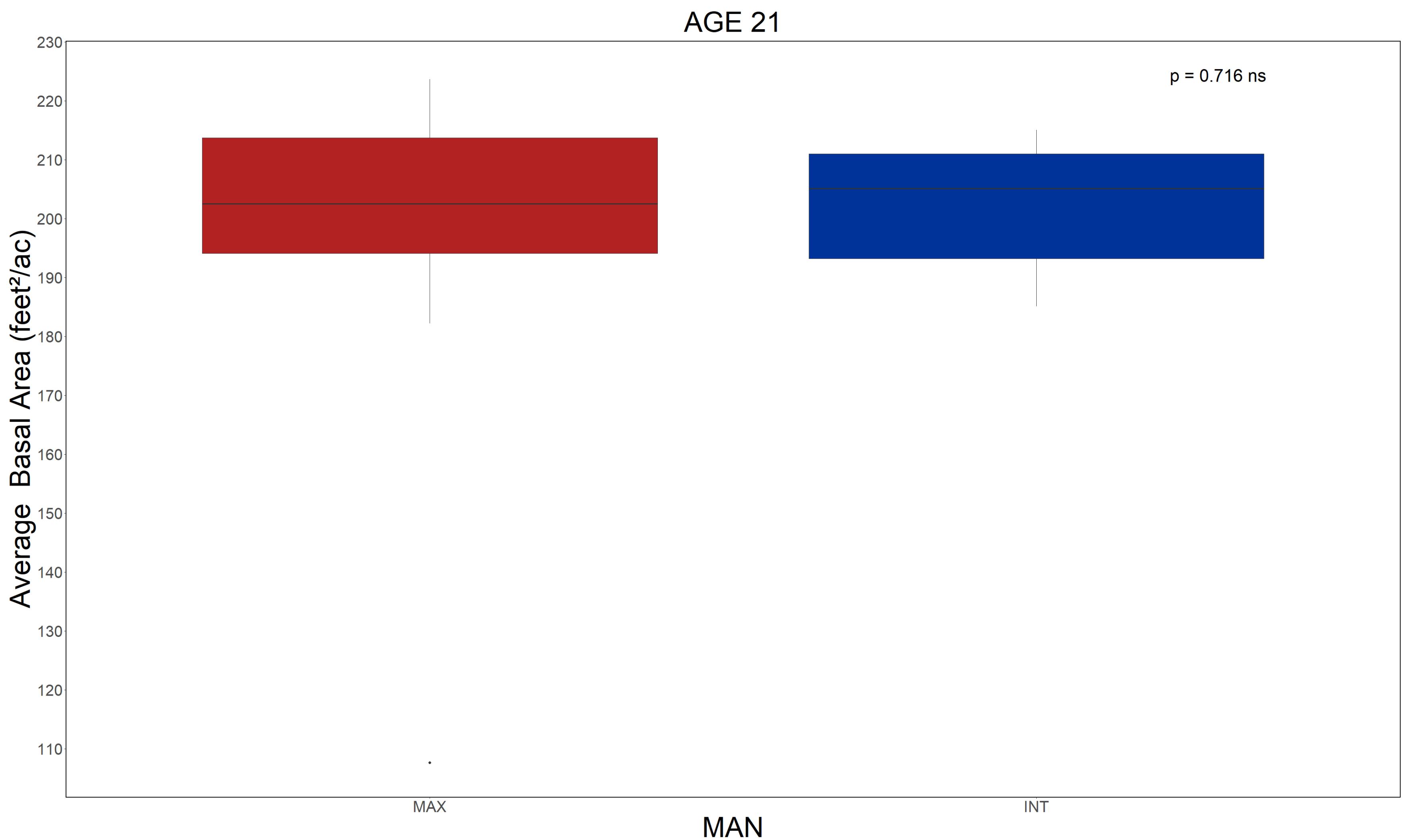

Figure 2.29: Box-plot of two-sample t-test for basal area per acre estimated at age 21, based on Weibull CDF, comparing maximum (MAX) management and intensive (INT) management intensity at an initial planting density (PLTPA) of 1200 trees per acre. Significance is based on p-values with $\alpha = 0.05$: **(ns)** not significant, **(*)** significant, **(**)** very significant, and **(***)** highly significant.

;

Table 2.34: One-inch diameter classification based on DBH (Diameter at Breast Height at 4.5' or 1.3 meters) assuming a measurement precision of 0.1 inch.

DBH Range (inches)	Class
$\leq$ 1.5	1"
1.6 – 2.5	2"
2.6 – 3.5	3"
3.6 – 4.5	4"
4.6 – 5.5	5"
5.6 – 6.5	6"
6.6 – 7.5	7"
7.6 – 8.5	8"
8.6 – 9.5	9"
9.6 – 10.5	10"
10.6 – 11.5	11"
11.6 – 12.5	12"
12.6 – 13.5	13"
13.6 – 14.5	14"
14.6 – 15.5	15"
15.6 – 16.5	16"
16.6 – 17.5	17"
17.6 – 18.5	18"
18.6 – 19.5	19"
19.6 – 20.5	20"

Table 2.35: Precision on average parameter estimates across all ages, five planting densities, and two silvicultural management intensities.

AGE	PLTPA	INT		MAX	
		Error Index	RMSE	Error Index	RMSE
6	200	14.75	11.50	12.11	10.28
	450	48.96	38.01	51.07	39.68
	700	51.72	50.17	45.03	34.77
	950	80.61	55.26	50.57	35.10
	1200	84.23	63.17	58.63	43.70
8	200	18.91	14.38	22.15	16.52
	450	42.83	30.92	37.66	29.85
	700	50.23	40.19	39.82	32.18
	950	81.20	54.90	47.15	37.67
	1200	70.08	55.95	47.71	39.22
10	200	16.49	13.08	14.17	11.45
	450	36.53	25.58	34.54	25.21
	700	41.35	32.55	38.69	30.92
	950	62.41	48.05	45.69	36.60
	1200	69.43	48.71	56.69	43.79
12	200	17.20	13.25	16.24	13.03
	450	37.06	26.20	29.29	22.37
	700	31.10	26.58	35.93	28.07
	950	61.04	48.23	43.32	33.22
	1200	62.35	47.87	40.57	35.32
15	200	17.05	14.57	16.67	14.15
	450	28.89	23.02	26.04	20.91
	700	28.96	23.67	28.21	21.93
	950	40.55	34.40	28.57	24.73
	1200	48.67	39.49	30.90	23.57
18	200	14.02	12.20	14.87	12.63
	450	23.33	20.59	20.19	16.98
	700	23.63	19.11	21.88	17.78
	950	31.52	25.97	28.96	21.13
	1200	34.64	26.19	27.94	20.49
21	200	14.05	13.28	11.81	12.31
	450	28.53	23.13	20.05	15.77
	700	17.38	15.48	18.76	14.36
	950	30.59	26.17	26.17	19.17
	1200	29.09	22.35	21.09	15.86

Chapter 3

Accounting for environmental co-variables in diameter distributions of loblolly pine (*Pinus taeda L.*) plantations[1]

[1]Maciel, G.O.P., B. P. Bullock, S.M. Kinane, and S. Sandoval. To be submitted to *Forest Ecology and Management*.

3.1 Abstract

Diameter distribution models have been shown to be a powerful tool for characterizing forest structure and forest dynamics. Using diameter distributions, stand tables can be generated to support forest managers in making decisions about the future development of a stand. However, traditional diameter distribution models typically use stand-level variables, which may not account for the effect of environmental co-variables on forest structure. In this study environmental co-variables were included in the diameter distribution modeling process to improve the three-parameter Weibull distribution estimation. Results from this study indicate that environmental co-variables such as maximum temperature, water deficit, and precipitation were important for recovering the four percentiles used in this study. Additionally, by accounting for environmental co-variables in the diameter distribution modeling process, part of the diameter variability could be explained that was previously attributed only to the effects of age and planting density. Based on the error index test and RMSE results, improvements in goodness-of-fit and precision in the three-parameter Weibull distribution were achieved, particularly at younger and mid-rotation ages, with more notable enhancements observed in the middle and higher planting densities levels.

3.2 Introduction

Globally, many models have been developed to characterize forest dynamics and forest structure; these models are the foundation of growth and yield systems (G&Y). G&Y systems use traditional variables (e.g., average diameter, quadratic mean diameter, average total height of the dominant trees, site index, basal area, tree per acre), as they explain the growth and productivity for even-aged planted systems quite well. The major goal of G&Y systems besides the characterization of forests is to provide information to forest managers for decision-making. The information is based on predictions of current conditions and then projections for future conditions. With predictions and projections, forest managers can make informed decisions around management practices such as thinning, fertilization, weed and vegetation control, and fire prescriptions to increase the site productivity and achieve the landowner objectives. Using silviculture to manipulate the site is important for growth and forest development; for example, thinning is an effective forest management technique to increase individual tree DBH tree and reduce tree mortality (Clutter et al., 1983; Weiskittel et al., 2011). This technique helps decrease competition between trees, and consequently for nutrients, forest health, and drought effects (Hennessey et al., 1992; Nyland, 2016; Zhao et al., 2025). Additionally, fertilization treatments have been shown to increase tree development in sites with nutrient deficiencies (Matziris and Zobel, 1976; Gough et al., 2004; Jackson et al., 2008). Although traditional site manipulation can improve site productivity, many studies have suggested that growth and survival of forests might be affected by climatic changes (Overpeck et al., 1990, 1991).

Wood characteristics (e.g., diameter growth) are highly affected by environmental covariables (Dougherty et al., 1994). An increase in temperature, for example, affects tree development by decreasing forest productivity (Clark et al., 2003). On the other hand, soil-available water and nutrient availability, individually or in conjunction, increase forest productivity, and water availability has a higher effect on forest biomass (McMurtrie et al., 1990; Poorter et al., 2017).

Traditional G&Y models face challenges in capturing the effects of environmental co-variables to characterize the effect of climate changes in forest dynamics and forest structure (Reyer, 2015; Maréchaux et al., 2021; Boukhris et al., 2025). For example, diameter distribution models are one of many models that are integrated into the G&Y system. Many studies that used traditional diameter distribution models have focused only on how the diameter distribution is affected by different planting densities or by comparing different parameter estimation techniques (Sandoval et al., 2012; Bullock and Burkhart, 2005; Poudel and Cao, 2013). Although diameter distribution modeling is common and important for management decisions (e.g., fertilization, thinning, weed control treatment) and to represent forest dynamics by a distribution by DBH classes (Jokela et al., 2004), few studies have explored the integration of new variables as auxiliary variables, such as environmental co-variables into the diameter distribution modeling process. It has been shown that including environmental co-variables in the diameter distribution process can enhance performance by improving the goodness-of-fit (Guo et al., 2024). Accounting for physiological and environmental co-variables into G&Y systems can help us to understand the potential effects on forest productivity—for example, growth efficiency and annual moisture stress (McMurtrie et al., 1994; Weiskittel et al., 2011).

This research focuses on investigating how diameter distributions in the Western Gulf physiographic region is affected by the inclusion of environmental co-variables across different planting densities and ages in loblolly pine *(Pinus taeda L.)* plantations. While diameter distributions have been studied and used over the past 50 years to create stand tables and to characterize forest dynamics and structure, traditional models that rely solely on common variables are still widely used. There is a lack of research in the literature regarding environmental co-variables that can influence diameter distributions and potentially improve predictions.

3.3 Literature Review

Many studies have acknowledged the increasing impact of environmental co-variables on tree growth and yield due to climate change (Huang et al., 2011). It has been suggested that environmental co-variables can have both positive effects (e.g., increases in forest vigor, increased water use efficiency) and negative, with increases in mortality due to climate change (Allen et al., 2010). The frequency and the intensity of drought and increasing temperatures can affect tree growth and result in higher mortality risks (Allen et al., 2010; Meir et al., 2015; de Streel et al., 2022; Lévesque et al., 2014). It has been shown that environmental co-variables such as temperature and water deficit play a crucial role in tree survival (Matallana-Ramirez et al., 2021). Forest mortality index increases in long-term, while forest growth decreases due to higher water stress, warmer temperatures, and vapor pressure deficit (Breshears et al., 2005, 2009; Dannenberg et al., 2019). For trees located in regions where water limitation is an issue, precipitation is the most crucial factor affecting annual variation in diameter growth rates (Adhikari et al., 2021).

Traditional growth and yield systems have been created to assist forest management decisions with the assumptions that sites are stable over time. These models are not able to project the impact of variation in climate in predictions and the impact of change in the predictions (Skovsgaard and Vanclay, 2013; Elli et al., 2017). For that reason, scientific studies have been adapting models to account for climate change with the main goal of obtaining better and more accurate predictions (Lei et al., 2016; Fu et al., 2017; Elli et al., 2017). One way to obtain a more accurate estimation considering climate change is by accounting for environmental co-variables. Besides providing better predictions, they can also provide useful simulation of the effects of future climate change in forest dynamics (Guo et al., 2022). One study developed in the Western Gulf physiographic region with environmental co-variables related to precipitation (i.e., water deficit, excess water, and available water) showed to be important and could improve the estimation for dominant height (Koirala et al., 2021). This environmental co-variable showed to have a strong correlation with Weibull parameters estimation for diameter distributions (Sanquetta et al., 2014). The strong correlation between diameter distribution parameters and precipitation is due to higher precipitation, resulting in higher diameter ring growth and DBH increment (Watson and Luckman, 2001; Sanquetta et al., 2014).

As described in the previous chapters, diameter distribution models are part of the G&Y system and enable the characterization of forest structure with volume or tonnage by diameter classes. To obtain more accurate stand and stock tables, environmental co-variables are now considered in diameter distribution modeling. The Weibull distribution is one of the most common approaches to compute diameter distributions. One study developed using the Weibull function to characterize *Larix principis- rupprechttii* plantation diameter distributions across northern China included soil variables in the diameter distribution modeling process and showed that this co-variable could improve the Weibull parameter estimates. The scale and shape parameter showed to be sensitive when soil co-variable was included (Guo et al., 2024). Another study showed that environmental co-variables related to temperature and precipitation improved statistical model fit compared to traditional models, leading to better performance (Guo et al., 2022). These co-variables show potential for inclusion in diameter distribution modeling for growth and yield prediction under future climate change scenarios (Guo et al., 2022).

3.4 Methods

3.4.1 Study Area & Data Structure

For this chapter, only data from the intensive silvicultural management treatments from the WGCDS were used. This type of management was chosen because it is more closely aligned with common practices in the Western Gulf region for plantation forestry. The results of the diameter distribution modeling for stands under this type of management will be informative for landowners and forest industry, providing a reference, especially in cases where a stand and management characteristics are similar to those presented in this research. The analysis was conducted using data from the intensive management, as previously mentioned; installations that received thinning treatment were not considered for this analysis in this chapter. It is important to remember that the WGCDS includes five initial planting densities (PLTPA), two levels of silvicultural management (MAN): intensive (INT) and maximum (MAX) levels of management, two levels of thinning treatment (thin to 200 and 450 TPA), with measurements taken at ages 6, 8, 10, 12, 15, 18, and 21 years (more details can be found in Chapter I). In total, 484 plots were analyzed in this chapter, distributed across the following regions: Interior Flatwoods (IF), Lower Coastal Plain (LCP), and Upper Coastal Plain (UCP), representing 25.83%, 23.77%, and 50,40% of the data used in the analyzes, for each region respectively (Figure 3.1).

3.4.2 Environmental Data

PRISM Climate Data

Environmental data from Oregon State University PRISM Climate Group was the base to create the environmental database used in this analysis. The Parameter-elevation Regressions on Independent Slopes Models (PRISM) is considered to obtaining environmental dataset for agriculture, ecology, hydrology, and natural resource conservation studies. PRISM can be defined as a knowledge-based system to interpolate climate data in complex landscapes locations (Daly et al., 2008). The PRISM method consists of point data, a digital elevation model (DEM), other spatial data sets, and an encoded spatial climate knowledge. The DEM is considering the most important grid input on PRISM (Daly et al., 2008). PRISM provides many environmental datasets such as maximum, minimum, and mean temperature; precipitation; potential evapotranspiration; and others. The dataset covers short-term and long-term weather in the period from 1895 to present and across many different levels (i.e. daily, monthly, and yearly).

Water Storage Capacity Data

The environmental database was created using PRISM data, with water storage capacity data used as an auxiliary dataset. The data for the amount of water in the soil was obtained from the US Department of Agriculture, Natural Resources Conservation Service SSURGO, with data available since December 2024 through the Esri website. The layer used to create the database is based on 30 meters (m) raster produced by the Natural Resources Conservation Service (NRCS). The data is fixed, and available water storage is 0-150 centimeters (cm) weighted average.

Environmental Data Structure

To obtain the environmental co-variables from PRISM used in this chapter, the centroid was used based on latitude and longitude of each WGCDS INST. ArcGIS Pro (version 3.5.0) was used to create a buffer based on plot size and then transform the circle shapefile into a rectangle shapefile to follow the study plot design. Six environmental co-variables were taken from the PRISM dataset: Maximum ($\mathrm{Temp_{max}}$), Minimum ($\mathrm{Temp_{min}}$), and Mean ($\mathrm{Temp_{mean}}$), Precipitation (PPT), Hargreaves Potential Evaporation (PET), and Potential Water Deficit. The Hargreaves PET can be obtained using the maximum and minimum air temperature, and the extraterrestrial radiation (Equation 3.1) (Fisher and Pringle III, 2013). And the potential water deficit (WD) can be obtained from PPT and PET (Equation 3.2). Two more environmental co-variables were calculated and obtained based on PPT and PET: the excess of water (EW) and availability of water (AW) (Equation 3.3 – 3.4) (Koirala et al., 2021). The six environmental datasets from PRISM were taken monthly, over a period of 21 years (From 2001 to 2022) and at 4 kilometers (4000 m – 1/24-deg) of resolution aligning with the measurement dates and location of the study sites used in this research.

$$\mathrm{PET_0} = 0.023(0.408)\mathrm{Temp_{mean}} + 17.8)\mathrm{Temp_{max}} - \mathrm{Temp_{min}})^{0.5}\mathrm{R_a} \tag{3.1}$$

Where the PET is the potential evapotranspiration; Temp_{max} is the maximum air temperature (F); Temp_{min} is the minimum air temperature (F); $\text{Temp}_{\text{mean}}$ is the mean air temperature (F). R_a is the extraterrestrial radiation (MJ.m^{-2}), and 0.408 is a factor to transform MJ m^{-2} to mm. The location's latitude and the calendar day of the year are used to estimate the R_a.

$$\text{WD}_\text{j} = \sum_{i=1}^{n}[\text{PET}_{\text{i,j}} > \text{PPT}_{\text{i,j}}] = (\text{PET}_{\text{i,j}} - \text{PPT}_{\text{i,j}}) \tag{3.2}$$

$$\text{EW}_\text{j} = \sum_{i=1}^{n}[\text{PPT}_{\text{i,j}} > \text{PET}_{\text{i,j}}] = (\text{PPT}_{\text{i,j}} - \text{PET}_{\text{i,j}}) \tag{3.3}$$

$$\text{AW}_\text{j} = \sum_{i=1}^{n}([\text{PET}_{\text{i,j}} > \text{PPT}_{\text{i,j}}] = \text{PPT}_{\text{i,j}} + [\text{PPT}_{\text{i,j}} > \text{PET}_{\text{i,j}}]\text{PET}_{\text{i,j}}) \tag{3.4}$$

Where the WD, EW, AW are water deficit, excess of water, availability of water respectively; PET is potential evapotranspiration; PPT is the precipitation.

The water storage capacity (WSC) data was converted to imperial units and was integrated with the environmental database to calculate three additional co-variables for each INST (Equation 3.5 - 3.7): soil water deficiency (Soil_{WD}), soil water excess (Soil_{EW}), and soil water availability (Soil_{AW}) . Since the WSC data is constant, the values are the same for all years.

$$\text{Soil}_{\text{WD}_\text{j}} = \sum_{i=1}^{n}[\text{PET}_{\text{i,j}} > \text{PPT}_{\text{i,j}}](\text{PET}_{\text{i,j}} - \text{PPT}_{\text{i,j}}) + [\text{EW}_{\text{i,j}} > \text{S}_{\text{WSC}}]\text{S}_{\text{WSC}} + [\text{EW}_{\text{i,j}} < \text{S}_{\text{WSC}}]\text{EW}_{\text{i,j}} \tag{3.5}$$

$$\text{Soil}_{\text{EW}_\text{j}} = \sum_{i=1}^{n}[\text{PPT}_{\text{i,j}} > \text{PET}_{\text{i,j}}](\text{PPT}_{\text{i,j}} - \text{PET}_{\text{i,j}}) + [\text{WD}_{\text{i,j}} > \text{S}_{\text{WSC}}]\text{S}_{\text{WSC}} + [\text{WD}_{\text{i,j}} < \text{S}_{\text{WSC}}]\text{EW}_{\text{i,j}} \tag{3.6}$$

$$\mathrm{Soil}_{\mathrm{AW}_j} = \sum_{i=1}^{n} [\mathrm{PET}_{i,j} > \mathrm{PPT}_{i,j}]\,\mathrm{PPT}_{i,j} + (\mathrm{PPT}_{i,j} - \mathrm{PET}_{i,j}) + \mathrm{PET}_{i,j} \\ + [\mathrm{EW}_{i,j} > \mathrm{S}_{\mathrm{WSC}}]\,\mathrm{S}_{\mathrm{WSC}} + [\mathrm{EW}_{i,j} < \mathrm{S}_{\mathrm{WSC}}]\,\mathrm{EW}_{i,j} \qquad (3.7)$$

Where $\mathrm{Soil}_{\mathrm{WD}_j}$, $\mathrm{Soil}_{\mathrm{EW}_j}$, and $\mathrm{Soil}_{\mathrm{AW}_j}$ represent soil water deficiency, soil water excess, and soil water availability, respectively; $\mathrm{S}_{\mathrm{WSC}}$ denotes the soil water storage capacity; and the terms PPT, PET, WD, EW, and AW were defined previously.

The environmental co-variables were selected between the year of the first growing season and the growing season of measurement. The year of measurement differs for INST and AGE (the period after which the trees were measured), and the average was calculated by INST, AGE, and PLTPA. Further details are provided in Table 3.7.

3.4.3 Analysis & Approaches

The selection analysis for choosing the environmental co-variables to include in diameter distribution modeling was based on the lasso regression technique (Tibshirani, 1996). The goal of using lasso regression was to select possibles environmental co-variables that could improve the prediction of percentiles of the diameter distributions and avoid any issues of multicolineality.

K-fold Cross-Validation

The k-fold cross-validation was used in the entire analysis. The cross-validation (CV) approach is a technique in which the dataset is divided into two datasets, a training dataset and a testing dataset (Yang and Huang, 2014). This technique is the simplest to estimate prediction error, by estimating the expected extra-sample error $\mathrm{Err} = \mathrm{E}[\mathrm{L}(\mathrm{Y}, \hat{f}(\mathrm{X}))]$, the average generalization error when the technique $\hat{f}(\mathrm{X})$ is applied to an independent test sample from the joint distribution of X and Y (Hastie et al., 2001). The k-fold CV technique split the dataset randomly into k fold of approximately equal size. With k-fold, each time a k-fold is used as testing $(k-1)$, and one part of dataset is available to fit the model. After the process of CV, the average prediction error based on the testing dataset across all k-fold is computed. For k-fold CV approach is common set 5 or 10 folds, this decision depends on the objective of the analysis and the dataset size. With 5 or 10 folds, the expectation is to estimate the expected error (Err), because the training sets in each fold are slightly different from the original training set (Hastie et al., 2001; Yang and Huang, 2014; Koirala et al., 2021).

Lasso Regression

Lasso regression is a powerful approach very commonly used for linear and generalized linear models (Nardi and Rinaldo, 2011). Developed by Tibshirani (1996), lasso regression is a technique for variable selection and parameter estimation simultaneously, making this approach highly preferred by researchers (Wang et al., 2007). The lasso regression technique is based on regularization penalty (Equation 3.8). The lambda controls the adjustment through regularizing to the estimate, by reducing the coefficients toward to 0 as the lambda increases, in some cases the coefficients can be exactly 0 (Zhao and Yu, 2006; Zou, 2006).

$$\hat{\beta}_{\mathrm{lasso}} = \arg\min_{\beta} \left\| \mathrm{y} - \sum_{\mathrm{j}=1}^{\mathrm{p}} \mathrm{x_j}\beta_{\mathrm{j}} \right\|^2 + \lambda \sum_{\mathrm{j}=1}^{\mathrm{p}} |\beta_{\mathrm{j}}| \tag{3.8}$$

Where y is the response vector, $\mathrm{x_j}$ is the predictor variable corresponding to the j-th column of matrix X; β_{j} are the coefficients; $\left\| \mathrm{y} - \sum_{\mathrm{j}=1}^{\mathrm{p}} \mathrm{x_j}\beta_{\mathrm{j}} \right\|^2$ is the residual sum of squares (RSS); λ is a non-negative regularization parameter; $\sum_{\mathrm{j}=1}^{\mathrm{p}} |\beta_{\mathrm{j}}|$ is the L1 penalty, where $|\beta_{\mathrm{j}}|$ denotes the L1 norm — the sum of the absolute values of the vector's entries.

The fivefold cross-validation approach was used through lasso regression in this analysis. The eleven environmental co-variables, along with the INST, DBH percentiles were used as response variables in the lasso regression. The analysis was performed for all four desired percentiles separately. As previously mentioned, lasso regression was developed for linear models. The percentiles prediction models used in the analysis are non-linear, but they become linear when the natural logarithm is applied. Therefore, the lasso regression method was considered appropriate for this analysis

3.4.4 Diameter Distribution Modeling

Percentile Regression Models

The performance of percentile regression models were conducted in two phases. This sub-subsection describes the first phase, while the next sub-subsection covers the second phase. In this phase, the goal was to compare the performance of the three base models used to predict the 0^{th}, 25^{th}, 50^{th}, 95^{th} percentiles of DBH distribution. The performances of the percentile regressions were evaluated using k-fold cross-validation. The regressions were computed at two levels, For the first level (i.e. the general level) the base models used the common predictor variables (e.g., HD, Dq, BA, AGE) and combined the three regional datasets into a single dataset, with fivefold cross-validation. For the second level (i.e., the regional level), the base models were applied separately to each region (LCP, UCP, and IF), creating three regional datasets. Tenfold cross-validation was performed within each region, and the results from the three datasets were then combined to compute the three-parameter Weibull distribution.

The first model (M1) was used in chapter II, developed by Jiang and Brooks (2009) (JB). In this model, the logarithm dominant tree height, logarithm age, logarithm quadratic mean diameter, and logarithm of the 50^{th} diameter (D_{50}) percentile of the dataset, were used to predict the diameter percentiles (Equations 2.16 - 2.19). The second model (M2) was developed by Cao (2004) (Cao). In this model, the variables are relative spacing, number of trees per acre, dominant tree height, and age were used to predict diameter percentiles, and it was also used to estimate the D_q used in M1 in chapter II (Equation 2.24). The third model (M3) was developed by Harrison and Borders (1996), a model from Plantation Management Research Cooperative (PMRC). In this model, basal area and number of trees per acre were used to predict diameter percentiles (Equation 3.9).

$$\ln(P_x) = \beta_1 + \beta_2 \ln\left(\frac{BA}{TPA}\right) \tag{3.9}$$

Where P_x is the percentiles (D_0, D_{25}, D_{50}, D_{95}); BA is basal area per acre; TPA is tree per acre, β_1 and β_2 coefficients to be estimate; ln is the natural logarithm.

All models were adapted to the WGCDS dataset, in which the PLTPA variable was included as a continuous variable. With that, the modified base models for the three models can be written as:

- Model 1 (M1):

$$D_0 = \exp\left[\beta_{10} + \beta_{11}\ln(D_q) + \beta_{12}\ln(AGE) + \beta_{13}\ln\left(\frac{1}{HD}\right) + \beta_{14}PLTPA\right] + \epsilon_1 \tag{3.10}$$

$$D_{25} = \exp\left[\beta_{20} + \beta_{21}\ln(D_{50}) + \beta_{22}\ln(AGE) + \beta_{23}PLTPA\right] + \epsilon_2 \tag{3.11}$$

$$D_{50} = \exp\left[\beta_{30} + \beta_{31}\ln(D_q) + \beta_{32}PLTPA\right] + \epsilon_3 \tag{3.12}$$

$$D_{95} = \exp\left[\beta_{40} + \beta_{41}\ln(D_{50}) + \beta_{42}\ln(AGE) + \beta_{43}\ln\left(\frac{1}{HD}\right) + \beta_{44}PLTPA\right] + \epsilon_4 \tag{3.13}$$

- Model 2 (M2):

$$D_0 = \exp\left[\beta_{10} + \beta_{11}\ln(RS) + \beta_{12}\ln(N) + \beta_{13}\ln(HD) + \frac{\beta_{14}}{AGE} + \beta_{15}PLTPA\right] + \epsilon \quad (3.14)$$

$$D_{25} = \exp\left[\beta_{20} + \beta_{21}\ln(RS) + \beta_{22}\ln(N) + \beta_{23}\ln(HD) + \frac{\beta_{24}}{AGE} + \beta_{25}PLTPA\right] + \epsilon \quad (3.15)$$

$$D_{50} = \exp\left[\beta_{30} + \beta_{31}\ln(RS) + \beta_{32}\ln(N) + \beta_{33}\ln(HD) + \frac{\beta_{34}}{AGE} + \beta_{35}PLTPA\right] + \epsilon \quad (3.16)$$

$$D_{95} = \exp\left[\beta_{40} + \beta_{41}\ln(RS) + \beta_{42}\ln(N) + \beta_{43}\ln(HD) + \frac{\beta_{44}}{AGE} + \beta_{45}PLTPA\right] + \epsilon \quad (3.17)$$

- Model 3 (M3):

$$\ln(D_0) = \beta_{10} + \beta_{11}\ln\left(\frac{BA}{TPA} + \beta_{12}PLTPA\right) \quad (3.18)$$

$$\ln(D_{25}) = \beta_{20} + \beta_{21}\ln\left(\frac{BA}{TPA} + \beta_{22}PLTPA\right) \quad (3.19)$$

$$\ln(D_{50}) = \beta_{30} + \beta_{31}\ln\left(\frac{BA}{TPA} + \beta_{32}PLTPA\right) \quad (3.20)$$

$$\ln(D_{95}) = \beta_{40} + \beta_{41}\ln\left(\frac{BA}{TPA} + \beta_{42}PLTPA\right) \quad (3.21)$$

Percentiles Regression Models & Environmental Co-variables

For this second phase, the goal was to adapt the three base models described in the previous sub-subsection and compare the performance of the results for the adapted models. To avoid model complexity and variability, just one environmental co-variable (ϕ) was considered to include in each percentile regression. Based on lasso regression results, the environmental co-variables with coefficient different from 0 were chosen to add in the percentile regression analysis (Equation 3.22 - 3.33). The final four regression that are combined and form the adapted models was based on those with the lowest AIC for each percentile. All terms were previously defined.

- Model 4 (M4):

$$D_0 = \exp\left[\beta_{10} + \beta_{11}\ln(D_q) + \beta_{12}\ln(\text{AGE}) + \beta_{13}\ln\left(\frac{1}{\text{HD}}\right) + \beta_{14}\text{PLTPA} + \beta_{15}\phi\right] + \epsilon_1 \tag{3.22}$$

$$D_{25} = \exp\left[\beta_{20} + \beta_{21}\ln(D_{50}) + \beta_{22}\ln(\text{AGE}) + \beta_{23}\text{PLTPA} + \beta_{24}\phi\right] + \epsilon_2 \tag{3.23}$$

$$D_{50} = \exp\left[\beta_{30} + \beta_{31}\ln(D_q) + \beta_{32}\text{PLTPA} + +\beta_{33}\phi\right] + \epsilon_3 \tag{3.24}$$

$$D_{95} = \exp\left[\beta_{40} + \beta_{41}\ln(D_{50}) + \beta_{42}\ln(\text{AGE}) + \beta_{43}\ln\left(\frac{1}{\text{HD}}\right) + \beta_{44}\text{PLTPA} + \beta_{45}\phi\right] + \epsilon_4 \tag{3.25}$$

- Model 5 (M5):

$$D_0 = \exp\left[\beta_{10} + \beta_{11}\ln(\text{RS}) + \beta_{12}\ln(\text{N}) + \beta_{13}\ln(\text{HD}) + \frac{\beta_{14}}{\text{AGE}} + \beta_{15}\text{PLTPA} + \beta_{16}\phi\right] + \epsilon_1 \tag{3.26}$$

$$D_{25} = \exp\left[\beta_{20} + \beta_{21}\ln(\text{RS}) + \beta_{22}\ln(\text{N}) + \beta_{23}\ln(\text{HD}) + \frac{\beta_{24}}{\text{AGE}} + \beta_{25}\text{PLTPA} + \beta_{26}\phi\right] + \epsilon_2 \tag{3.27}$$

$$D_{50} = \exp\left[\beta_{30} + \beta_{31}\ln(\text{RS}) + \beta_{32}\ln(\text{N}) + \beta_{33}\ln(\text{HD}) + \frac{\beta_{34}}{\text{AGE}} + \beta_{35}\text{PLTPA} + \beta_{36}\phi\right] + \epsilon_3 \tag{3.28}$$

$$D_{95} = \exp\left[\beta_{40} + \beta_{41}\ln(\text{RS}) + \beta_{42}\ln(\text{N}) + \beta_{43}\ln(\text{HD}) + \frac{\beta_{44}}{\text{AGE}} + \beta_{45}\text{PLTPA} + \beta_{46}\phi\right] + \epsilon_4 \tag{3.29}$$

- Model 6 (M6):

$$\ln(D_0) = \beta_{10} + \beta_{11}\ln\left(\frac{\text{BA}}{\text{TPA}} + \beta_{12}\text{PLTPA} + \beta_{13}\phi\right) \tag{3.30}$$

$$\ln(D_{25}) = \beta_{20} + \beta_{21}\ln\left(\frac{\text{BA}}{\text{TPA}} + \beta_{22}\text{PLTPA} + \beta_{23}\phi\right) \tag{3.31}$$

$$\ln(D_{50}) = \beta_{30} + \beta_{31}\ln\left(\frac{\text{BA}}{\text{TPA}} + \beta_{32}\text{PLTPA} + \beta_{33}\phi\right) \tag{3.32}$$

$$\ln(D_{95}) = \beta_{40} + \beta_{41}\ln\left(\frac{\text{BA}}{\text{TPA}} + \beta_{42}\text{PLTPA} + \beta_{44}\phi\right) \tag{3.33}$$

As in the approach described in the previous sub-subsection, two levels of percentile modeling were applied in this phase. For the first level (i.e. the general level), the three regional datasets were combined into a single dataset. (i.e., the regional level), the base models were applied separately to each region (LCP, UCP, and IF),creating three regional dataset, and the results from the three regions were then combined to compute the three-parameter Weibull distribution. The fivefold cross-validation took place in the first level, and tenfold was used in the second level.

As described in Chapter II, the Seemingly Unrelated Regression (SUR) approach (Zellner, 1962) is commonly used in simultaneous regression modeling to account for correlated error terms. For this reason, the SUR approach was incorporated into the cross-validation process to mitigate the error correlation between the four percentile regressions across the three base and adapted models.

Following the same approaches performed in Chapter II, the Weibull probability density function estimates (Equations 2.26 - 2.30), cumulative density function (Equation 1.5), trees per acre and basal area prediction (Equation 2.31), and goodness of fit test were computed for this chapter (Equations 2.32 and 2.33).

3.4.5 Comparison

The three base percentile regression models and the three adapted models (accounting for environmental co-variables) for both levels of modeling were compared based on model fitting and validation statistics: Akaike Information Criterion (AIC) and root mean square error (RMSE) as fitting statistics, and with the R-squared value.

3.5 Results

3.5.1 General & Regional Level - Base Models

Percentile Regression Models

The three base models were compared using several statistical results (Table 3.1 - 3.2). for the general level, the three regional datasets were combined into a single dataset, while for the regional level, each dataset was used separately for its respective region (LCP, UCP, and IF). The results for D_0 percentiles showed that M1 obtained the lower RMSE, higher R^2, and lower AIC. For D_{25}, M3 performed better compared to the two other models, the M3 had the lower RMSE and AIC, and M1 higher R^2. The M1 and M3 performed simialarly for percentile D_{50} but with slightly differences for RMSE and AIC. Following a similar result of D_{25} and D_{50}, the M3 obtained the lower RMSE, the height R^2, and lower AIC. M2 showed the poorest statistical results for all four percentile regressions compared to M1 and M3.

The regional level shows that for the IF region, based on the statistical performance, M3 provided the lowest RMSE and AIC for all four percentiles, while M1 showed the highest R^2 for almost all percentiles, except to D_0 percentile; for this percentile M3 had the highest R^2. For the LCP region, the results can be found in Table 3.3. M2 had the highest R^2 values, and M1 the lowest RMSE and AIC for the D_0 percentile. For the D_{25} percentile, M3 obtained the lowest RMSE and AIC, and the highest R^2. For the D_{50} percentile, M1 and M3 obtained similar RMSE and AIC values, both being the lowest, and the highest R^2. Finally, for the D_{95} percentile, M3 obtained the lowest RMSE and AIC, and the highest R^2. The results of the percentile regressions for the UCP region can be found in Table 3.4. For the D_0 percentile, M2 obtained the lowest RMSE and AIC, and the highest R^2. For the D_{25} percentile, M3 obtained the lowest RMSE and AIC, and the highest R^2. For the D_{50} percentile, both M3 and M1 obtained the lowest RMSE, the highest R^2, and the lowest AIC. Following the same results from other percentiles, M3 showed the lowest RMSE and AIC, and highest R^2 for D_{95} percentile.

Error Index

Results from the average error index (EI) by age and PLTPA for the general level are presented in Table 3.5. At age 6 for 200 and 1200 PLTPA the M2 obtained the lower EI; for 450 and 700 PLTPA, M1 proved the lower EI; for 950 PLTPA the M3 had the lower EI. M2 provided the lower EI for all five PLTPA at age 8. For 200, 700, and 950 PLTPA at age 10 the M2 had the lower EI, and for PLTPA 450, and 1200 M1 had the lower EI. M1 had the lower EI for 200 and 1200 PLTPA at age 12, and M2 had the lower for 450, 700, 900

PLTPA. M2 had the lower EI for all PLTPA except to 1200 PLTPA; for this PLTPA M1 could provide a slight improvement at age 15. For age 18, M1 had lower EI at 200, 700, and 1200 PLTPA, and M2 at 450 and 950 PLTPA. At age 21 the M2 had lower EI for 200, 450, and 700 PLTPA, and M1 for 950, 1200 PLTPA.

For the regional level, the results for the EI (Table 3.6) showed that at age 6, M1 had the lowest EI values for 200, 450, and 1200 PLTPA, while M2 had the lowest for 700 PLTPA and M3 for 950 PLTPA. At age 8, the M1 and M3 models presented similar EI values for 950 PLTPA, with M1 showing the lowest EI for 200 PLTPA, M3 for 450 and 1200 PLTPA, and M2 for 700 PLTPA. At age 10, M1 had the lowest EI for 200 PLTPA and 450, M2 for 700 and 1200 PLTPA, and M3 for 950 PLTPA. At age 12, M2 had the lowest EI for almost all PLTPA values, except for 1200 PLTPA, where M1 performed better. A similar trend was observed at age 15, but in this case M2 had the lowest EI across all PLTPA values. At age 18, M1 and M3 showed similar EI values for 200 PLTPA, while M2 had the lowest for the remaining densities. Finally, at age 21, M1 had the lowest EI for 200 and 950 PLTPA, whereas M2 had the lowest for 450, 700, and 1200 PLTPA.

RMSE

The RMSE was used to analyze the precision of Weibull PDF obtained from the percentile prediction across the three regions used in this analysis, across the general and regional level of modeling. For the general level of modeling in Table 3.5, for 200 PLTPA M2 had better performance at ages 8, 10, 12, 15 and at age 21. M1 performed better at age 18. For 450 PLTPA M1 obtained better results at ages 10 and 21, while M2 obtained better results for the other ages. At 700 PLTPA for age 6, 10, and 18 the M1 could have a better precision for PDF, and at ages 8, 12, and 21 M2 could have a better precision. At age 15 both model M1 and M3 shows a similar result. M2 showed better precision for 5 of 7 ages (8, 10, 12, 15, and 18), M3 at age 6 and M1 at 21. For 1200 PLTPA M2 provided the better PDF precision at ages 6, 8, and 21, and M1 at ages 10, 12, 15, and 18.

The results for RMSE for PDF based on three percentiles models for the regional level of modeling can be found in Table 3.6. For 200 PLTPA, M1 had better PDF precision at ages 6 – 10, M2 at ages 12 and 15, and M3 at ages 18 and 21. For PLTPA 450 M1 provided better precision at ages 6, 8, and 10 and M2 at ages 12, 15, 18, and 21. For PLTPA 700 M2 had better precision for all ages. For 950 PLTPA M1 had better precision at ages 10 and 21, M2 at ages 12, 15, and 18 and M3 at ages 6 and 8. For 1200 PLTPA M1 had better precision at age 6 and 8, M2 at ages 12, 15, and 18 and M3 at ages 10 and 21.

3.5.2 Comparison - General & Regional Level - Base Models

Percentile Regression Models

The results for the D_0 percentile across the three regions are presented in Figures 3.2 – 3.4. For the IF region, in all five PLTPA, models M1 and M3 provided predictions closer to the observed D_0 percentile for the general modeling level. M1 and M3 showed similar performance for this percentile, with no major differences, and this trend extended to all PLTPA. Model M2, however, consistently underestimated across all five PLTPA, with the largest discrepancies observed in 200, 450, and 700 PLTPA. At the regional modeling level, M2 provided improved predictions compared with the general level, and this improvement extended to all PLTPA. All three models performed better between ages 6 and 10. In 200 PLTPA, M1 and M3 underestimated at ages 6, 8, and 10 and overestimated the percentile at ages 12, 15, 18, and 21, while M2 showed the opposite behavior.

Similar to the IF region, the regional-level modeling for the LCP region produced better predictions compared with the general level. However, unlike the IF region, M2 consistently overestimated across all five PLTPA and in nearly all ages for the general level. In 200 PLTPA, the three models showed larger differences in overestimation for the general level compared with the other PLTPA.

Unlike the results for IF and LCP, the modeling level did not significantly affect predictions in the UCP region. Only for 200, 450, and 1200 PLTPA there was a visible improvement for M2, where predictions showed better performance.

The results for the D_{25} percentile across the three regions are presented in Figures 3.5 – 3.7. For the IF region, M2 consistently underestimated across all PLTPA and ages for the general modeling level. In contrast, M1 and M3 achieved better performance. For the regional level, an improvement was observed, particularly for M2, which, together with the other models, produced satisfactory predictions. Similarly, in the LCP region, regional-level modeling improved predictions, especially for M2, which had overestimated the D_{25} percentile for the general level. As with the D_0 percentile, the modeling levels for the D_{25} percentile in the UCP region did not result in visible or significant differences across PLTPA values and ages. When the dataset was analyzed separately for each region (regional level), the D_{50} percentile in the IF region showed improvement compared with the combined three-region dataset (general level). Model M2 was the most affected, as it underestimated the percentiles for the general level. A similar pattern was observed in the LCP region, where M2 overestimated the D_{50} percentile for the general level but performed better for the regional level. In contrast, predictions in the UCP region were not influenced by modeling level for this percentile (Figures 3.8–3.10). Following the same pattern observed for the other percentiles, results for the D_{95} indicated that, in the IF and LCP regions, the regional-level modeling improved predictions compared with the general level (Figures 3.11–3.13). However, as with the previous percentiles, differences in modeling level did not affect predictions in the UCP region.

Goodness-of-fit

As mentioned in Chapter II, the Error Index (EI) is used to evaluate model performance. The EI results for the three regions, comparing the two modeling levels, are presented in Figures (3.14 - 3.16). As expected, the EI results for the IF region showed lower values overall for the regional level. This trend was observed in all three models for 450 PLTPA across all ages. For 200, 950, and 1200 PLTPA, the lowest EI values for the general level occurred only at age 6. In 700 PLTPA, the general level showed the lowest values between ages 18 and 21 for all three models. Models M1 and M3 showed similar results, which is not surprising given their similarity in the percentile prediction results.

For the LCP region, in 450, 700, and 950 PLTPA, the regional level showed lower EI values across all ages and for all three models. In 200 PLTPA, no significant differences were observed between modeling levels, ages, or models. In 1200 PLTPA, the EI for the regional level was lower for all models up to age 18, while at age 21, the general level presented the lowest EI values.

Unlike the other regions, but not unexpectedly based on the percentile regression results, the EI results for the UCP region did not show notable differences between the two modeling levels. The EI values shows that the general and regional levels overlap each other across most ages and for all three models (Figure 3.16).

For RMSE, as expected, the RMSE results were similar to the error index results, showing that the PDF obtained from percentile regressions for the regional level presented better precision with lower RMSE. The IF and LCP regions showed the most improvement. This increase in precision occurred at all ages for PLTPA 450 and at almost all ages for PLTPA 950, except at age 6 in the IF region; in the LCP region, both levels were similar at age 21. For PLTPA 200, the IF region showed better precision only at age 6, while in the LCP region improvement was observed at all ages, although with a slight difference.

For PLTPA 700 in the IF region, the general level showed better precision only at age 18 for models M1 and M3, and at age 6 for the 1200 density. In the LCP region, at PLTPA 1200, the regional level of modeling showed better precision at almost all ages, with a small difference at age 21. On the other hand, the UCP region did not show significant notable effects between the general and regional modeling levels (Figures 3.17 - 3.19).

3.5.3 Lasso Regression

The results for lasso regression can be found in Figure 3.20. Based on the results, WD was the environmental co-variable that showed that it might be important in the prediction of all four DBH percentiles. This co-variable showed greater weight, causing its coefficient to decrease more slowly toward zero compared to other environmental co-variables. PPT also showed greater weight for the four percentiles; however, its coefficients decreased toward zero earlier than those of WD.

With a similar behavior, the co-variable $Temp_{max}$ also appeared to be important, but it presented a negative coefficient, suggesting that higher maximum temperatures are associated with lower values of the response variable. The co-variable $Temp_{min}$ showed that it might be important for all four percentiles, but with less weight compared to the three co-variables mentioned previously. This co-variable had greater weight in percentiles D_0 and D_{95}, causing its coefficients to decrease more slowly compared to percentiles D_{25} and D_{50}. As mentioned earlier, lasso regression applies penalization. After penalization, the environmental co-variables that appeared to be important for the prediction of DBH percentiles can be found in Table 3.7. Percentile D_0 had the highest number of important co-variables, with five; D_{25} had three; D_{50} had only two important co-variables, and D_{95} had three. The co-variable WD appeared in all percentiles, as expected based on the lasso regression selection process. AW co-variable appeared for almost all percentiles except D_0. Koirala et al. (2021) obtained a similar result using lasso for the selection of environmental co-variables to model dominant height in the Western Gulf region. In their study, the variables AW and WD were found to be important for the prediction of dominant height (HD) in that region. The co-variable $Temp_{max}$ appeared in the result for percentiles D_0 and D_{25}, while PPT appeared for D_0 and D_{95}, and $Temp_{min}$ appeared in the result only for percentile D_0.

3.5.4 General & Regional Level - Adapted Models Accounting for Environmental Co-variables

Percentile Regression Models

With environmental co-variables based on lasso regression results, 15 new models were tested. The final three adapted models accounting for environmental co-variables were selected based on the lower AIC values for each percentile regression (Table 3.8). The chosen adapted models were M4, M5, and M6 (Equations 3.34 – 3.45) (Figure 3.21).

- Model 4 (M4):

$$D_0 = \exp\left[\beta_{10} + \beta_{11}\ln(D_q) + \beta_{12}\ln(AGE) + \beta_{13}\ln\left(\frac{1}{HD}\right) + \beta_{14}PLTPA + \beta_{15}Temp_{max}\right] + \epsilon_1 \quad (3.34)$$

$$D_{25} = \exp\left[\beta_{20} + \beta_{21}\ln(D_{50}) + \beta_{22}\ln(AGE) + \beta_{23}PLTPA + \beta_{24}Temp_{max}\right] + \epsilon_2 \quad (3.35)$$

$$D_{50} = \exp\left[\beta_{30} + \beta_{31}\ln(D_q) + \beta_{32}PLTPA + \beta_{33}WD\right] + \epsilon_3 \quad (3.36)$$

$$D_{95} = \exp\left[\beta_{40} + \beta_{41}\ln(D_{50}) + \beta_{42}\ln(AGE) + \beta_{43}\ln\left(\frac{1}{HD}\right) + \beta_{44}PLTPA + \beta_{45}PPT\right] + \epsilon_4 \quad (3.37)$$

- Model 5 (M5):

$$D_0 = \exp\left[\beta_{10} + \beta_{11}\ln(RS) + \beta_{12}\ln(N) + \beta_{13}\ln(HD) + \frac{\beta_{14}}{AGE} + \beta_{15}PLTPA + \beta_{16}Temp_{max}\right] + \epsilon_1 \quad (3.38)$$

$$D_{25} = \exp\left[\beta_{20}+\beta_{21}\ln(\mathrm{RS})+\beta_{23}\ln(\mathrm{N})+\beta_{24}\ln(\mathrm{HD})+\frac{\beta_{25}}{\mathrm{AGE}}+\beta_{26}\mathrm{PLTPA}+\beta_{27}\mathrm{Temp}_{\mathrm{max}}\right]+\epsilon_2 \quad (3.39)$$

$$D_{50} = \exp\left[\beta_{30}+\beta_{31}\ln(\mathrm{RS})+\beta_{32}\ln(\mathrm{N})+\beta_{33}\ln(\mathrm{HD})+\frac{\beta_{34}}{\mathrm{AGE}}+\beta_{35}\mathrm{PLTPA}+\beta_{36}\mathrm{WD}\right]+\epsilon_3 \quad (3.40)$$

$$D_{95} = \exp\left[\beta_{40}+\beta_{41}\ln(\mathrm{RS})+\beta_{42}\ln(\mathrm{N})+\beta_{43}\ln(\mathrm{HD})+\frac{\beta_{44}}{\mathrm{AGE}}+\beta_{45}\mathrm{PLTPA}+\beta_{46}\mathrm{PPT}\right]+\epsilon \quad (3.41)$$

- Model 6 (M6):

$$\ln(D_0) = \beta_{10} + \beta_{11}\ln\left(\frac{\mathrm{BA}}{\mathrm{TPA}} + \beta_{12}\mathrm{PLTPA} + \beta_{13}\mathrm{Temp}_{\mathrm{max}}\right) \quad (3.42)$$

$$\ln(D_{25}) = \beta_{20} + \beta_{21}\ln\left(\frac{\mathrm{BA}}{\mathrm{TPA}} + \beta_{22}\mathrm{PLTPA} + \beta_{23}\mathrm{Temp}_{\mathrm{max}}\right) \quad (3.43)$$

$$\ln(D_{50}) = \beta_{30} + \beta_{31}\ln\left(\frac{\mathrm{BA}}{\mathrm{TPA}} + \beta_{32}\mathrm{PLTPA} + \beta_{33}\mathrm{WD}\right) \quad (3.44)$$

$$\ln(D_{95}) = \beta_{40} + \beta_{41}\ln\left(\frac{\mathrm{BA}}{\mathrm{TPA}} + \beta_{42}\mathrm{PLTPA} + \beta_{43}\mathrm{PPT}\right) \quad (3.45)$$

The three adapted models modeled for the general level obtained p-value <0.05 with 95% confidence intervals (CI) for the environmental co-variables included, confirming the lasso regression results that these co-variables are important to estimate the four percentiles (Table 3.9 - 3.20). The three models were compared based on statistical results. These results for the general level can be found in Table 3.21. For the D_0 percentile, M4 showed the lowest RMSE, while M5 obtained the lowest AIC and the highest R^2. M6, on the other hand, presented the highest RMSE, the highest AIC, and the lowest R^2. Based on these results, M5 demonstrated the best performance in predicting this percentile. However, the difference between the models was not statistically significant. The statistical results for the D_{25} percentile showed that M6 had the best performance, with the lowest RMSE, the lowest AIC, and the highest R^2, compared to models M4 and M5. For the D_{50} percentile, the performance results showed that M5 achieved the lowest AIC but had the highest RMSE. Models M4 and M6 performed similarly, with the lowest RMSE, the highest R^2 values, and the highest AIC values, compared to M5. M6 demonstrated the best performance for the D_{95} percentile, with the lowest RMSE, the highest R^2, and the lowest AIC. The second-best model was M4, with better statistical results compared to M5.

The performance results for regional level for the four percentiles, shows that in the IF region (Table 3.22) the D_0 percentile, M6 showed the best performance, with the lowest RMSE, lowest AIC, and highest R^2. M5 had the highest RMSE, the second-highest R^2, and the highest AIC. Similar to the D_0 percentile, M6 also showed the best performance for the D_{25} percentile, with the lowest RMSE, lowest AIC, and highest R^2. M4 was the second-best model for predicting this percentile. Models M4 and M6 showed similar performance for percentile D_{50}, being the top two models for this percentile. For the D_{95} percentile, M6 achieved the best results in terms of RMSE, R^2, and AIC. M4 had a lower RMSE and higher R^2 than M5, although M5 recorded the lowest AIC. In the LCP region, M4 achieved the lowest RMSE and AIC for predicting the D_0 percentile, while M5 obtained the highest R^2. For the D_{25} percentile, M6 had the lowest RMSE and highest R^2, while M5 had the lowest AIC compared to the other two models. M4 and M6 yielded similar results for the D_{50} percentile, with the lowest RMSE and highest R^2, while M5 had the lowest AIC. For the

D_{95} percentile, M6 showed the best RMSE and R^2, and M2 recorded the lowest AIC (Table 3.23). The M2 demonstrated the best performance in the UCP region for the D_0 percentile, with the best results for RMSE, R^2, and AIC. For the D_{25} percentile, M6 showed the best predictive performance, with the best statistical results. As with the previous percentile, M6, together with M4, were the models with the best performance for the D_{50} percentile. Following the same trend observed for D_{25} and D_{50}, M6 also performed well for D_{95}, showing the best RMSE and R^2, although it had the worst AIC for this percentile (Table 3.24).

Error Index

The results for the EI accounting for environmental co-variables for the general modeling level can be found in Table 3.25. At age 6, model M4 showed the best performance, with lower values for 200, 450, and 700 PLTPA. For 950 and 1200 PLTPA, however, M6 had the best performance. At age 8, M4 performed better for 200, 700, and 1200 PLTPA, while M5 was superior for 450 and 950 PLTPA. At age 10, M4 had the best performance only for 200, M6 for 950, and M5 for 450, 700, and 1200 PLTPA. At age 12, M4 performed better for 700 and 1200 PLTPA, while M5 was superior for 450 and 950 PLTPA, and M6 for 200 PLTPA. At age 15, M5 performed better for 200, 450, and 1200 PLTPA, while M4 was superior for 950 and M6 for 700 PLTPA. At age 18, M4 showed the best performance for 200, 700, 950, and 1200 PLTPA, while M5 performed better for 450 PLTPA. Finally, at age 21, M4 had the best performance for 200, 950, and 1200 PLTPA, while M5 was superior for 450 and 700 PLTPA. However, all differences reported above among between three models were very small.

The EI results for the regional modeling level showed that, for 200 and 700 PLTPA, M5 achieved the best performance with the lowest EI values (Table 3.26). For 450 and 1200 PLTPA, M4 performed best, while for 950 PLTPA, M6 had the lowest EI. At age 8, M5 showed the best performance for 450, 950, and 1200 PLTPA, M4 for 700 PLTPA, and both M4 and M6 for 200 PLTPA. At age 10, M5 achieved the best performance for 200, 700, and 1200 PLTPA, while M4 performed best for 450 and 950 PLTPA. At age 12, M5 stood out with the best performance across all PLTPA. Similarly, at age 15, M5 maintained the best performance for nearly all PLTPA, except for 950 PLTPA, where M6 was superior. At age 18, M4 performed best for 450, while M5 showed the best results for 700, 950, and 1200 PLTPA. For PLTPA 200, M4 and M5 performed equally well. At age 21, M5 showed the best performance for 200, 450, 700, and 1200 PLTPA, while M4 was superior for 950 PLTPA.

RMSE

For the general level following the same pattern observed for the EI at age 6, M4 showed higher precision with lower RMSE values for 200, 450, and 700 PLTPA, while M6 had lower values for 950 and 1200 PLTPA. At age 8, M5 achieved higher accuracy for 450, 950, and 1200 PLTPA, M4 for 700 PLTPA, and M6 for 200 PLTPA. At age 10, the results were similar to those of the Error Index: M5 had higher precision with lower RMSE values for 450, 700, and 1200 PLTPA; M4 for 200; and M6 for 950 PLTPA. At age 12, M5 achieved lower RMSE values for 450, 950, and 1200 PLTPA, while M6 showed lower values for 200 and 700 PLTPA, thus demonstrating higher precision for these cases. At age 15, M5 showed the highest precision with lower RMSE values for 200, 450, 700, and 1200 PLTPA, while M6 had the lowest RMSE for 950 PLTPA. At age 18, M4 stood out with the highest precision for 200, 700, 950, and 1200 PLTPA, while for 450 PLTPA both M4 and M5 showed lower RMSE compared to M6. At age 21, M4 showed higher precision for PLTPA 200, 450, and 950, M5 for PLTPA 700, and M6 for 1200 PLTPA (Table 3.25).

Regional level RMSE shows that at age 6, M4 showed the highest accuracy for 200, 450, and 1200 PLTPA, while M5 performed best for 700, and M6 had the lowest RMSE for 950 PLTPA. At age 8, both M4 and M5 showed high accuracy, with M4 having lower RMSE for 200 and 450, and M5 for 700, 950, and 1200 PLTPA. At age 10, M5 stood out with the best accuracy for all PLTPA, except for 700 PLTPA, where M5 and M6 showed similar performance. As at age 10, M5 showed the best accuracy, with the lowest RMSE across all

PLTPA at age 12. Similar results were observed at age 15, with M5 performing best for nearly all PLTPA, except for 950 PLTPA. At age 18, M4 showed the highest accuracy for 200 and 950 PLTPA, while M5 performed best for 450, 700, and 1200 PLTPA. At age 21, M5 showed the best accuracy for 200 and 450 PLTPA, M6 for 950 and 1200 PLTPA, and M4 for 700 PLTPA (Table 3.26).

3.5.5 Comparison - General & Regional Level - Models Accounting for Environmental Co-variables

Percentile Regression Models

The results for D_0 for the three models accounting for environmental co-variables for the IF, LCP, and UCP regions can be found in Figures 3.22 - 3.24. For the IF region at 200 PLTPA, models M4 and M6 overestimated D_0 for ages 15, 18, and 21 and underestimated for ages 6 and 8 at both modeling levels. Model M2 achieved improved precision for the regional level, resulting in predictions closer to the observed percentiles. For 450 PLTPA, there were no significant differences in D_0 predictions between the two modeling levels. At 700 PLTPA, all three models underestimated the D_0 percentile for the general level. For the regional level, for ages 6, 8, 10, 12, and 15, D_0 percentile predictions from the three models were closer to the observed values. However, for ages 18 and 21, models M4 and M6 underestimated the D_0 percentile, while M5 overestimated. At 950 PLTPA, all three models underestimated the D_0 percentile for ages 12, 15, and 18. At age 21, models M4 and M6 also underestimated, while M5 overestimated for the general level. At 1200 PLTPA, the three models underestimated the D_0 percentile between ages 15 and 21 for the general level, while for the regional level, M5 overestimated for these ages. The other two models produced similar results to the general level, underestimating at ages 15 and 21. For the LCP region, the regional level showed better performance, with predictions closer to the values observed at 200 PLTPA. At 450 PLTPA, the general level achieved better performance. A similar result was observed at 700 PLTPA, where the general level outperformed the regional level. At 950 PLTPA, the general level underestimated the percentiles, while the regional level overestimated. At 1200 PLTPA, both levels underestimated the D_0 percentile. The results for the UCP region did not show significant differences; both levels achieved similar results.

The results for the prediction of the D_{25} percentile showed similarity across the three regions (Figure 3.25 - 3.27). The regional level showed better performance, with improvement in percentile predictions at that level. The improvement is more evident for ages 15, 18, and 21 in the IF region at 200, 950, and 1200 PLTPA; for ages 12, 15, 18, and 21 in the LCP region at 200 PLTPA; and for ages 18 and 21 in the UCP region at 200 PLTPA.

As in the D_{25} percentile predictions, regional-level modeling achieved better predictions for D_{50} (Figures 3.28 - 3.30). Improvement occurred across all PLTPA and age groups in the IF region. For the LCP region, in general, the regional level showed better performance compared to the general level. However, at 200 PLTPA (age 15), 450 PLTPA (ages 12 and 15), and 1200 PLTPA (ages 15 and 18), the regional level resulted in underestimation of the D_{50} percentile. In the UCP region, predictions remained close; both levels showed good performance in predicting the D_{50} percentile.

Predictions for D_{95} were better for the regional level for the IF and LCP regions across all ages. For the UCP region, both modeling levels showed good performance, with a slight improvement for the regional level for 700, 950, and 1200 PLTPA at age 21. Model M2 was the one that showed the greatest improvement across all percentiles, regions, and age groups (Figure 3.31 - 3.33).

Goodness-of-fit

The results of the error index accounting for environmental co-variables for two levels of modeling and for the IF, LCP, and UCP regions can be found in Figures 3.34 - 3.36. Similar to the EI results for the models without environmental co-variables, the regional modeling level showed better performance, presenting lower error index values for the IF region. For 200 PLTPA, the error index for the regional level was lower across all ages in model M5, and for almost all ages in models M4 and M6, except at age 6, where the general model had a lower error index. A similar result was observed in 450 PLTPA, where the regional EI was lower at all ages in models M4 and M6, and almost all ages in M5, except at age 6, where the general level presented the lowest value. In 700 PLTPA, the three models had similar results: the regional level showed lower EI from age 6, 8, 10, 12, and 15. At age 18, for the general level showed higher EI for models M4 and M6, while for M5 there was no significant difference. At age 21, the regional level had a higher EI, a consistent result across all three models. For 950 and 1200 PLTPA presented the same pattern: for the general level had lower EI at age 6, while the regional level had lower EI from age 8 onwards, extending up to age 21 for all three models.

In the LCP region, the regional modeling level yielded lower EI for all ages in PLTPA for models M4 and M6, with more pronounced differences between ages 8, 10, and 18. For M5, the regional EI was higher at age 6, but followed the same trend as M4 and M6 between ages 8 and 18, where the difference between the two modeling levels became more evident. For 450 PLTPA, EI did not show significant differences at age 8 for models M4 and M5, nor at age 21 for M4, M5, and M6. However, at age 8, for the general level was slightly better for M5. For 700 PLTPA, the EI for the regional level was lower for almost all ages across the three models, except at age 21—where no significant difference was observed—and at age 18 for M4, which also showed no relevant difference between modeling levels. Models M4 and M5 showed similar results for 950 PLTPA, where the regional EI was higher only at age 15. For M6, the regional EI was lower between ages 8 and 18, and at age 21, both modeling levels were similar across all three models. For 1200 PLTPA, the regional EI was slightly higher at age 21 for models M4 and M6. On the other hand, between ages 8 and 18, the regional EI was consistently lower in all three models.

Unlike the behavior observed in the IF and LCP regions, in the UCP region, the differences between modeling levels were not significant. For 200 PLTPA, this difference was only noticeable for M5 at ages 8 and 12. In 450 PLTPA, the regional EI was lower at age 12 for all models, and at ages 8 and 10 for M5. 700 PLTPA showed minor differences at ages 10 and 12 across all three models. For 950 PLTPA, differences were observed from ages 6, 8, 10, 12, 15, and 18 for M5, where the regional level had lower EI; from ages 8 to 12 for M4; and from ages 10 and 12 for M6. Finally, in 1200 PLTPA, for the general level EI was lower at age 8 for all models. At age 18, the regional level had a lower EI for M4 and M5. For the other ages, no significant differences were found between modeling levels.

For RMSE results, the regional levels showed better precision compared to the general level for all planting densities and almost all ages for the three models for region IF (Figure 3.37). For 200 PLTPA M4 and M6, the regional had lower precision compared to the general level at age 6. For 700 PLTPA, the general level obtains better precision at ages 18 and 21 for M4 and M6, and for M5 both levels showed similar precision. For 950 and 1200 PLTPA the three models for the regional level obtained better precision for all ages, except at age 6. For 450 PLTPA for all models the regional level resulted in better precision for all ages. Similar behavior can be observed for RMSE results for the LCP region. (Figure 3.38). For 200 PLTPA, the regional level showed better precision for all ages and for all models. For 450 PLTPA, the regional level showed better precision for almost all ages, except at age 8 for M5, and at age 21 for all three models. For 700 and 1200 PLTPA, the general and regional levels showed similar precision at 21 for all three models; for the other ages, the regional level was superior, showing better precision for all three models. for 950 PLTPA, the general level showed better precision at age 15 for M5 and similar precision at age 21 for all three models. The RMSE results for the UCP region showed no significant difference at 200 PLTPA for M4 and M6. For M5, there was a small difference at ages 6, 8, 10, and 12, with the regional level showing higher precision. For 450 PLTPA, the regional level showed better precision at ages 12, 15, 18, and 21, while at 950 PLTPA it was better for ages 6, 8, and 10. For 700 PLTPA, the difference in precision is more noticeable only at age 21, with the regional level showing better RMSE. Similar results can be found for 1200 PLTPA (Figure 3.39).

3.5.6 Comparison - Base models & Adapted Models Accounting for Environmental Co-variables

Percentiles Estimation

Analyzing the output for D_0 percentile predictions for the general level in the base model and accounting for environmental co-variable models, both seem to predict similiar. All three models provided better predictions for higher PLTPA (700, 950, and 1200) and for juvenile stands (6, 10, 12 ages). On the other hand, for lower PLTPA (200), the three models showed poor performance (Figure 3.40). The base model created by Jiang and Brooks, as well as the models developed by PMRC researchers, underestimated the D_0 percentile for juvenile stands by 10.53% on average and by 9.94% when accounting for environmental co-variables. They overestimated the D_0 percentile for mature stands by 6.8% on average and by 6.9% on average when accounting for environmental co-variables. Cao's base model underestimated the D_0 percentile for juvenile stand by 2.75% and by 3.13% when accounting for environmental co-variables and underestimated for mature stands by 3.5% and by 1.2% when accounting for environmental co-variables. The three regression models seem to have a better performance for larger percentile diameters (D_{25}, D_{50}, D_{95}), since the models provided an adequate prediction for these percentiles in the base model and when accounting for environmental co-variables (Figures 3.41- 3.43). No notable difference was found between the base and the environmental co-variable models for the regional level; by analyzing the output for the three regression models it was noticed that both predictions were similar. Both approaches performed better at high PLTPA and poorly at low PLTPA, for D_0 percentile predictions. The three models underestimated at certain ages (6, 10, and 12) and overestimated at others (15, 18, and 21) in lower PLTPA (Figure 3.44). For larger percentiles both approaches showed decent performance without notable differences, confirming that the three models are reliable for predicting large percentiles (Figures 3.45 - 3.47). However, models accounting for environmental co-variables did not show notable improvement in percentile predictions compared to base model predictions.

Percentiles Residuals

Residuals vs. predicted value plot for percentiles estimation for the general level are presented in Figure 3.48 – 3.51. The results for D_0 percentile for the six models appear to be similar, showing a homoscedasticity for lower PLTPA (200 and 450) for all ages. On the other hand, the residuals for higher PLTPA (700, 950, and 1200) display heteroscedasticity behavior. For D_{25} percentile the behavior is a mixture; ages 6, 8, 10, 12, and 15 appear to show homoscedasticity for all five PLTPA and the same behavior at age 18 for 950 PLTPA. At ages 18 and 21 for 200, 450, 700 and 1200 PLTPA the residuals have heteroscedasticity behavior. For percentile D_{50}, JB and the PMRC model systems show a strong similar result; all six models display homoscedasticity behavior all for PLTPA and ages. For D_{95} percentile the six models appear to be similar; the results display homoscedasticity behavior for all five PLTPA and ages. For the regional level (Figures 3.52 - 3.55), the residuals for D_0 percentile for all six models, for base and adapted, display a similar trend for each year and PLTPA; the homoscedasticity behavior is present for all PLTPA and ages. For D_{25} percentile, the residuals for all six models show bias at ages 6, 18, and 21 for all PLTPA. At ages 8, 10, 12, and 15 the homoscedasticity behavior is present for all PLTPA, the models appear similar for all six models. Similar to the general level, the residuals for JB and PMRC for base and adapted models for D_{50} percentile show a strong similarity. The base and adapted models display homoscedasticity behavior for all five PLTPA and seven ages. For D_{95} percentile, the residuals for 200, 450, 700, and 1200 PLTPA appear biased with heteroscedasticity behavior for all base and adapted modes at age 6. At ages 8, 10, 12, 15, 18, and 21 all six models for base and adapted appear to have similar results and homoscedasticity behavior.

Weibull three-parameter estimation

Based on the general level results, in the estimation of the location (a) parameter from the Weibull distribution, it can be observed that Cao's base model (M2) and Cao's adapted model accounting for environmental co-variables (M5) showed greater differences compared to JB's base model (M1), JB's adapted model (M4), PMRC's base model (M3), and its adapted model (M6). For PLTPA 200, the a parameter estimated by Cao's adapted model showed higher value in some INST compared to the same INST under Cao's base model. In other INST, the adapted model presented lower a parameter values compared to the base model for the same INST, and this pattern was consistent across all ages. Similar results were observed for the other PLTPA levels. For the JB and PMRC models, the difference between the a parameter of the base and adapted models was more evident in the lower densities (200 and 450 PLTPA) (Figure 3.56). A similar pattern was found for the b parameter, where Cao's base and adapted models exhibited greater differences. Likewise, both higher and lower b parameter values were observed in some INST for all five PLTPA levels and across all ages. For the JB and PMRC models, this behavior was observed at PLTPA 200, 450, and 750 (Figure 3.57). For the c parameter, INST in juvenile age shows more evident difference between the base and adapted models, with more higher difference in low PLTPA (Figure 3.58).

For the regional level (Figure 3.59), similar to the general-level results for 200 PLTPA, the a parameter for the adapted model exhibited higher values compared to the corresponding parameters from the base model. For 450 PLTPA, differences between parameters were observed at ages 18 and 20 for all three adapted models, and at ages 10 and 12 for the Cao and JB models. For 700 PLTPA, the Cao model showed greater differences at ages 18 and 20, while for the JB model, this occurred at age 12. For the PMRC model, the difference between the base and adapted models was not substantial. For 950 and 1200 PLTPA, both the base and adapted models showed very similar a parameter values, with no notable difference between the two approaches.

Regarding the scale (b) parameter (Figure 3.60), the adapted models accounting for environmental co-variables generally yielded higher parameter values. This result was evident at ages 8, 10, 12, 15, 18, and 20. However, for some INST, the adapted models produced lower b values, similar to the pattern found for the general level. For 700 PLTPA, differences between parameters were most evident at age 20 across all models, and at age 18 for the Cao model. For 950 PLTPA, differences were observed at ages 15, 18, and 20 for the Cao and JB models. For 1200 PLTPA, only the Cao model showed a visible difference between the b parameters of the base and adapted models with environmental co-variables.

For the shape (c) parameter, the results for 200 PLTPA indicate a difference at age 6 for the Cao and JB models. In some INST, Cao's adapted model yielded higher c parameter values, while in others it showed lower values compared to Cao's base model. For JB, on the other hand, the adapted model accounting for environmental co-variables generally produced lower c parameter values compared to its base model. At ages 8, 10, and 12, the c parameters of Cao's adapted model were higher than those from Cao's base model, whereas at ages 18 and 20, the adapted model yielded lower parameter values. For JB, the results were mixed: in some INST the adapted model produced higher c values, while in others it produced lower ones. A similar pattern was observed for the PMRC model. A comparable behavior was also found for 450, 700, and 950 PLTPA, where for certain INST and ages, the adapted models presented higher c parameter values, while for others they showed lower values (Figure 3.61).

By averaging the three-parameter Weibull model, all changes represent differences between the adapted models and their respective base models across five PLTPA levels and ages. These results, presented for both the general and regional levels, are shown in Tables 3.27–3.29. Cao's adapted model shows changes in the a parameter at 200 PLTPA at ages 6, 15, 18, and 20 by 2.20%, 2.69%, 3.33%, and 6.49%, respectively. Similarly, JB's adapted model shows changes at ages 6, 8, 10, 18, and 21 by 26.09%, 1.30%, 1.01%, 0.99%, and 1.47%, respectively. PMRC's adapted model shows changes in the a parameter at ages 6, 8, 10, 12, and 15 by 3.62%, 0.74%, 1.01%, 0.86%, and 0.93%, respectively. At 450 PLTPA, changes in the a parameter are observed at age 6 for the Cao, JB, and PMRC adapted models, by 3.99%, 8.57%, and 3.50%, respectively. For 700 PLTPA, the Cao and PMRC adapted models show changes in the a parameter at age 6 by 6.75% and 2.00%, respectively. For 950 PLTPA, changes in the a parameter occur at age 15 for Cao's and JB's adapted models, and at age 6 for PMRC's adapted model, with differences of 3.16%, 1.56%, and 3.26%, respectively. At 1200 PLTPA, Cao's adapted model shows changes in the *a* parameter at ages 6, 8, and 15 by 9.04%, 4.19%, and 2.22%, respectively. JB's adapted model shows a change of 2.19% at age 10, while PMRC's adapted model shows changes of 3.76% and 2.19% at ages 6 and 8, respectively (Figure 3.62).

For the *b* parameter, Cao's adapted model shows a change of 1.59% at age 8 and the highest change of 8.27% at age 21 for 200 PLTPA. JB's adapted model shows a change of 1.67% at age 15, while PMRC's adapted model shows a change of 1.23% at age 18. At 450 PLTPA, Cao's adapted model shows changes of 0.32% at age 8 and 5.17% at age 21. JB's adapted model shows a change of 1.61% at age 12, and PMRC's adapted model shows a change of 1.79% at age 18. For 700 PLTPA, Cao's and JB's adapted models show changes in the *b* parameter at age 21 by 2.64% and 1.38%, respectively, while PMRC's adapted model shows a change of 1.22% at age 18. Similar results are observed at 950 PLTPA, where Cao's adapted model shows a change of 2.98% and PMRC's adapted model shows a change of 0.84%, both at age 21. At 1200 PLTPA, Cao's and PMRC's adapted models show changes in the *b* parameter at age 21 by 4.26% and 3.33%, respectively (Figure 3.63).

Regarding the *c* parameter, Cao's adapted model shows a change of 4.06% at age 21 compared to the base model at 200 PLTPA. JB's adapted model presents changes at ages 8, 18, and 21 by 2.91%, 3.27%, and 6.60%, respectively. PMRC's adapted model shows changes at ages 8, 18, and 21 by 1.46%, 1.70%, and 2.95%, respectively.At 450 PLTPA, Cao's adapted model shows changes of 2.42% and 4.78% at ages 18 and 21, respectively. JB's adapted model shows changes at ages 8, 18, and 21 by 3.06%, 2.66%, and 3.00%, respectively, while PMRC's adapted model shows changes at ages 8 and 21 by 1.78% and 1.49%, respectively.For 700 PLTPA, both Cao's and PMRC's adapted models show changes at age 18, with differences of 1.32%. JB's adapted model shows changes at ages 8, 18, and 21 by 2.09%, 1.41%, and 1.44%, respectively. PMRC's adapted model also shows changes at ages 8, 18, and 20 by 1.06%, 1.29%, and 1.86%, respectively. For 950 PLTPA, Cao's adapted model shows a change of

1.18% at age 18. JB's adapted model shows changes at ages 8 and 18 by 1.87% and 1.74%, respectively, while PMRC's adapted model shows changes at the same ages by 1.18% and 1.05%, respectively. At 1200 PLTPA, Cao's adapted model shows a change of 1.05% at age 8. JB's adapted model shows changes of 2.15% and 1.50% at ages 8 and 10, respectively. PMRC's adapted model shows changes of 1.38% and 1.21% at ages 8 and 21, respectively (Figure 3.64).

The Weibull three-parameter results for the regional level of modeling are presented in Tables 3.31–3.33. For 200 PLTPA, Cao's adapted model shows effects of environmental co-variables at ages 6 and 8, with changes in the a parameter of 12.90% and 4.10%, respectively. JB's and PMRC's adapted models also show effects of environmental co-variables, with changes of 11.30% and 2.00% at age 6, and 4.92% and 8.23% at age 21, respectively. At 450 PLTPA, the three adapted models show changes in the a parameter of 3.09%, 6.36%, and 3.49% for Cao, JB, and PMRC, respectively. For 700 PLTPA, the three adapted models show their greatest changes at age 6, with differences of 6.25% for Cao, 4.44% for JB, and 3.79% for PMRC. At 950 PLTPA, Cao's adapted model shows changes in the a parameter at ages 6 and 8 by 4.69% and 2.16%, respectively. JB's adapted model shows changes at ages 6, 8, and 18 by 2.34%, 3.28%, and 1.65%, respectively, while PMRC's adapted model shows changes at ages 10 and 21 by 1.60% and 1.21%, respectively. For 1200 PLTPA, Cao's adapted model shows a change in the a parameter of 8.08% at age 6. JB's adapted model shows a change of 1.89% at age 10, and PMRC's adapted model shows a change of 3.34% at age 6 (Figure 3.62).

For the b parameter for the regional level, for 200 PLTPA, Cao's adapted model shows changes at ages 6, 8, and 15 by 17.47%, 2.30%, and 2.09%, respectively. JB's adapted model shows changes at ages 6 and 21 by 2.66% and 6.26%, respectively, while PMRC's adapted model shows a change of 11.48% at age 21. At 450 PLTPA, Cao's adapted model shows changes at ages 8 and 18 by 1.03% and 2.76%, respectively. JB's adapted model shows changes at ages 15, 18, and 21 by 0.81%, 2.94%, and 5.17%, respectively, while PMRC's adapted model shows a change of 0.96% at age 21. For 700, 950, and 1200 PLTPA, the differences between the averages of the base and adapted models, accounting for environmental covariables, do not show notable variation (Figure 3.63).

Regarding the c parameter, Cao's adapted model shows changes at 200 PLTPA at ages 6, 15, 18, and 21 by 15.90%, 2.13%, 3.63 and 3.80%, respectively, compared to the c parameter from Cao's base model. JB's adapted model shows changes at ages 6 and 21 by 4.22% and 6.47%, respectively, while PMRC's adapted model shows a change of 11.21% at age 21. At 450 PLTPA, Cao's adapted model shows changes at ages 6 and 18 by 2.48% and 3.44%, respectively. JB's adapted model shows changes at ages 6, 18, and 21 by 4.14%, 3.43%, and 3.54%, respectively, while PMRC's adapted model shows a change of 2.41% at age 6. For 700, 950, and 1200 PLTPA, the differences between the base and adapted models for all three models do not show notable variation in the c parameter (Figure 3.64).

3.6 Discussion

The inclusion of environmental co-variables produced different results depending on planting density, modeling level (i.e., general and regional) and age.

For the percentile predictions, all base and adapted models provided better predictions for higher PLTPA and for juvenile stands for the first level (i.e. the general level) combined the three regional datasets into a single dataset. The regression models seem to have a better performance for larger percentile diameters, since the models provided an adequate prediction in the base model and when accounting for environmental co-variables.

No notable difference was found between the base and the adapted models for the second level (i.e., the regional level), with the three regional datasets applied separately for the three regions (LCP, UCP, and IF); by analyzing the output for the regression models it was noticed that both base and adapted models percentiles predictions were similar.

The models underestimated the percentiles predictions at certain ages and overestimated at others in lower PLTPA. For larger percentiles, both approaches showed decent performance without notable differences, confirming that the all models are reliable for predicting large percentiles. The adapted models accounting for environmental co-variables does not show notable improvement in percentile predictions compared to base models predictions. This might be due to the difficulty in detecting relationships between environmental co-variables (i.e., precipitation, maximum and minimum temperature) and ecological processes (e.g., tree growth), since environmental datasets are often available at finer temporal scales (daily, monthly), whereas ecological datasets (e.g., DBH, HD) are measured over much longer intervals (years) (Tredennick et al., 2021). Although including environmental co-variables in the percentile models does not seem to provide notable improvement in the percentiles predictions, the AIC results for all percentiles and the three adapted models for the general level of modeling decreased. The model most affected by environmental co-variables ($Temp_{max}$, WD, PPT) for the general level was the one created by Cao, especially for the percentile of D_{25}. The models created by Jiang and Brooks and by Cao showed improvements when environmental co-variables is included in the D_0 percentile regression for the regional level.

Regarding the Weibull three-parameter estimation, by accounting for environmental co-variables an effect on the a parameter for both the general and regional modeling levels can be observed in some specific age and PLTPA. The inclusion of these variables—specifically: $Temp_{max}$ associated with the D_0 percentile and WD associated with the D_{50} percentile, as well as tree density (trees per plot)— notable changes this parameter compared to the a parameter from base model. Tree growth is strongly influenced by climatic conditions, where increases in temperature (within non-limiting ranges) and adequate water availability enhance diameter growth rates (D'Orangeville et al., 2018; Anderson-Teixeira et al., 2022; Huang et al., 2021). By including precipitation co-variable in the estimation of the D_{95} percentile, an effect on the c parameter is observed in some ages, and PLTPA, with decrease values from the adapted model compared to the base model, with strong notable evidence for the regional level. The negative trend can be explain by the fact of under conditions of high precipitation, the greater availability of soil water enhances tree growth, as trees have sufficient water to develop more rapidly (Yan et al., 2025). Consequently, smaller trees tend to exhibit lower mortality rates and higher chances of survival, while dominant trees can grow faster. Thus, in scenarios with higher precipitation and greater tree growth potential, the *c* parameter tends to become flatter, showing a negative relationship with precipitation (Sanquetta et al., 2014; Guo et al., 2024; Yan et al., 2025), which indicates a greater concentration of individuals in larger diameter classes, and obtain lower *c* parameter values. The estimation of the Weibull *b* parameter is not based on a specific percentile, as shown in Equation 2.30. This parameter is computed using the estimated location parameter, D_q, and the gamma-1 and gamma-2 functions, in which the *c* parameter is employed (Equation 2.28 - 2.29). The *b* parameter showed mixed results, this parameter has sensitive and strongly influenced by the D_q; as D_q increases, the *b* parameter also tends to increase (Yan et al., 2025). The decrease in this parameter at certain ages may be associated with the use of the gamma function in its computation, since this function depends on the *c* parameter. Because the *c* parameter is affected by precipitation, it can indirectly influence the *b* parameter through the gamma functions, resulting in a decreases on *b* parameter (Guo et al., 2022).

At low PLTPA, the Weibull PDF from parameters used percentiles estimated by accounting for environmental co-variables shows no notable improvement in goodness-of-fit (EI) or precision (RMSE) compared to Weibull PDF from the base models for the general level. This result suggests that at low PLTPA, environmental resources such as light, water, and nutrients are not limiting, and thus environmental co-variables have a minimal impact on characterizing tree growth and diameter distribution (Forrester et al., 2013). In contrast, at medium and high densities, all Weibull PDFs from adapted models demonstrated better performance, particularly at younger ages. These results can be explained by the fact that, at low planting densities, environmental resources such as precipitation, light, and soil nutrients are more readily available for trees to capture because the competition is not as intensive as in the higher planting densities, since the site is not fully occupied (Forrester et al., 2013). It seems that at these ages environmental co-variables were important to obtain a lower EI values. These trends are expected and also make biological sense when considering tree development, since growth peaks during the early stages of a plantation. For highest PLTPA, besides the fact that trees reach peak growth within this age range (6, 8, 10, 12), competition increases with greater planting density by trees competing for the same nutrients that make environmental co-variables important and essential for tree development (Figures 3.65–3.66).

For the regional modeling level, the inclusion of environmental co-variables in the percentiles estimation model improved the performance of the Weibull PDF across most planting densities and ages. These results indicate that incorporating environmental co-variables enhances Weibull PDF accuracy by capturing part of the spatial and temporal variability in site conditions that affect tree growth (Forrester et al., 2013; Weiskittel et al., 2011). Regarding model precision, results were generally consistent across densities and Weibull PDF based on parameter from the adapted percentiles estimated. At lower densities, base and adapted Weibull PDF shows similar precision, suggesting that environmental effects are less relevant under low competition. However, at moderate and higher densities, the adapted Weibull PDF shows improved precision, especially during early stand development(Figures 3.67–3.68). These improvements highlight the role of environmental factors—such as precipitation and temperature —in influencing tree competition and growth variability under denser forest stand conditions (Pretzsch, 2010; Forrester et al., 2013).

3.7 Conclusions

Overall, an improvement in diameter distributions fit was observed when environmental co-variables were included in the modeling process. Precipitation, maximum temperature, and water deficit were shown to be important based on lasso regression in diameter percentiles in the Western Gulf region of the United States. Based on AIC, a reduction was observed when these environmental co-variables were incorporated into the prediction of the percentiles.

The models used in this study to predict percentiles performed better in predicting larger percentiles compared to the prediction of the minimum diameter percentile.

For the regional level where three regional datasets were applied separately for the three regions (LCP, UCP, and IF) in the percentile regression models, showed that both the base models and those accounting for environmental co-variables showed better performance for all percentiles and across the five PLTPA levels, compared to the general level, where the three regional datasets were combined into a single dataset. By including environmental co-variables in the percentile predictions models, we take into account the effects of environmental co-variables on the diameter distribution development of the forest stands in the Western Gulf physiographic region.

Based on the general-level results, the estimation of the Weibull parameters indicated that Cao's model was more strongly affected by the inclusion of environmental co-variables, showing greater differences in the Weibull three-parameter (location, scale, and shape) between its base and adapted versions compared to those observed for the JB and PMRC models. For the a parameter, Cao's adapted model presented both higher and lower values across installations, with this pattern consistent for all ages and planting densities. The JB and PMRC models also showed noticeable differences between their base and adapted versions, mainly at lower densities (200 and 450 PLTPA). Similar behavior was observed for the b parameter, where Cao's models showed the largest variations, while for the c parameter, the greatest differences occurred at juvenile ages and in lower planting densities. For the regional level, the adapted models generally produced higher a and b parameter values, particularly at younger ages and in low to medium planting densities. However, as planting density increased, the differences between the base and adapted models became smaller, indicating a reduced effect of environmental co-variables under higher competition. The c parameter tended to decrease in the adapted models at older ages, suggesting a reduction in the upper tail of the diameter distribution. The inclusion of environmental co-variables improved parameter estimation, especially for Cao's adapted model, highlighting the importance of considering environmental factors when modeling diameter distributions across varying stand conditions. When computing the three-parameter Weibull distribution using the percentile-based parameter recovery approach, the estimation of the location, scale, and shape parameters incorporated environmental covariables. This inclusion was achieved by adapting the percentile regression models to account for environmental effects within the model formulation. With this technique, we were able to achieve better performance in estimating the Weibull three-parameter, with a reduction in both the Error Index and RMSE.

3.8 References

Adhikari, A., Masters, R. E., Adams, H., Mainali, K. P., Zou, C. B., Joshi, O., and Will, R. E. (2021). Effects of climate variability and management on shortleaf pine radial growth across a forest-savanna continuum in a 34-year experiment. *Forest Ecology and Management*, 491:119125.

Allen, C. D., Macalady, A. K., Chenchouni, H., Bachelet, D., McDowell, N., Vennetier, M., Kitzberger, T., Rigling, A., Breshears, D. D., Hogg, E. T., Gonzalez, P., Fensham, R., Zhang, Z., Castro, J., Demidova, N., Lim, J.-H., Allard, G., Running, S. W., Semerci, A., and Cobb, N. (2010). A global overview of drought and heat-induced tree mortality reveals emerging climate change risks for forests. *Forest Ecology and Management*, 259(4):660–684. Adaptation of Forests and Forest Management to Changing Climate.

Anderson-Teixeira, K. J., Herrmann, V., Rollinson, C. R., Gonzalez, B., Gonzalez-Akre, E. B., Pederson, N., Alexander, M. R., Allen, C. D., Alfaro-Sánchez, R., Awada, T., et al. (2022). Joint effects of climate, tree size, and year on annual tree growth derived from tree-ring records of ten globally distributed forests. *Global Change Biology*, 28(1):245–266.

Boukhris, I., Marano, G., Dalmonech, D., Valentini, R., and Collalti, A. (2025). Modeling forest growth under current and future climate. *Current Forestry Reports*, 11(1):17.

Breshears, D. D., Cobb, N. S., Rich, P. M., Price, K. P., Allen, C. D., Balice, R. G., Romme, W. H., Kastens, J. H., Floyd, M. L., Belnap, J., Anderson, J. J., Myers, O. B., and Meyer, C. W. (2005). Regional vegetation die-off in response to global-change-type drought. *Proceedings of the National Academy of Sciences*, 102(42):15144–15148.

Breshears, D. D., Myers, O. B., Meyer, C. W., Barnes, F. J., Zou, C. B., Allen, C. D., McDowell, N. G., and Pockman, W. T. (2009). Tree die-off in response to global change-type drought: mortality insights from a decade of plant water potential measurements.

Frontiers in Ecology and the Environment, 7(4):185–189.

Bullock, B. P. and Burkhart, H. E. (2005). Juvenile diameter distributions of loblolly pine characterized by the two-parameter weibull function. *New Forests*, 29:233–244.

Cao, Q. V. (2004). Predicting parameters of a weibull function for modeling diameter distribution. *Forest Science*, 50(5):682–685.

Clark, D. A., Piper, S., Keeling, C. D., and Clark, D. (2003). Tropical rain forest tree growth and atmospheric carbon dynamics linked to interannual temperature variation during 1984–2000. *Proceedings of the national academy of sciences*, 100(10):5852–5857.

Clutter, J. L., Fortson, J. C., Pienaar, L. V., Brister, G. H., and Bailey, R. L. (1983). *Timber management: a quantitative approach.* John Wiley 'I&' Sons, Inc., New York.

Daly, C., Halbleib, M., Smith, J. I., Gibson, W. P., Doggett, M. K., Taylor, G. H., Curtis, J., and Pasteris, P. P. (2008). Physiographically sensitive mapping of climatological temperature and precipitation across the conterminous united states. *International Journal of Climatology*, 28(15):2031–2064.

Dannenberg, M. P., Wise, E. K., and Smith, W. K. (2019). Reduced tree growth in the semi-arid united states due to asymmetric responses to intensifying precipitation extremes. *Science Advances*, 5(10):eaaw0667.

de Streel, G., Lebourgeois, F., Ammer, C., Barbeito, I., Bielak, K., Bravo-Oviedo, A., Brazaitis, G., Coll, L., Collet, C., del Río, M., Den Ouden, J., Drössler, L., Heym, M., Hurt, V., Kurylyak, V., Löf, M., Lombardi, F., Matovic, B., Motta, R., Osadchuk, L., Pach, M., Pereira, M., Pretzsch, H., Sitko, R., Skrzyszewski, J., Sramek, V., Svoboda, M., Verheyen, K., Zlatanov, T., and Ponette, Q. (2022). Regional climate moderately influences species-mixing effect on tree growth-climate relationships and drought resistance for beech and pine across europe. *Forest Ecology and Management*, 520:120317.

Dougherty, P. M., Whitehead, D., and Vose, J. M. (1994). Environmental influences on the phenology of pine. *Ecological Bulletins*, pages 64–75.

D'Orangeville, L., Houle, D., Duchesne, L., Phillips, R. P., Bergeron, Y., and Kneeshaw, D. (2018). Beneficial effects of climate warming on boreal tree growth may be transitory. *Nature communications*, 9(1):3213.

Elli, E., Caron, B., Behling, A., Eloy, E., Souza, V. Q. D., Schwerz, F., and Stolzle, J. (2017). Climatic factors defining the height growth curve of forest species. *iForest - Biogeosciences and Forestry*, (3):547–553.

Fisher, D. K. and Pringle III, H. (2013). Evaluation of alternative methods for estimating reference evapotranspiration. *Agricultural Sciences*, 4(8):51–60.

Forrester, D. I., Wiedemann, J. C., Forrester, R. I., and Baker, T. G. (2013). Effects of planting density and site quality on mean tree size and total stand growth of eucalyptus globulus plantations. *Canadian Journal of Forest Research*, 43(9):846–851.

Fu, L., Sun, W., and Wang, G. (2017). A climate-sensitive aboveground biomass model for three larch species in northeastern and northern china. *Trees*, 31.

Gough, C., Seiler, J., and Maier, C. A. (2004). Short-term effects of fertilization on loblolly pine (pinus taeda l.) physiology. *Plant, Cell & Environment*, 27(7):876–886.

Guo, H., Lei, X., You, L., Zeng, W., Lang, P., and Lei, Y. (2022). Climate-sensitive diameter distribution models of larch plantations in north and northeast china. *Forest Ecology and Management*, 506:119947.

Guo, H., Liu, X., and Liu, D. (2024). Soil-sensitive weibull distribution models of larix principis-rupprechtii plantations across northern china. *Forests*, 15(9).

Hastie, T., Tibshirani, R., and Friedman, J. (2001). *The Elements of Statistical Learning*. Springer Series in Statistics. Springer New York Inc., New York, NY, USA.

Hennessey, T., Dougherty, P., Cregg, B., and Wittwer, R. (1992). Annual variation in needle fall of a loblolly pine stand in relation to climate and stand density. *Forest Ecology and Management*, 51(4):329–338.

Huang, J., Abt, B., Kindermann, G., and Ghosh, S. (2011). Empirical analysis of climate change impact on loblolly pine plantations in the southern united states. *Natural Resource Modeling*, 24(4):445–476.

Huang, X., Dai, D., Xiang, Y., Yan, Z., Teng, M., Wang, P., Zhou, Z., Zeng, L., and Xiao, W. (2021). Radial growth of pinus massoniana is influenced by temperature, precipitation, and site conditions on the regional scale: A meta-analysis based on tree-ring width index. *Ecological Indicators*, 126:107659.

Jackson, B. E., Wright, R. D., Browder, J. F., Harris, J. R., and Niemiera, A. X. (2008). Effect of fertilizer rate on growth of azalea and holly in pine bark and pine tree substrates. *HortScience*, 43(5):1561–1568.

Jiang, L. and Brooks, J. R. (2009). Predicting diameter distributions for young longleaf pine plantations in southwest georgia. *Southern Journal of Applied Forestry*, 33(1):25–28.

Jokela, E. J., Dougherty, P. M., and Martin, T. A. (2004). Production dynamics of intensively managed loblolly pine stands in the southern united states: a synthesis of seven long-term experiments. *Forest ecology and management*, 192(1):117–130.

Koirala, A., Montes, C. R., and Bullock, B. P. (2021). Modeling dominant height using stand and water balance variables for loblolly pine in the western gulf, us. *Forest Ecology and Management*, 479:118610.

Lei, X., Yu, L., and Hong, L. (2016). Climate-sensitive integrated stand growth model (cs-isgm) of changbai larch (larix olgensis) plantations. *Forest Ecology and Management*, 376:265–275.

Lévesque, M., Rigling, A., Bugmann, H., Weber, P., and Brang, P. (2014). Growth response of five co-occurring conifers to drought across a wide climatic gradient in central europe. *Agricultural and Forest Meteorology*, 197:1–12.

Maréchaux, I., Langerwisch, F., Huth, A., Bugmann, H., Morin, X., Reyer, C. P., Seidl, R., Collalti, A., Dantas de Paula, M., Fischer, R., Gutsch, M., Lexer, M. J., Lischke, H., Rammig, A., Rödig, E., Sakschewski, B., Taubert, F., Thonicke, K., Vacchiano, G., and Bohn, F. J. (2021). Tackling unresolved questions in forest ecology: The past and future role of simulation models. *Ecology and Evolution*, 11(9):3746–3770.

Matallana-Ramirez, L. P., Whetten, R. W., Sanchez, G. M., and Payn, K. G. (2021). Breeding for climate change resilience: A case study of loblolly pine (pinus taeda l.) in north america. *Frontiers in Plant Science*, Volume 12 - 2021.

Matziris, D. I. and Zobel, B. J. (1976). Effect of fertilization on growth and quality characteristics of loblolly pine. *Forest Ecology and Management*, 1:21–30.

McMurtrie, R., Rook, D., and Kelliher, F. (1990). Modelling the yield of pinus radiata on a site limited by water and nitrogen. *Forest Ecology and Management*, 30(1-4):381–413.

McMurtrie, R. E., Gholz, H. L., Linder, S., and Gower, S. T. (1994). Climatic factors controlling the productivity of pine stands: a model-based analysis. *Ecological Bulletins*, pages 173–188.

Meir, P., Mencuccini, M., and Dewar, R. C. (2015). Drought-related tree mortality: addressing the gaps in understanding and prediction. *New Phytologist*, 207(1):28–33.

Nardi, Y. and Rinaldo, A. (2011). Autoregressive process modeling via the lasso procedure. *Journal of Multivariate Analysis*, 102(3):528–549.

Nyland, R. D. (2016). *Silviculture: concepts and applications*. Waveland Press.

Overpeck, J. T., Bartlein, P. J., and Webb, T. (1991). Potential magnitude of future vegetation change in eastern north america: Comparisons with the past. *Science*, 254(5032):692–695.

Overpeck, J. T., Rind, D., and Goldberg, R. (1990). Climate-induced changes in forest disturbance and vegetation. *Nature*, 343(6253):51–53.

Poorter, L., van der Sande, M. T., Arets, E. J., Ascarrunz, N., Enquist, B. J., Finegan, B., Licona, J. C., Martínez-Ramos, M., Mazzei, L., Meave, J. A., et al. (2017). Biodiversity and climate determine the functioning of neotropical forests. *Global ecology and biogeography*, 26(12):1423–1434.

Poudel, K. P. and Cao, Q. V. (2013). Evaluation of methods to predict weibull parameters for characterizing diameter distributions. *Forest Science*, 59(2):243–252.

Pretzsch, H. (2010). Forest dynamics, growth and yield: From measurement to model. springer.

Reyer, C. (2015). Forest productivity under environmental change—a review of stand-scale modeling studies. *Current Forestry Reports*, 1.

Sandoval, S., Cancino, J., Rubilar, R., Esquivel, E., Acuna, E., Munoz, F., and Espinosa, M. (2012). Probability distributions in high-density dendroenergy plantations. *Forest Science*, 58(6):663–672.

Sanquetta, C. R., Behling, A., Dalla Corte, A. P., Péllico Netto, S., Rodrigues, A. L., and Simon, A. A. (2014). A model based on environmental factors for diameter distribution in black wattle in brazil. *PLOS ONE*, 9(6):1–11.

Skovsgaard, J. P. and Vanclay, J. K. (2013). Forest site productivity: a review of spatial and temporal variability in natural site conditions. *Forestry: An International Journal of Forest Research*, 86(3):305–315.

Tibshirani, R. (1996). Regression shrinkage and selection via the lasso. *Journal of the Royal Statistical Society. Series B (Methodological)*, 58(1):267–288.

Tredennick, A. T., Hooker, G., Ellner, S. P., and Adler, P. B. (2021). A practical guide to selecting models for exploration, inference, and prediction in ecology. *Ecology*, 102(6):e03336.

Wang, H., Li, G., and Tsai, C.-L. (2007). Regression coefficient and autoregressive order shrinkage and selection via the lasso. *Journal of the Royal Statistical Society. Series B (Statistical Methodology)*, 69(1):63–78.

Watson, E. and Luckman, B. H. (2001). Dendroclimatic reconstruction of precipitation for sites in the southern canadian rockies. *The Holocene*, 11(2):203–213.

Weiskittel, A. R., Hann, D. W., Kershaw Jr, J. A., and Vanclay, J. K. (2011). *Forest growth and yield modeling.* Hoboken, NJ: John Wiley 'I&' Sons, 169-172 p.

Yan, Y., Zhang, Z., Jiang, L., and Gaire, D. (2025). Climate and soil influence diameter distribution: a case study for pinus koraiensis plantations in northeast china. *European Journal of Forest Research*, pages 1–15.

Yang, Y. and Huang, S. (2014). Suitability of five cross validation methods for performance evaluation of nonlinear mixed-effects forest models – a case study. *Forestry: An International Journal of Forest Research*, 87(5):654–662.

Zellner, A. (1962). An efficient method of estimating seemingly unrelated regressions and tests for aggregation bias. *Journal of the American statistical Association*, 57(298):348–368.

Zhao, D., Bullock, B. P., Wang, M., Kinane, S. M., and Queiroz, T. (2025). Growth and structural responses of loblolly pine plantations to first and second thinning, and post-thinning treatments in the southeastern us. *Forest Ecology and Management*, 594:122975.

Zhao, P. and Yu, B. (2006). On model selection consistency of lasso. *Journal of Machine Learning Research*, 7(90):2541–2563.

Zou, H. (2006). The adaptive lasso and its oracle properties. *Journal of the American Statistical Association*, 101(476):1418–1429.

3.9 Tables and Figures

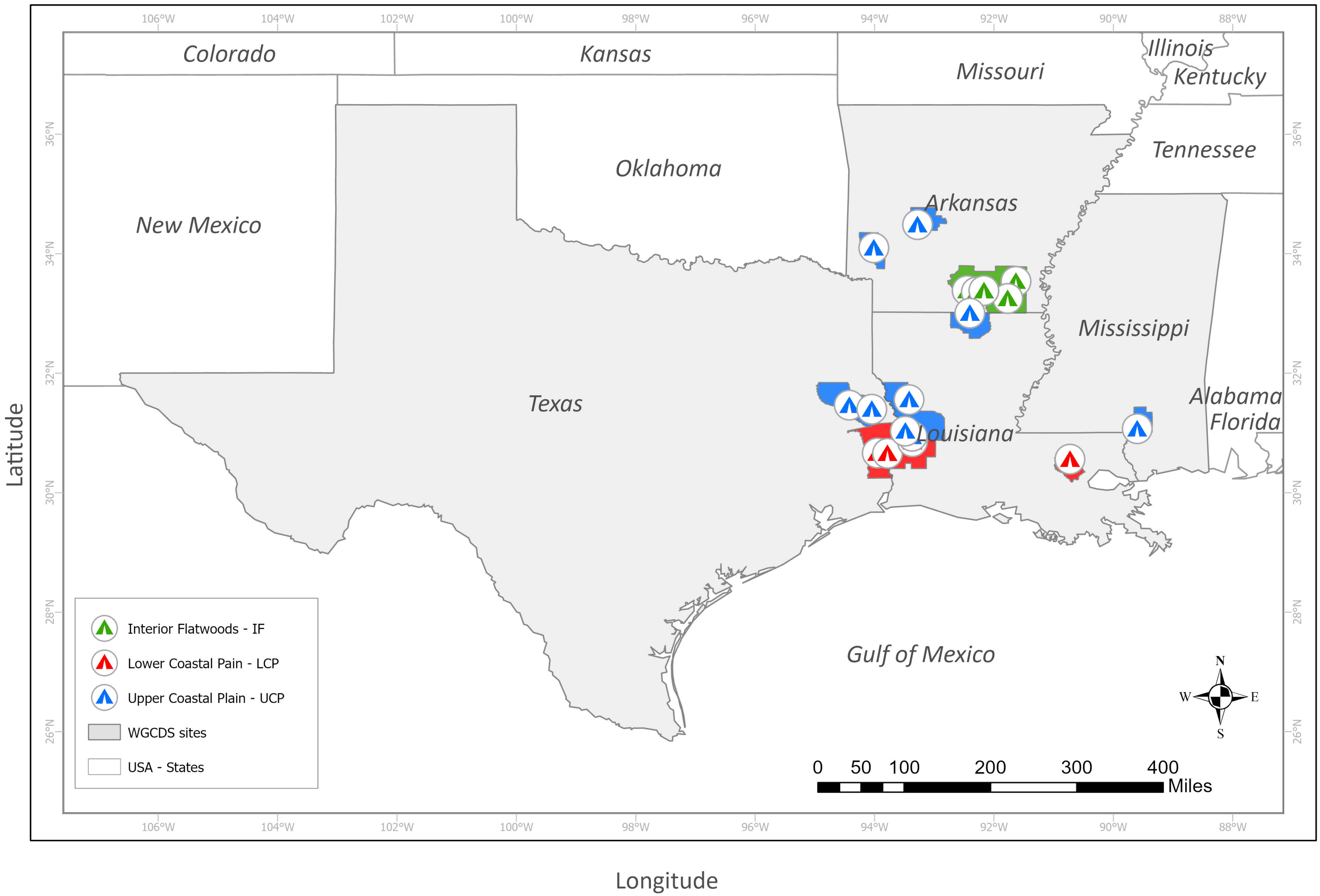

Figure 3.1: Western Gulf Culture Density Study installations across Interior Flatwoods, Lower Coastal Plain, and, Upper Coastal Plain regions.

Table 3.1: Environmental co-variables period by installation (INST) and stand age (AGE) for loblolly pine plantation in the Western Gulf physiography region in the United States.

INST	AGE (years)	Env. Cov. Period (from/to)
1–9	8	2001–2008
	10	2001–2010
	12	2001–2012
	15	2001–2015
	18	2001–2018
	21	2001–2021
10–13	8	2002–2009
	10	2002–2011
	12	2002–2013
	15	2002–2016
	18	2002–2019
	21	2002–2022
14–18	6	2003–2008
	8	2003–2010
	10	2003–2012
	12	2003–2014
	15	2003–2017
	18	2003–2021

Table 3.2: Performance of the three regression models (M1, M2, and M3) across four percentiles (D_0, D_{25}, D_{50}, and D_{95}) conducted for the general modeling level aggregated across three regions, seven ages and five planting densities.

PCT	M1			M2			M3		
	RMSE	R^2	AIC	RMSE	R^2	AIC	RMSE	R^2	AIC
D_0	1.005	0.709	234.001	1.080	0.686	269.889	1.007	0.705	243.648
D_{25}	0.304	0.976	-1553.255	0.571	0.923	-991.646	0.276	0. 979	-1616.787
D_{50}	0.151	0.995	-2410.317	0.514	0.947	-1241.026	0.151	0.995	-2410.312
D_{95}	0.434	0.972	-1629.019	0.619	0.953	-1337.451	0.366	0.978	-1721.227

Table 3.3: Performance of the three regression models (M1, M2, and M3) across four percentiles (D_0, D_{25}, D_{50}, and D_{95}) for region IF.

PCT	RMSE			R^2			AIC		
	M1	M2	M3	M1	M2	M3	M1	M2	M3
D_0	0.859	0.960	0.843	0.741	0.739	0.749	42.041	47.665	39.171
D_{25}	0.201	0.341	0.182	0.992	0.977	0.992	-539.865	-411.479	-547.292
D_{50}	0.126	0.322	0.126	0.997	0.982	0.997	-682.043	-455.552	-682.057
D_{95}	0.308	0.465	0.219	0.986	0.972	0.993	-495.220	-403.678	-582.595

Table 3.4: Performance of the three regression models (M1, M2, and M3) across four percentiles (D_0, D_{25}, D_{50}, and D_{95}) for region LCP.

PCT	RMSE			R^2			AIC		
	M1	M2	M3	M1	M2	M3	M1	M2	M3
D_0	1.101	1.112	1.140	0.665	0.668	0.634	86.602	90.212	99.988
D_{25}	0.394	0.482	0.349	0.966	0.947	0.974	-315.571	-269.034	-343.455
D_{50}	0.215	0.447	0.215	0.992	0.968	0.992	-499.655	-347.602	-499.662
D_{95}	0.568	0.788	0.415	0.962	0.936	0.980	-356.465	-283.263	-420.992

Table 3.5: Performance of the three regression models (M1, M2, and M3) across four percentiles (D_0, D_{25}, D_{50}, and D_{95}) for region UCP.

PCT	RMSE			R^2			AIC		
	M1	M2	M3	M1	M2	M3	M1	M2	M3
D_0	0.978	0.927	1.000	0.732	0.739	0.723	84.987	78.814	93.639
D_{25}	0.276	0.386	0.238	0.978	0.955	0.982	-808.648	-644.332	-856.825
D_{50}	0.116	0.306	0.116	0.997	0.975	0.997	-1308.447	-823.352	-1308.418
D_{95}	0.359	0.432	0.324	0.975	0.967	0.979	-842.519	-773.717	-879.958

Table 3.6: Precision of the Weibull three-parameter, conducted for the general modeling level aggregated across three regions, seven ages and five planting densities for three percentile-based models (M1, M2, and M3).

AGE	PLTPA	M1		M2		M3	
		Error Index	RMSE	Error Index	RMSE	Error Index	RMSE
6	200	13.50	13.03	12.05	13.64	15.93	14.85
	450	40.64	40.90	45.54	44.56	45.43	45.27
	700	60.10	52.12	61.91	52.54	66.75	55.71
	950	74.00	57.78	73.85	58.29	68.82	54.00
	1200	60.77	55.84	59.72	54.13	62.56	57.26
8	200	20.11	18.89	19.46	18.16	20.00	18.79
	450	40.31	38.17	39.17	38.01	40.26	38.51
	700	59.79	55.64	59.14	54.59	60.80	55.14
	950	84.60	71.09	83.11	69.22	84.11	69.69
	1200	71.23	69.09	70.32	68.70	72.15	69.83
10	200	15.84	17.12	15.80	16.92	16.30	17.35
	450	35.51	33.44	36.82	33.82	36.78	34.09
	700	40.15	40.76	40.02	41.10	40.49	41.07
	950	65.83	61.40	63.59	60.74	63.64	60.76
	1200	69.65	60.57	70.46	61.22	70.21	60.93
12	200	15.72	16.08	15.78	15.47	16.02	15.99
	450	39.59	33.93	38.23	32.38	39.53	33.64
	700	33.56	36.31	33.29	35.81	33.92	36.25
	950	64.82	63.29	62.66	61.92	64.10	62.82
	1200	56.31	55.49	57.07	56.06	57.53	56.07
15	200	15.86	16.32	14.08	15.16	15.41	16.21
	450	27.25	27.00	25.62	25.56	27.06	26.89
	700	28.96	30.82	28.90	30.82	28.91	31.12
	950	41.96	45.40	40.89	43.69	42.90	45.41
	1200	42.04	44.57	42.17	45.40	43.15	46.38
18	200	13.68	14.24	14.28	14.82	13.99	14.67
	450	21.26	24.20	20.88	23.59	22.04	25.15
	700	20.67	23.34	21.54	23.85	21.68	24.46
	950	33.71	37.39	32.89	36.41	34.86	38.67
	1200	32.04	33.98	33.07	35.19	34.83	36.36
21	200	10.76	11.84	10.23	11.24	11.24	12.15
	450	26.84	26.90	25.56	27.24	27.60	28.40
	700	19.06	21.80	18.03	21.17	19.08	22.55
	950	27.71	33.38	29.57	33.41	28.35	34.35
	1200	27.08	30.37	27.90	29.64	27.41	30.29

Table 3.7: Precision of the Weibull three-parameter, conducted for the regional modeling level across seven ages and five planting densities for three percentile models (M1, M2, and M3).

AGE	PLTPA	M1		M2		M3	
		Error Index	RMSE	Error Index	RMSE	Error Index	RMSE
6	200	17.76	16.89	24.43	22.82	22.60	20.37
	450	38.37	36.17	45.20	42.06	42.69	40.41
	700	61.69	49.04	59.61	47.13	63.61	49.83
	950	83.83	67.71	83.44	68.60	82.43	67.18
	1200	76.61	64.81	79.07	66.08	77.16	65.38
8	200	16.62	15.91	17.01	16.08	16.77	16.12
	450	34.92	33.19	34.97	33.42	34.53	33.49
	700	45.28	44.27	44.01	43.20	44.99	44.15
	950	65.32	56.95	65.44	57.00	65.31	56.84
	1200	67.14	61.04	68.23	61.20	66.54	60.89
10	200	14.21	14.47	14.25	14.67	14.49	14.78
	450	30.00	28.97	31.40	29.26	30.97	29.61
	700	32.81	33.17	32.27	32.44	32.98	32.92
	950	50.49	48.19	50.91	48.97	50.03	48.25
	1200	51.93	49.09	51.31	49.27	51.85	48.87
12	200	12.32	12.35	12.18	12.18	12.61	12.46
	450	32.71	28.71	31.89	27.91	32.88	28.95
	700	26.15	28.71	25.71	28.01	25.84	28.32
	950	48.69	46.98	45.28	45.68	47.57	46.67
	1200	43.46	43.52	43.50	43.27	43.68	44.09
15	200	11.22	12.23	10.59	11.70	11.11	12.11
	450	20.63	20.91	19.35	20.01	20.69	21.00
	700	24.45	24.53	23.17	23.84	24.03	24.32
	950	32.70	35.14	32.12	34.94	32.63	35.06
	1200	33.22	36.46	33.08	36.39	34.16	37.73
18	200	10.86	11.45	11.18	11.79	10.86	11.46
	450	17.28	20.08	16.75	19.60	18.03	20.50
	700	21.26	23.36	18.67	21.60	21.26	24.01
	950	24.09	27.61	22.75	26.70	24.95	28.47
	1200	26.27	27.82	25.42	26.95	28.12	29.55
21	200	8.39	10.02	8.69	9.95	8.57	9.74
	450	21.17	22.65	20.59	22.41	21.85	23.14
	700	18.20	19.75	16.40	17.83	18.87	20.83
	950	22.15	27.01	24.07	28.21	23.18	27.98
	1200	27.25	29.73	26.59	29.61	27.34	29.53

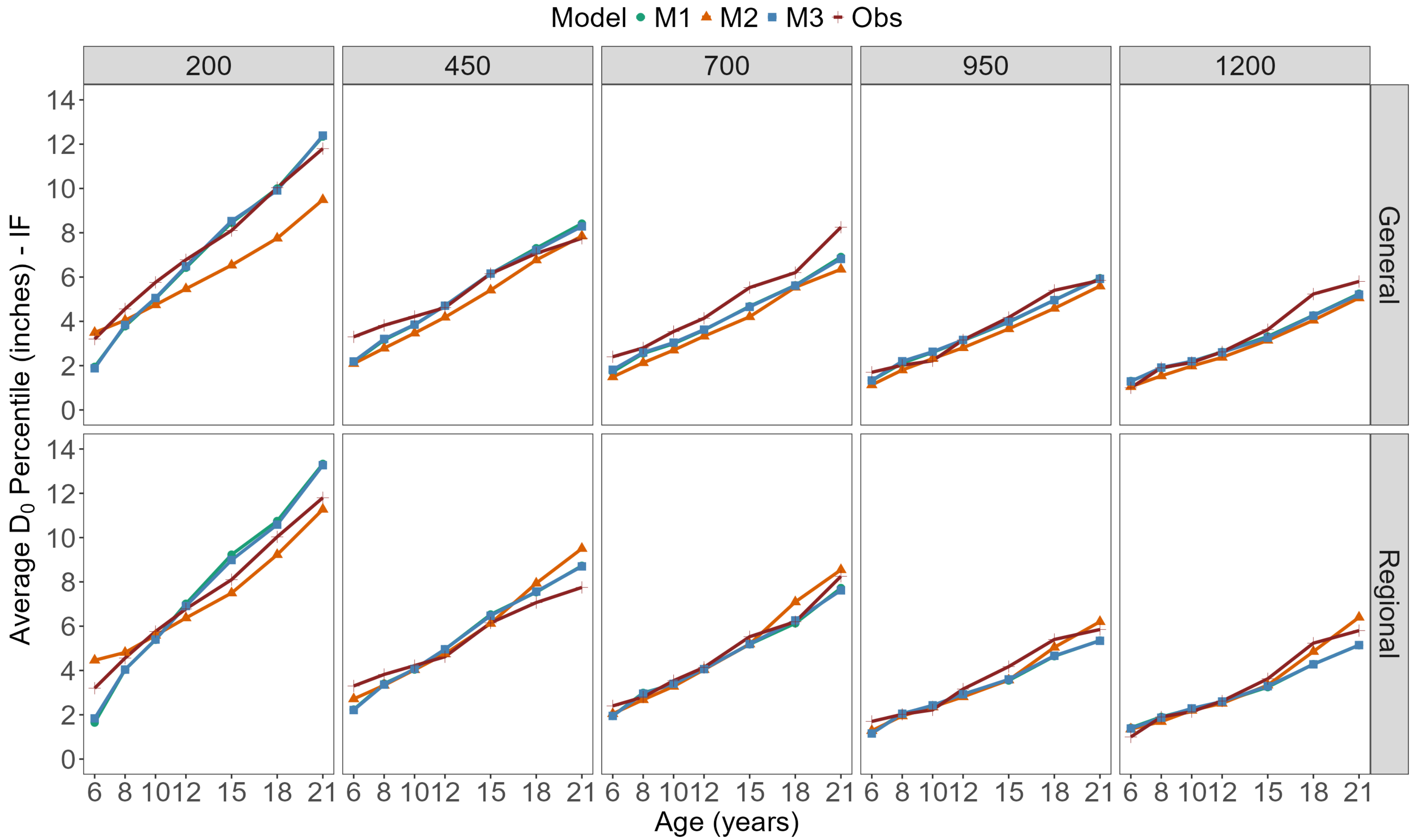

Figure 3.2: Average D_0 percentile values for three regression models (M1, M2, and M3), across two modeling levels and five planting densities, for the IF installations in the WGCDS.

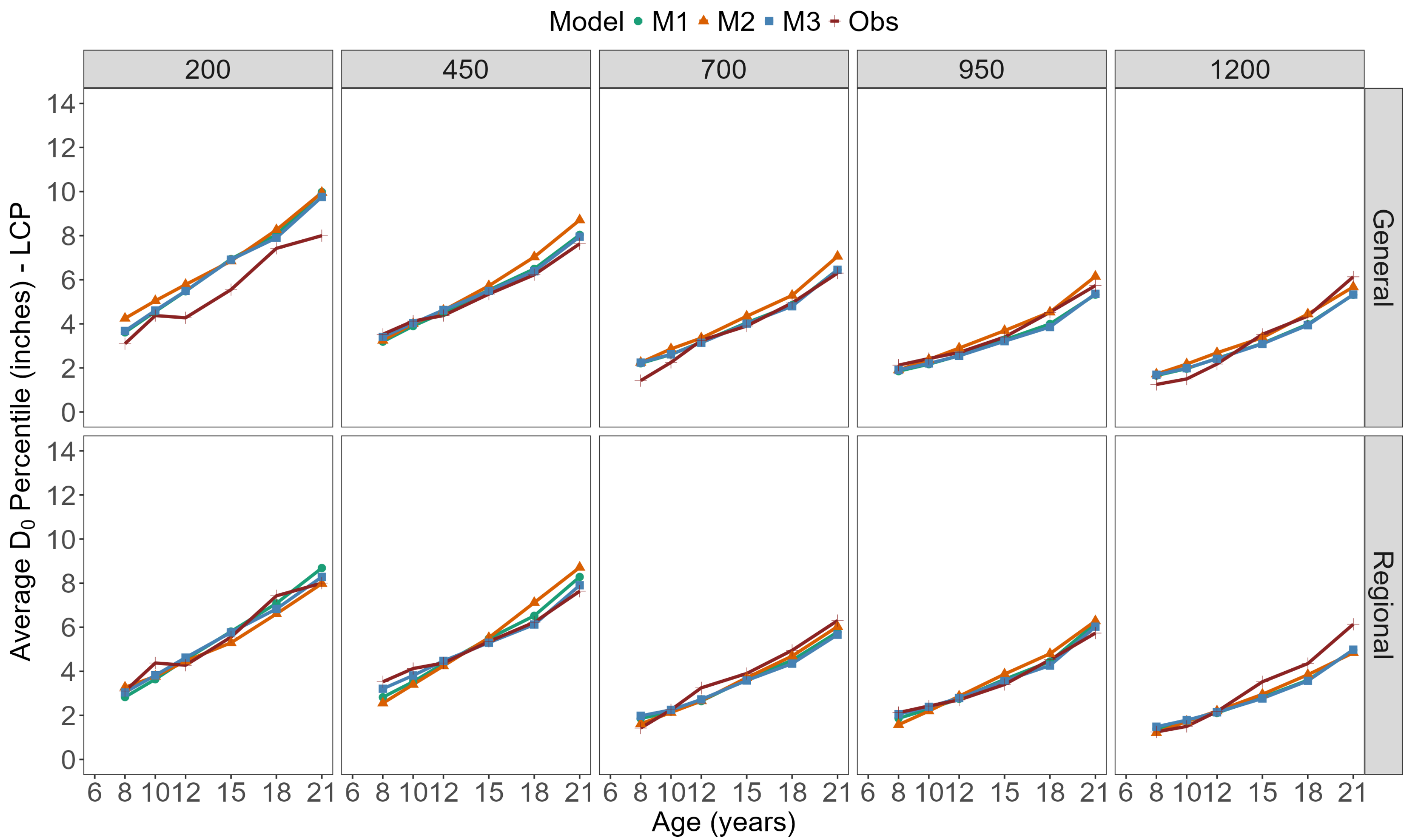

Figure 3.3: Average D_0 percentile values for three regression models (M1, M2, and M3), across two modeling levels and five planting densities, for the LCP installations in the WGCDS.

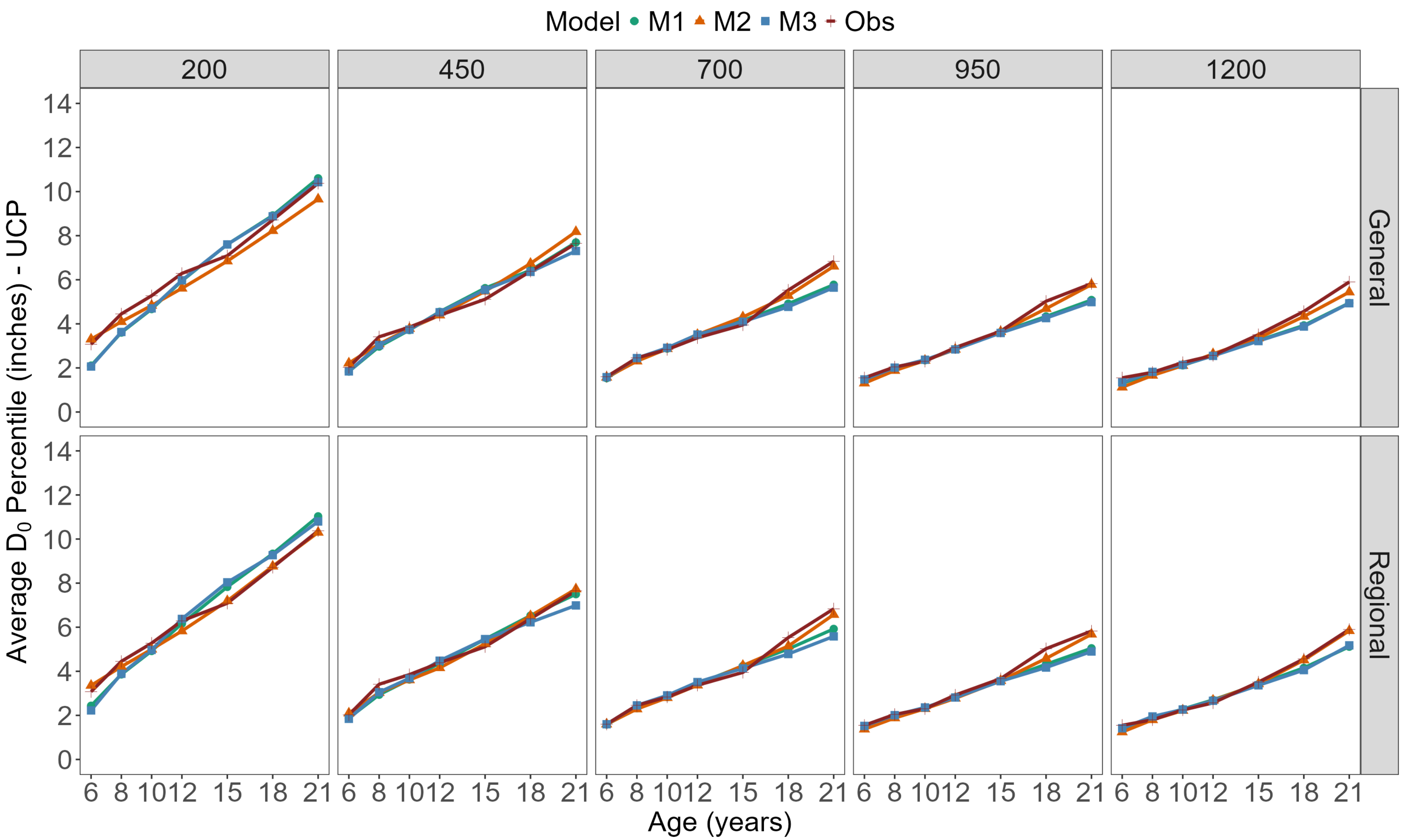

Figure 3.4: Average D_0 percentile values for three regression models (M1, M2, and M3), across two modeling levels and five planting densities, for the UCP installations in the WGCDS.

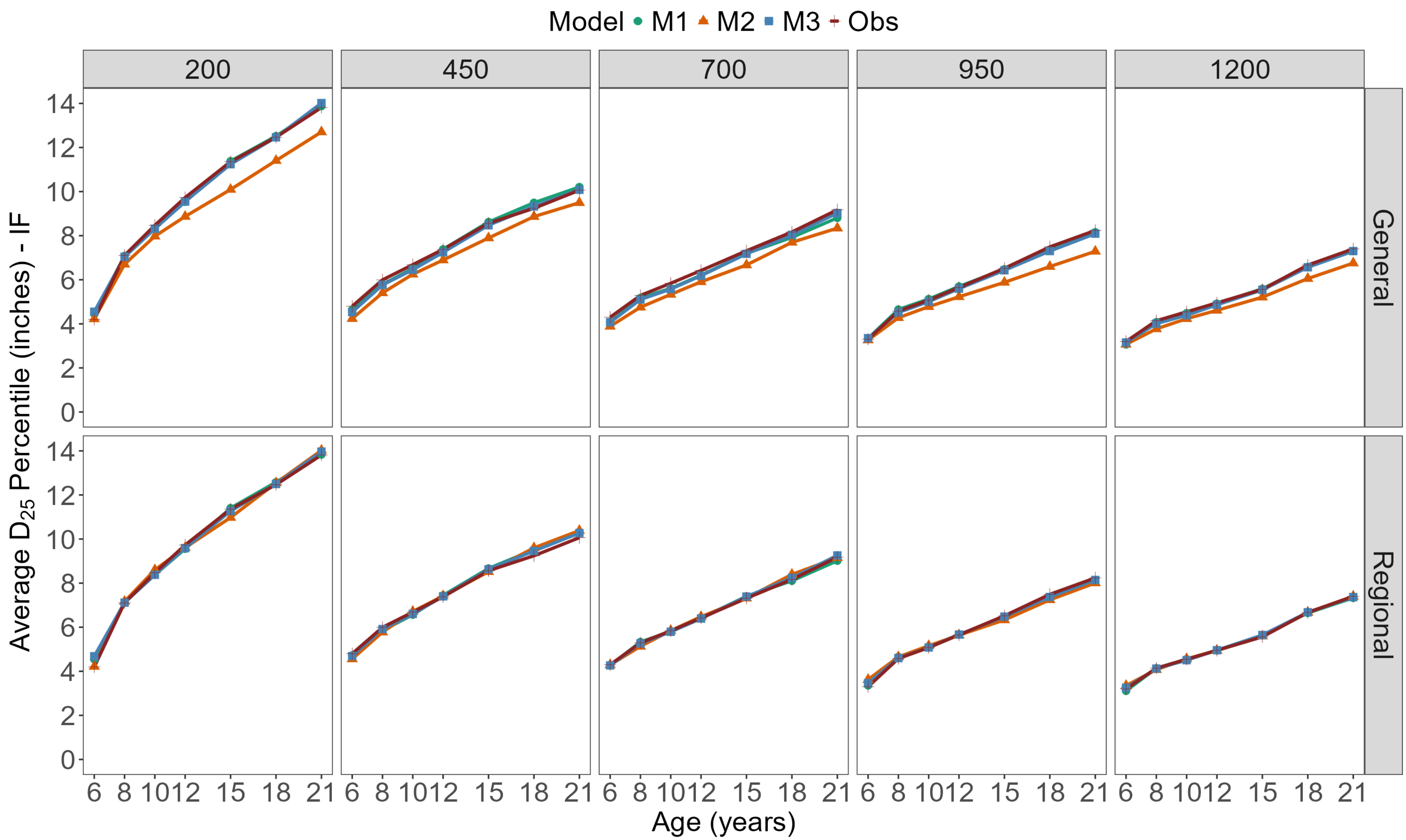

Figure 3.5: Average D_{25} percentile values for three regression models (M1, M2, and M3), across two modeling levels and five planting densities, for the IF installations in the WGCDS.

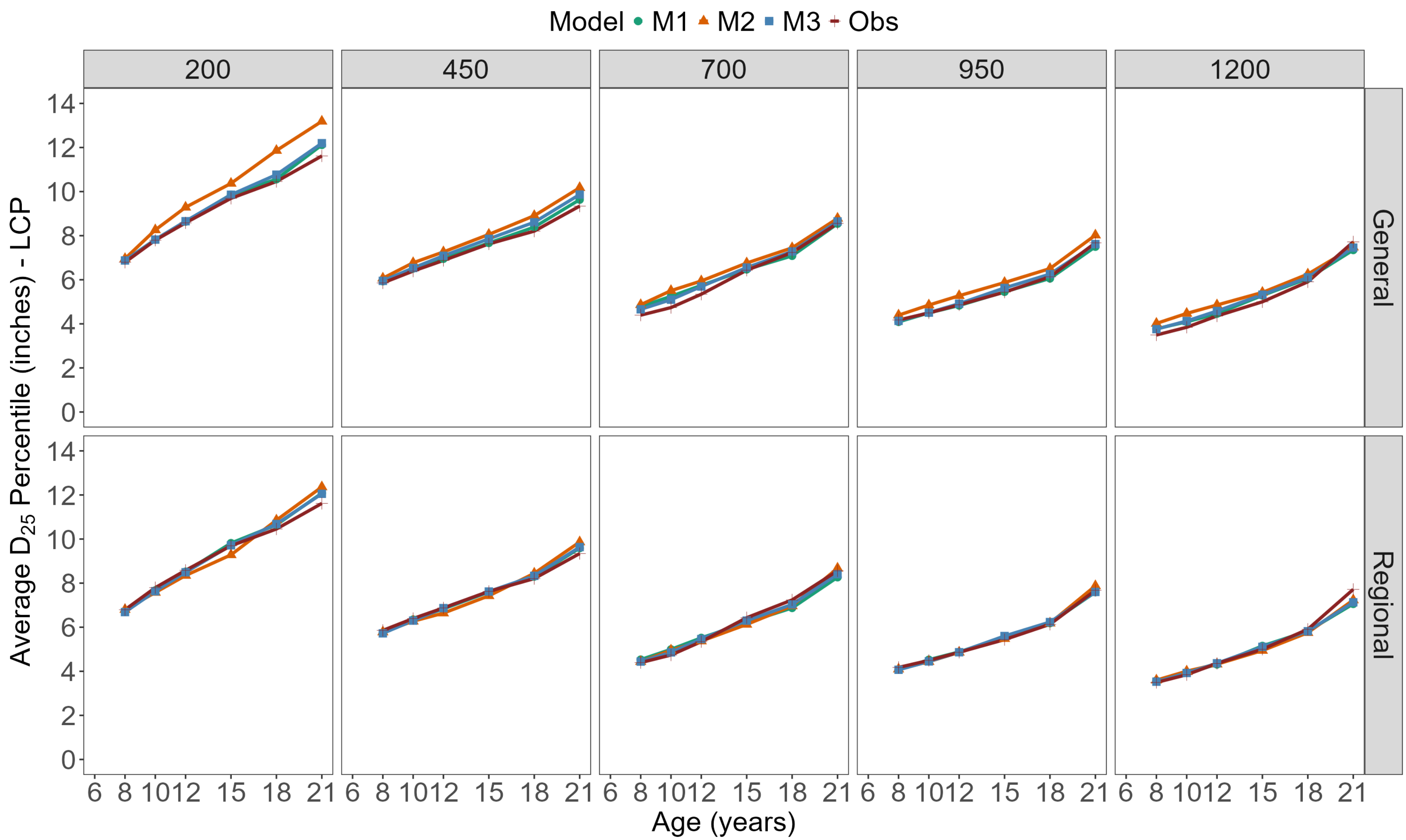

Figure 3.6: Average D_{25} percentile values for three regression models (M1, M2, and M3), across two modeling levels and five planting densities, for the LCP installations in the WGCDS.

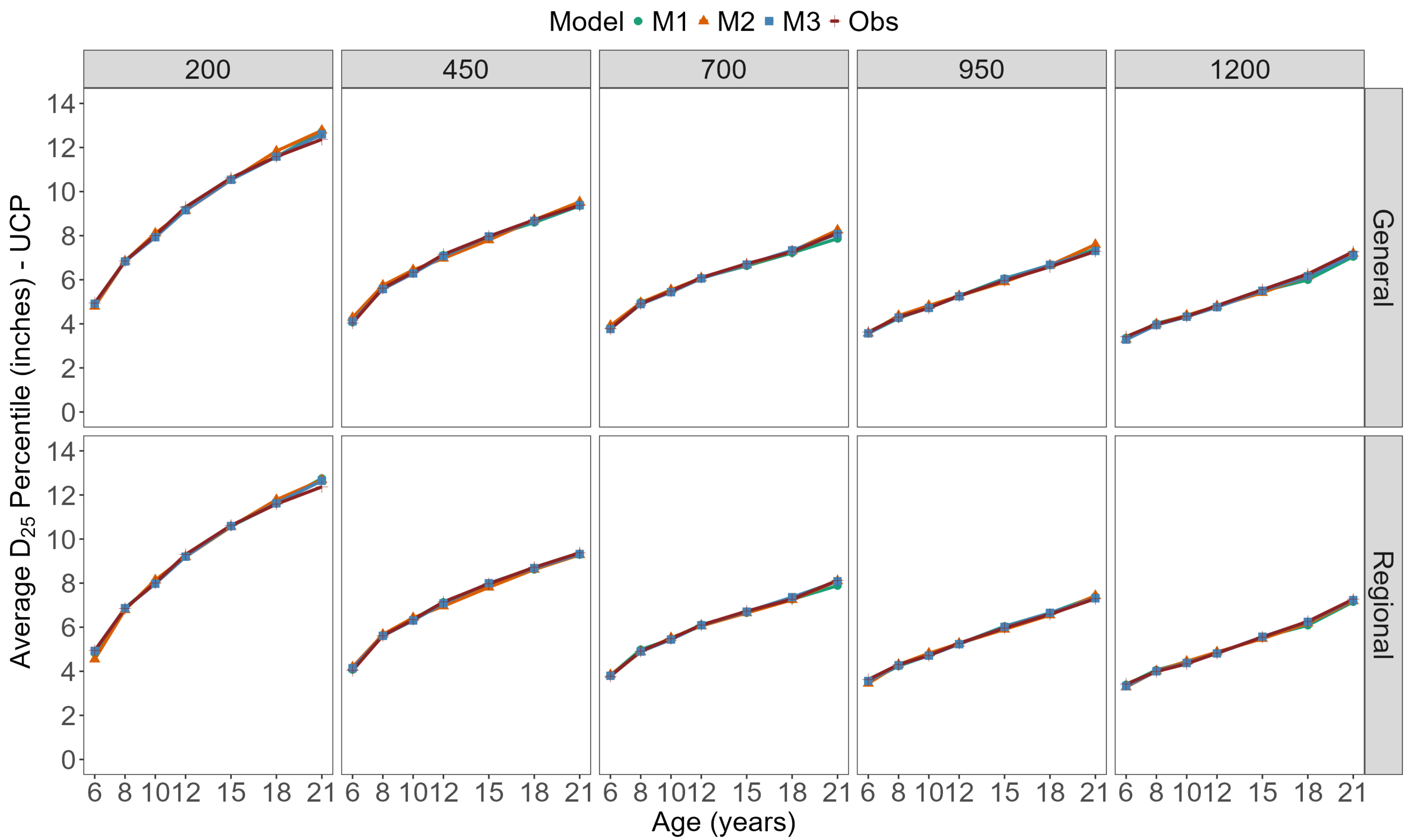

Figure 3.7: Average D_{25} percentile values for three regression models (M1, M2, and M3), across two modeling levels and five planting densities, for the UCP installations in the WGCDS.

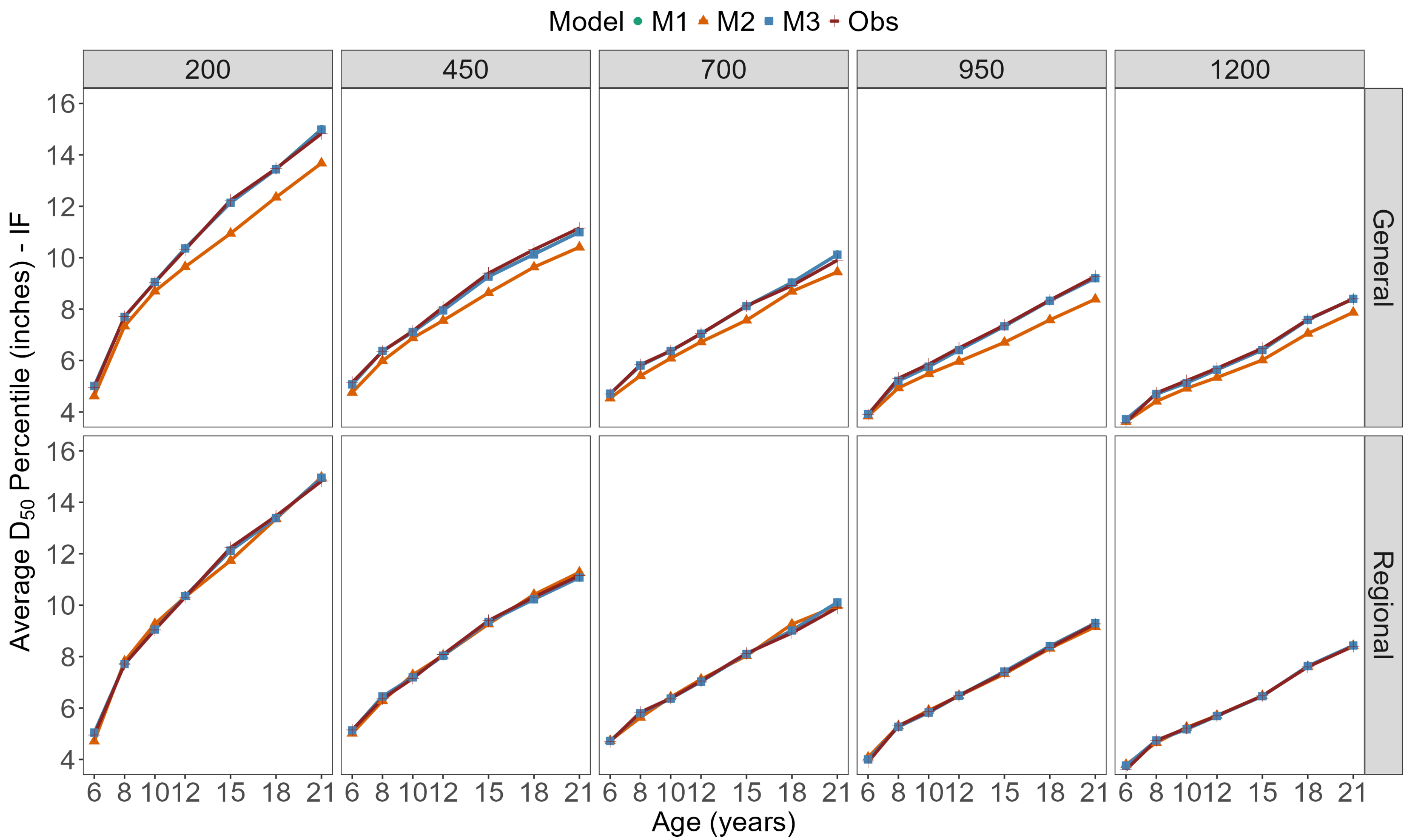

Figure 3.8: Average D_{50} percentile values for three regression models (M1, M2, and M3), across two modeling levels and five planting densities, for the IF installations in the WGCDS.

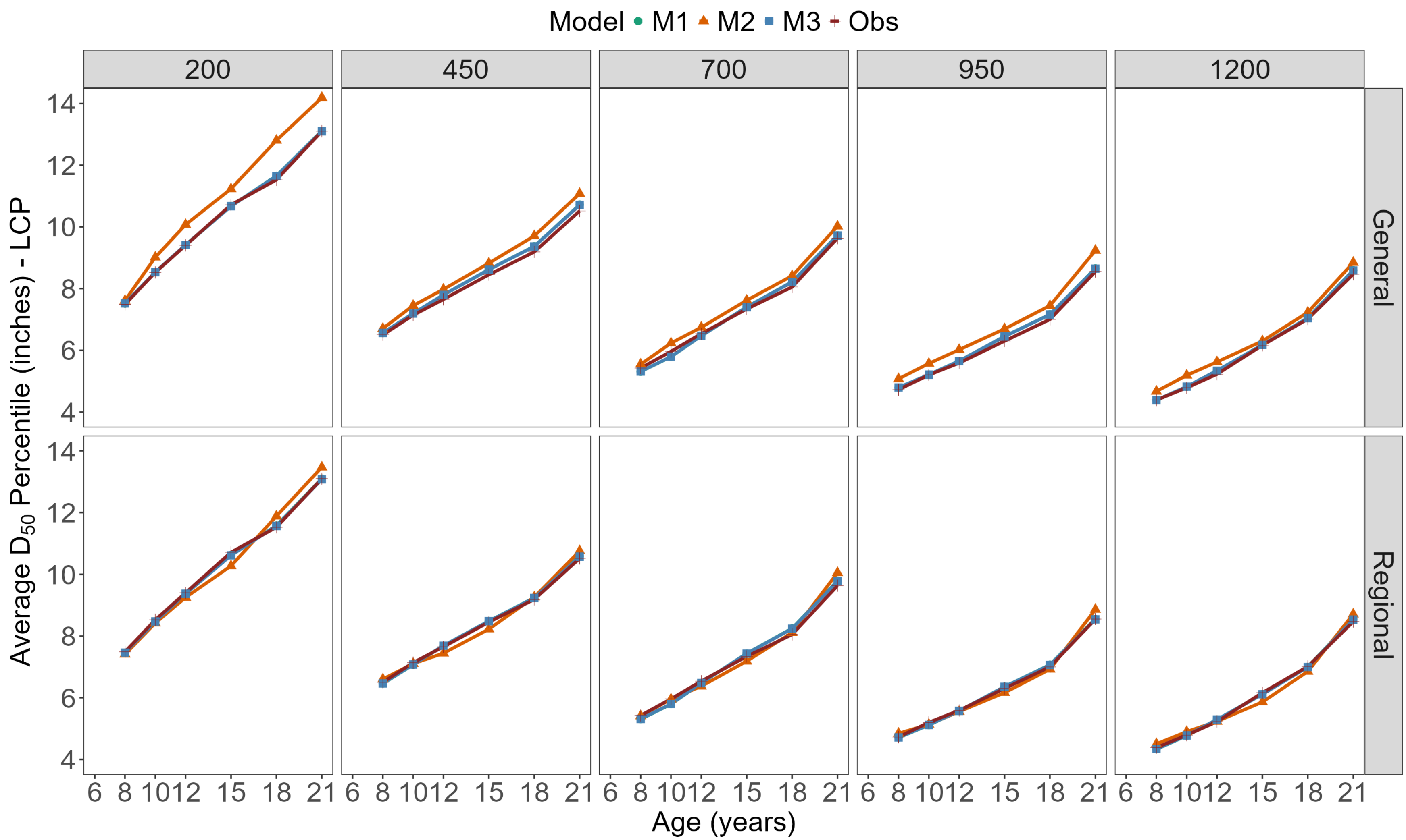

Figure 3.9: Average D_{50} percentile values for three regression models (M1, M2, and M3), across two modeling levels and five planting densities, for the LCP installations in the WGCDS.

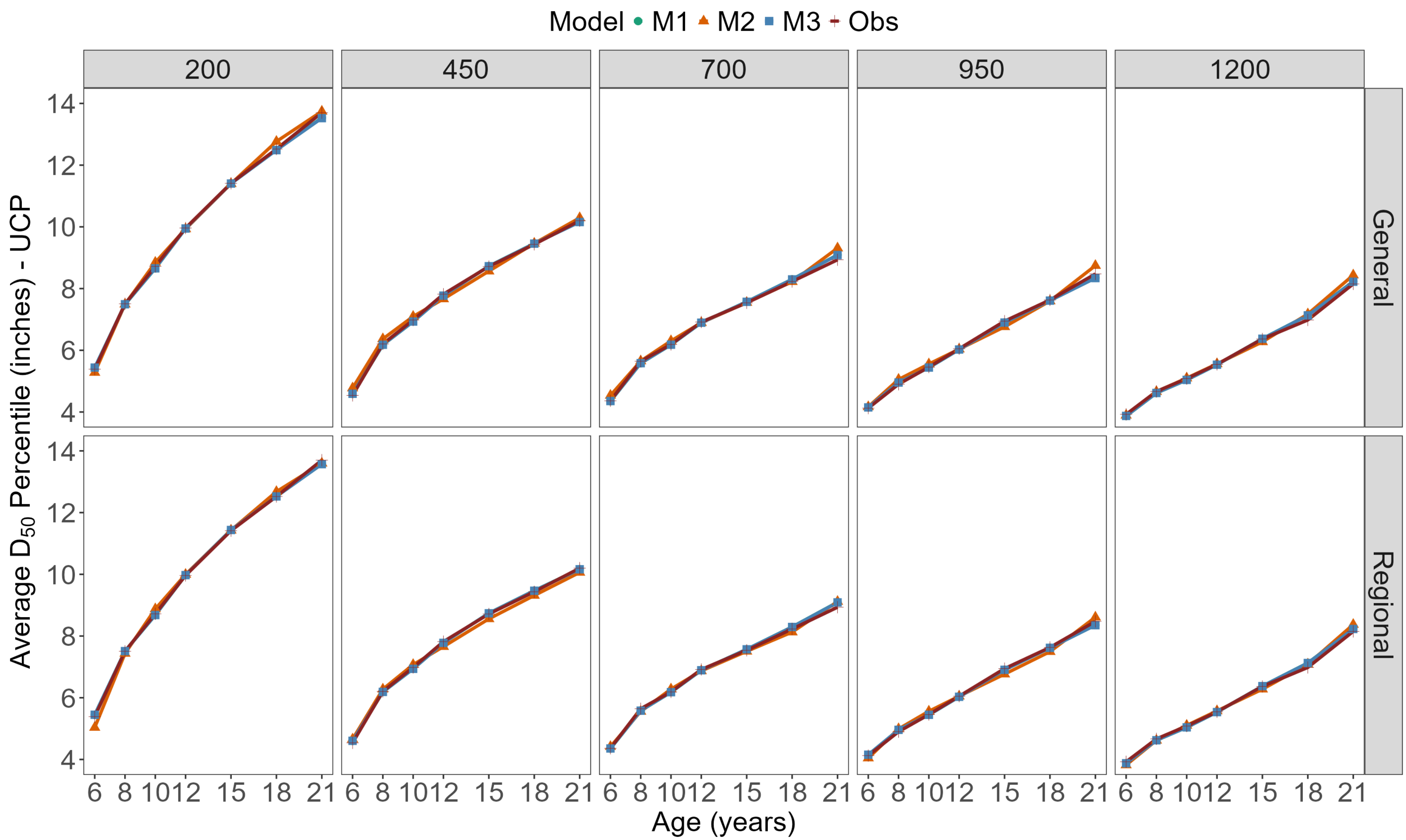

Figure 3.10: Average D_{50} percentile values for three regression models (M1, M2, and M3), across two modeling levels and five planting densities, for the UCP installations in the WGCDS.

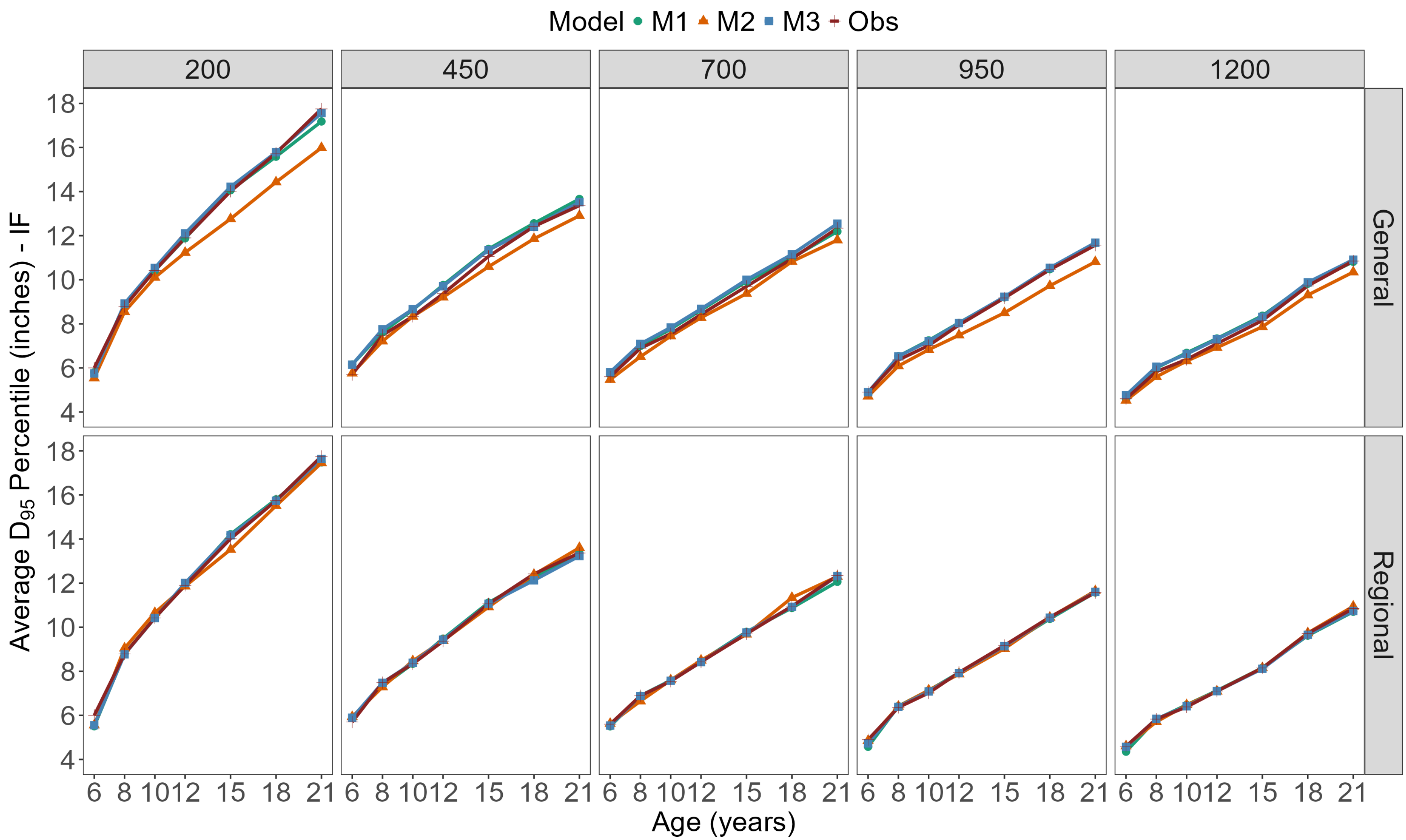

Figure 3.11: Average D_{95} percentile values for three regression models (M1, M2, and M3), across two modeling levels and five planting densities, for the IF installations in the WGCDS.

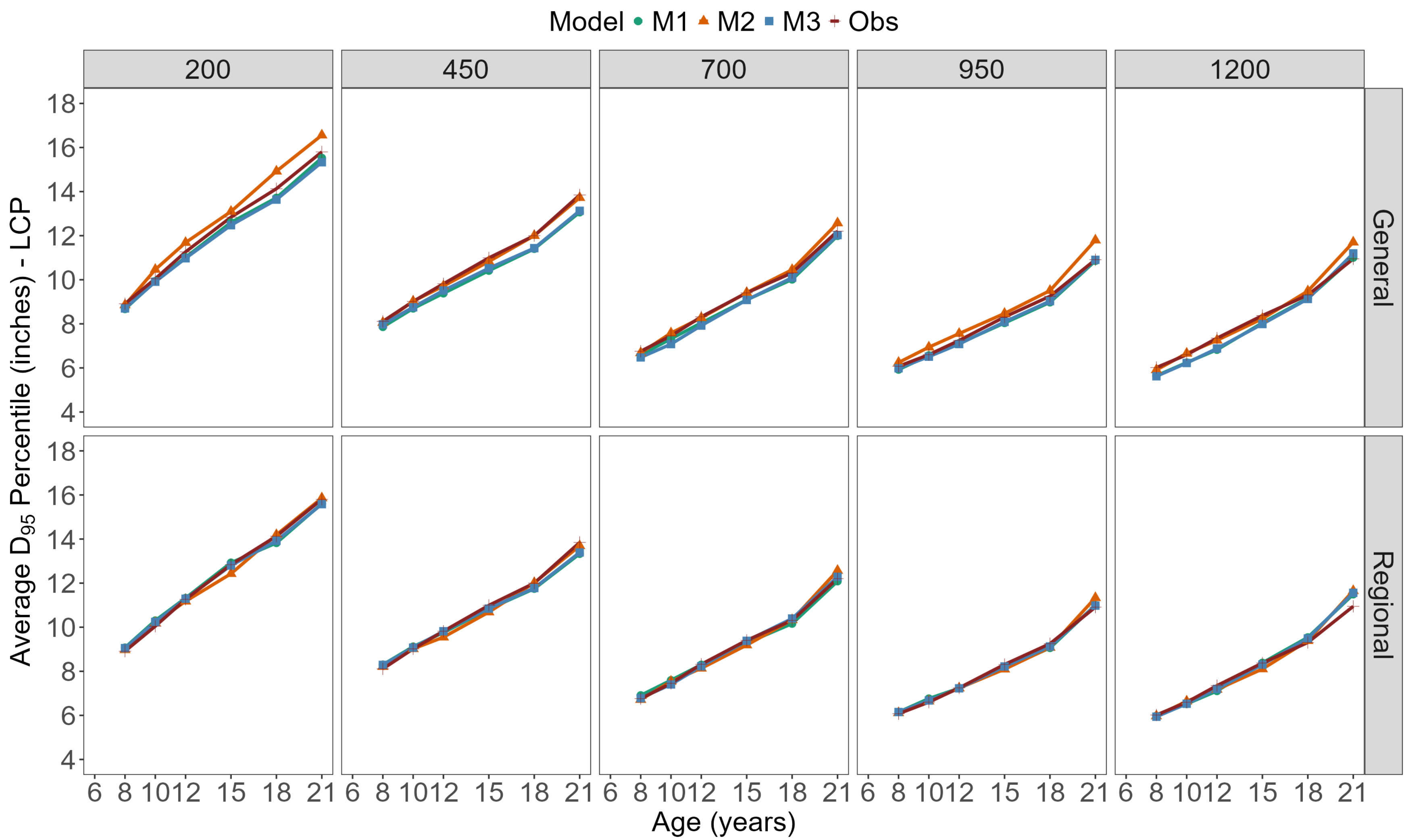

Figure 3.12: Average D_{95} percentile values for three regression models (M1, M2, and M3), across two modeling levels and five planting densities, for the LCP installations in the WGCDS.

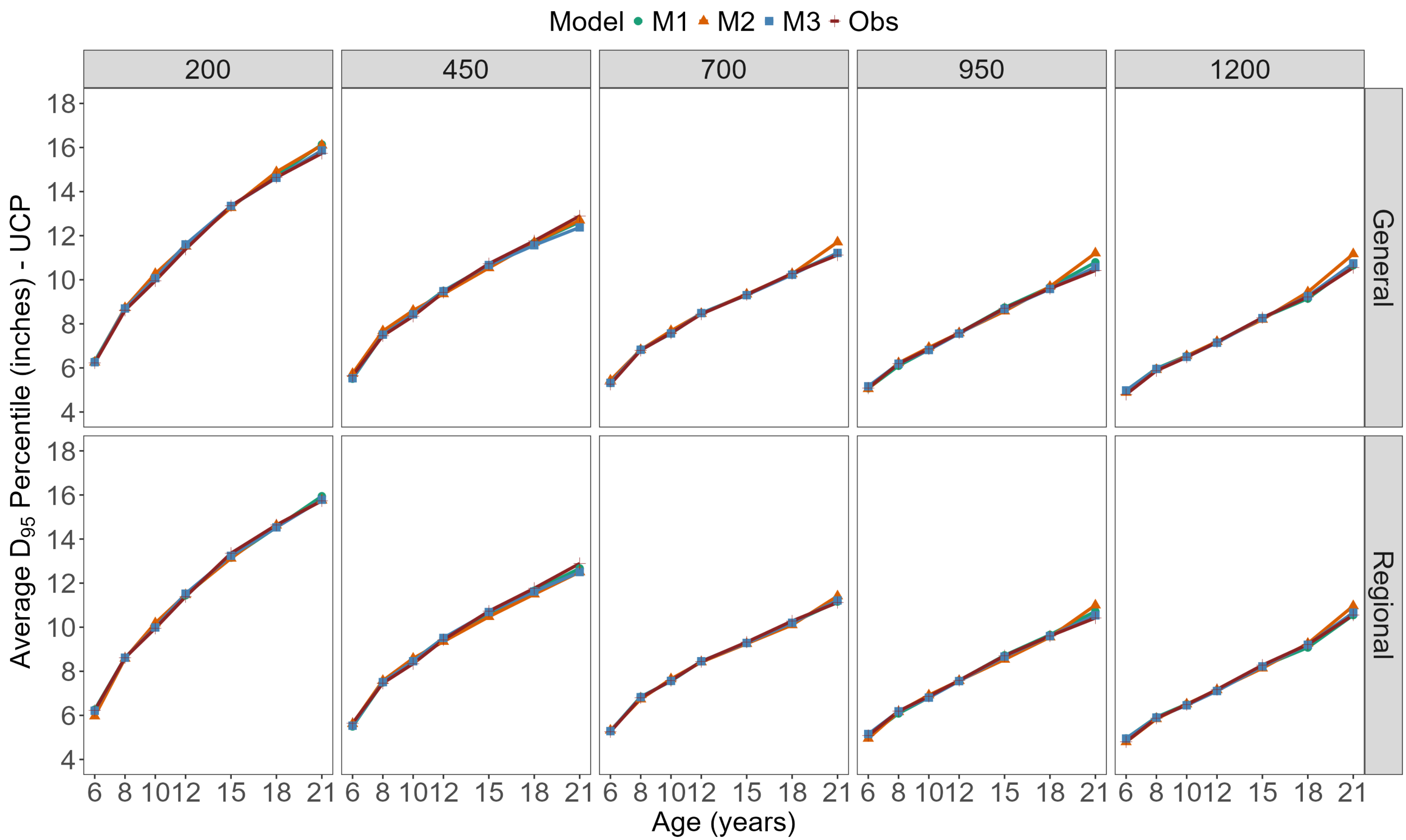

Figure 3.13: Average D_{95} percentile values for three regression models (M1, M2, and M3), across two modeling levels and five planting densities, for the UCP installations in the WGCDS.

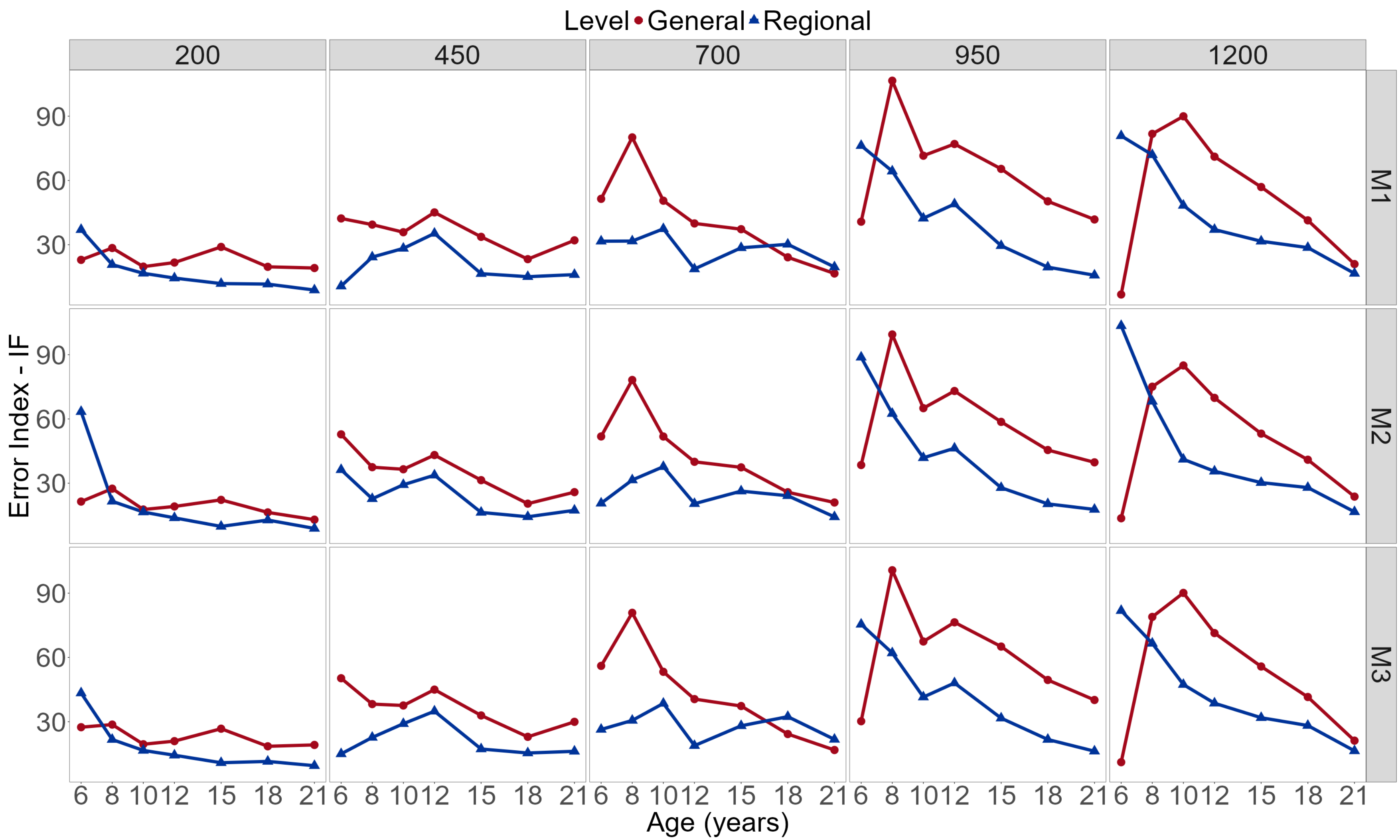

Figure 3.14: Error Index based on three regression models (M1, M2, and M3), across two modeling levels and five planting densities, for the IF installations in the WGCDS.

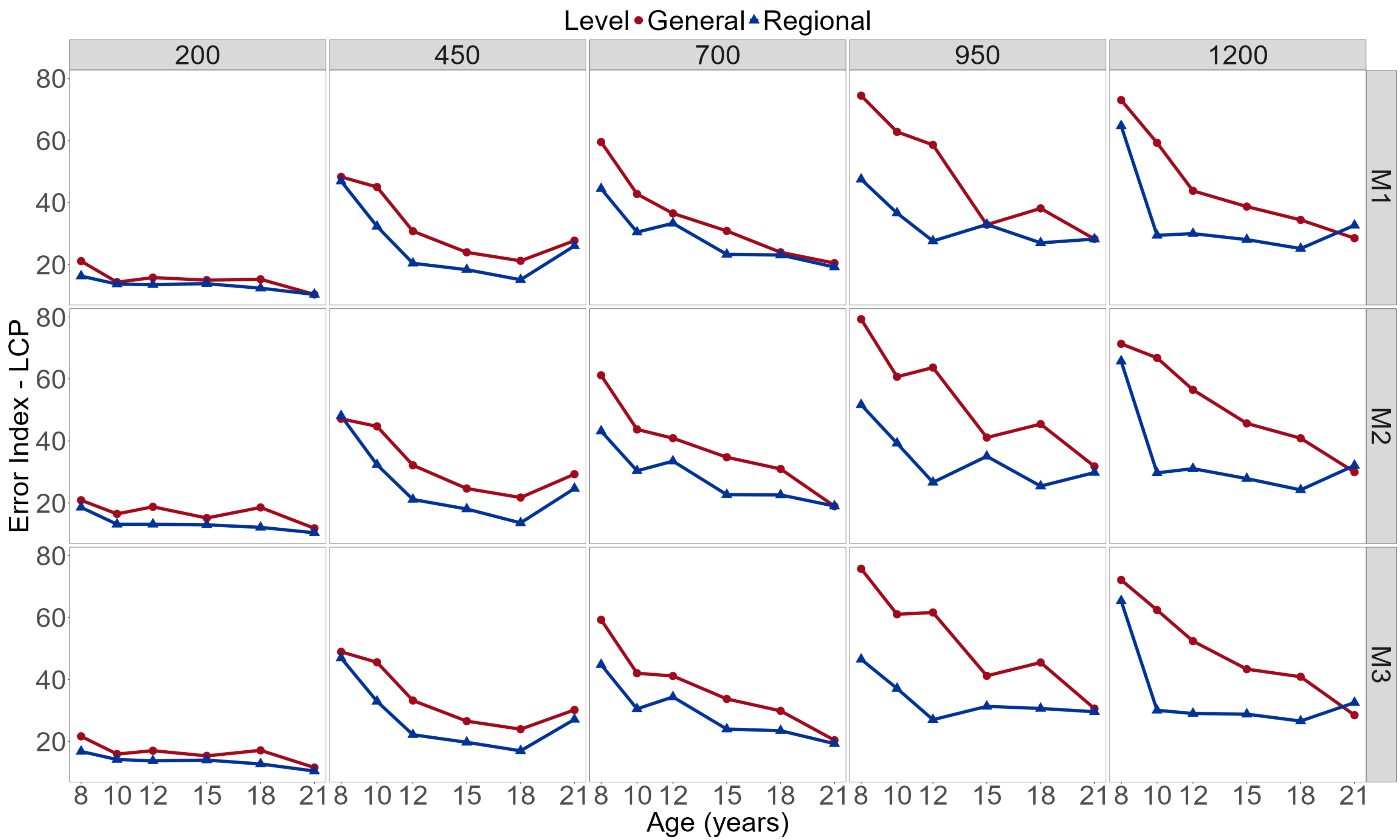

Figure 3.15: Error Index based on three regression models (M1, M2, and M3), across two modeling levels and five planting densities, for the LCP installations in the WGCDS.

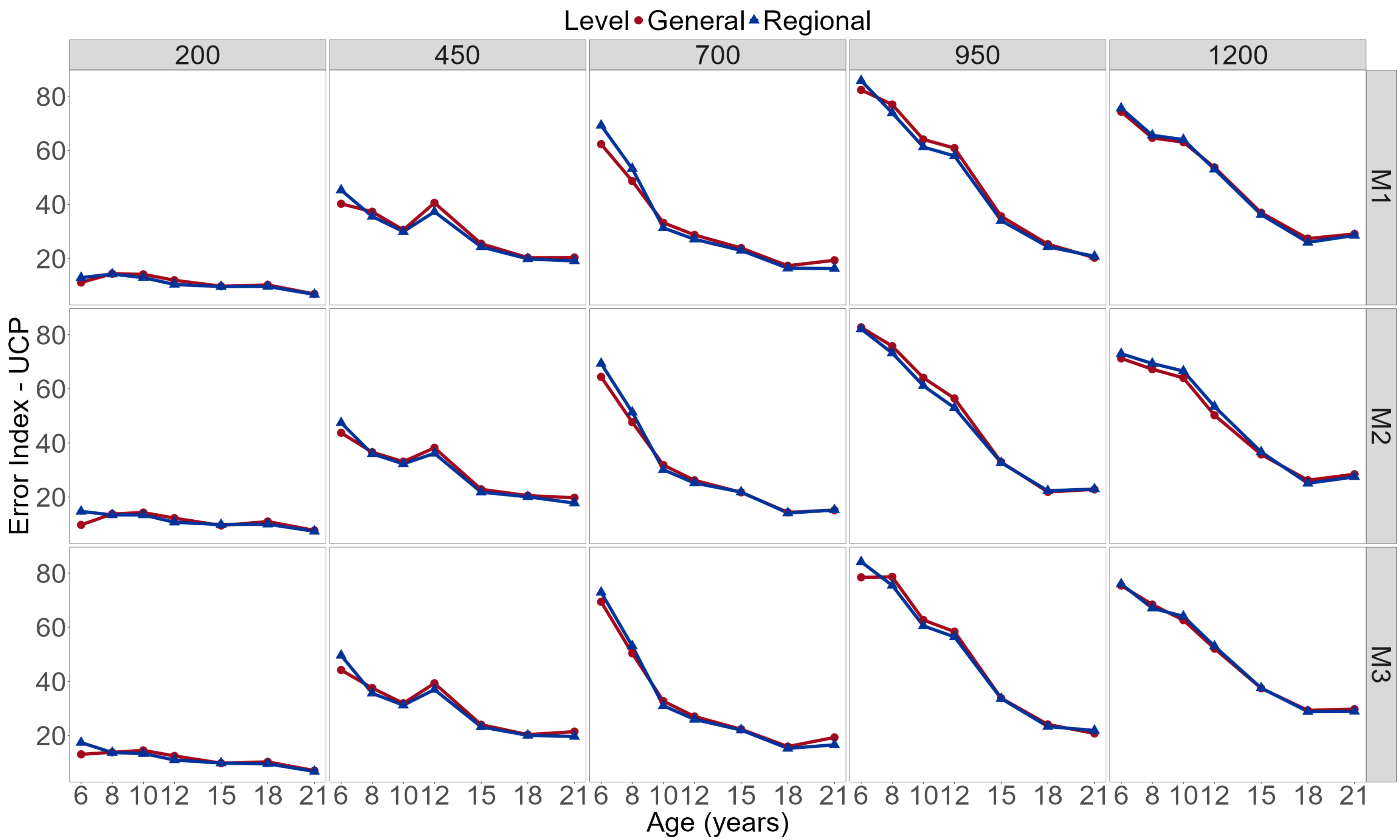

Figure 3.16: Error Index based on three regression models (M1, M2, and M3), across two modeling levels and five planting densities, for the UCP installations in the WGCDS.

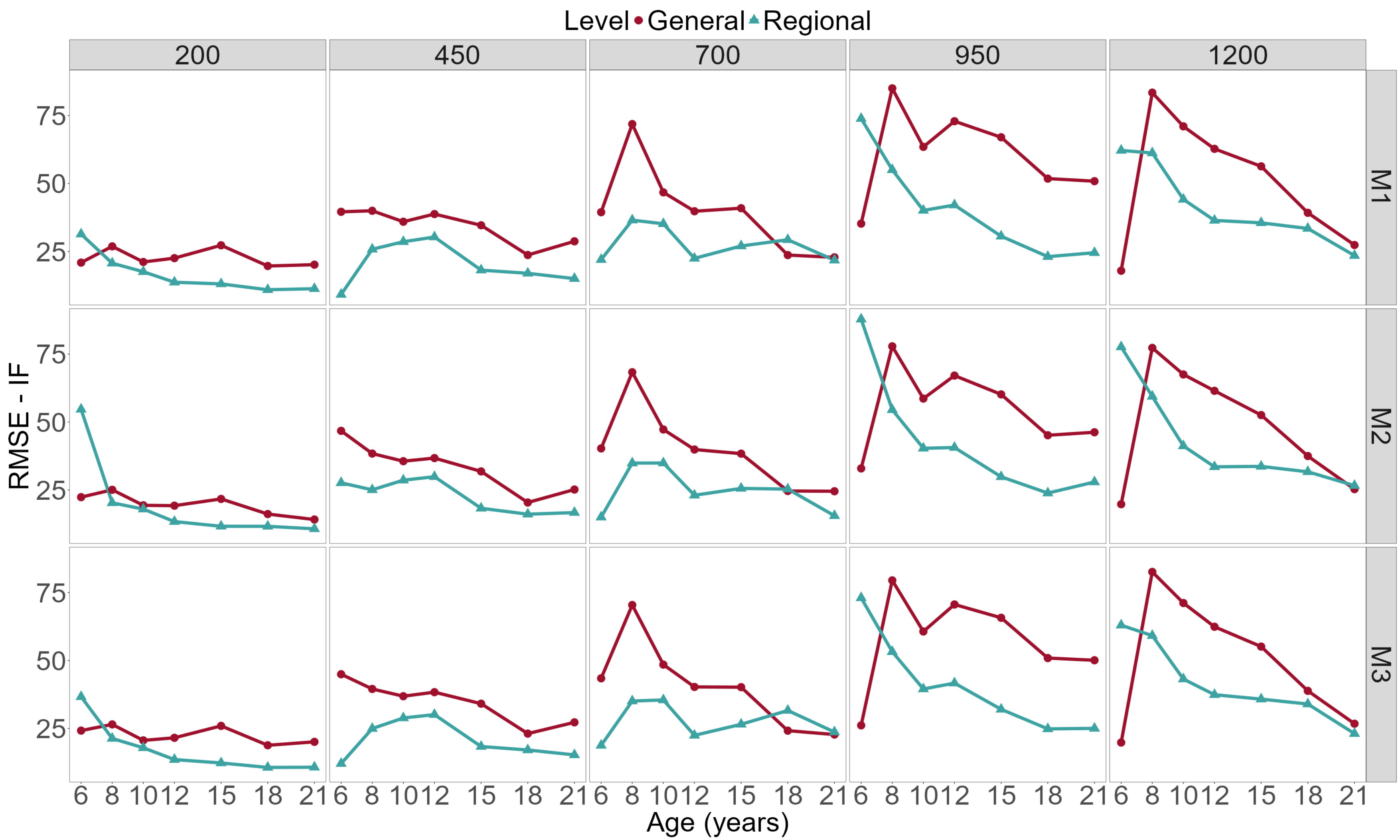

Figure 3.17: RMSE based on three regression models (M1, M2, and M3), across two modeling levels and five planting densities, for the UCP installations in the WGCDS.

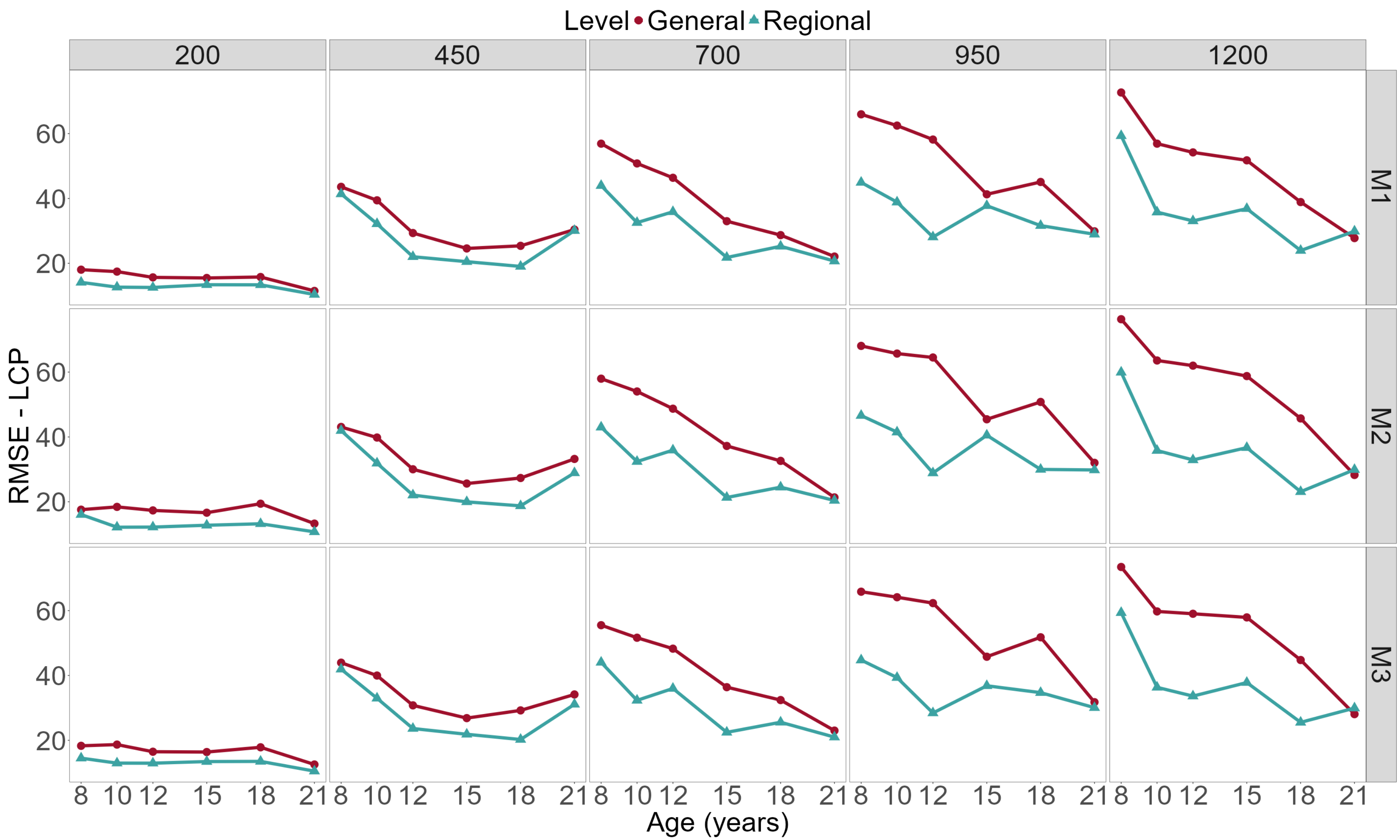

Figure 3.18: RMSE based on three regression models (M1, M2, and M3), across two modeling levels and five planting densities, for the UCP installations in the WGCDS.

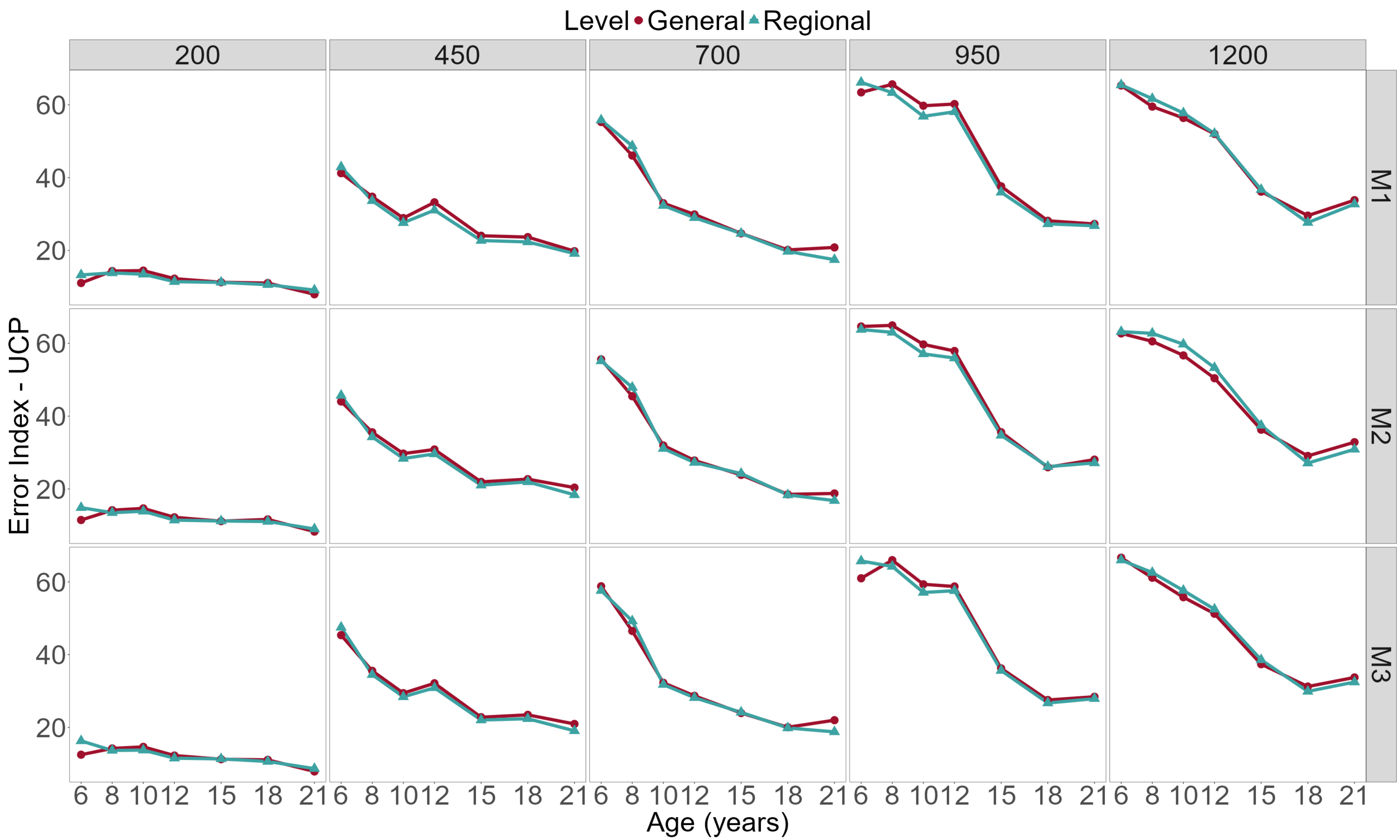

Figure 3.19: RMSE based on three regression models (M1, M2, and M3), across two modeling levels and five planting densities, for the UCP installations in the WGCDS.

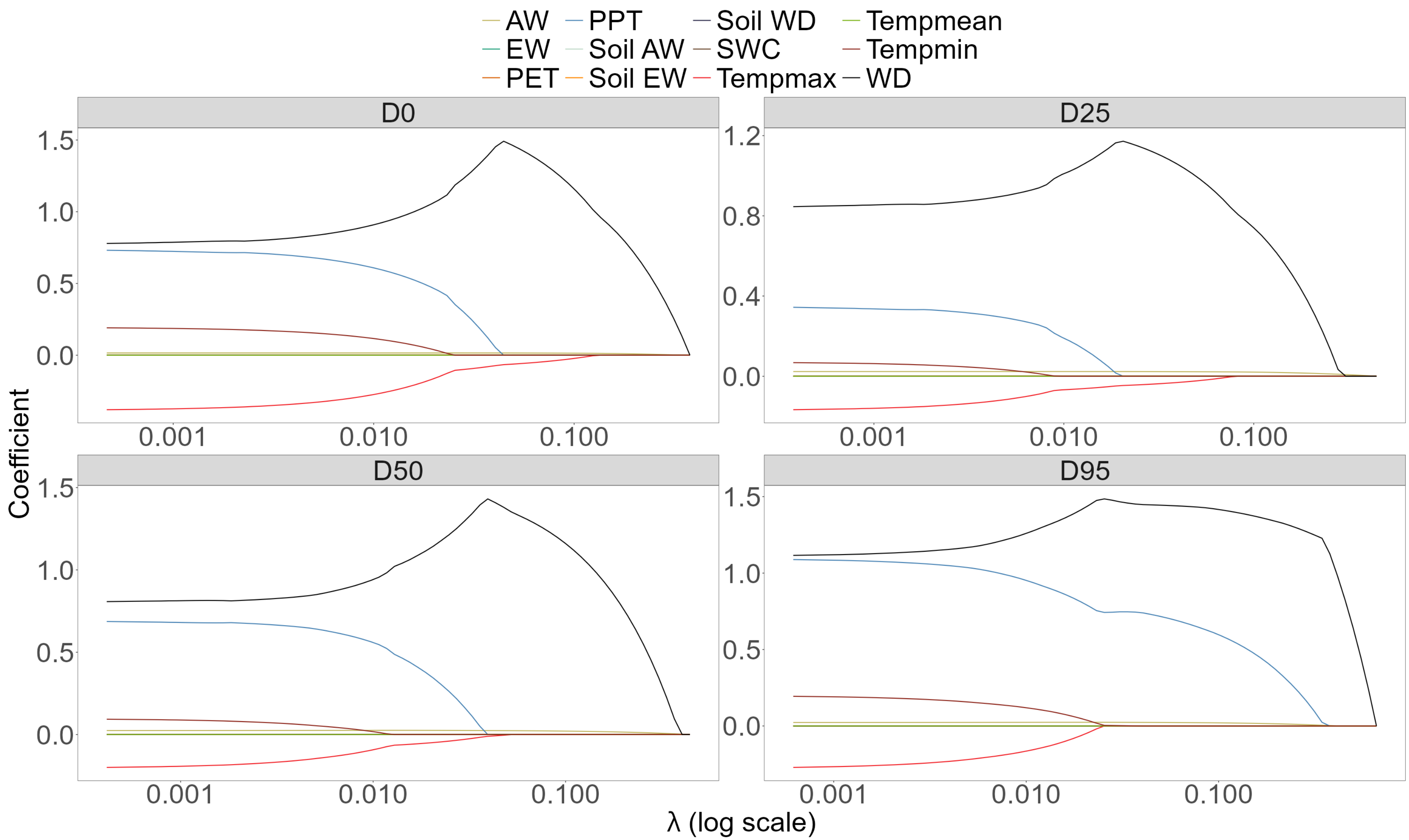

Figure 3.20: Lasso shrinkage of coefficient for percentiles D_0, D_{25}, D_{50}, and D_{95}: each line represents an environmental co-variable coefficient as a function of percentile.

Table 3.8: Coefficients obtained from the lasso regression after the penalty for percentiles D_0, D_{25}, D_{50}, and D_{95}.

PCT	Env. Cov.	Coeff
D_0	$Temp_{max}$	-0.355
D_0	$Temp_{min}$	0.174
D_0	PPT	0.709
D_0	PET	0.016
D_0	WD	0.818
D_{25}	$Temp_{max}$	-0.008
D_{25}	WD	0.882
D_{25}	AW	0.022
D_{50}	WD	1.257
D_{50}	AW	0.022
D_{95}	PPT	0.664
D_{95}	WD	1.435
D_{95}	AW	0.022

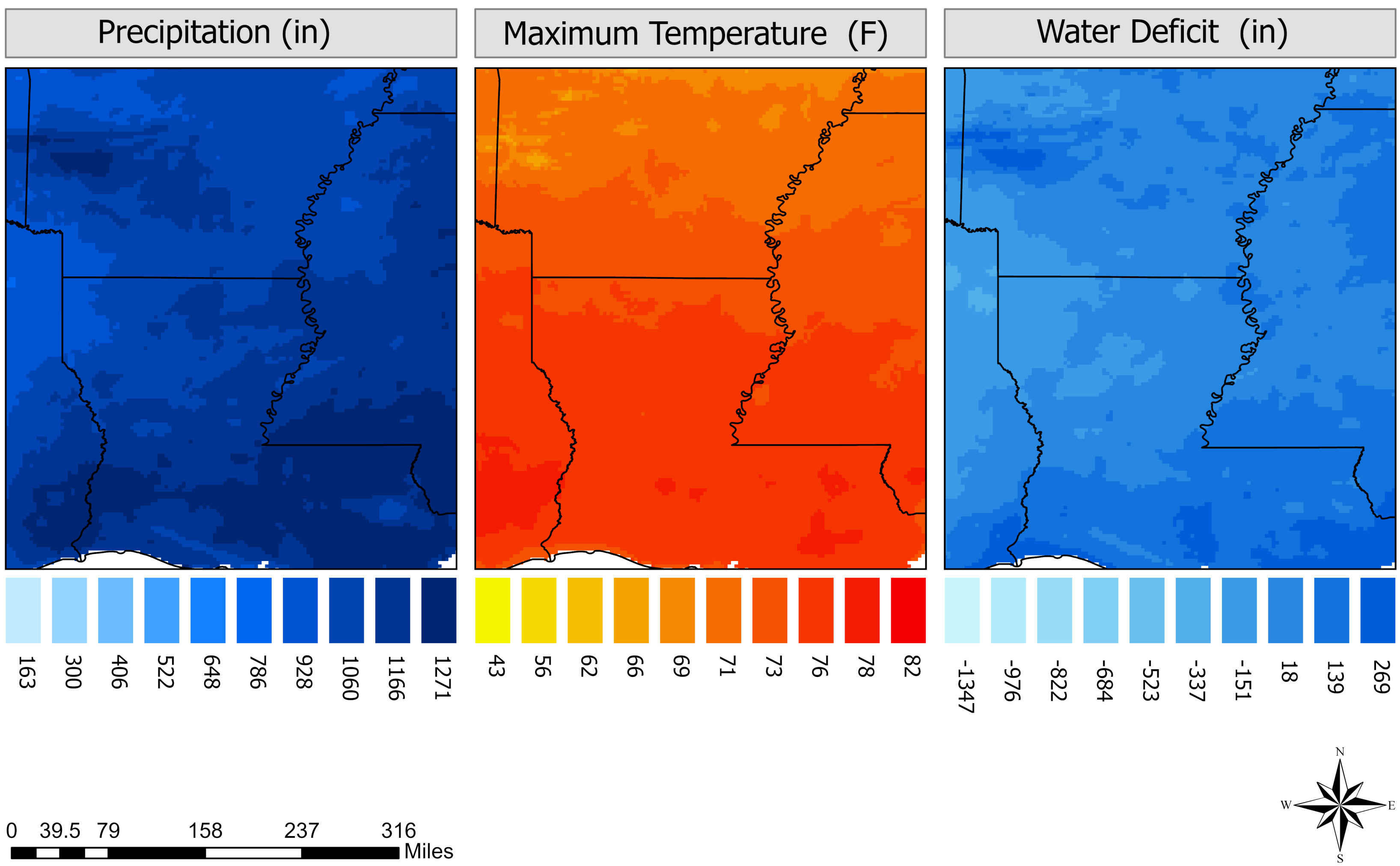

Figure 3.21: Western Gulf physiography region Map showing environmental co-variables selected by lasso regression included into the percentile regression models: Precipitation (PPT), Maximum Temperature ($Temp_{max}$), and Water Deficit (WD).

Table 3.9: Akaike Information Criterion (AIC) and Bayesian Information Criterion (BIC) for 15 models for the general level. Base indicates base model; environmental co-variables defined previously.

Model	PCT	Structure	AIC	BIC	Model	PCT	Structure	AIC	BIC
M4 (JB)	D_0	Base + $Temp_{max}$	210.37	252.19	M11 (Cao)	D_0	Base + PPT	239.64	285.65
	D_{25}	Base + $Temp_{max}$	-1583.78	-1546.14		D_{25}	Base + AW	-995.60	-949.60
	D_{50}	Base + WD	-2426.55	-2393.10		D_{50}	Base + AW	-1246.40	-1200.40
	D_{95}	Base + PPT	-1712.55	-1670.72		D_{95}	Base + PPT	-1340.88	-1294.87
M5 (Cao)	D_0	Base + $Temp_{max}$	204.16	250.16	M12 (PMRC)	D_0	Base + PPT	241.21	274.67
	D_{25}	Base + $Temp_{max}$	-1275.85	-1229.85		D_{25}	Base + AW	-1616.60	-1583.15
	D_{50}	Base + WD	-1300.55	-1254.55		D_{50}	Base + AW	-2412.88	-2379.43
	D_{95}	Base + PPT	-1340.88	-1294.87		D_{95}	Base + PPT	-1871.83	-1838.37
M6 (PMRC)	D_0	Base + $Temp_{max}$	235.27	268.73	M13 (JB)	D_0	Base + $Temp_{min}$	220.15	261.97
	D_{25}	Base + $Temp_{max}$	-1684.00	-1650.55		D_{25}	Base + $Temp_{max}$	-1583.78	-1546.14
	D_{50}	Base + WD	-2426.56	-2393.10		D_{50}	Base	-2410.32	-2381.04
	D_{95}	Base + PPT	-1871.83	-1838.37		D_{95}	Base + AW	-1628.74	-1586.92
M7 (JB)	D_0	Base + WD	234.97	276.80	M14 (Cao)	D_0	Base + $Temp_{min}$	222.49	268.49
	D_{25}	Base + WD	-1577.91	-1540.27		D_{25}	Base + $Temp_{max}$	-1275.85	-1229.85
	D_{50}	Base + WD	-2426.55	-2393.10		D_{50}	Base	-1241.03	-1199.20
	D_{95}	Base + WD	-1687.65	-1645.83		D_{95}	Base + AW	-1336.55	-1290.54
M8 (Cao)	D_0	Base + WD	260.28	306.28	M15 (PMRC)	D_0	Base + $Temp_{min}$	238.21	271.66
	D_{25}	Base + WD	-1070.15	-1024.15		D_{25}	Base + $Temp_{max}$	-1684.00	-1650.55
	D_{50}	Base + WD	-1300.55	-1254.55		D_{50}	Base	-2410.31	-2381.04
	D_{95}	Base + WD	-1336.57	-1290.57		D_{95}	Base + AW	-1723.46	-1689.99
M9 (PMRC)	D_0	Base + WD	244.62	278.08	M16 (JB)	D_0	Base + $Temp_{max}$	210.37	252.19
	D_{25}	Base + WD	-1673.12	-1639.67		D_{25}	Base	-1553.26	-1519.80
	D_{50}	Base + WD	-2426.56	-2393.10		D_{50}	Base	-2410.32	-2381.04
	D_{95}	Base + WD	-1805.69	-1772.23		D_{95}	Base	-1629.02	-1591.38
M10 (JB)	D_0	Base + PPT	228.65	270.47	M17 (Cao)	D_0	Base + $Temp_{max}$	204.16	250.16
	D_{25}	Base + AW	-1551.47	-1513.83		D_{25}	Base	-991.65	-949.83
	D_{50}	Base + AW	-2412.89	-2379.43		D_{50}	Base	-1241.03	-1199.20
	D_{95}	Base + PPT	-1712.55	-1670.72		D_{95}	Base	-1337.45	-1295.63
					M18 (PMRC)	D_0	Base + $Temp_{max}$	235.27	268.73
						D_{25}	Base	-1616.79	-1587.51
						D_{50}	Base	-2410.31	-2381.04
						D_{95}	Base	-1721.23	-1691.95

Table 3.10: Coefficients estimates from the D_0 percentile regression accounting for maximum temperature co-variable, M4.

	Estimate	Std. Error	t value	$Pr(>\|t\|)$
(Intercept)	0.9073	0.6143	1.4769	0.1404
$\ln D_q$	0.9995	0.2274	4.3959	0.0000
lnAGE	0.2320	0.1237	1.8751	0.0614
HD	-0.2968	0.2095	-1.4165	0.1573
PLTPA450	-0.0247	0.0659	-0.3747	0.7080
PLTPA700	-0.1585	0.0918	-1.7279	0.0847
PLTPA950	-0.2182	0.1102	-1.9797	0.0483
PLTPA1200	-0.2473	0.1237	-2.0001	0.0461
$Temp_{max}$	-0.0413	0.0090	-4.5787	0.0000

Table 3.11: Coefficients estimates from the D_{25} percentile regression accounting for maximum temperature co-variable, M4.

	Estimate	Std. Error	t value	$Pr(>\|t\|)$
(Intercept)	0.2294	0.0821	2.7956	0.0054
$\ln D_{50}$	1.0676	0.0209	50.9893	0.0000
lnAGE	-0.0257	0.0136	-1.8930	0.0590
PLTPA450	0.0045	0.0083	0.5427	0.5876
PLTPA700	-0.0192	0.0100	-1.9285	0.0544
PLTPA950	-0.0231	0.0117	-1.9736	0.0490
PLTPA1200	-0.0303	0.0131	-2.3228	0.0206
$Temp_{max}$	-0.0053	0.0010	-5.2967	0.0000

Table 3.12: Coefficients estimates from the D_{50} percentile regression accounting for water deficit co-variable, M4.

	Estimate	Std. Error	t value	$Pr(>\|t\|)$
(Intercept)	0.0441	0.0091	4.8627	0.0000
$\ln D_q$	0.9829	0.0039	250.0868	0.0000
PLTPA450	-0.0135	0.0030	-4.5091	0.0000
PLTPA700	-0.0049	0.0032	-1.5533	0.1210
PLTPA950	-0.0139	0.0033	-4.1813	0.0000
PLTPA1200	-0.0217	0.0035	-6.2550	0.0000
WD	-0.0196	0.0030	-6.4527	0.0000

Table 3.13: Coefficients estimates from the D_{95} percentile regression accounting for precipitation co-variable, M4.

	Estimate	Std. Error	t value	Pr(> $\|t\|$)
(Intercept)	-0.0985	0.0335	-2.9427	0.0034
$\ln D_{50}$	0.8896	0.0208	42.8464	0.0000
lnAGE	0.0244	0.0140	1.7385	0.0828
HD	-0.0545	0.0187	-2.9065	0.0038
PLTPA450	0.0213	0.0077	2.7874	0.0055
PLTPA700	0.0111	0.0095	1.1754	0.2404
PLTPA950	0.0225	0.0111	2.0233	0.0436
PLTPA1200	0.0439	0.0124	3.5375	0.0004
PPT	0.0490	0.0050	9.8268	0.0000

Table 3.14: Coefficients estimates from the D_0 percentile regression accounting for maximum temperature co-variable, M5.

	Estimate	Std. Error	t value	Pr(> $\|t\|$)
(Intercept)	-1.1527	1.4727	-0.7827	0.4342
RS	2.1149	0.5830	3.6274	0.0003
lnTPA	0.1031	0.1194	0.8637	0.3882
lnHD	1.5771	0.1974	7.9874	0.0000
AGE	-1.5116	1.2635	-1.1964	0.2321
PLTPA450	-0.0942	0.0715	-1.3184	0.1880
PLTPA700	-0.3114	0.0972	-3.2051	0.0014
PLTPA950	-0.4317	0.1183	-3.6488	0.0003
PLTPA1200	-0.5082	0.1320	-3.8490	0.0001
$Temp_{max}$	-0.0565	0.0077	-7.3814	0.0000

Table 3.15: Coefficients estimates from the D_{25} percentile regression accounting for maximum temperature co-variable, M5.

	Estimate	Std. Error	t value	$Pr(>\|t\|)$
(Intercept)	4.2619	0.3181	13.3997	0.0000
RS	-1.2440	0.1263	-9.8468	0.0000
lnTPA	-0.2641	0.0258	-10.2381	0.0000
lnHD	0.3494	0.0426	8.2091	0.0000
AGE	-0.1104	0.2731	-0.4043	0.6862
PLTPA450	-0.1735	0.0154	-11.2326	0.0000
PLTPA700	-0.2892	0.0210	-13.7854	0.0000
PLTPA950	-0.3558	0.0255	-13.9374	0.0000
PLTPA1200	-0.4112	0.0285	-14.4350	0.0000
$Temp_{max}$	-0.0210	0.0015	-14.3357	0.0000

Table 3.16: Coefficients estimates from the D_{50} percentile regression accounting for water deficit co-variable, M5.

	Estimate	Std. Error	t value	$Pr(>\|t\|)$
(Intercept)	3.8679	0.3059	12.6431	0.0000
RS	-1.3873	0.1230	-11.2743	0.0000
lnTPA	-0.3714	0.0251	-14.7891	0.0000
lnHD	0.2220	0.0409	5.4297	0.0000
AGE	-0.3182	0.2679	-1.1880	0.2354
PLTPA450	-0.1005	0.0151	-6.6748	0.0000
PLTPA700	-0.1477	0.0205	-7.2022	0.0000
PLTPA950	-0.1765	0.0250	-7.0724	0.0000
PLTPA1200	-0.2036	0.0279	-7.3037	0.0000
WD	-0.0456	0.0102	-4.4766	0.0000

Table 3.17: Coefficients estimates from the D_{95} percentile regression accounting for precipitation co-variable, M5.

	Estimate	Std. Error	t value	$Pr(>\|t\|)$
(Intercept)	3.3761	0.2939	11.4889	0.0000
RS	-1.0410	0.1180	-8.8230	0.0000
lnTPA	-0.3110	0.0239	-13.0298	0.0000
lnHD	0.2611	0.0394	6.6308	0.0000
AGE	-1.0111	0.2560	-3.9503	0.0001
PLTPA450	-0.0611	0.0143	-4.2640	0.0000
PLTPA700	-0.1122	0.0194	-5.7707	0.0000
PLTPA950	-0.1276	0.0236	-5.3989	0.0000
PLTPA1200	-0.1309	0.0264	-4.9644	0.0000
PPT	0.0236	0.0068	3.4523	0.0006

Table 3.18: Coefficients estimates from the D_0 percentile regression accounting for maximum temperature co-variable, M6.

	Estimate	Std. Error	t value	$Pr(>\|t\|)$
(Intercept)	3.5933	0.5199	6.9111	0.0000
lnBA/TPA	0.8531	0.0303	28.1474	0.0000
PLTPA450	0.1262	0.0469	2.6920	0.0074
PLTPA700	0.0897	0.0493	1.8199	0.0694
PLTPA950	0.0989	0.0518	1.9102	0.0567
PLTPA1200	0.1163	0.0541	2.1475	0.0323
$Temp_{max}$	-0.0167	0.0068	-2.4671	0.0140

Table 3.19: Coefficients estimates from the D_{25} percentile regression accounting for maximum temperature co-variable, M6.

	Estimate	Std. Error	t value	$Pr(>\|t\|)$
(Intercept)	2.8987	0.0647	44.8212	0.0000
lnBA/TPA	0.5046	0.0042	120.9351	0.0000
PLTPA450	-0.0179	0.0065	-2.7804	0.0056
PLTPA700	-0.0386	0.0068	-5.6959	0.0000
PLTPA950	-0.0561	0.0071	-7.8761	0.0000
PLTPA1200	-0.0745	0.0075	-9.9979	0.0000
$Temp_{max}$	-0.0049	0.0008	-5.7917	0.0000

Table 3.20: Coefficients estimates from the D_{50} percentile regression accounting for water deficit co-variable, M6.

	Estimate	Std. Error	t value	$Pr(>\|t\|)$
(Intercept)	2.6040	0.0026	1007.4111	0.0000
lnBA/TPA	0.4902	0.0020	247.5465	0.0000
PLTPA450	-0.0140	0.0030	-4.6731	0.0000
PLTPA700	-0.0058	0.0032	-1.8312	0.0677
PLTPA950	-0.0150	0.0033	-4.5051	0.0000
PLTPA1200	-0.0230	0.0035	-6.6057	0.0000
WD	-0.0176	0.0034	-5.1344	0.0000

Table 3.21: Coefficients estimates from the D_{95} percentile regression accounting for precipitation co-variable, M6.

	Estimate	Std. Error	t value	$Pr(>\|t\|)$
(Intercept)	2.5833	0.0180	143.8551	0.0000
lnBA/TPA	0.4913	0.0035	140.9200	0.0000
PLTPA450	0.0331	0.0053	6.2236	0.0000
PLTPA700	0.0456	0.0056	8.1448	0.0000
PLTPA950	0.0591	0.0059	10.0245	0.0000
PLTPA1200	0.0806	0.0062	13.0602	0.0000
PPT	0.0361	0.0036	10.0791	0.0000

Table 3.22: Performance of the three regression models (M4, M5, and M6) across four percentiles (D_0, D_{25}, D_{50}, and D_{95}) accounting for environmental co-variables.

PCT	M4			M5			M6		
	RMSE	R^2	AIC	RMSE	R^2	AIC	RMSE	R^2	AIC
D_0	1.002	0.720	210.369	1.005	0.725	204.158	1.007	0.709	235.271
D_{25}	0.294	0.977	-1583.778	0.449	0.952	-1275.850	0.258	0.981	-1684.003
D_{50}	0.150	0.995	-2426.554	0.497	0.952	-1300.555	0.150	0.995	-2426.557
D_{95}	0.403	0.977	-1712.545	0.633	0.950	-1340.876	0.326	0.983	-1871.829

Table 3.23: Performance of the three regression models (M4, M5, and M6) across four percentiles (D_0, D_{25}, D_{50}, and D_{95}) for region IF, accounting for environmental co-variable models.

PCT	RMSE			R^2			AIC		
	M4	M5	M6	M4	M5	M6	M4	M5	M6
D_0	0.869	0.894	0.854	0.747	0.754	0.756	40.034	41.675	37.075
D_{25}	0.202	0.344	0.175	0.992	0.977	0.993	-540.973	-412.387	-559.931
D_{50}	0.126	0.322	0.127	0.997	0.982	0.997	-680.224	-454.829	-680.238
D_{95}	0.308	0.464	0.218	0.987	0.972	0.993	-496.544	-403.115	-585.705

Table 3.24: Performance of the three regression models (M4, M5, and M6) across four percentiles (D_0, D_{25}, D_{50}, and D_{95}) for region LCP, accounting for environmental co-variable models.

PCT	RMSE			R^2			AIC		
	M4	M5	M6	M4	M5	M6	M4	M5	M6
D_0	1.041	1.073	1.102	0.699	0.705	0.641	73.433	75.014	99.461
D_{25}	0.374	0.462	0.343	0.970	0.955	0.976	-331.189	-288.660	-353.093
D_{50}	0.214	0.453	0.214	0.992	0.967	0.992	-500.422	-346.128	-500.430
D_{95}	0.568	0.793	0.416	0.961	0.934	0.980	-355.853	-281.308	-419.922

Table 3.25: Performance of the three regression models (M4, M5, and M6) across four percentiles (D_0, D_{25}, D_{50}, and D_{95}) for region UCP, accounting for environmental co-variable models.

PCT	RMSE			R^2			AIC		
	M4	M5	M6	M4	M5	M6	M4	M5	M6
D_0	0.988	0.954	1.014	0.747	0.753	0.723	69.361	62.933	92.682
D_{25}	0.277	0.366	0.239	0.978	0.959	0.982	-807.293	-678.546	-858.836
D_{50}	0.120	0.310	0.118	0.997	0.974	0.997	-1306.626	-821.387	-1306.597
D_{95}	0.339	0.420	0.305	0.979	0.970	0.982	-889.209	-800.223	-930.701

Table 3.26: Precision of the Weibull three-parameter accounting for environmental co-variables, conducted fot the general modeling level across seven ages and five planting densities for three percentile models (M4, M5, and M6).

AGE	PLTPA	M4		M5		M6	
		Error Index	RMSE	Error Index	RMSE	Error Index	RMSE
6	200	16.24	15.21	18.19	19.14	17.37	16.09
	450	42.05	42.29	47.73	46.66	45.92	45.66
	700	61.46	52.71	66.07	55.23	66.55	55.30
	950	79.72	62.29	82.59	64.46	74.98	58.36
	1200	64.73	57.98	66.90	58.95	63.27	57.58
8	200	20.06	18.94	21.17	19.30	20.09	18.88
	450	38.65	37.23	36.04	35.45	39.23	37.85
	700	59.94	55.18	61.08	56.09	60.96	55.19
	950	82.93	69.97	79.94	67.70	82.50	68.90
	1200	68.92	66.55	66.24	64.00	69.71	67.57
10	200	16.07	17.10	16.83	17.14	16.13	17.21
	450	33.48	31.87	31.99	30.54	34.62	32.63
	700	38.83	39.94	38.41	39.54	38.90	40.05
	950	67.18	61.00	68.89	60.61	64.91	60.36
	1200	67.23	59.60	65.66	58.70	68.00	59.56
12	200	16.09	16.55	16.68	16.45	16.02	16.36
	450	38.67	33.38	36.44	32.48	38.86	33.30
	700	34.29	36.54	34.56	36.28	33.93	36.10
	950	64.18	63.07	62.39	61.28	63.44	62.54
	1200	55.86	55.69	57.06	55.59	56.90	55.97
15	200	16.66	16.86	15.96	16.30	16.26	16.75
	450	28.23	27.47	27.31	26.61	27.46	27.14
	700	29.46	30.93	29.47	30.75	28.77	30.87
	950	43.17	46.05	44.03	46.66	43.37	45.83
	1200	42.32	45.10	41.76	44.99	42.65	46.17
18	200	13.86	14.10	14.96	15.17	14.26	14.56
	450	20.89	24.05	20.49	24.02	21.38	24.50
	700	20.00	23.02	21.25	23.63	20.76	23.75
	950	33.40	37.46	33.76	38.01	34.24	38.23
	1200	31.82	33.73	33.52	34.91	34.18	35.67
21	200	11.79	12.63	12.28	12.78	11.93	12.65
	450	27.67	27.19	27.27	28.42	27.28	27.53
	700	18.07	21.12	17.13	20.75	18.42	21.90
	950	29.26	34.58	31.91	36.79	29.57	35.01
	1200	27.51	31.44	29.67	33.25	27.63	30.93

Table 3.27: Precision of the Weibull three-parameter accounting for environmental co-variables, conducted for the regional modeling level across seven ages and five planting densities for three percentile models (M4, M5, and M6).

AGE	PLTPA	M4		M5		M6	
		Error Index	RMSE	Error Index	RMSE	Error Index	RMSE
6	200	17.22	16.67	16.74	17.75	22.04	19.98
	450	38.15	35.99	47.73	43.95	43.09	40.81
	700	59.67	47.89	58.05	46.94	62.29	49.00
	950	82.53	66.56	83.04	67.20	81.72	66.42
	1200	73.95	62.92	74.19	63.14	74.86	63.84
8	200	17.06	16.25	17.67	16.33	17.05	16.38
	450	34.72	33.27	34.22	33.13	34.47	33.71
	700	45.95	44.80	46.48	44.48	46.06	44.68
	950	63.95	56.04	61.65	54.19	64.68	56.66
	1200	66.40	60.12	64.97	59.19	66.66	60.78
10	200	13.80	14.18	13.70	14.14	14.19	14.54
	450	30.01	28.65	30.45	28.35	31.32	29.58
	700	33.15	33.46	32.60	33.03	32.83	33.04
	950	50.00	47.62	50.73	47.56	50.03	48.15
	1200	49.95	47.56	46.89	46.24	50.51	47.82
12	200	12.33	12.43	12.14	12.17	12.48	12.45
	450	32.16	28.02	31.62	27.40	33.02	28.81
	700	25.94	28.90	25.91	28.18	25.46	28.27
	950	46.29	46.30	44.17	44.15	47.28	46.31
	1200	42.70	42.90	42.64	42.42	43.19	43.61
15	200	11.37	12.30	10.51	11.68	11.23	12.09
	450	20.29	20.90	19.55	20.34	20.26	20.90
	700	23.74	23.88	22.50	23.25	23.55	23.88
	950	32.91	34.98	32.82	35.52	32.55	34.73
	1200	32.24	35.46	31.73	34.99	33.93	37.24
18	200	10.60	11.10	11.16	11.56	10.88	11.33
	450	17.65	20.71	17.65	20.51	18.39	20.82
	700	21.58	23.32	19.63	21.76	21.44	24.03
	950	23.74	27.21	22.72	27.29	24.98	28.26
	1200	25.41	27.26	25.23	26.92	27.75	29.36
21	200	10.54	11.43	8.50	9.84	10.53	11.26
	450	21.61	23.64	21.24	23.27	22.27	23.67
	700	17.99	19.37	17.90	19.76	18.94	20.84
	950	21.71	26.47	24.39	28.41	23.36	28.11
	1200	27.05	29.46	25.94	30.18	27.22	29.17

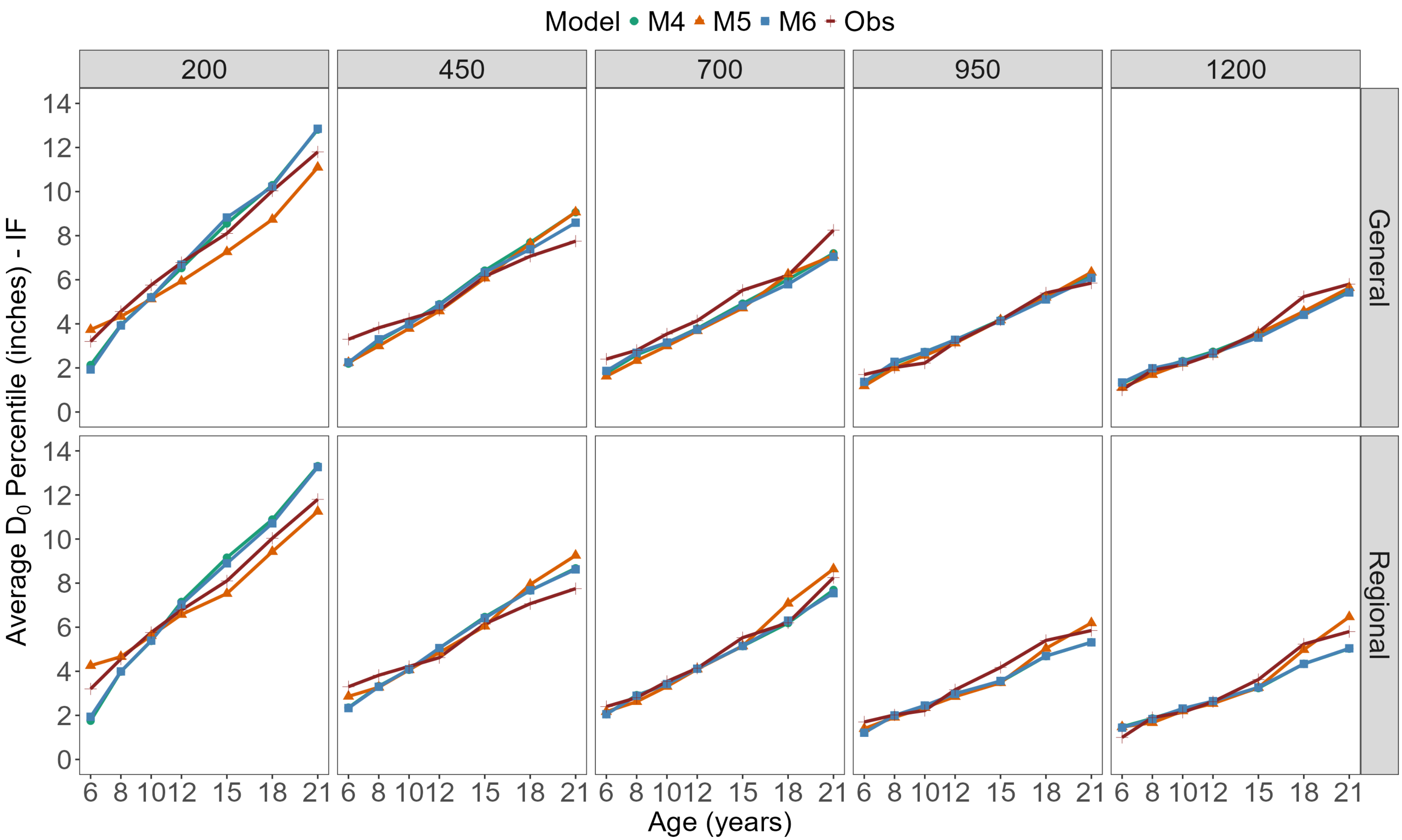

Figure 3.22: Average D_0 percentile values for three regression models (M4, M5, and M6) accounting for environmental co-variables, across two modeling levels and five planting densities, for the IF installations in the WGCDS.

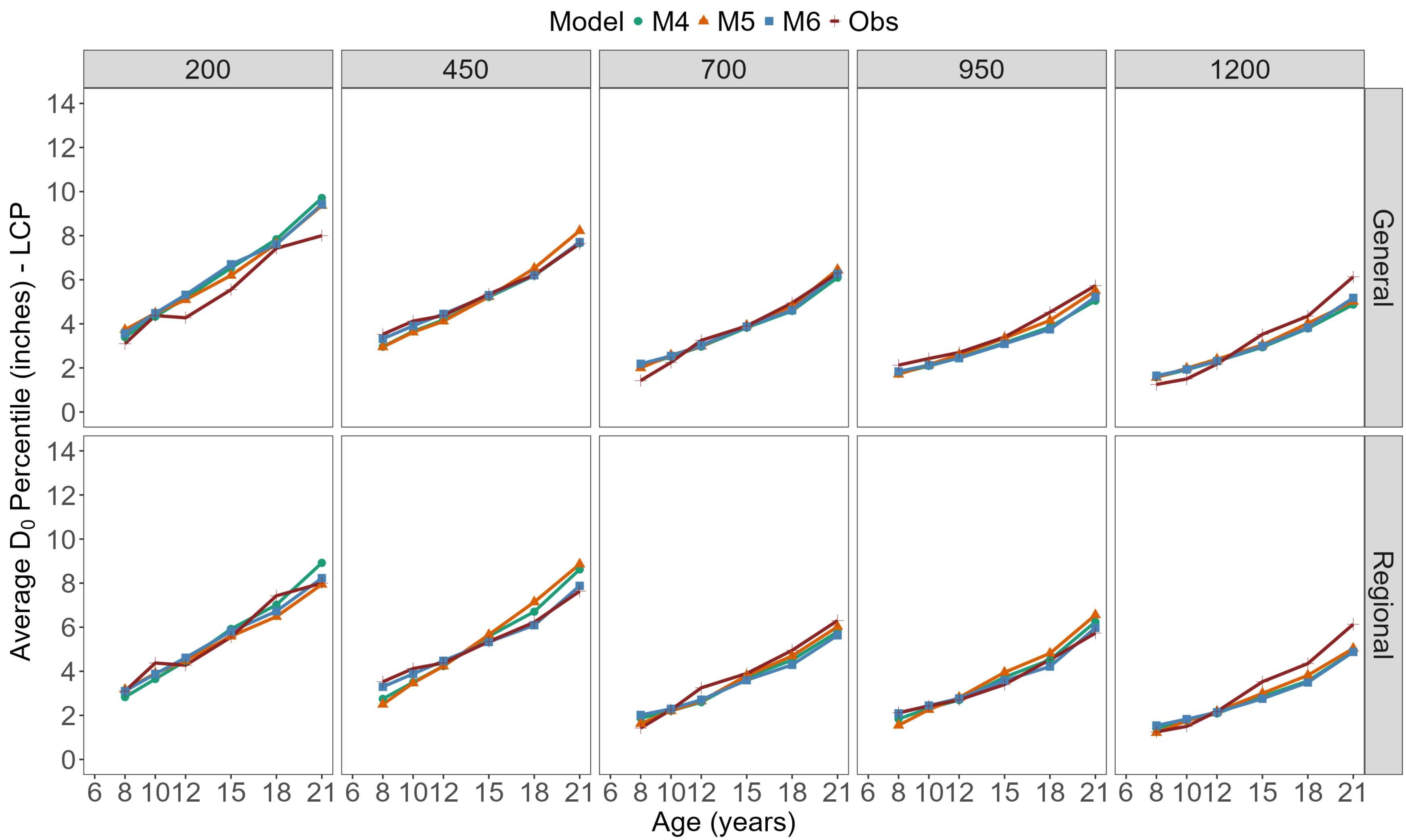

Figure 3.23: Average D_0 percentile values for three regression models (M4, M5, and M6) accounting for environmental co-variables, across two modeling levels and five planting densities, for the LCP installations in the WGCDS.

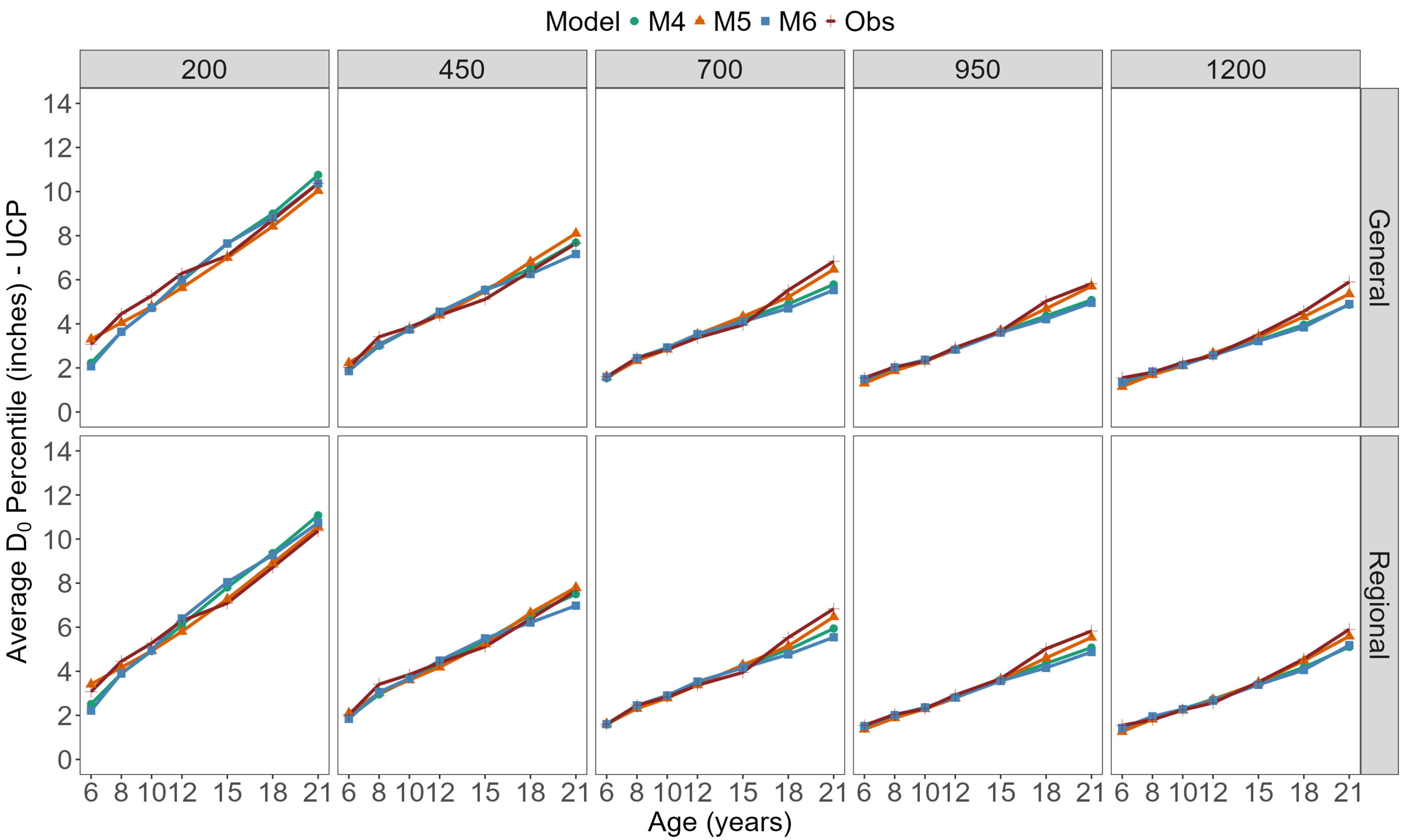

Figure 3.24: Average D_0 percentile values for three regression models (M4, M5, and M6) accounting for environmental co-variables, across two modeling levels and five planting densities, for the UCP installations in the WGCDS.

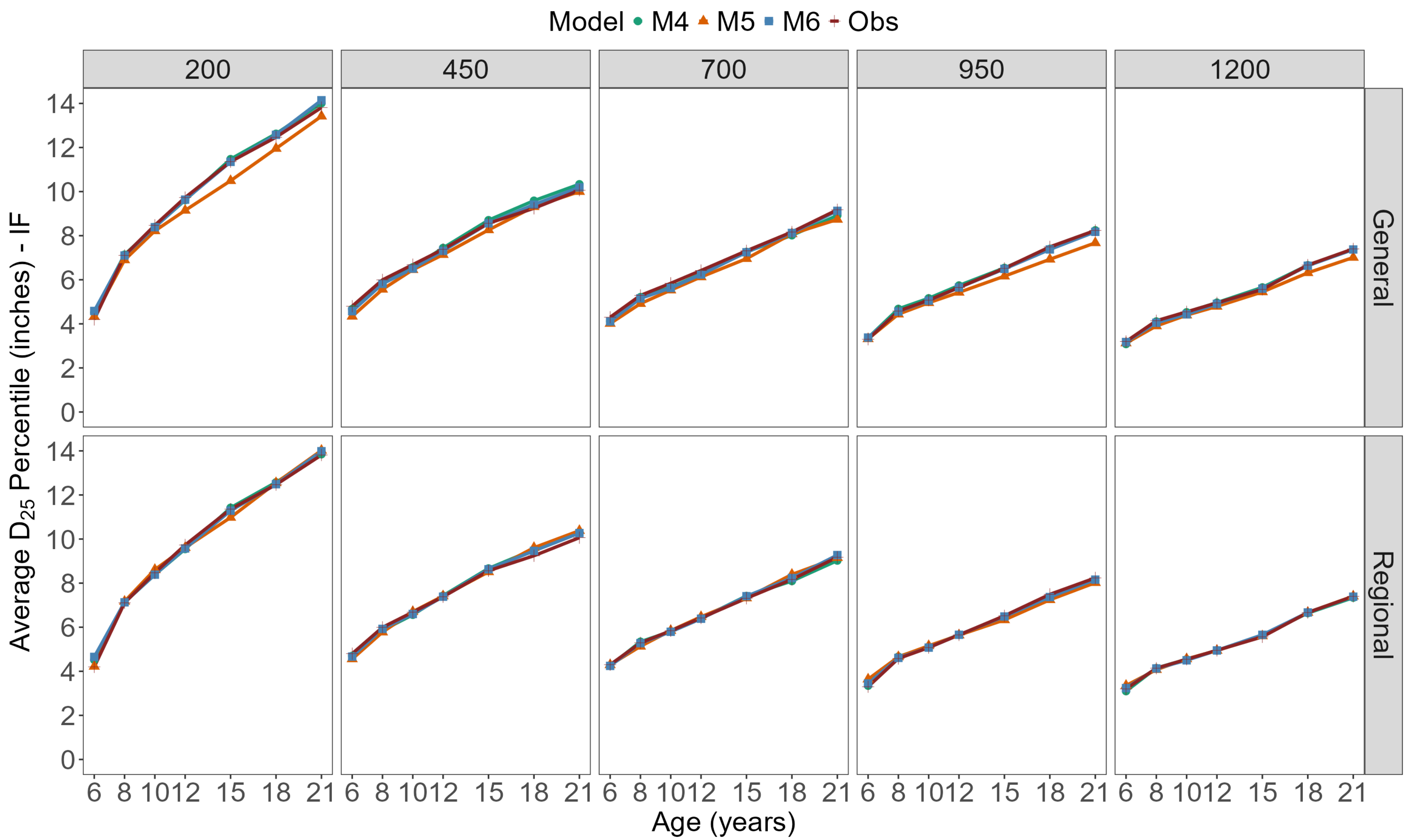

Figure 3.25: Average D_{25} percentile values for three regression models (M4, M5, and M6) accounting for environmental co-variables, across two modeling levels and five planting densities, for the IF installations in the WGCDS.

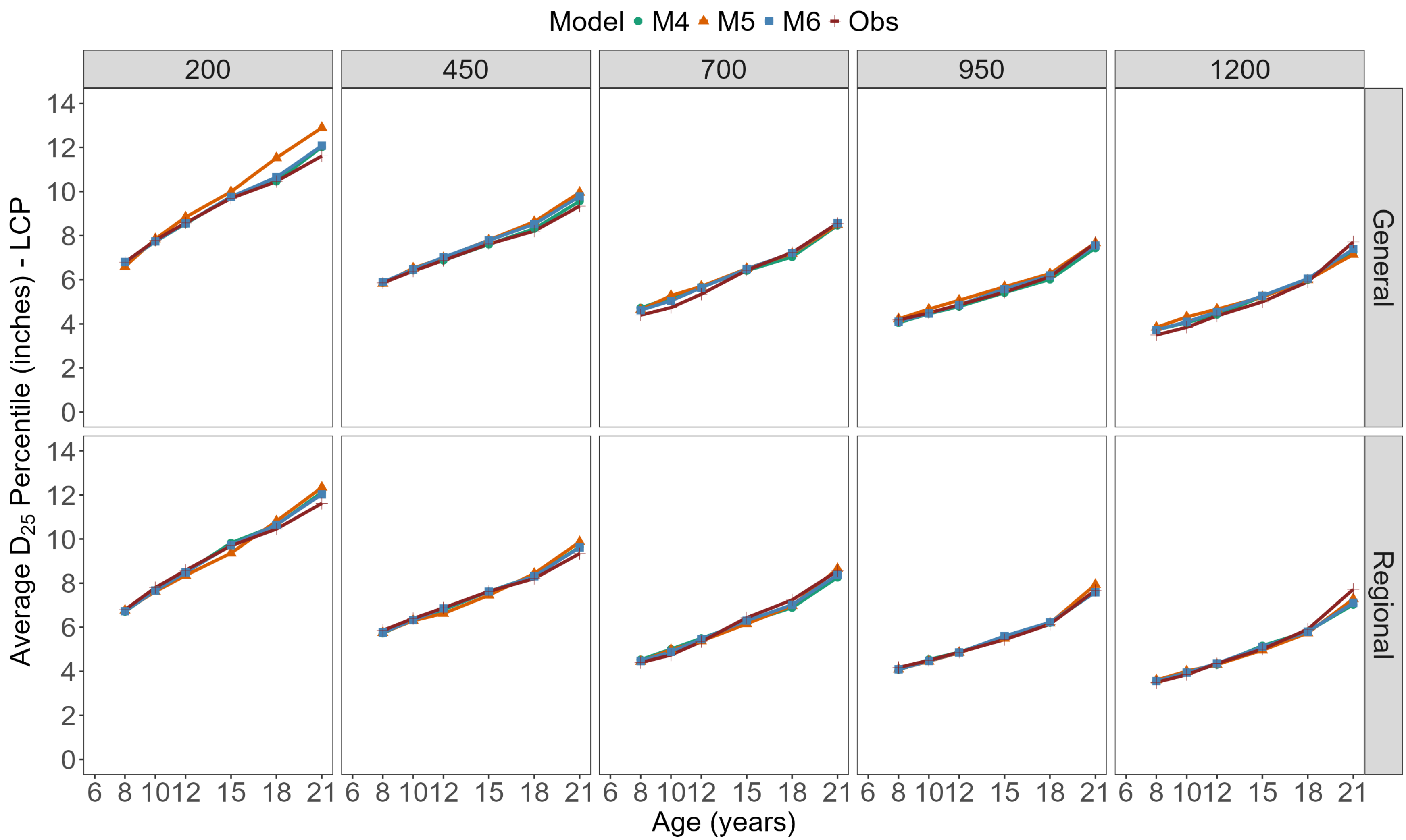

Figure 3.26: Average D_{25} percentile values for three regression models (M4, M5, and M6) accounting for environmental co-variables, across two modeling levels and five planting densities, for the LCP installations in the WGCDS.

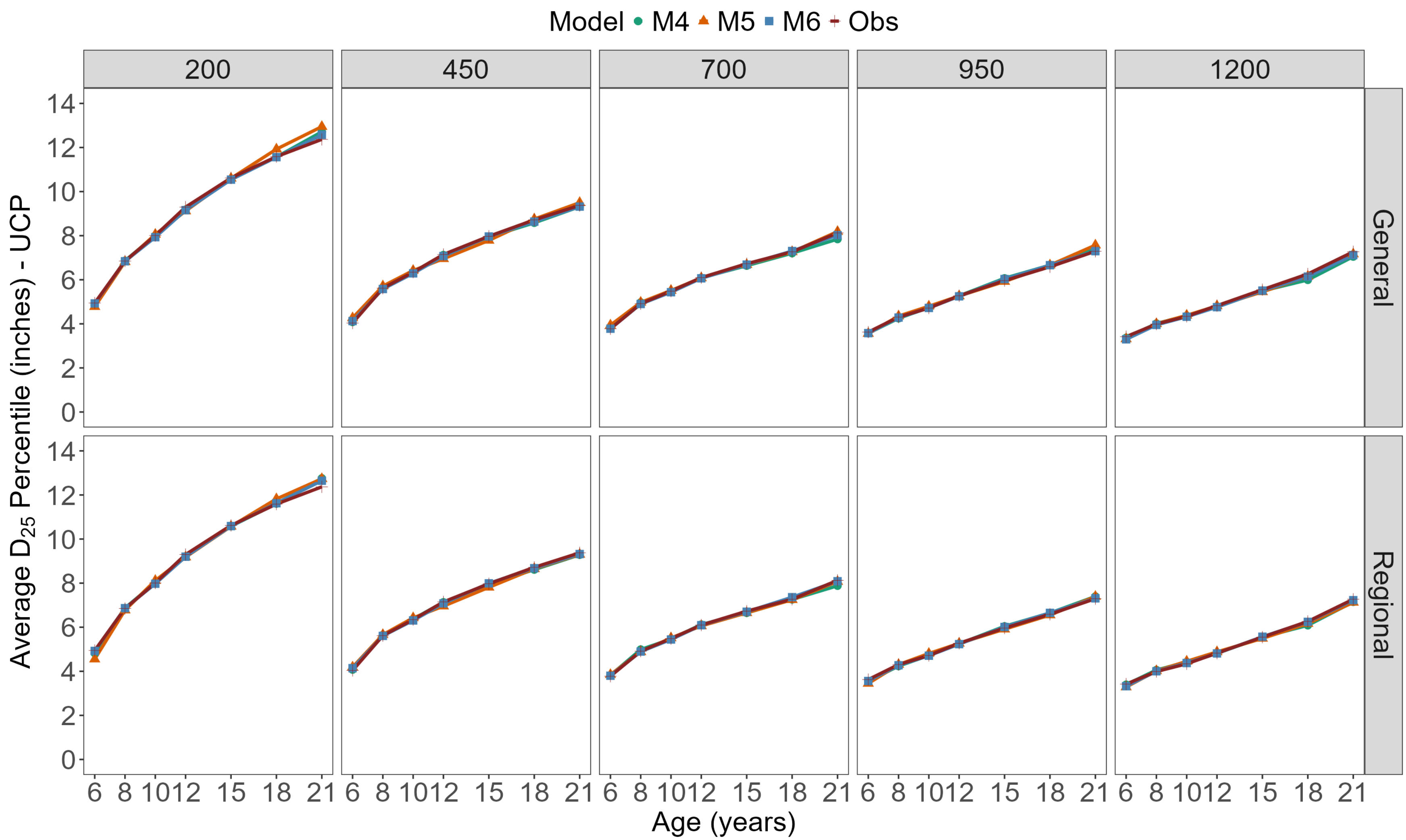

Figure 3.27: Average D_{25} percentile values for three regression models (M4, M5, and M6) accounting for environmental co-variables, across two modeling levels and five planting densities, for the UCP installations in the WGCDS.

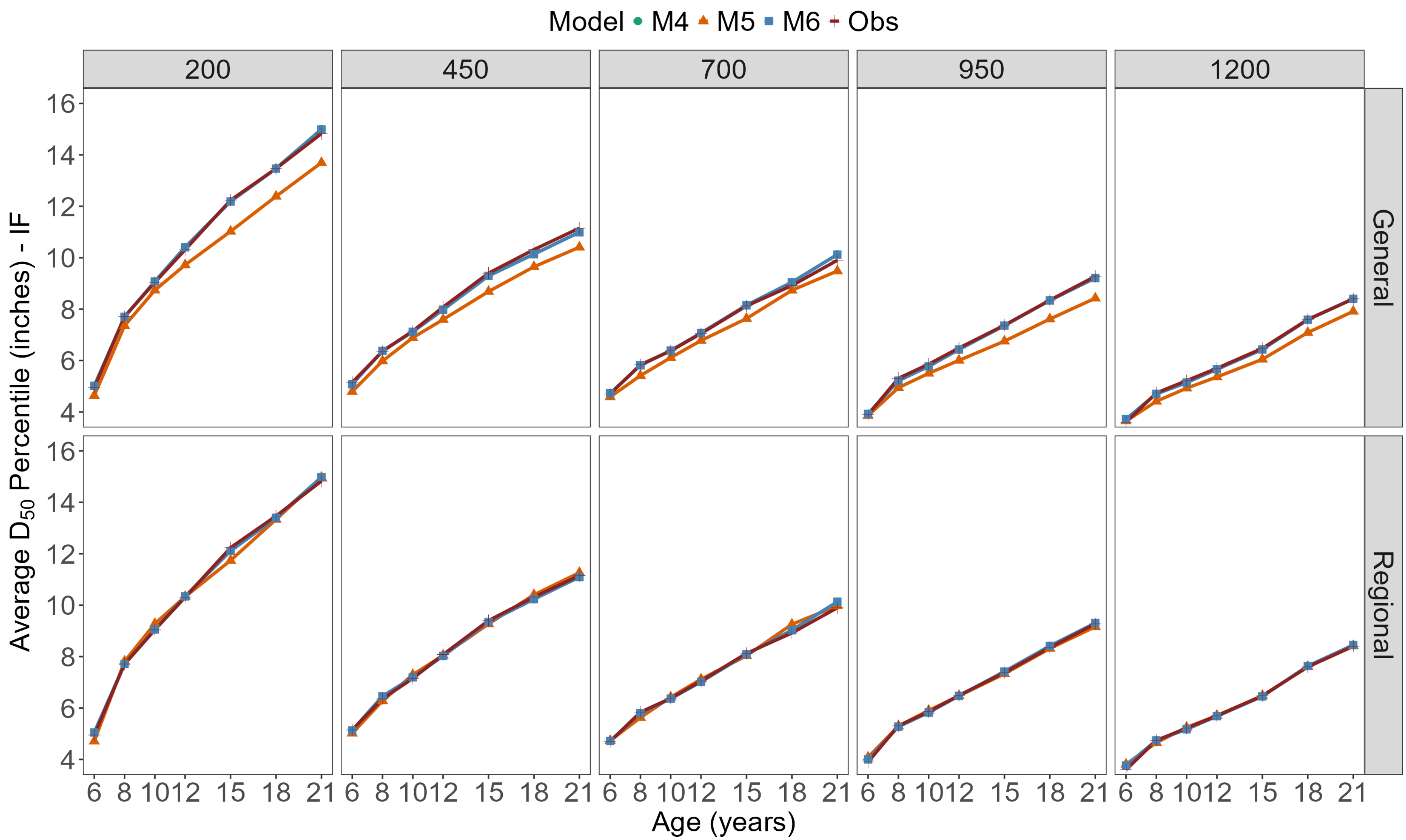

Figure 3.28: Average D_{50} percentile values for three regression models (M4, M5, and M6) accounting for environmental covariables, across two modeling levels and five planting densities, for the IF installations in the WGCDS.

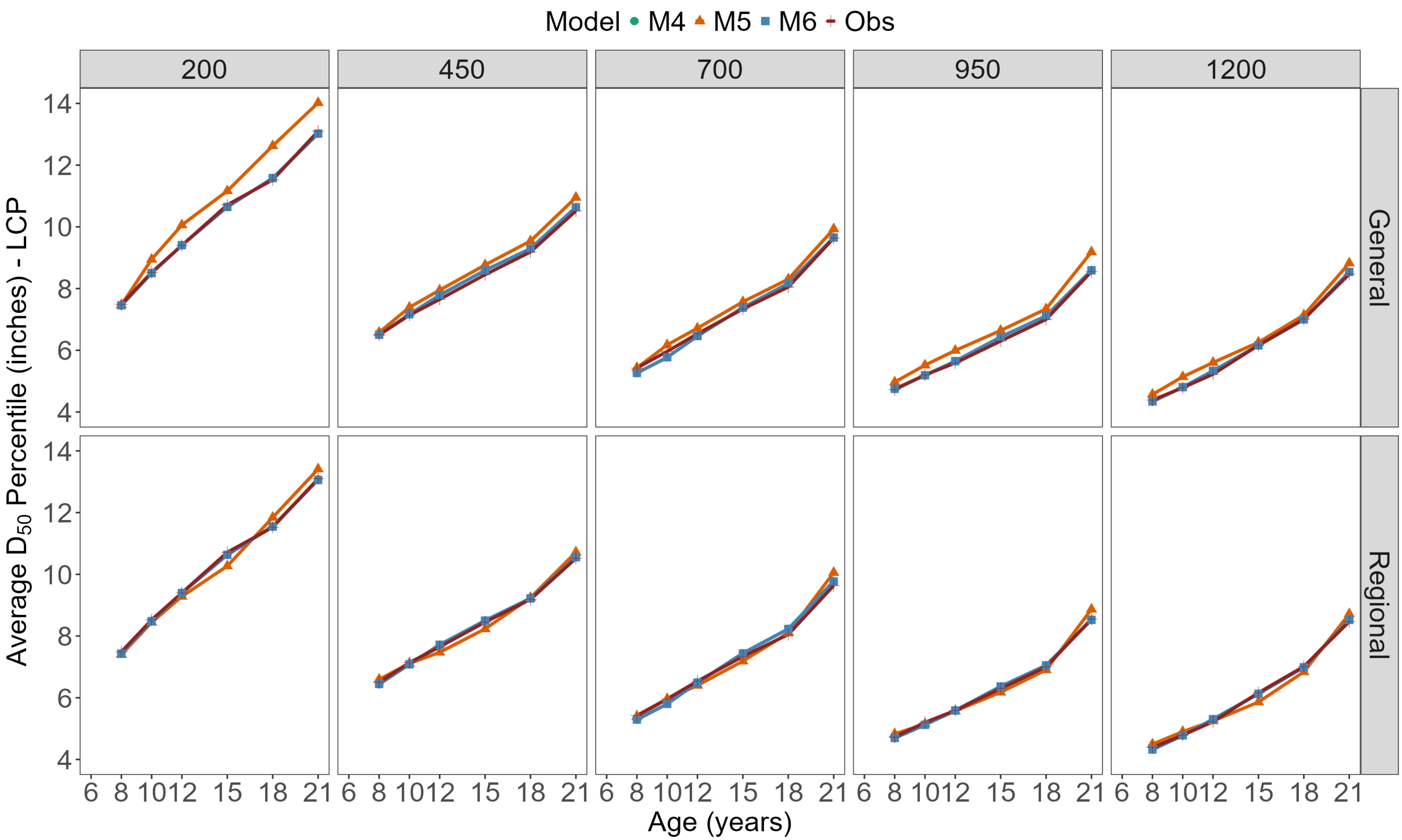

Figure 3.29: Average D_{50} percentile values for three regression models (M4, M5, and M6) accounting for environmental co-variables, across two modeling levels and five planting densities, for the LCP installations in the WGCDS.

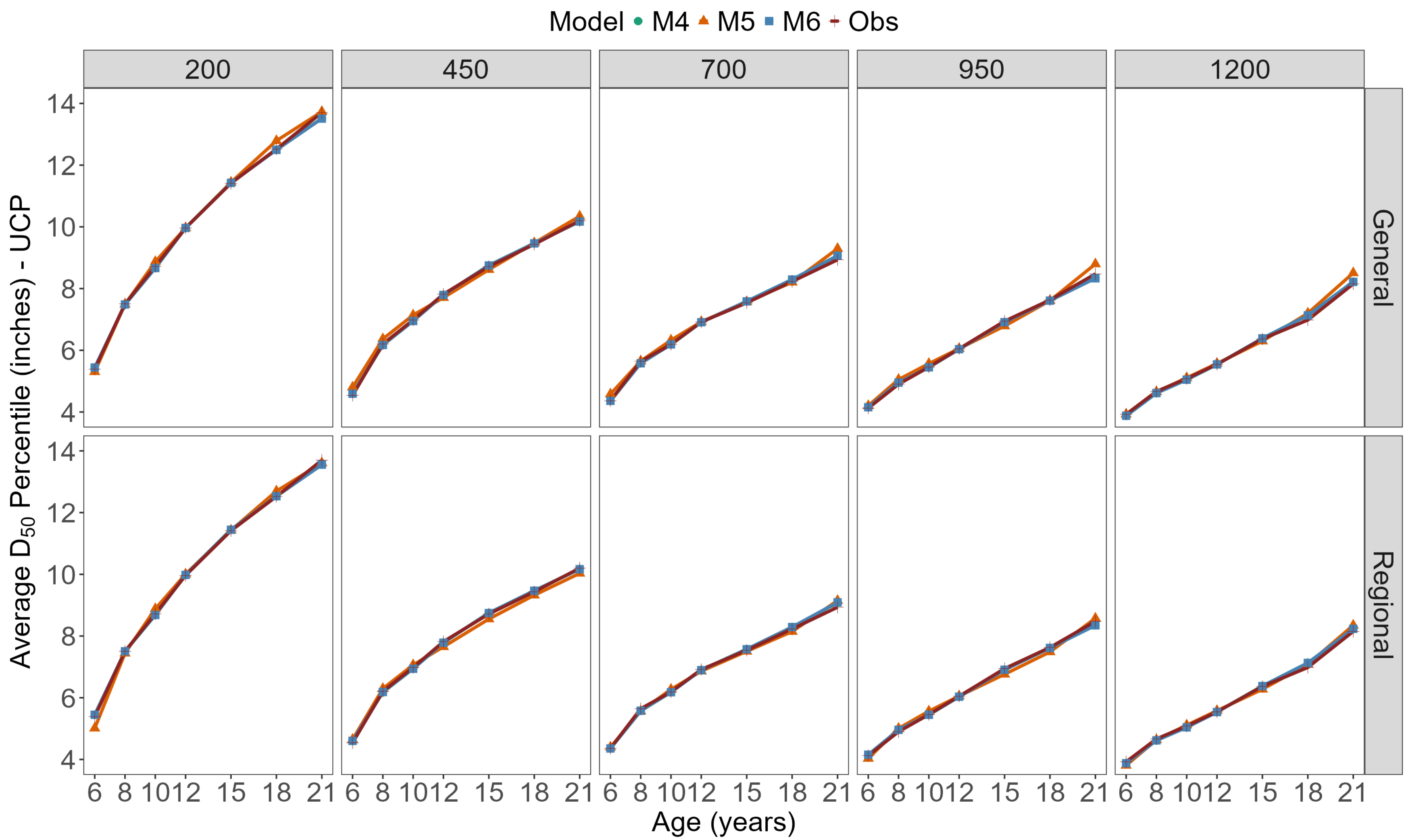

Figure 3.30: Average D_{50} percentile values for three regression models (M4, M5, and M6) accounting for environmental co-variables, across two modeling levels and five planting densities, for the UCP installations in the WGCDS.

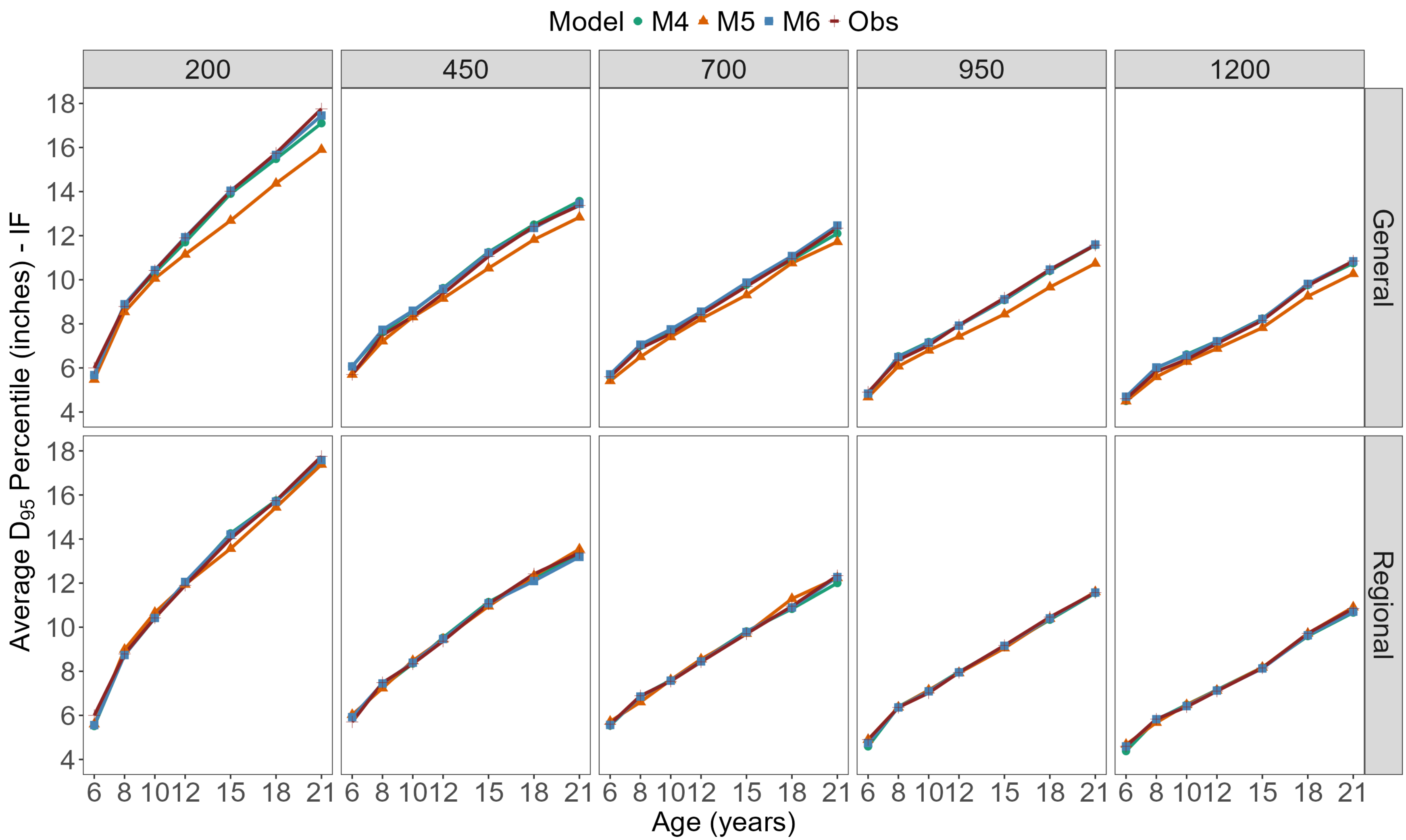

Figure 3.31: Average D_{95} percentile values for three regression models (M4, M5, and M6) accounting for environmental co-variables, across two modeling levels and five planting densities, for the IF installations in the WGCDS.

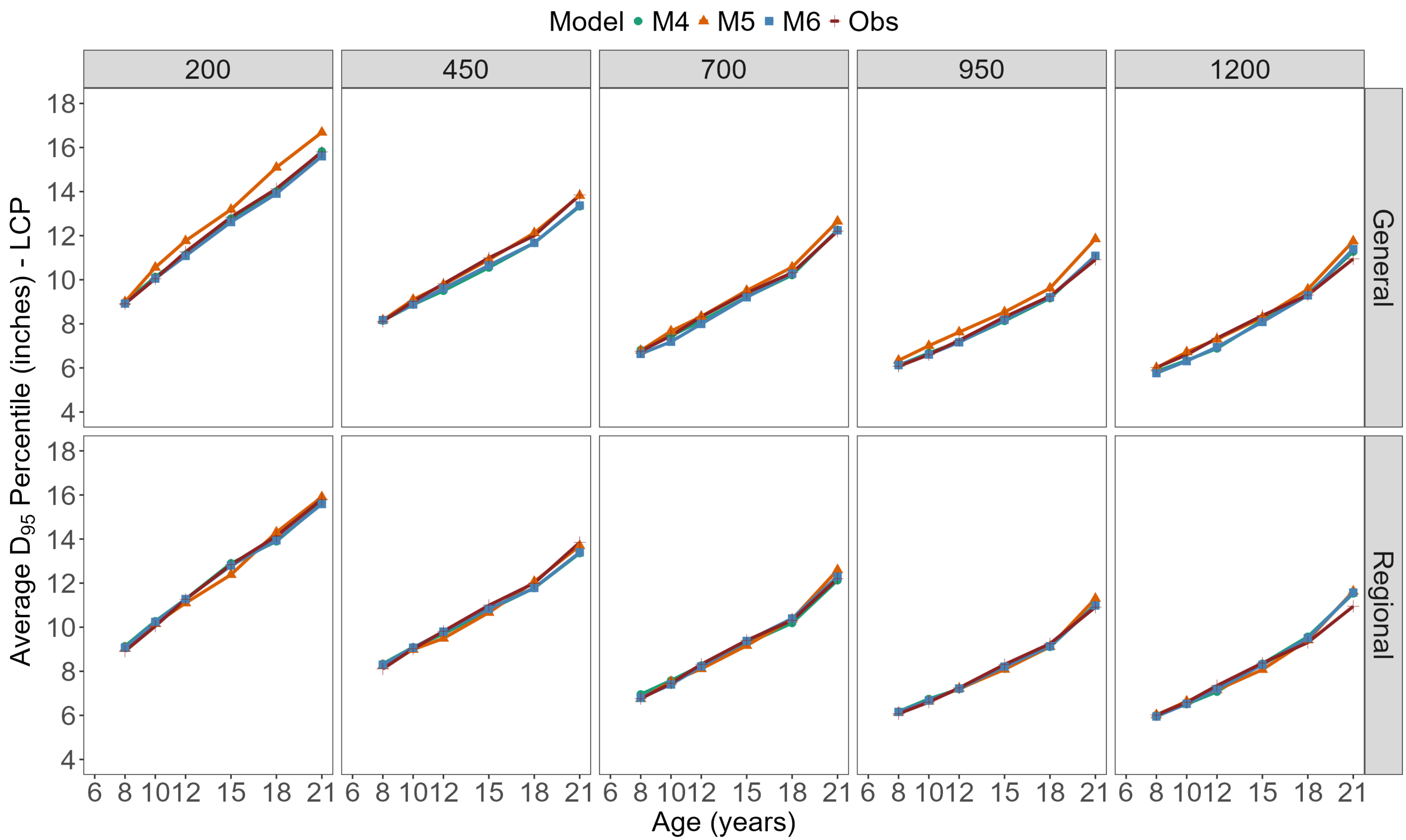

Figure 3.32: Average D_{95} percentile values for three regression models (M4, M5, and M6) accounting for environmental co-variables, across two modeling levels and five planting densities, for the LCP installations in the WGCDS.

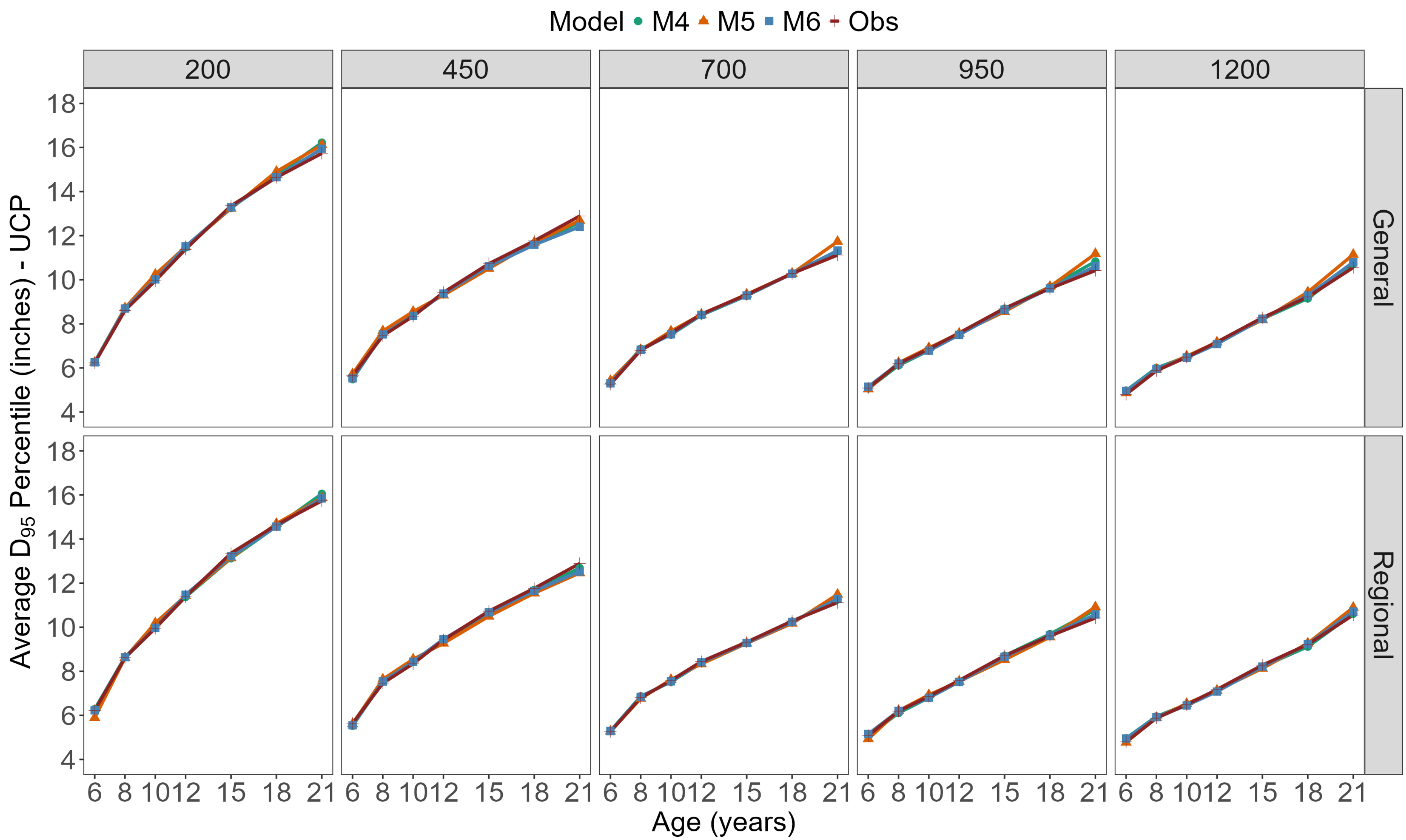

Figure 3.33: Average D_{95} percentile values for three regression models (M4, M5, and M6) accounting for environmental co-variables, across two modeling levels and five planting densities, for the UCP installations in the WGCDS.

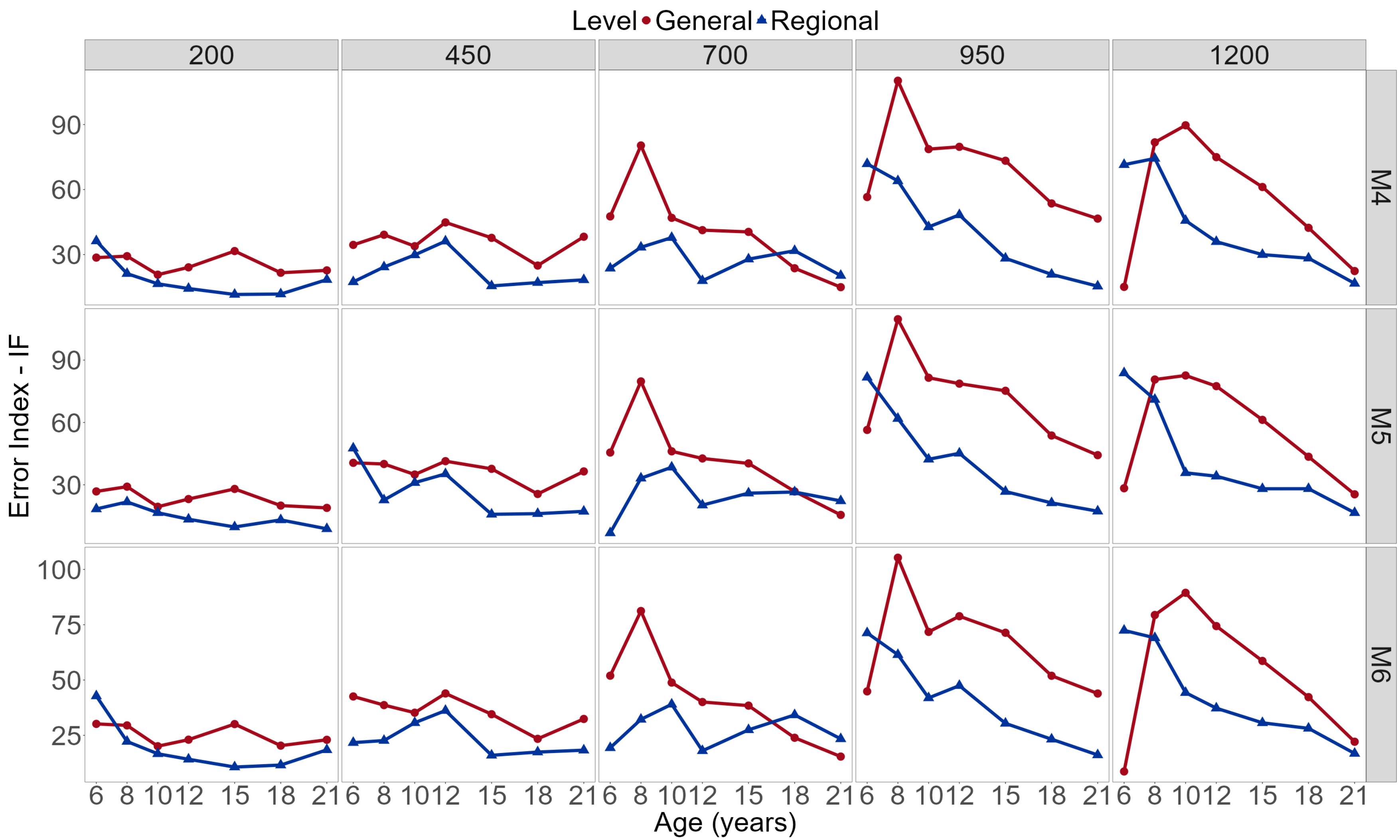

Figure 3.34: Error Index based on three regression models (M4, M5, and M6) accounting for environmental co-variables, across two modeling levels and five planting densities, for the IF installations in the WGCDS.

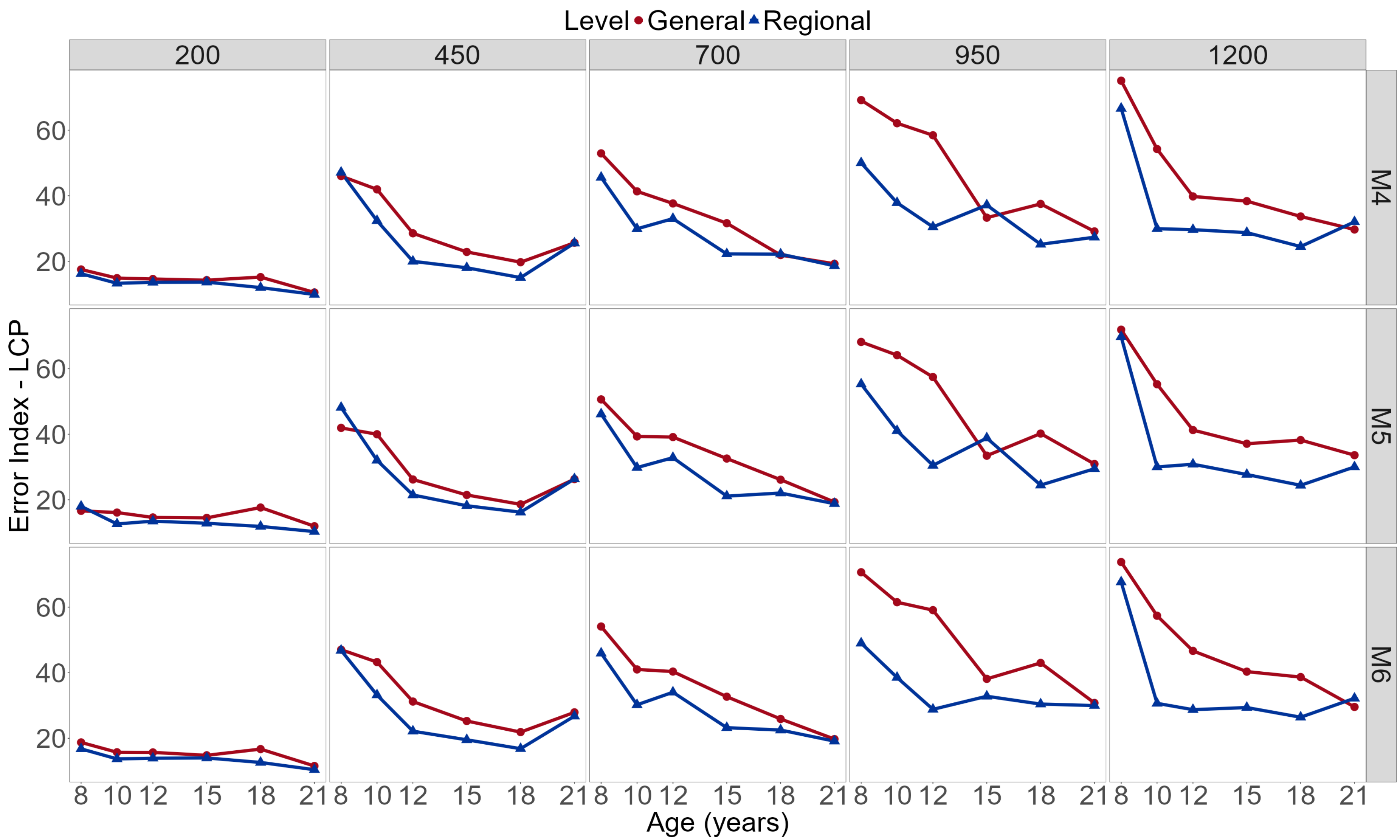

Figure 3.35: Error Index based on three regression models (M4, M5, and M6) accounting for environmental co-variables, across two modeling levels and five planting densities, for the LCP installations in the WGCDS.

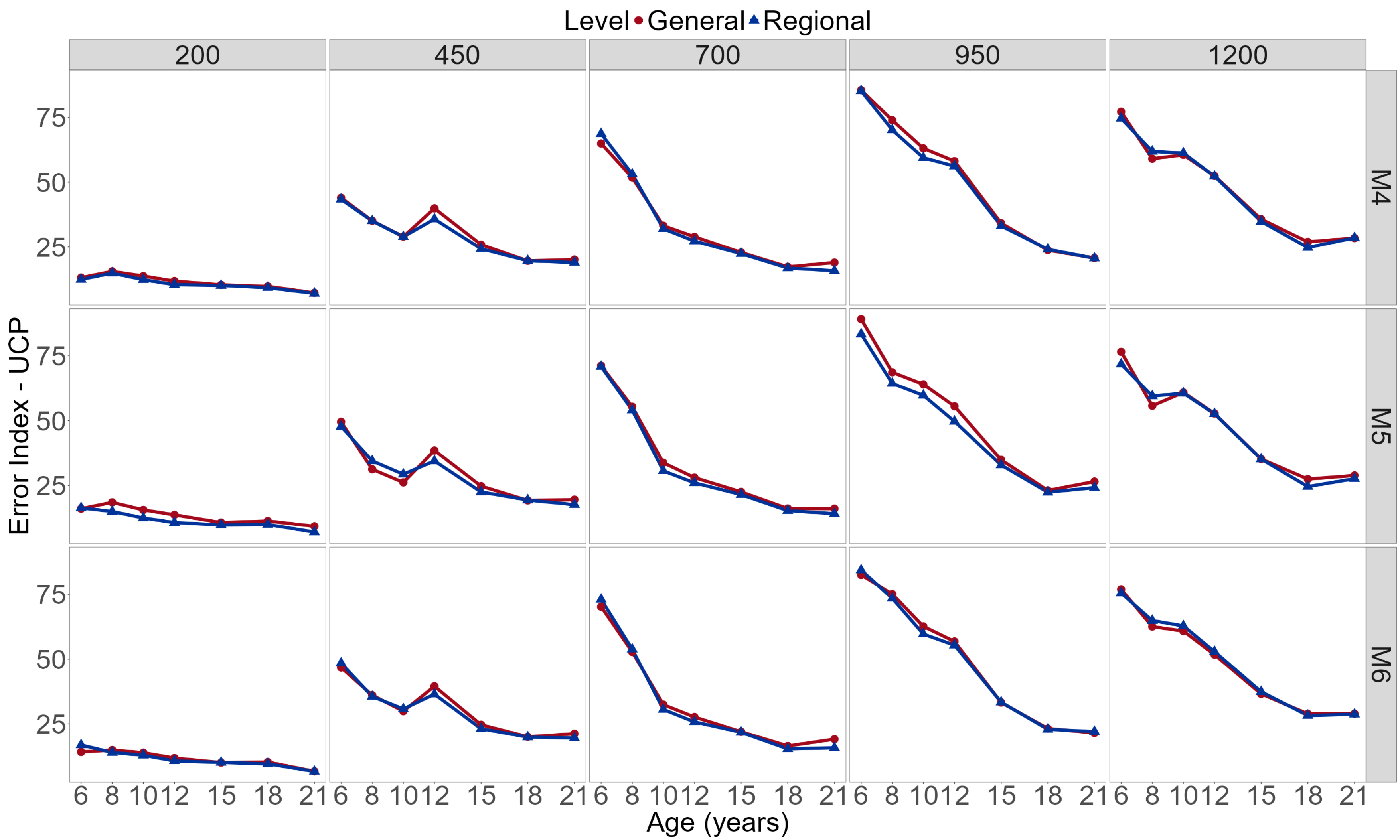

Figure 3.36: Error Index based on three regression models (M4, M5, and M6) accounting for environmental co-variables, across two modeling levels and five planting densities, for the UCP installations in the WGCDS.

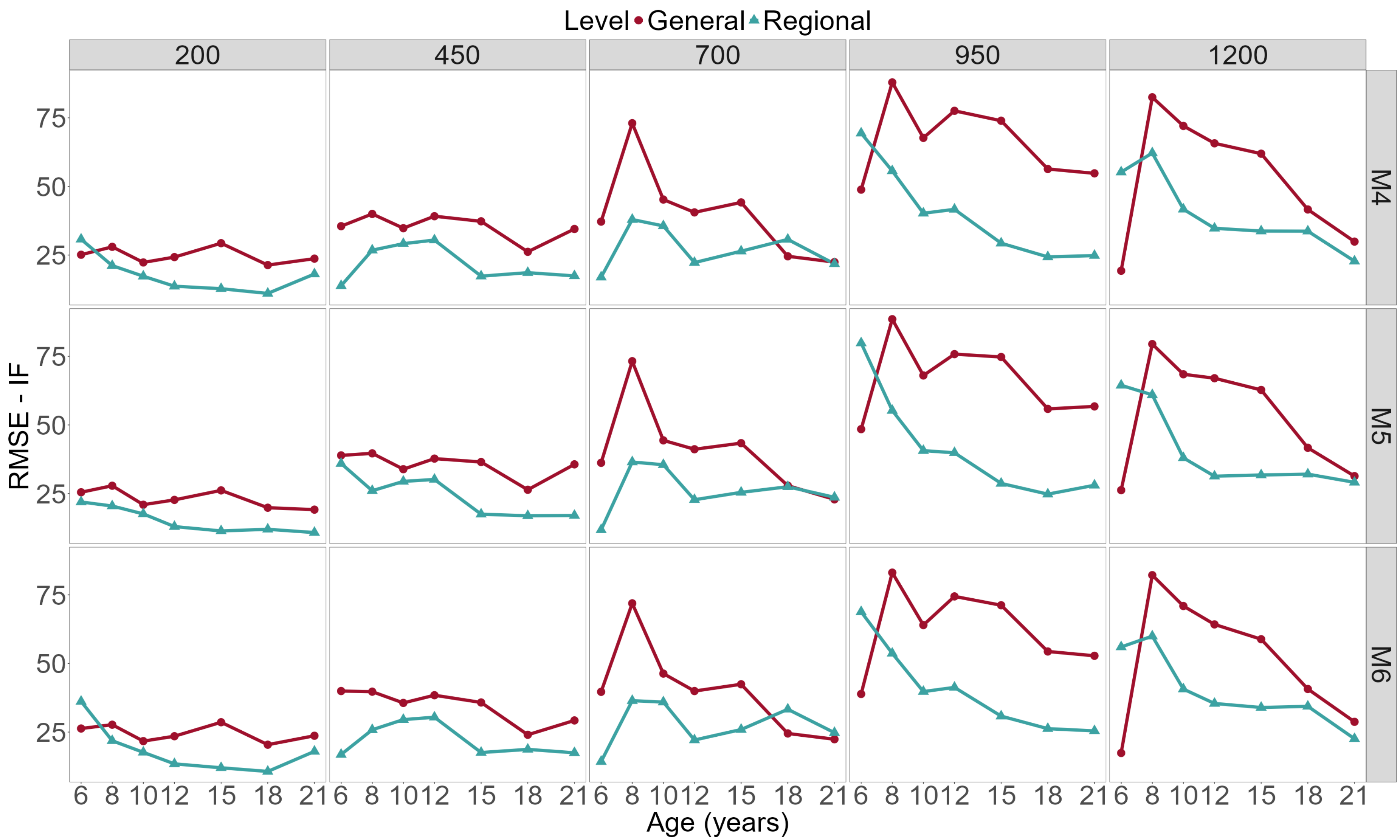

Figure 3.37: RMSE based on three regression models (M4, M5, and M6) accounting for environmental co-variables, across two modeling levels and five planting densities, for the IF installations in the WGCDS.

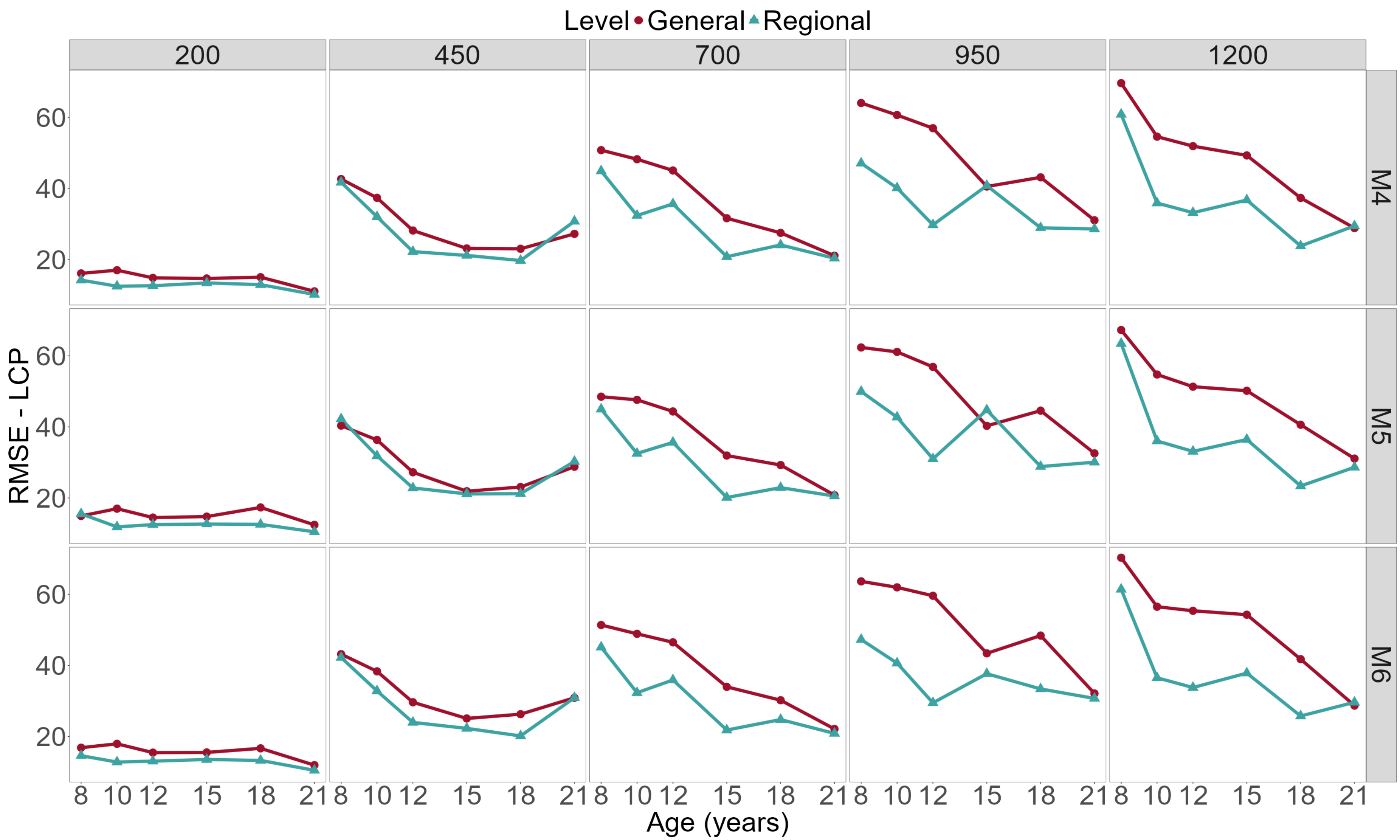

Figure 3.38: RMSE based on three regression models (M4, M5, and M6) accounting for environmental co-variables, across two modeling levels and five planting densities, for the LCP installations in the WGCDS.

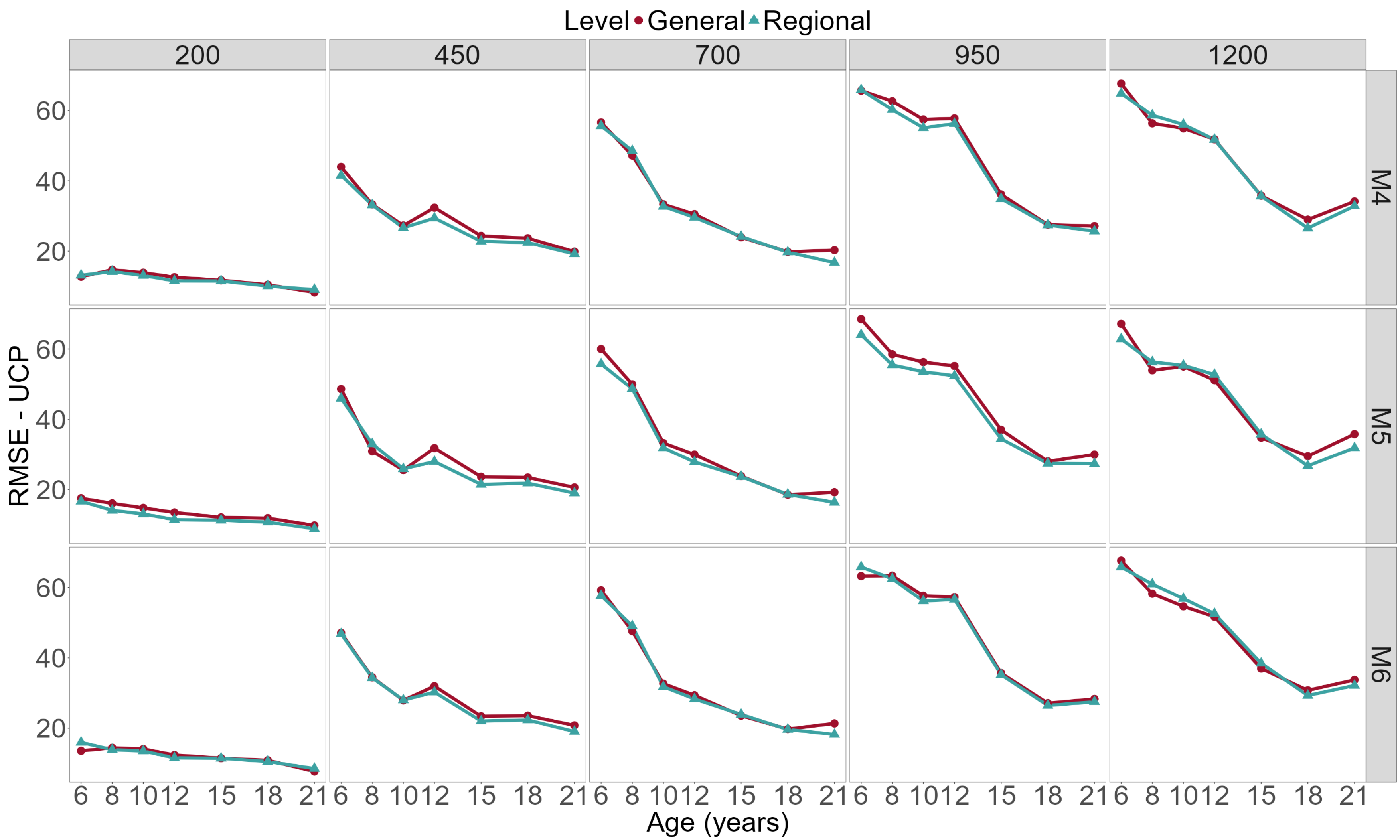

Figure 3.39: RMSE based on three regression models (M4, M5, and M6) accounting for environmental co-variables, across two modeling levels and five planting densities, for the UCP installations in the WGCDS.

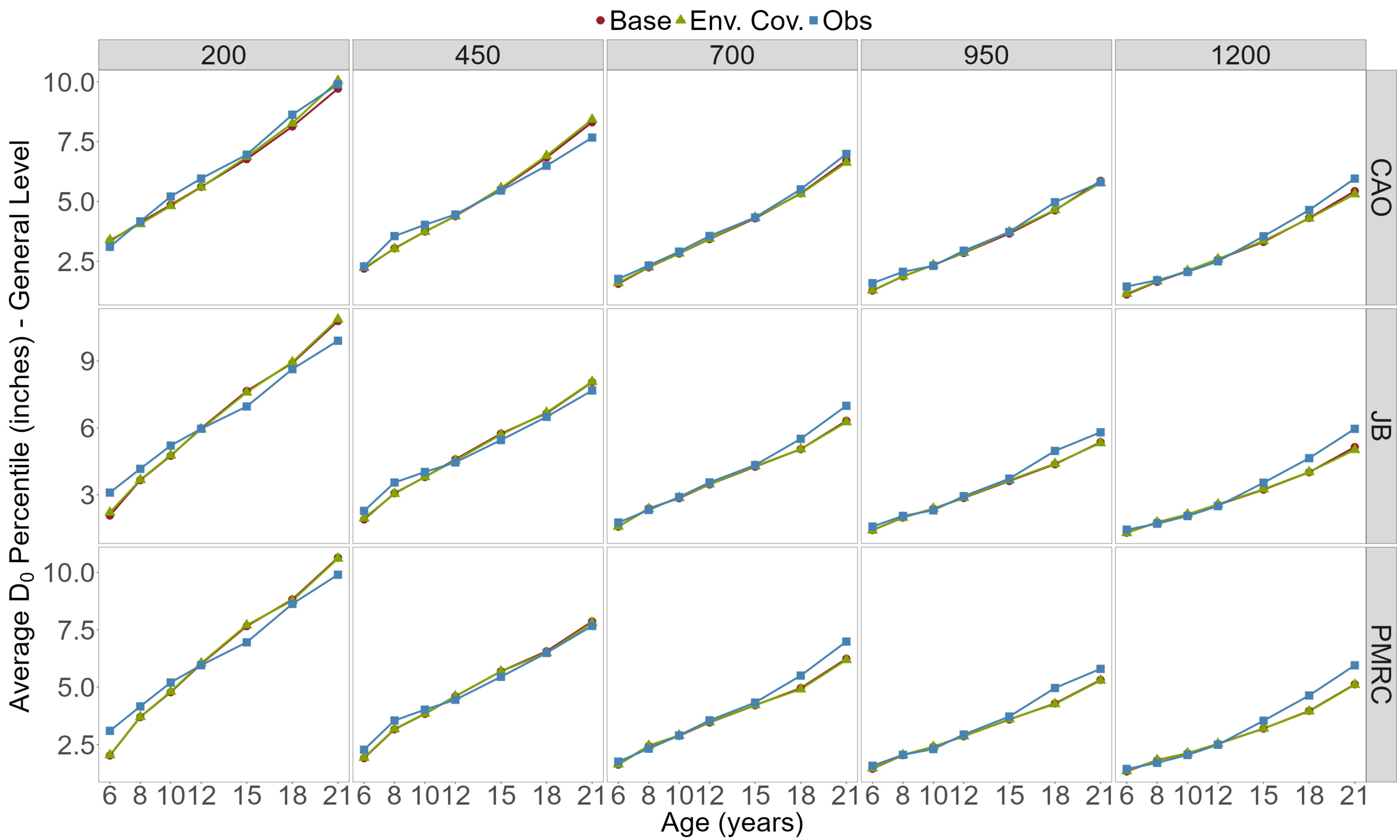

Figure 3.40: Results from three models for the D_0 percentile under two modeling approaches: (i) the base model (without environmental co-variables), and (ii) the adapted model (accounting for environmental co-variables), conducted for the general modeling level, and the percentile from observed. The predictions are plotted across all ages and five planting densities.

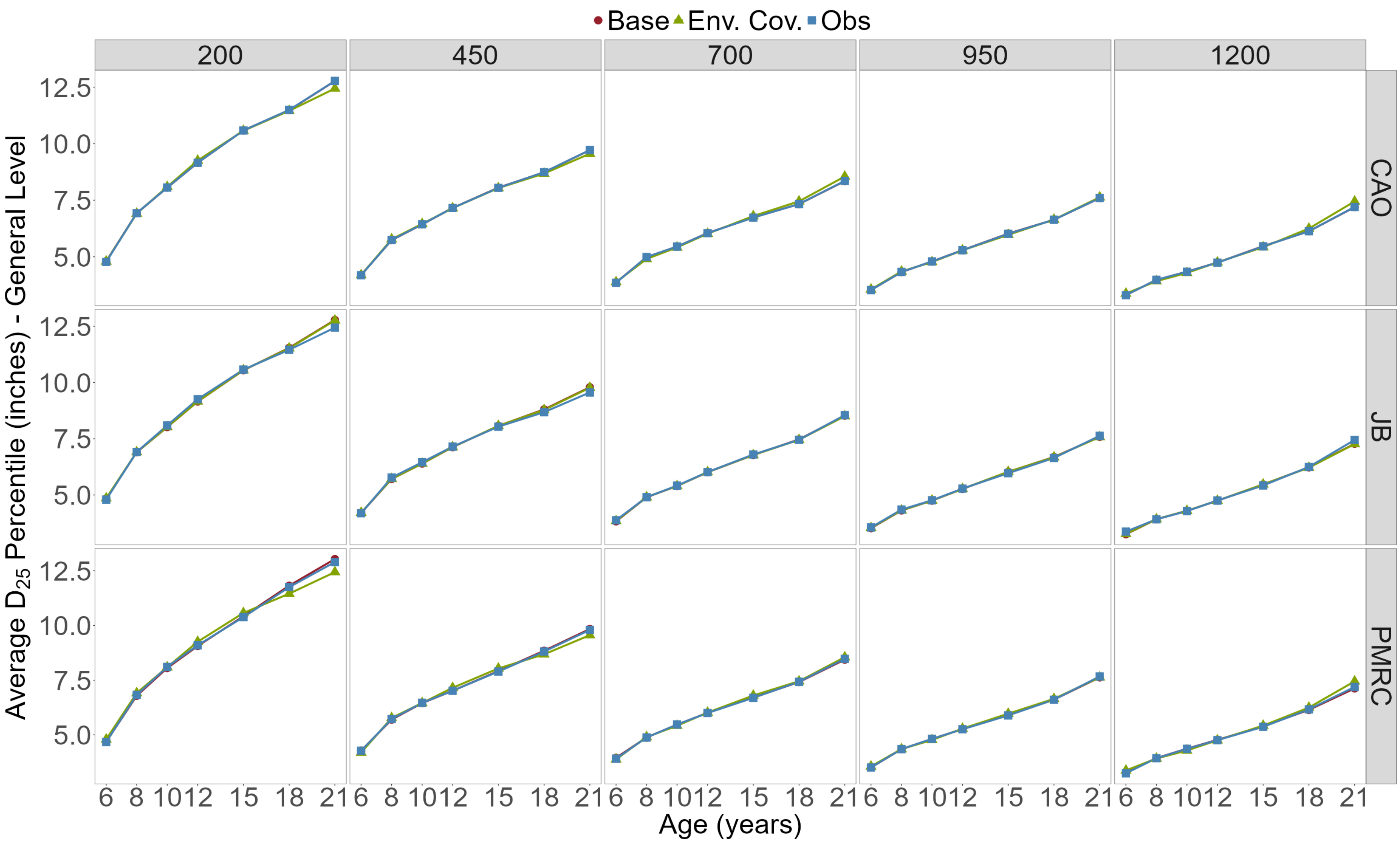

Figure 3.41: Results from three models for the D_{25} percentile under two modeling approaches: (i) the base model (without environmental co-variables), and (ii) the adapted model (accounting for environmental co-variables), conducted fot the general modeling level, and the percentile from observed. The predictions are plotted across all ages and five planting densities.

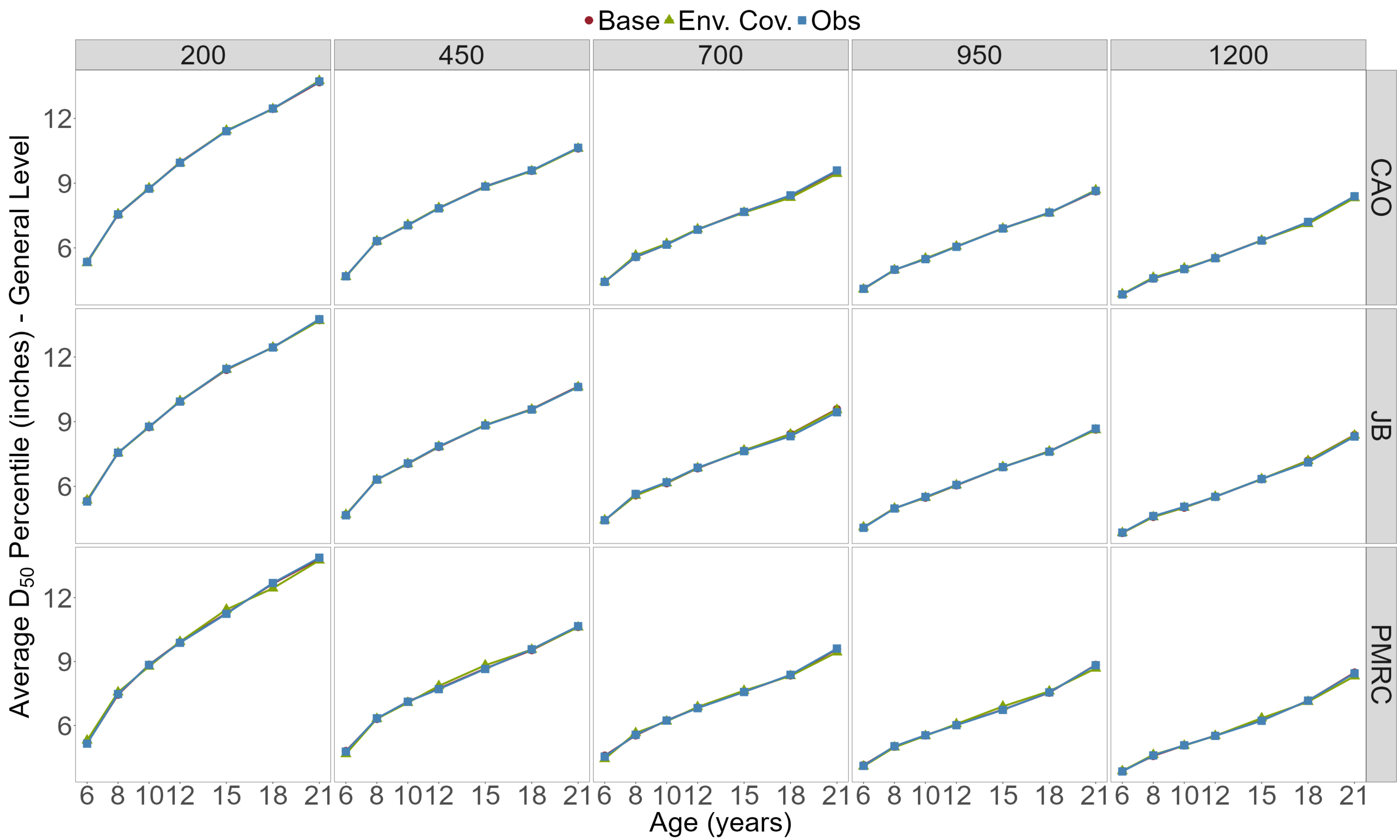

Figure 3.42: Results from three models for the D_{50} percentile under two modeling approaches: (i) the base model (without environmental co-variables), and (ii) the adapted model (accounting for environmental co-variables), conducted for the general modeling level, and the percentile from observed. The predictions are plotted across all ages and five planting densities.

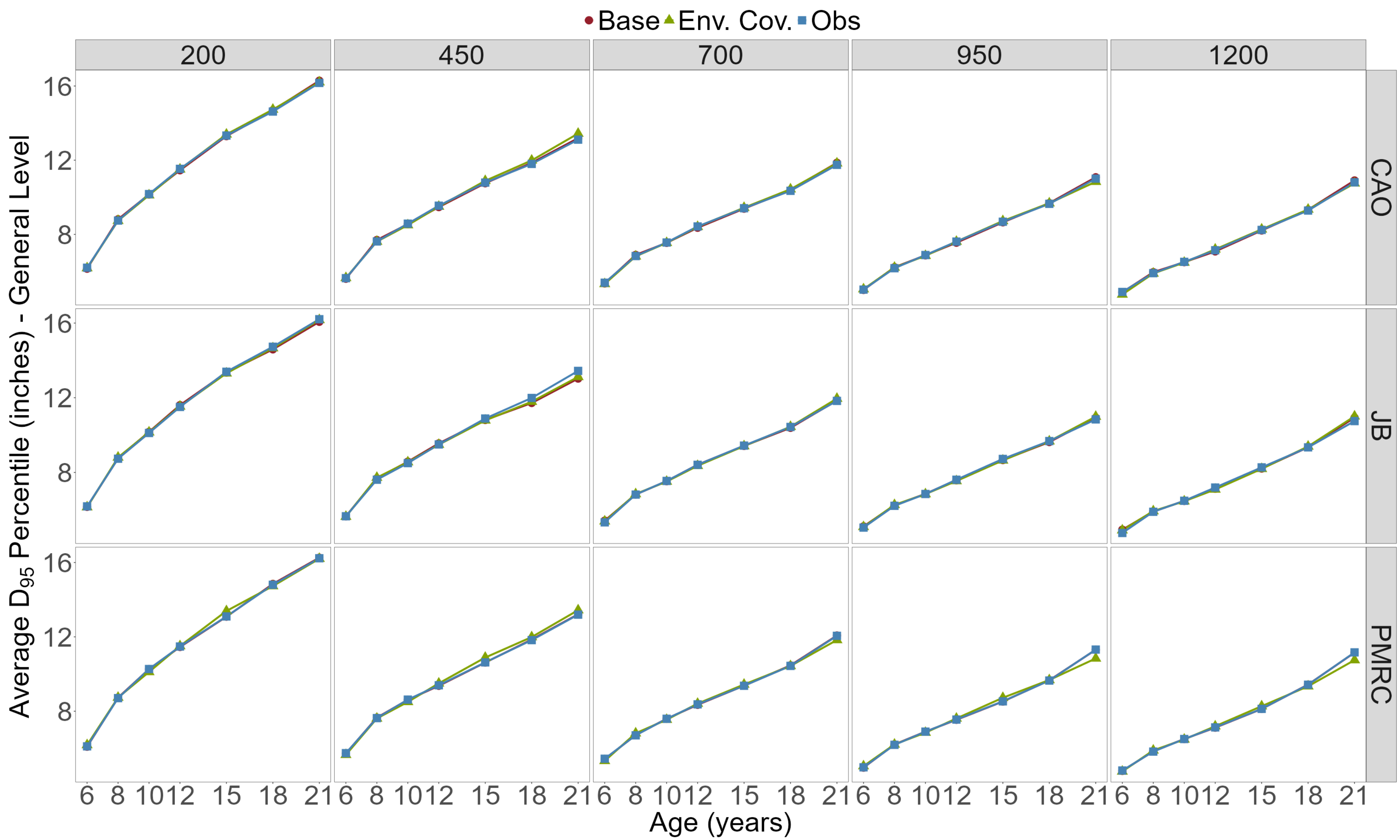

Figure 3.43: Results from three models for the D_{95} percentile under two modeling approaches: (i) the base model (without environmental co-variables), and (ii) the adapted model (accounting for environmental co-variables), conducted for the general modeling level, and the percentile from observed. The predictions are plotted across all ages and five planting densities.

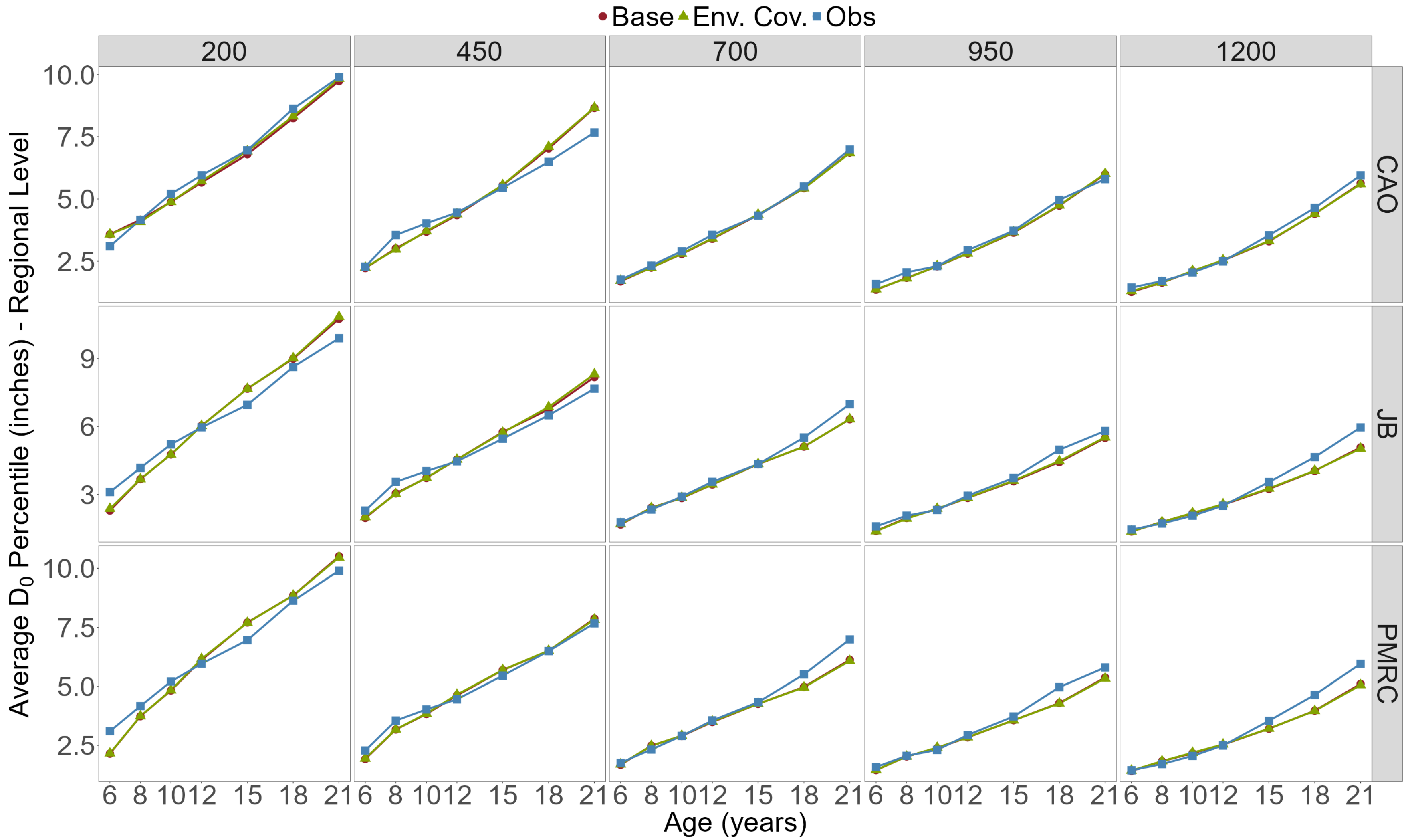

Figure 3.44: Results from three models for the D_0 percentile under two modeling approaches: (i) the base model (without environmental co-variables), and (ii) the adapted model (accounting for environmental co-variables), conducted for the regional modeling level, and the percentile from observed. The predictions are plotted across all ages and five planting densities.

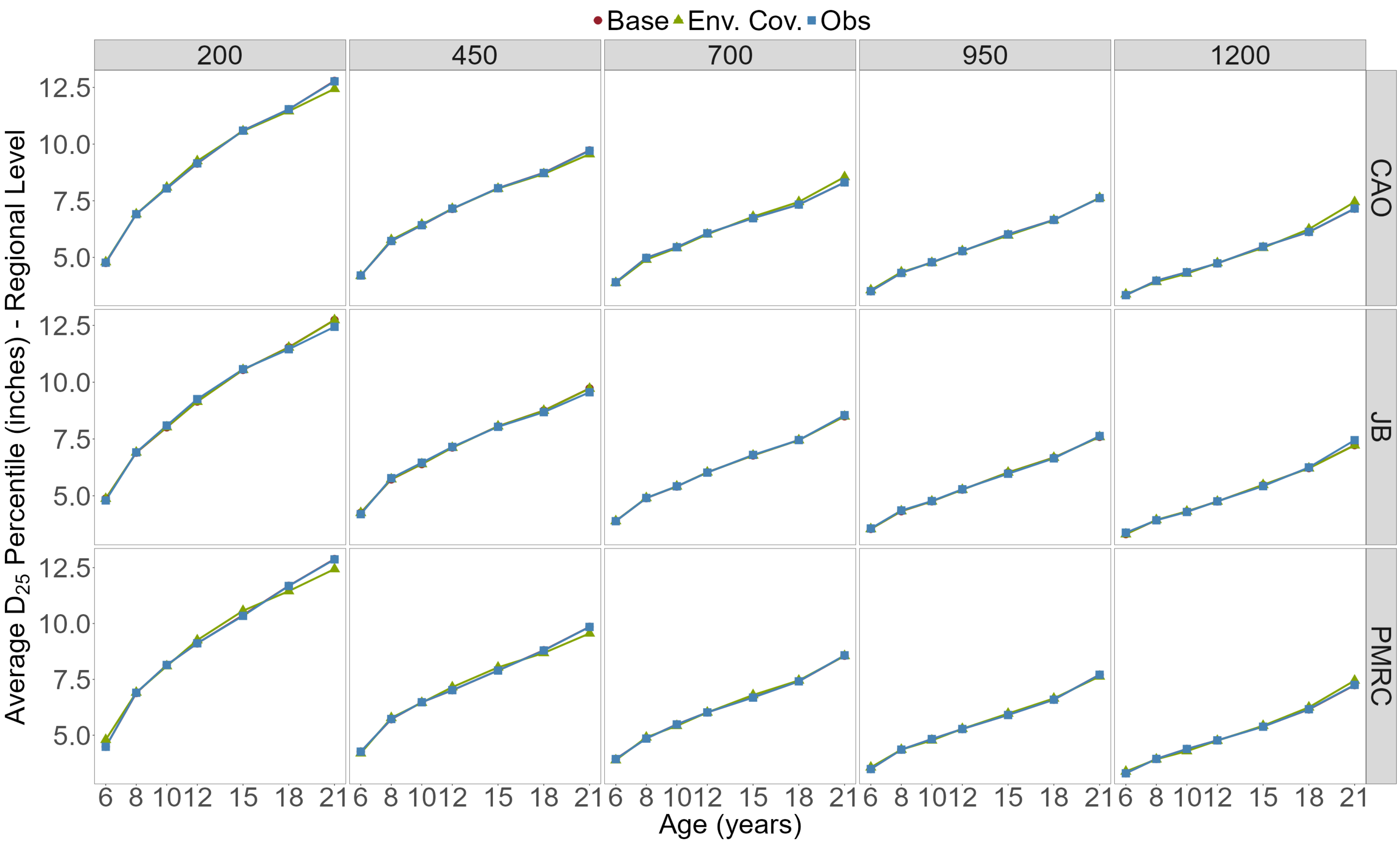

Figure 3.45: Results from three models for the D_{25} percentile under two modeling approaches: (i) the base model (without environmental co-variables), and (ii) the adapted model (accounting for environmental co-variables), conducted for the regional modeling level, and the percentile from observed. The predictions are plotted across all ages and five planting densities.

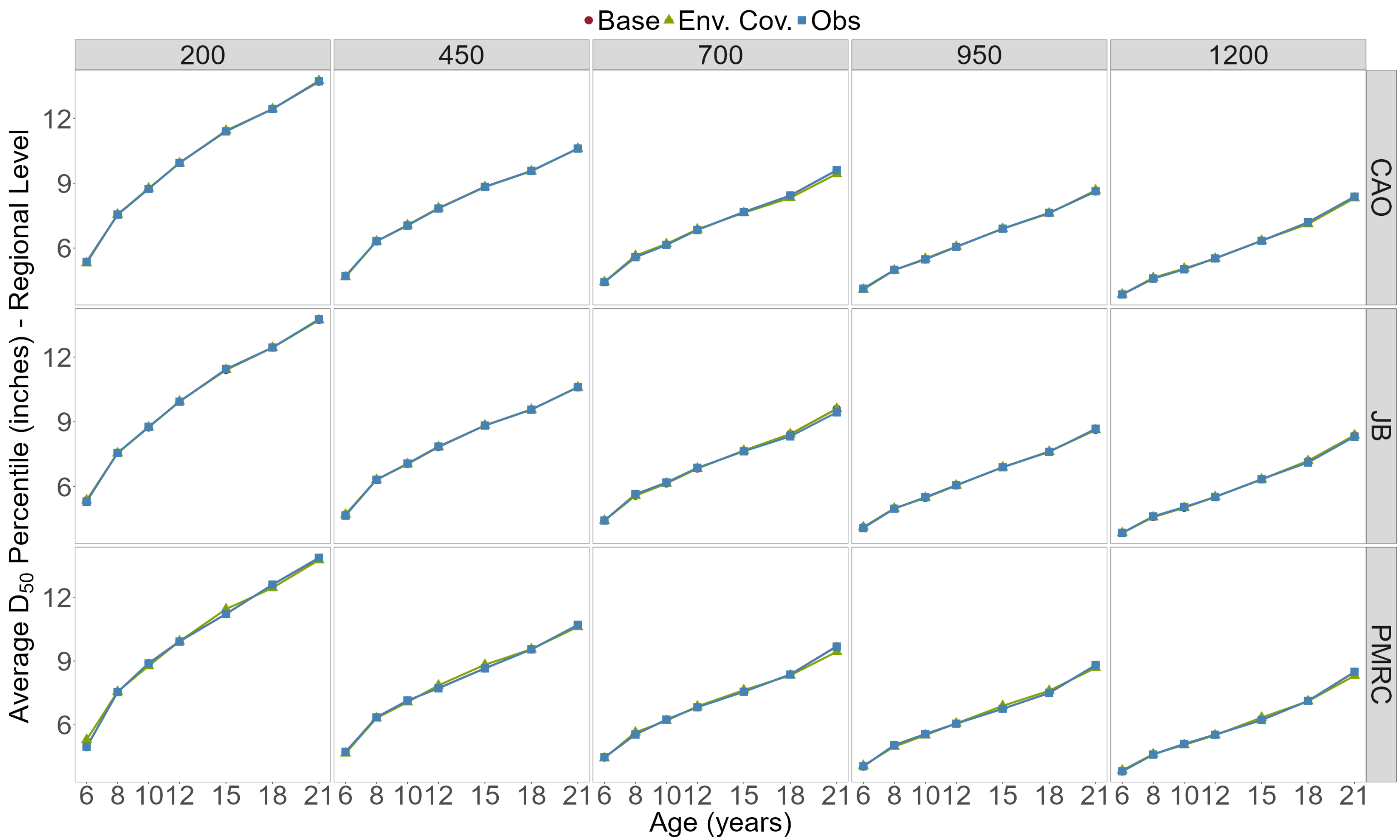

Figure 3.46: Results from three models for the D_{50} percentile under two modeling approaches: (i) the base model (without environmental co-variables), and (ii) the adapted model (accounting for environmental co-variables), conducted for the regional modeling level, and the percentile from observed. The predictions are plotted across all ages and five planting densities.

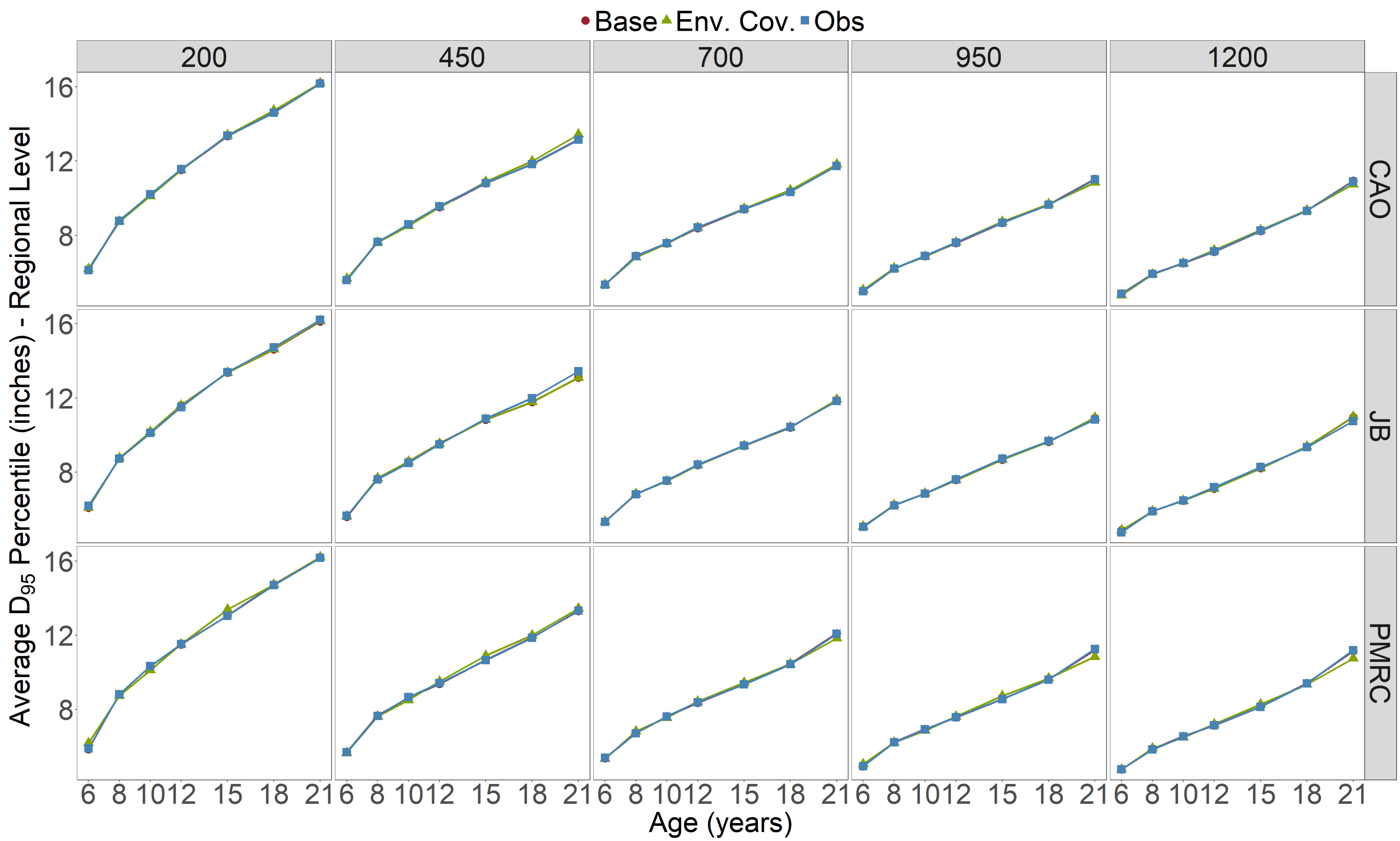

Figure 3.47: Results from three models for the D_{95} percentile under two modeling approaches: (i) the base model (without environmental co-variables), and (ii) the adapted model (accounting for environmental co-variables), conducted for the regional modeling level, and the percentile from observed. The predictions are plotted across all ages and five planting densities.

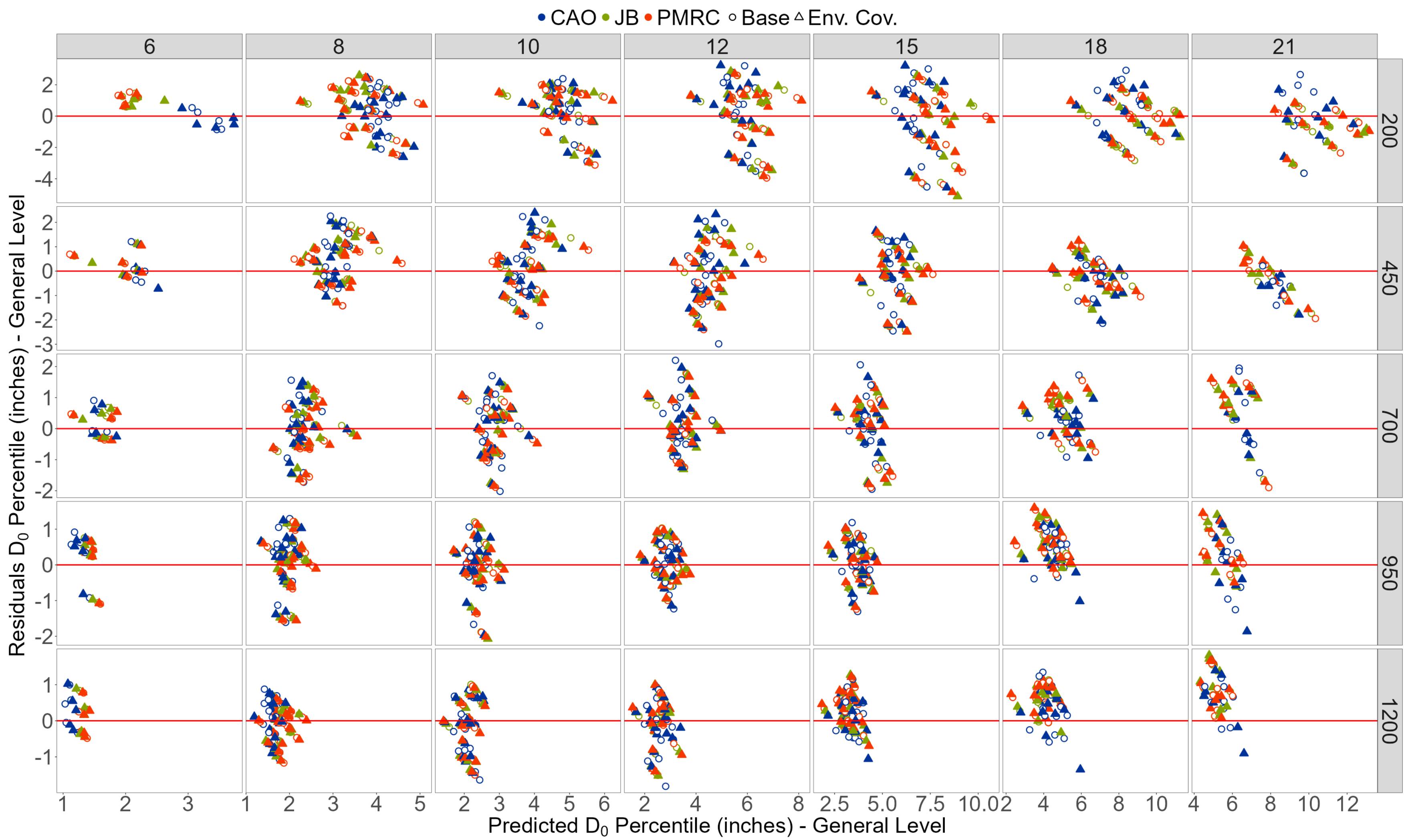

Figure 3.48: Residuals (obs. – pred.) from the 484 plots for three models for the D_0 percentile under two modeling approaches: (i) the base model (without environmental co-variables), and (ii) the adapted model (accounting for environmental co-variables), conducted for the general modeling level. Residuals are plotted against predicted percentiles across all seven ages and five planting densities.

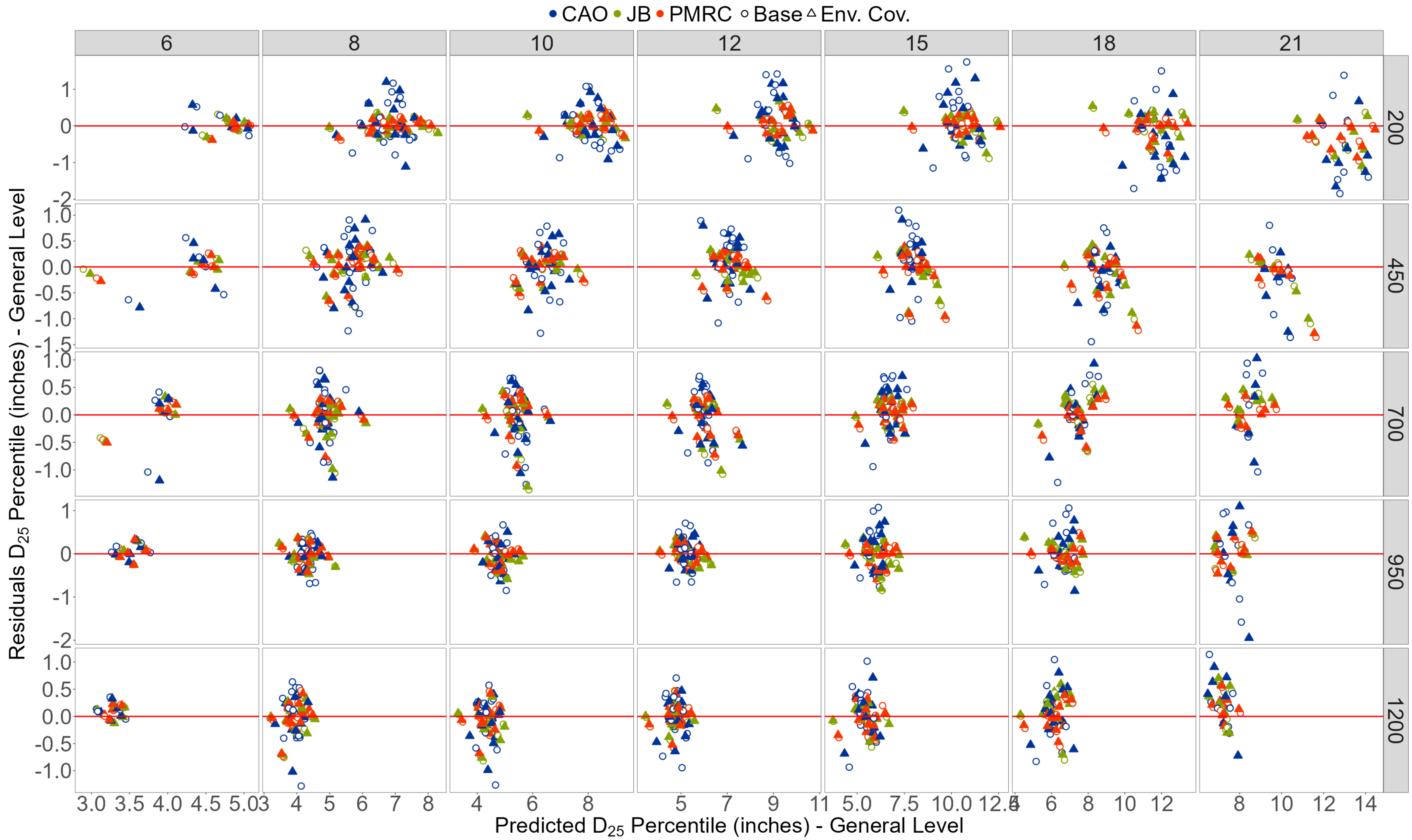

Figure 3.49: Residuals (obs. – pred.) from the 484 plots for three models for the D_{25} percentile under two modeling approaches: (i) the base model (without environmental co-variables), and (ii) the adapted model (accounting for environmental co-variables), conducted at a general modeling level. Residuals are plotted against predicted percentiles across all seven ages and five planting densities.

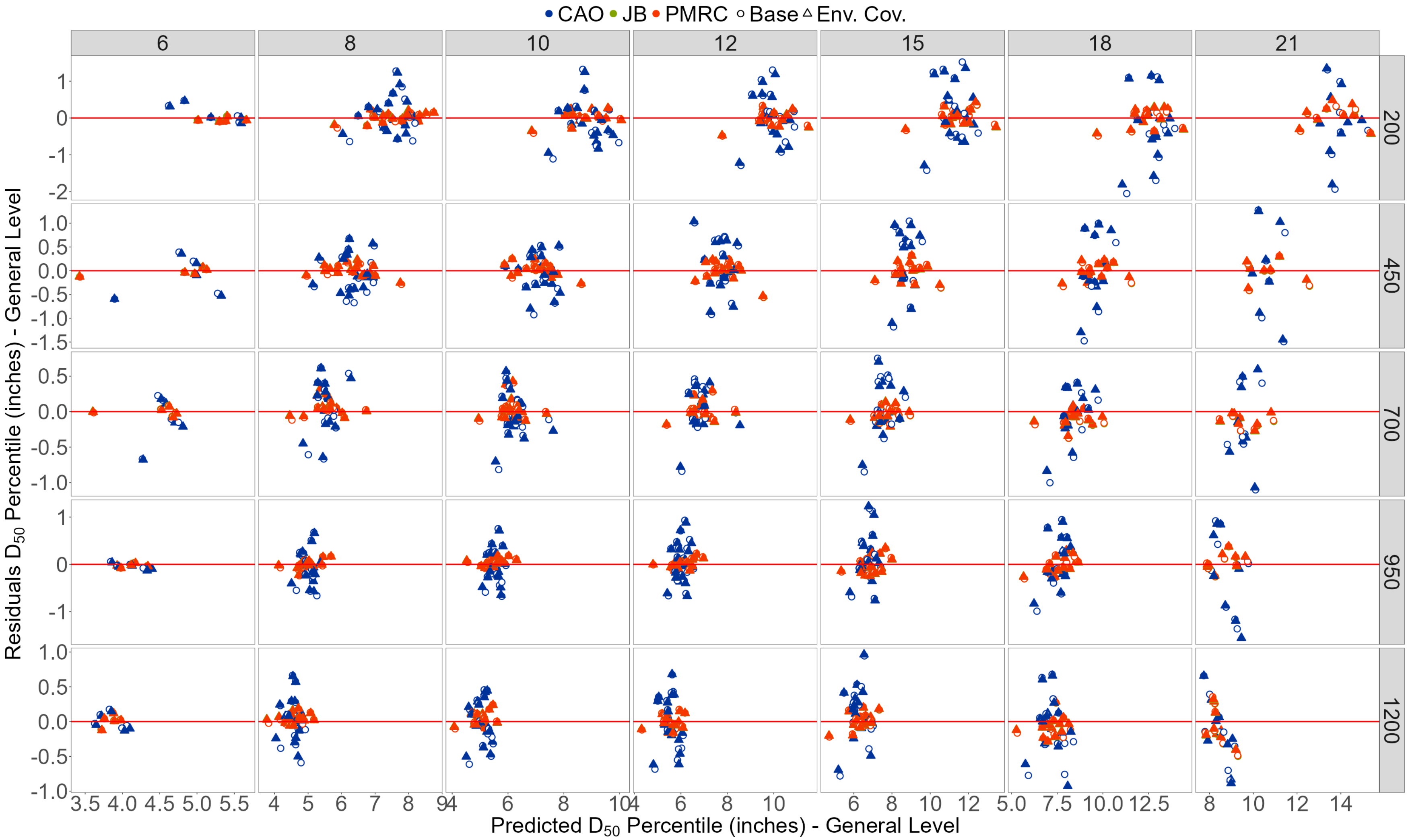

Figure 3.50: Residuals (obs. – pred.) from the 484 plots for three models for the D_{50} percentile under two modeling approaches: (i) the base model (without environmental co-variables), and (ii) the adapted model (accounting for environmental co-variables), conducted for the general modeling level. Residuals are plotted against predicted percentiles across all seven ages and five planting densities.

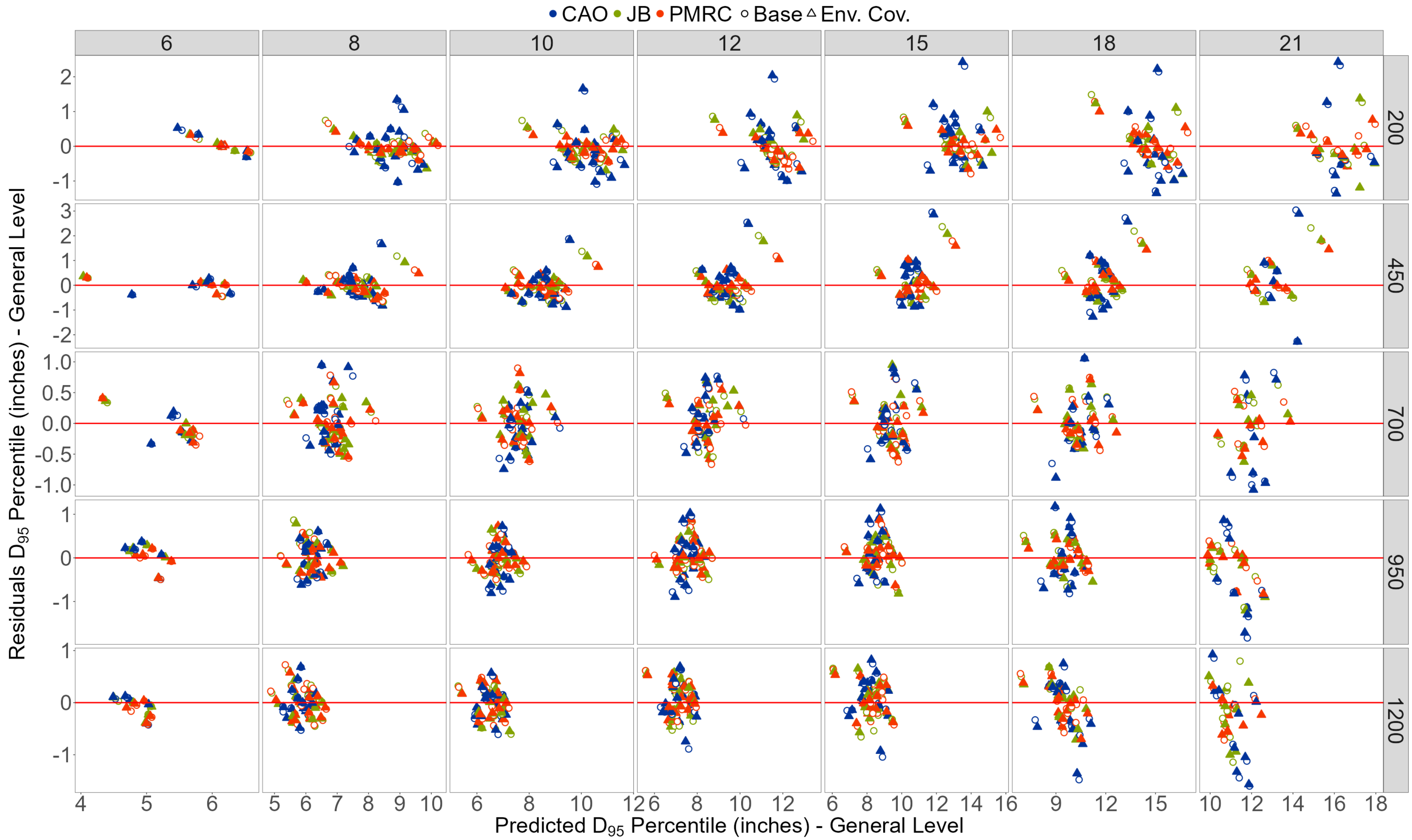

Figure 3.51: Residuals (obs. – pred.) from the 484 plots for three models for the D_{95} percentile under two modeling approaches: (i) the base model (without environmental co-variables), and (ii) the adapted model(accounting for environmental co-variables), conducted for the general modeling level. Residuals are plotted against predicted percentiles across all seven ages and five planting densities

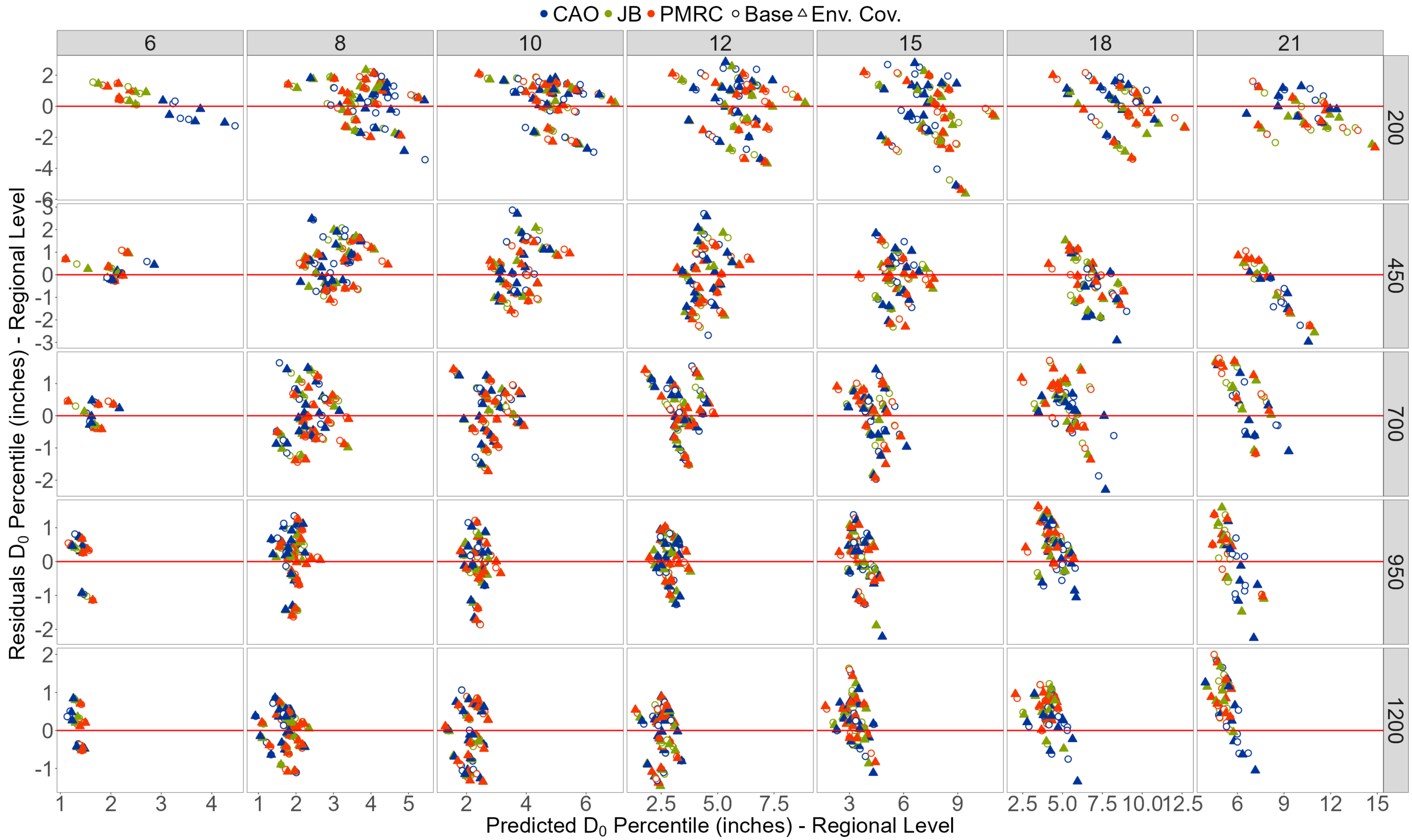

Figure 3.52: Residuals (obs. – pred.) from the 484 plots for three models for the D_0 percentile under two modeling approaches: (i) the base model (without environmental co-variables), and (ii) the adapted model (accounting for environmental co-variables), conducted for the regional modeling level. Residuals are plotted against predicted percentiles across all seven ages and five planting densities.

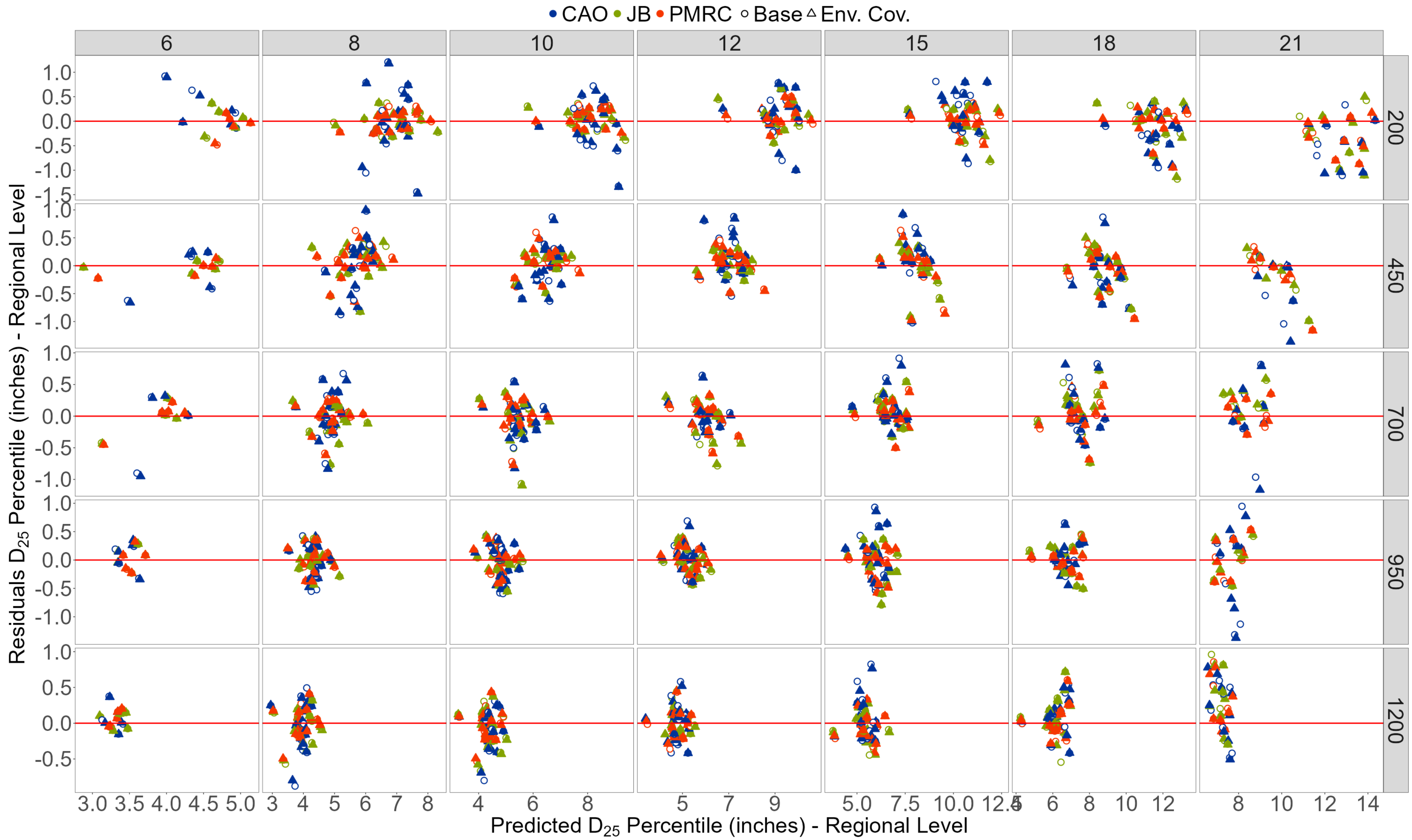

Figure 3.53: Residuals (obs. – pred.) from the 484 plots for three models for the D_{25} percentile under two modeling approaches: (i) the base model (without environmental co-variables), and (ii) the adapted model (accounting for environmental co-variables), conducted for the regional modeling level. Residuals are plotted against predicted percentiles across all seven ages and five planting densities.

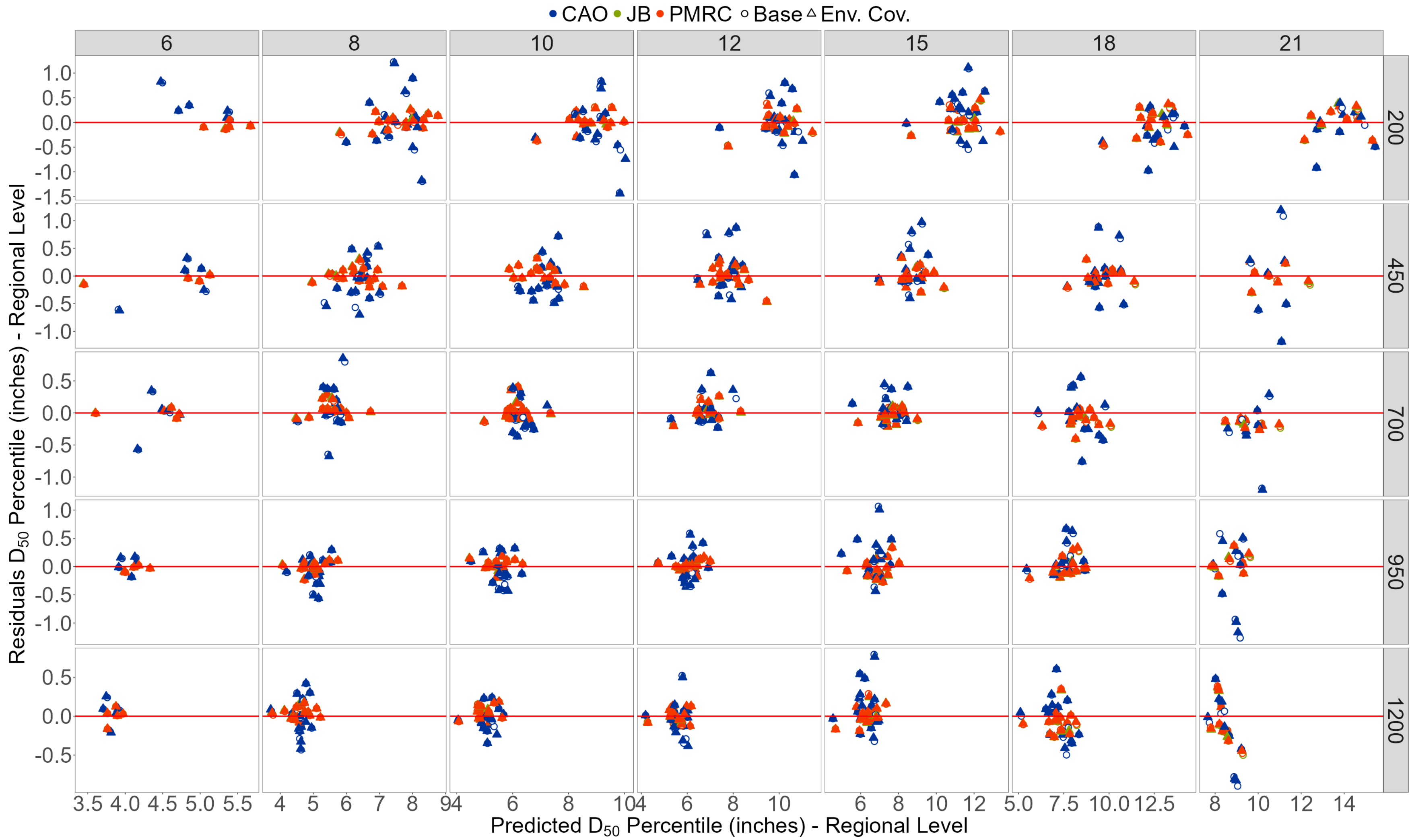

Figure 3.54: Residuals (obs. – pred.) from the 484 plots for three models for the D_{50} percentile under two modeling approaches: (i) the base model (without environmental co-variables), and (ii) the adapted model (accounting for environmental co-variables), conducted for the regional modeling level. Residuals are plotted against predicted percentiles across all seven ages and five planting densities

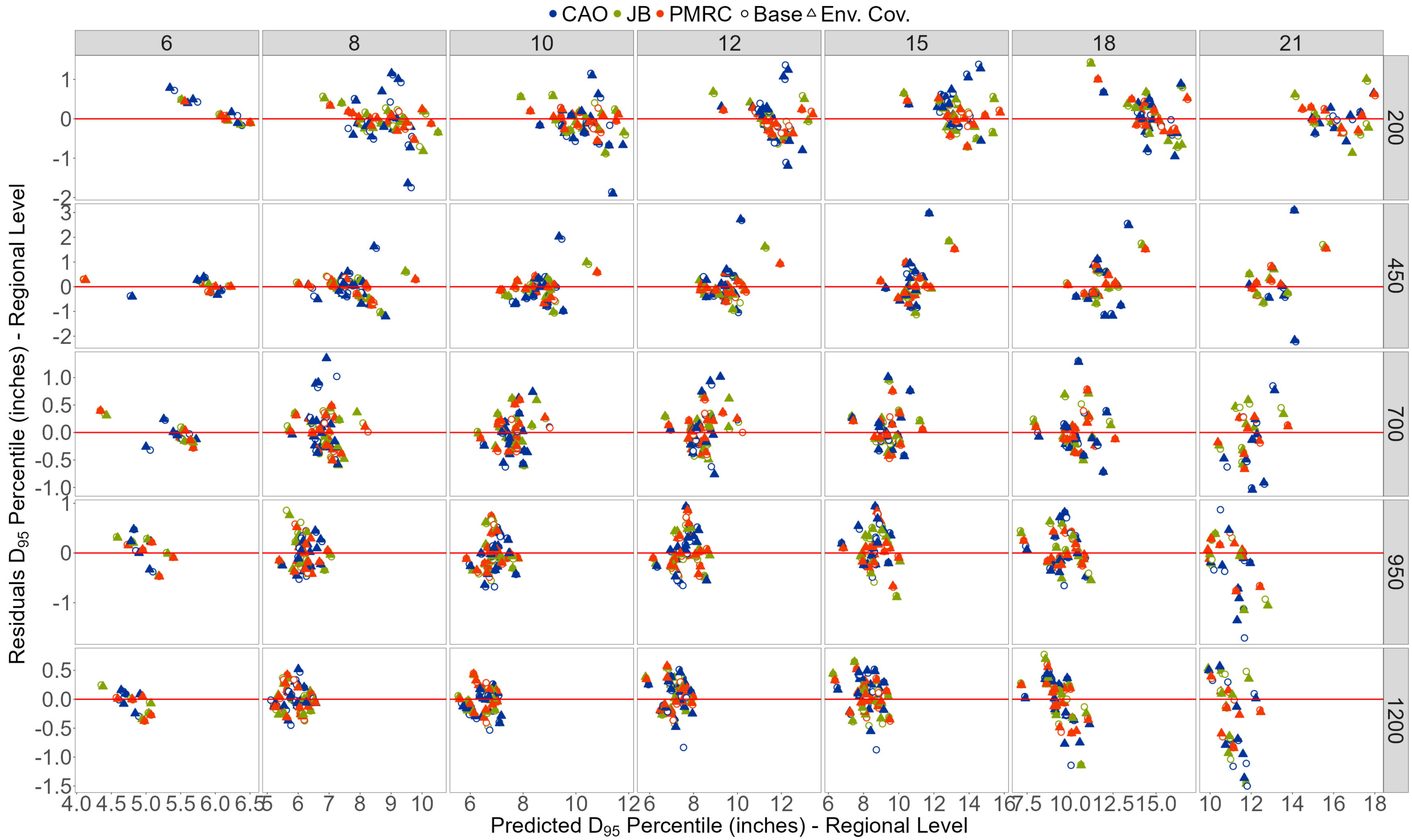

Figure 3.55: Residuals (obs. – pred.) from the 484 plots for three models for the D_{95} percentile under two modeling approaches: (i) the base model (without environmental co-variables), and (ii) the adapted model (accounting for environmental co-variables), conducted for the regional modeling level. Residuals are plotted against predicted percentiles across all seven ages and five planting densities.

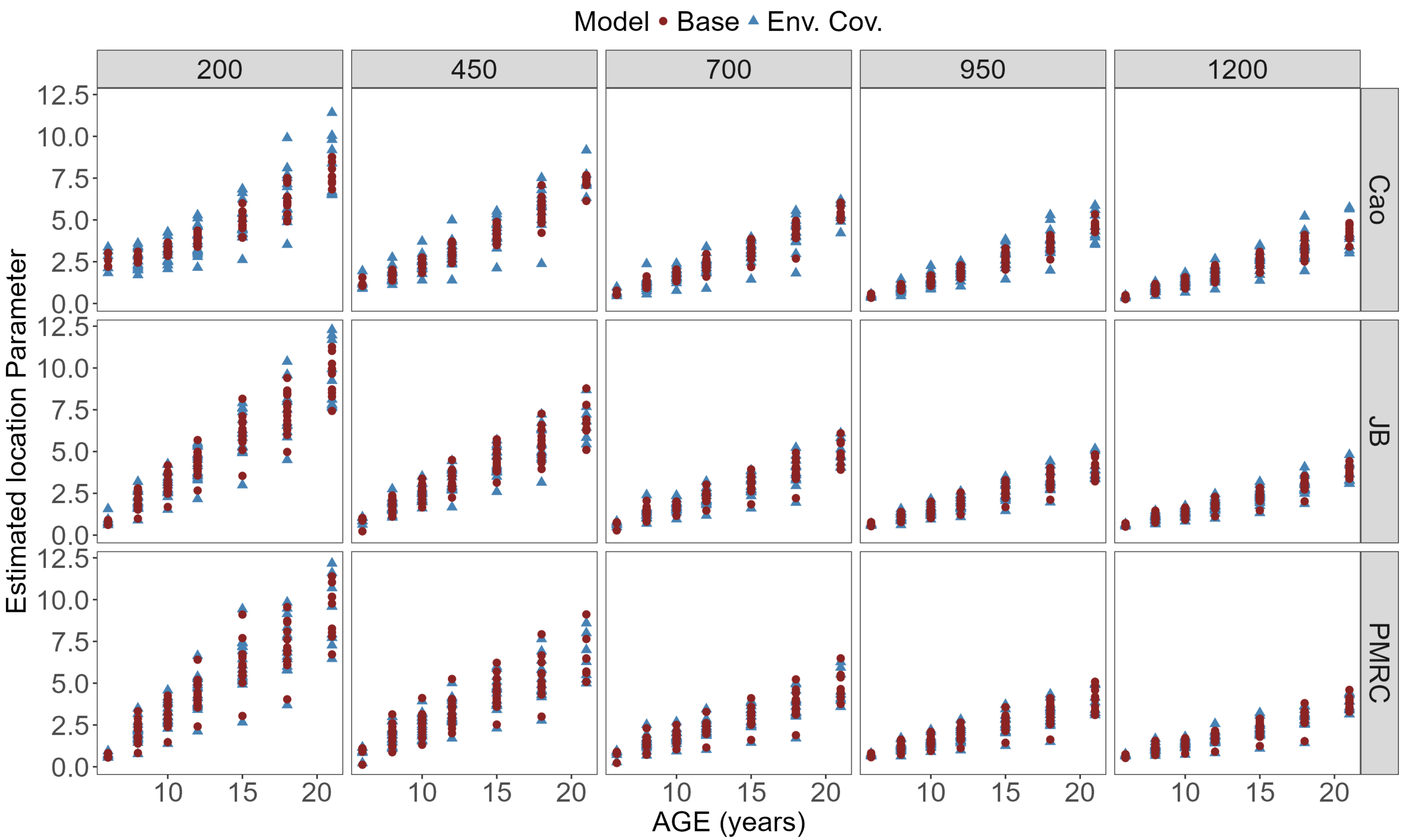

Figure 3.56: Weibull location parameter estimated for diameter distribution based on three percentiles models under two modeling approaches: (i) the base model (without environmental co-variables), and (ii) the adapted model (accounting for environmental co-variables), conducted for the general modeling level. across seven ages and five planting densities.

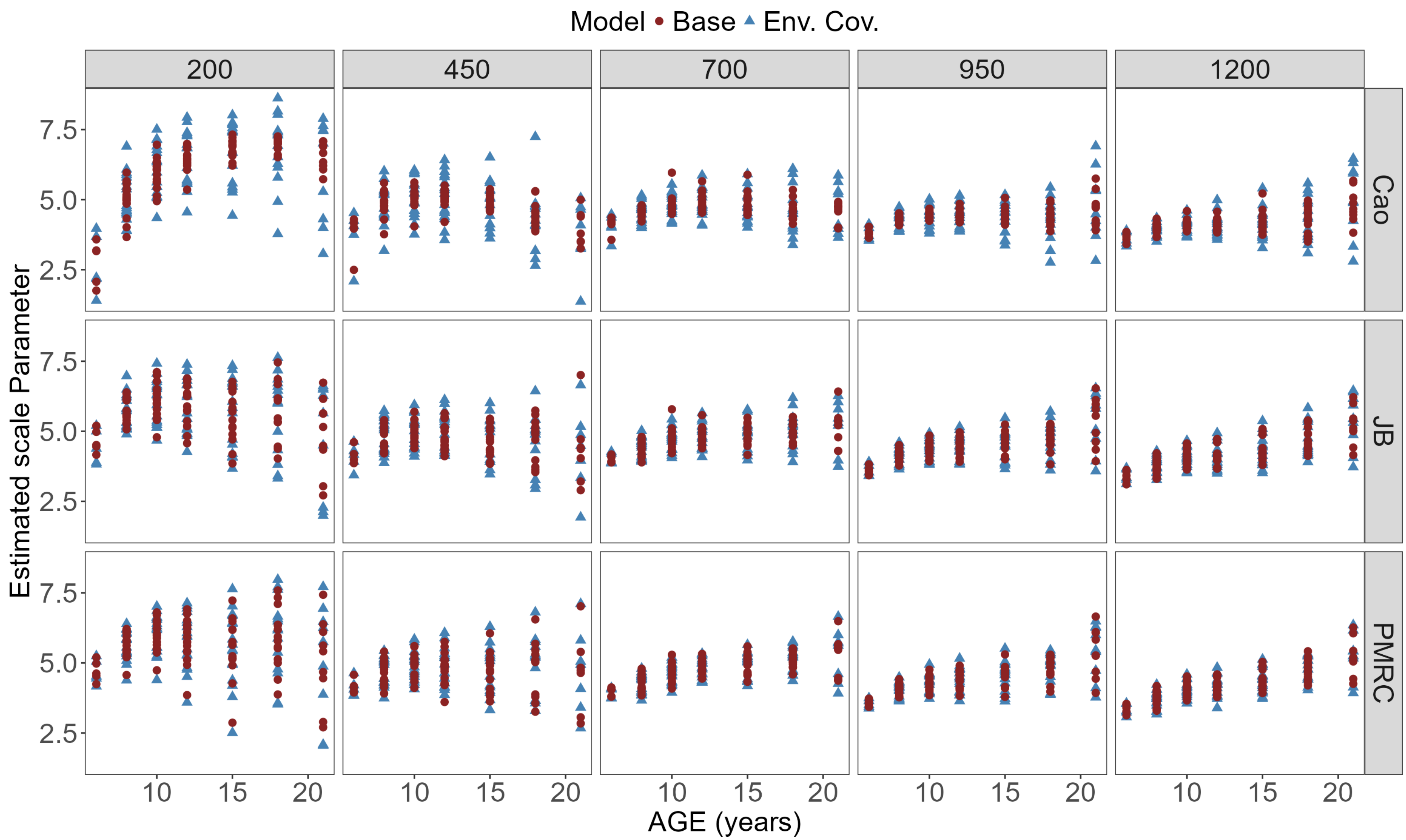

Figure 3.57: Weibull scale parameter estimated for diameter distribution based on three percentiles models under two modeling approaches: (i) the base model (without environmental co-variables), and (ii) the adapted model (accounting for environmental co-variables), conducted for the general modeling level. across seven ages and five planting densities.

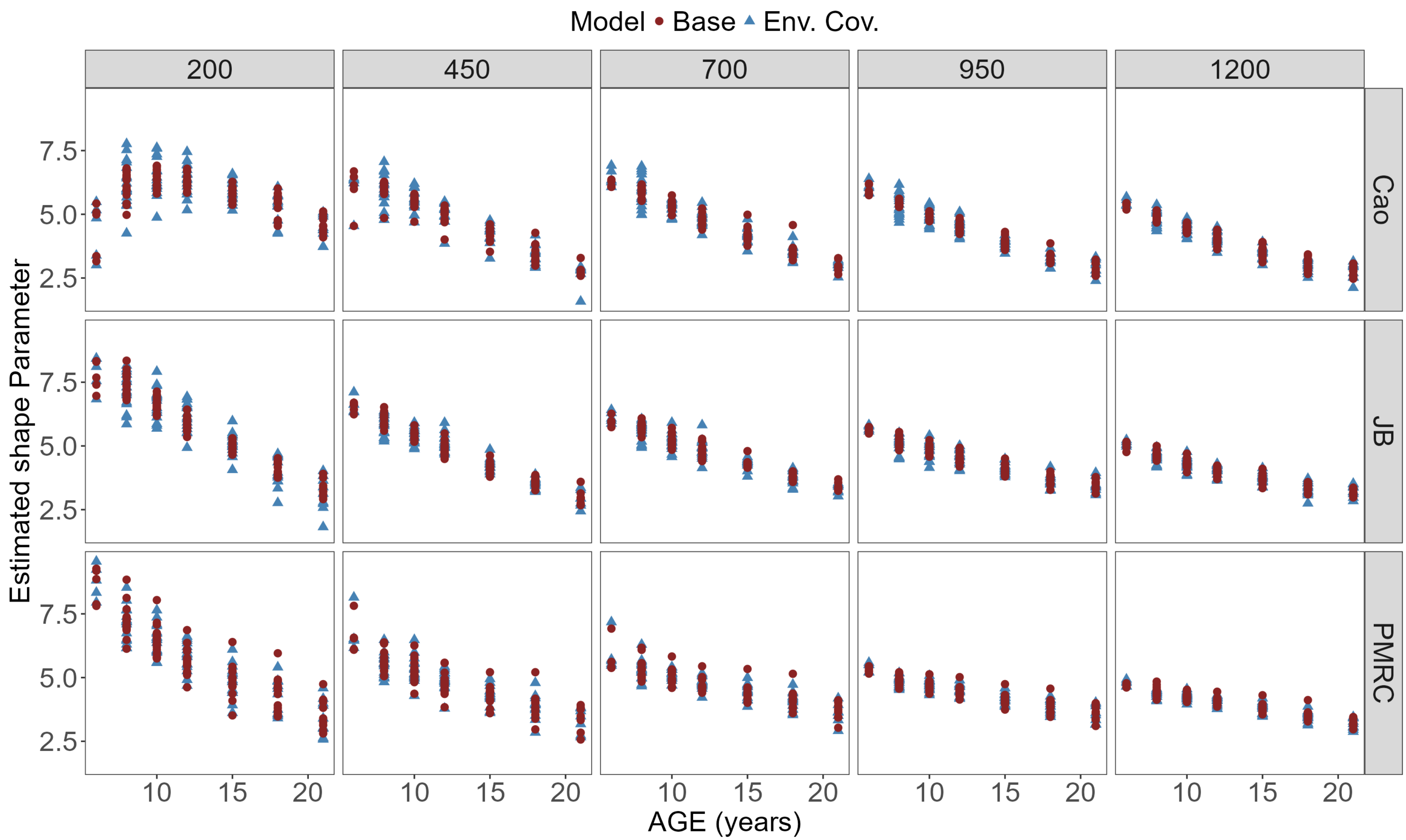

Figure 3.58: Weibull shape parameter estimated for diameter distribution based on three percentiles models under two modeling approaches: (i) the base model (without environmental co-variables), and (ii) the adapted model (accounting for environmental co-variables), conducted for the general modeling level. across seven ages and five planting densities.

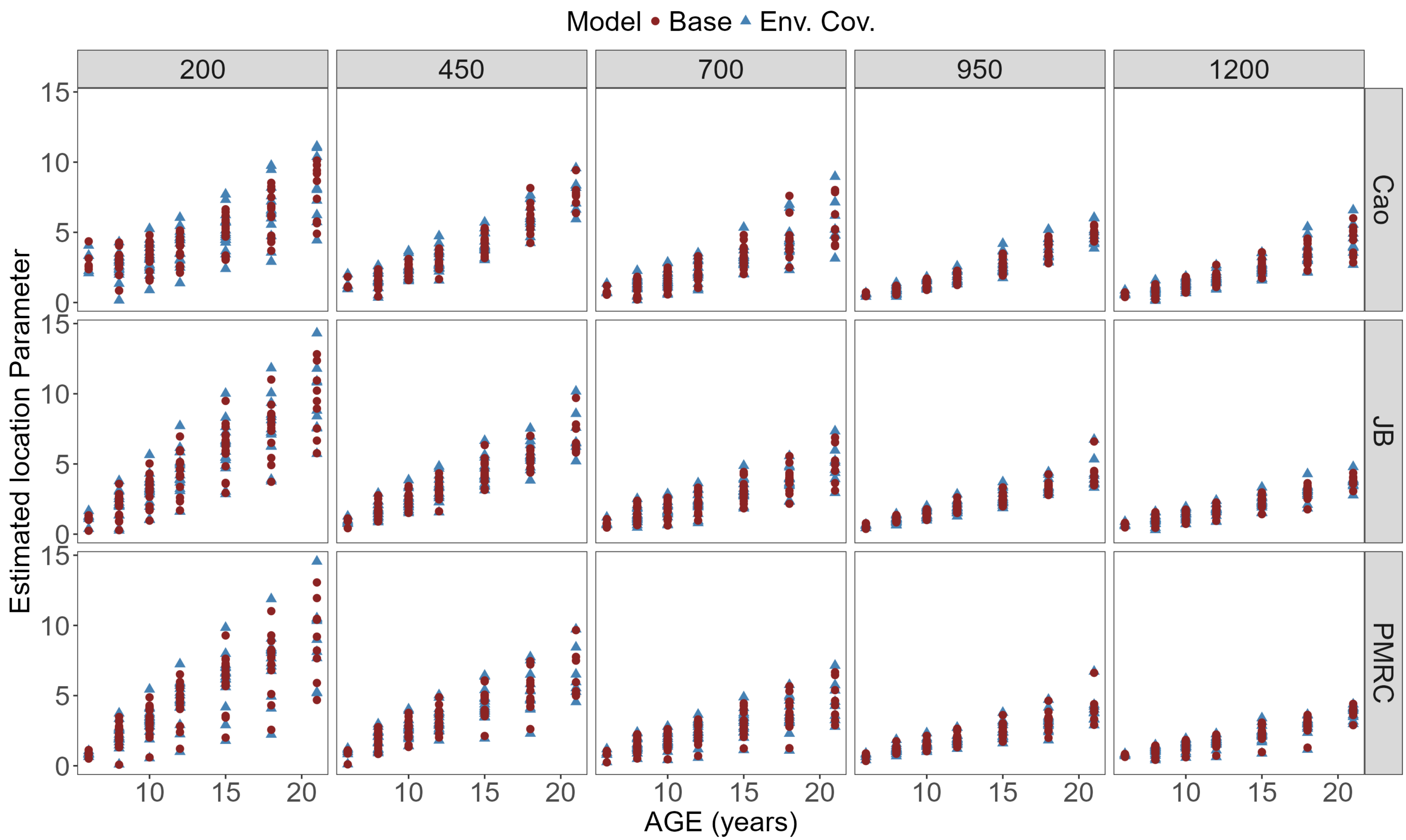

Figure 3.59: Weibull location parameter estimated for diameter distribution based on three percentiles models under two modeling approaches: (i) the base model (without environmental co-variables), and (ii) the adapted model (accounting for environmental co-variables), conducted for the regional modeling level. across seven ages and five planting densities.

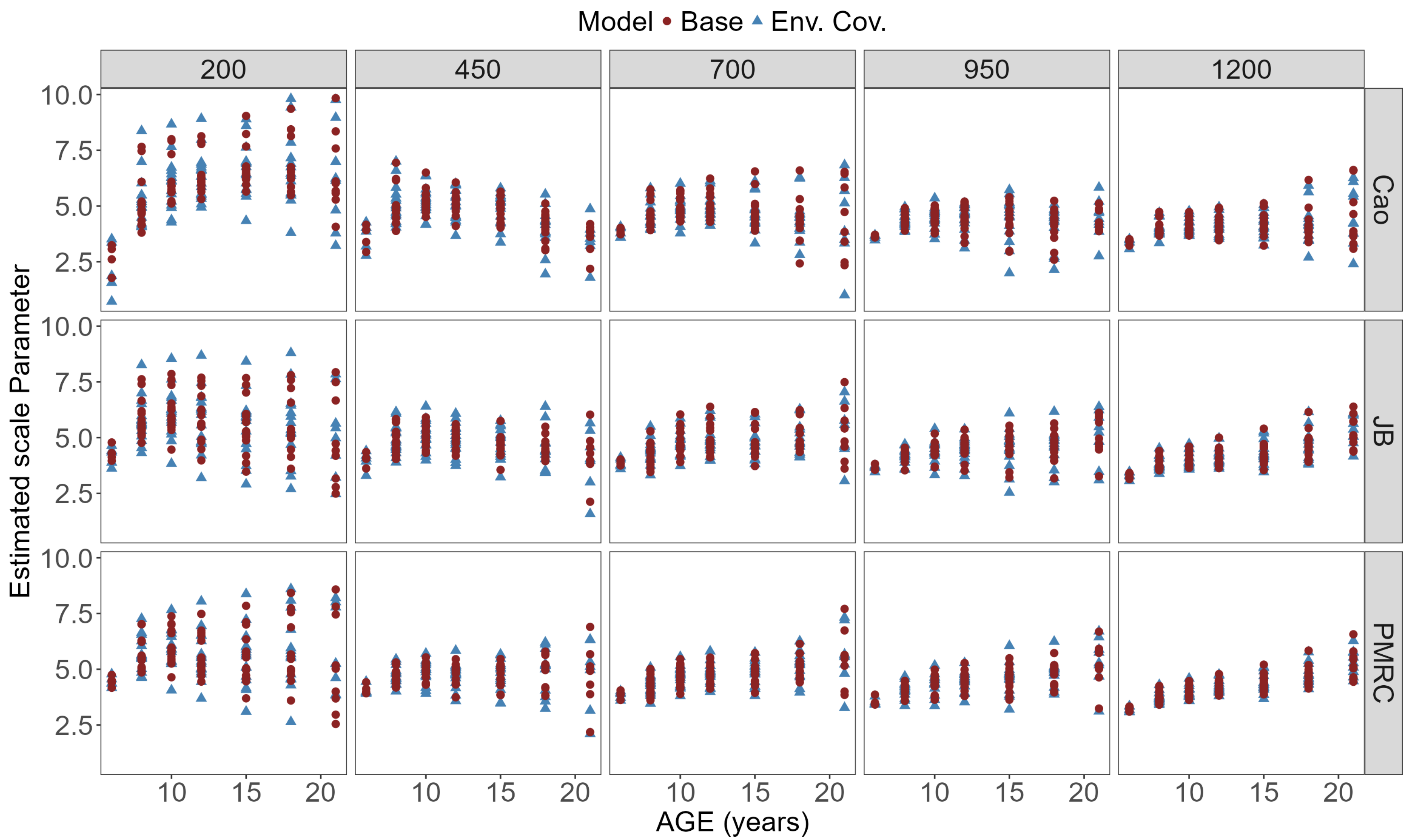

Figure 3.60: Weibull scale parameter estimated for diameter distribution based on three percentiles models under two modeling approaches: (i) the base model (without environmental co-variables), and (ii) the adapted model (accounting for environmental co-variables), conducted for the regional modeling level. across seven ages and five planting densities.

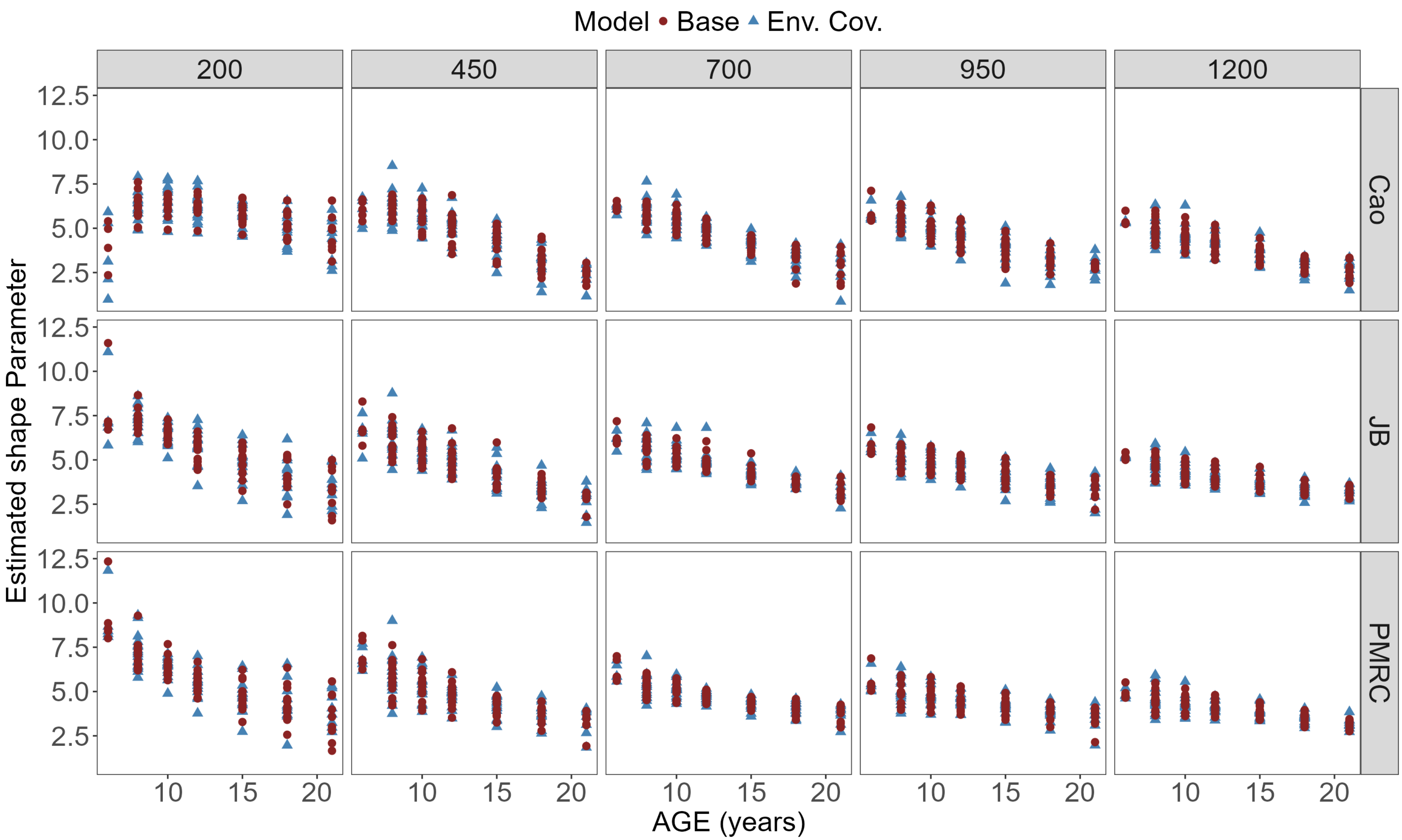

Figure 3.61: Weibull shape parameter estimated for diameter distribution based on three percentiles models under two modeling approaches: (i) the base model (without environmental co-variables), and (ii) the adapted model (accounting for environmental co-variables), conducted for the regional modeling level. across seven ages and five planting densities.

Table 3.28: Average three-parameter Weibull distribution for Cao model under two modeling approaches: (i) the base model (without environmental co-variables), and (ii) the adapted model (accounting for environmental co-variables), conducted for the general modeling level across seven ages and five planting densities.

AGE	PLTPA	Cao					
		Base Model			Env. Cov. Model		
		location ($\hat{a}$)	scale ($\hat{b}$)	shape ($\hat{c}$)	location ($\hat{a}$)	scale ($\hat{b}$)	shape ($\hat{c}$)
6	200	2.61	2.75	4.40	2.66	2.69	4.38
	450	1.19	3.79	5.97	1.24	3.74	5.98
	700	0.59	4.10	6.18	0.63	4.05	6.46
	950	0.45	3.79	5.97	0.45	3.79	6.04
	1200	0.39	3.65	5.36	0.42	3.62	5.53
8	200	2.72	5.03	6.20	2.65	5.11	6.20
	450	1.73	4.90	5.99	1.72	4.91	5.92
	700	1.16	4.59	5.88	1.19	4.56	5.88
	950	0.95	4.30	5.41	0.97	4.28	5.38
	1200	0.86	3.98	4.88	0.90	3.94	4.83
10	200	3.20	5.97	6.41	3.13	6.04	6.42
	450	2.40	5.08	5.50	2.38	5.09	5.55
	700	1.67	4.82	5.30	1.68	4.81	5.27
	950	1.41	4.42	4.92	1.40	4.42	4.94
	1200	1.29	4.09	4.43	1.31	4.07	4.45
12	200	3.82	6.42	6.28	3.78	6.45	6.36
	450	3.04	5.08	5.00	3.03	5.09	5.08
	700	2.25	4.87	4.78	2.27	4.85	4.84
	950	1.90	4.45	4.51	1.91	4.43	4.56
	1200	1.77	4.10	4.03	1.78	4.08	4.07
15	200	4.87	6.81	5.85	5.00	6.67	5.92
	450	4.21	4.92	4.23	4.26	4.86	4.24
	700	3.11	4.82	4.21	3.16	4.77	4.20
	950	2.69	4.44	3.90	2.78	4.35	3.89
	1200	2.45	4.19	3.53	2.50	4.13	3.54
18	200	6.17	6.98	5.40	6.38	6.76	5.34
	450	5.66	4.44	3.49	5.78	4.31	3.41
	700	4.20	4.58	3.57	4.19	4.60	3.52
	950	3.64	4.37	3.33	3.68	4.33	3.29
	1200	3.37	4.28	3.04	3.35	4.30	3.01
21	200	7.84	6.56	4.63	8.35	6.02	4.44
	450	7.21	3.99	2.78	7.40	3.78	2.65
	700	5.49	4.56	2.97	5.38	4.69	3.00
	950	4.68	4.65	2.93	4.54	4.79	2.96
	1200	4.25	4.79	2.74	4.05	4.99	2.77

Table 3.29: Average three-parameter Weibull distribution for JB model under two modeling approaches: (i) the base model (without environmental co-variables), and (ii) the adapted model (accounting for environmental co-variables), conducted for the general modeling level across seven ages and five planting densities.

AGE	PLTPA	JB					
		Base Model			Env. Cov. Model		
		location ($\hat{a}$)	scale ($\hat{b}$)	shape ($\hat{c}$)	location ($\hat{a}$)	scale ($\hat{b}$)	shape ($\hat{c}$)
6	200	0.73	4.66	7.74	0.93	4.46	7.87
	450	0.82	4.17	6.52	0.89	4.09	6.61
	700	0.65	4.04	5.97	0.66	4.02	6.13
	950	0.64	3.60	5.61	0.63	3.61	5.73
	1200	0.64	3.40	5.00	0.62	3.42	5.10
8	200	2.04	5.72	7.42	2.06	5.70	7.20
	450	1.78	4.84	6.04	1.75	4.87	5.86
	700	1.35	4.40	5.73	1.33	4.42	5.61
	950	1.12	4.13	5.15	1.11	4.14	5.05
	1200	1.03	3.81	4.66	1.04	3.81	4.56
10	200	3.08	6.08	6.62	3.11	6.05	6.66
	450	2.50	4.97	5.40	2.50	4.97	5.45
	700	1.74	4.75	5.21	1.77	4.72	5.21
	950	1.47	4.35	4.79	1.49	4.33	4.82
	1200	1.33	4.05	4.30	1.36	4.02	4.31
12	200	4.32	5.91	5.87	4.25	5.97	6.14
	450	3.27	4.84	4.89	3.19	4.92	5.12
	700	2.30	4.83	4.76	2.30	4.82	4.89
	950	1.91	4.44	4.48	1.92	4.43	4.58
	1200	1.73	4.13	3.99	1.76	4.10	4.06
15	200	6.05	5.59	4.95	5.96	5.68	5.10
	450	4.43	4.69	4.15	4.36	4.75	4.27
	700	3.04	4.89	4.29	3.07	4.86	4.32
	950	2.59	4.54	4.06	2.63	4.50	4.09
	1200	2.31	4.33	3.70	2.34	4.30	3.73
18	200	7.37	5.77	4.15	7.44	5.69	4.02
	450	5.40	4.72	3.60	5.45	4.66	3.50
	700	3.78	5.02	3.81	3.79	5.02	3.76
	950	3.27	4.75	3.66	3.31	4.71	3.60
	1200	2.97	4.70	3.38	2.99	4.68	3.33
21	200	9.46	4.88	3.32	9.59	4.72	3.10
	450	6.84	4.38	3.00	6.87	4.34	2.91
	700	4.94	5.15	3.40	4.87	5.22	3.35
	950	4.05	5.31	3.48	4.01	5.36	3.45
	1200	3.87	5.20	3.20	3.70	5.37	3.24

Table 3.30: Average three-parameter Weibull distribution for PMRC model under two modeling approaches: (i) the base model (without environmental co-variables), and (ii) the adapted model (accounting for environmental co-variables), conducted for the general modeling level across seven ages and five planting densities.

AGE	PLTPA	PMRC					
		Base Model			Env. Cov. Model		
		location ($\hat{a}$)	scale ($\hat{b}$)	shape ($\hat{c}$)	location ($\hat{a}$)	scale ($\hat{b}$)	shape ($\hat{c}$)
6	200	0.67	4.72	8.60	0.69	4.69	8.78
	450	0.83	4.15	6.63	0.86	4.12	6.75
	700	0.72	3.97	5.74	0.74	3.95	5.91
	950	0.68	3.57	5.29	0.70	3.54	5.40
	1200	0.67	3.37	4.69	0.69	3.34	4.78
8	200	2.10	5.66	7.20	2.12	5.65	7.10
	450	1.91	4.71	5.65	1.94	4.69	5.55
	700	1.42	4.33	5.36	1.44	4.31	5.31
	950	1.19	4.06	4.89	1.21	4.04	4.83
	1200	1.09	3.75	4.42	1.12	3.72	4.36
10	200	3.13	6.03	6.46	3.16	6.00	6.50
	450	2.56	4.91	5.24	2.57	4.89	5.30
	700	1.79	4.71	5.08	1.81	4.68	5.08
	950	1.51	4.32	4.70	1.51	4.31	4.73
	1200	1.35	4.03	4.25	1.35	4.03	4.27
12	200	4.37	5.86	5.71	4.40	5.82	5.82
	450	3.29	4.82	4.80	3.30	4.81	4.91
	700	2.30	4.83	4.72	2.31	4.81	4.80
	950	1.92	4.43	4.48	1.92	4.43	4.55
	1200	1.71	4.16	4.06	1.72	4.15	4.11
15	200	6.08	5.57	4.85	6.13	5.51	4.86
	450	4.37	4.75	4.26	4.36	4.76	4.29
	700	2.98	4.95	4.46	3.00	4.94	4.45
	950	2.56	4.58	4.16	2.57	4.56	4.18
	1200	2.28	4.37	3.80	2.28	4.37	3.82
18	200	7.26	5.87	4.41	7.19	5.94	4.34
	450	5.28	4.84	3.92	5.20	4.92	3.87
	700	3.67	5.13	4.15	3.61	5.20	4.10
	950	3.17	4.86	3.89	3.14	4.89	3.84
	1200	2.92	4.75	3.54	2.90	4.78	3.51
21	200	9.26	5.08	3.58	9.22	5.11	3.48
	450	6.59	4.65	3.39	6.51	4.72	3.34
	700	4.84	5.25	3.67	4.78	5.31	3.60
	950	4.00	5.36	3.57	3.98	5.39	3.54
	1200	3.86	5.21	3.23	3.83	5.23	3.19

Table 3.31: Average three-parameter Weibull distribution for Cao model under two modeling approaches: (i) the base model (without environmental co-variables), and (ii) the adapted model (accounting for environmental co-variables), conducted for the regional modeling level across seven ages and five planting densities.

AGE	PLTPA	Cao					
		Base Model			Env. Cov. Model		
		location ($\hat{a}$)	scale ($\hat{b}$)	shape ($\hat{c}$)	location ($\hat{a}$)	scale ($\hat{b}$)	shape ($\hat{c}$)
6	200	2.67	2.67	4.15	3.02	2.21	3.49
	450	1.25	3.67	6.06	1.29	3.63	5.91
	700	0.78	3.86	6.18	0.83	3.81	6.15
	950	0.57	3.64	5.86	0.60	3.61	5.80
	1200	0.59	3.41	5.43	0.64	3.36	5.34
8	200	2.77	5.06	6.14	2.65	5.17	6.25
	450	1.68	4.96	6.11	1.63	5.01	6.17
	700	1.17	4.58	5.78	1.17	4.58	5.83
	950	0.91	4.37	5.44	0.89	4.38	5.46
	1200	0.86	3.98	4.95	0.87	3.98	4.93
10	200	3.21	5.99	6.39	3.19	6.01	6.45
	450	2.30	5.18	5.67	2.32	5.15	5.69
	700	1.62	4.88	5.40	1.64	4.86	5.43
	950	1.34	4.51	5.01	1.34	4.50	5.00
	1200	1.30	4.09	4.49	1.31	4.08	4.48
12	200	3.89	6.38	6.22	3.94	6.32	6.21
	450	2.98	5.14	5.14	3.03	5.09	5.13
	700	2.21	4.93	4.91	2.23	4.90	4.95
	950	1.83	4.54	4.59	1.84	4.54	4.62
	1200	1.70	4.18	4.14	1.71	4.16	4.15
15	200	4.92	6.73	5.81	5.05	6.59	5.69
	450	4.24	4.88	4.25	4.25	4.88	4.23
	700	3.20	4.73	4.14	3.23	4.71	4.13
	950	2.66	4.48	3.92	2.68	4.45	3.91
	1200	2.43	4.21	3.58	2.45	4.19	3.60
18	200	6.37	6.72	5.22	6.49	6.60	5.03
	450	5.96	4.10	3.25	6.06	3.99	3.14
	700	4.34	4.43	3.42	4.33	4.44	3.39
	950	3.80	4.17	3.20	3.82	4.14	3.16
	1200	3.51	4.11	2.95	3.51	4.10	2.92
21	200	7.87	6.50	4.60	8.04	6.32	4.42
	450	7.71	3.55	2.42	7.73	3.50	2.44
	700	5.66	4.45	2.90	5.63	4.45	2.87
	950	4.88	4.44	2.88	4.87	4.44	2.92
	1200	4.49	4.52	2.60	4.42	4.59	2.66

Table 3.32: Average three-parameter Weibull distribution for JB model under two modeling approaches: (i) the base model (without environmental co-variables), and (ii) the adapted model (accounting for environmental co-variables), conducted for the regional modeling level across seven ages and five planting densities.

AGE	PLTPA	JB					
		Base Model			Env. Cov. Model		
		location ($\hat{a}$)	scale ($\hat{b}$)	shape ($\hat{c}$)	location ($\hat{a}$)	scale ($\hat{b}$)	shape ($\hat{c}$)
6	200	1.01	4.30	7.93	1.13	4.18	7.59
	450	0.88	4.04	6.80	0.94	3.98	6.52
	700	0.76	3.88	6.30	0.80	3.85	6.15
	950	0.58	3.63	5.84	0.57	3.65	5.80
	1200	0.69	3.31	5.23	0.69	3.31	5.18
8	200	2.05	5.78	7.24	2.05	5.78	7.25
	450	1.73	4.89	6.13	1.70	4.93	6.18
	700	1.37	4.37	5.61	1.36	4.39	5.67
	950	1.08	4.19	5.15	1.04	4.23	5.21
	1200	1.04	3.80	4.69	1.03	3.81	4.70
10	200	3.09	6.11	6.48	3.09	6.12	6.55
	450	2.40	5.08	5.51	2.41	5.07	5.54
	700	1.72	4.78	5.25	1.74	4.76	5.29
	950	1.43	4.41	4.83	1.45	4.39	4.83
	1200	1.39	4.00	4.31	1.41	3.99	4.30
12	200	4.39	5.86	5.71	4.38	5.87	5.79
	450	3.19	4.93	5.01	3.18	4.93	5.03
	700	2.25	4.89	4.88	2.26	4.87	4.92
	950	1.88	4.50	4.50	1.89	4.49	4.52
	1200	1.71	4.16	4.06	1.75	4.13	4.03
15	200	6.09	5.52	4.87	6.07	5.53	4.89
	450	4.44	4.68	4.17	4.40	4.72	4.20
	700	3.13	4.81	4.22	3.14	4.80	4.21
	950	2.53	4.61	4.12	2.56	4.58	4.10
	1200	2.32	4.33	3.73	2.35	4.30	3.72
18	200	7.51	5.56	4.13	7.54	5.52	4.07
	450	5.56	4.53	3.46	5.68	4.40	3.34
	700	3.86	4.94	3.76	3.85	4.95	3.73
	950	3.33	4.65	3.64	3.39	4.59	3.57
	1200	3.00	4.65	3.35	3.02	4.63	3.31
21	200	9.42	4.87	3.32	8.95	5.18	3.54
	450	7.07	4.24	2.83	7.26	4.02	2.73
	700	4.93	5.24	3.33	4.94	5.23	3.28
	950	4.26	5.09	3.37	4.29	5.05	3.33
	1200	3.77	5.29	3.17	3.72	5.35	3.19

Table 3.33: Average three-parameter Weibull distribution for PMRC model under two modeling approaches: (i) the base model (without environmental co-variables), and (ii) the adapted model (accounting for environmental co-variables), conducted for the regional modeling level across seven ages and five planting densities.

AGE	PLTPA	PMRC					
		Base Model			Env. Cov. Model		
		location ($\hat{a}$)	scale ($\hat{b}$)	shape ($\hat{c}$)	location ($\hat{a}$)	scale ($\hat{b}$)	shape ($\hat{c}$)
6	200	0.83	4.46	9.23	0.85	4.45	9.05
	450	0.83	4.08	7.13	0.86	4.06	6.94
	700	0.77	3.87	6.21	0.80	3.84	6.11
	950	0.67	3.54	5.54	0.68	3.53	5.49
	1200	0.76	3.24	4.92	0.79	3.22	4.84
8	200	2.14	5.68	7.17	2.15	5.67	7.21
	450	1.92	4.71	5.82	1.92	4.70	5.85
	700	1.48	4.27	5.29	1.47	4.28	5.33
	950	1.18	4.09	4.96	1.17	4.10	4.98
	1200	1.10	3.74	4.51	1.10	3.74	4.52
10	200	3.19	6.02	6.36	3.21	6.00	6.39
	450	2.54	4.93	5.34	2.57	4.90	5.34
	700	1.80	4.70	5.11	1.82	4.68	5.12
	950	1.48	4.36	4.75	1.50	4.34	4.73
	1200	1.40	3.99	4.28	1.43	3.96	4.26
12	200	4.52	5.73	5.50	4.57	5.68	5.48
	450	3.31	4.80	4.83	3.35	4.76	4.80
	700	2.33	4.80	4.78	2.36	4.77	4.77
	950	1.88	4.50	4.52	1.89	4.49	4.53
	1200	1.70	4.17	4.11	1.72	4.16	4.09
15	200	6.14	5.47	4.73	6.12	5.48	4.75
	450	4.36	4.76	4.25	4.37	4.75	4.25
	700	3.04	4.90	4.38	3.05	4.89	4.38
	950	2.52	4.63	4.18	2.52	4.62	4.18
	1200	2.29	4.36	3.81	2.29	4.36	3.82
18	200	7.31	5.76	4.30	7.30	5.76	4.29
	450	5.20	4.91	3.84	5.20	4.90	3.81
	700	3.69	5.11	4.06	3.67	5.14	4.06
	950	3.17	4.82	3.85	3.15	4.84	3.86
	1200	2.92	4.74	3.52	2.91	4.74	3.51
21	200	9.06	5.25	3.59	8.31	5.85	3.99
	450	6.62	4.72	3.23	6.57	4.76	3.29
	700	4.65	5.52	3.70	4.59	5.59	3.72
	950	4.10	5.26	3.52	4.05	5.31	3.55
	1200	3.82	5.24	3.18	3.77	5.30	3.20

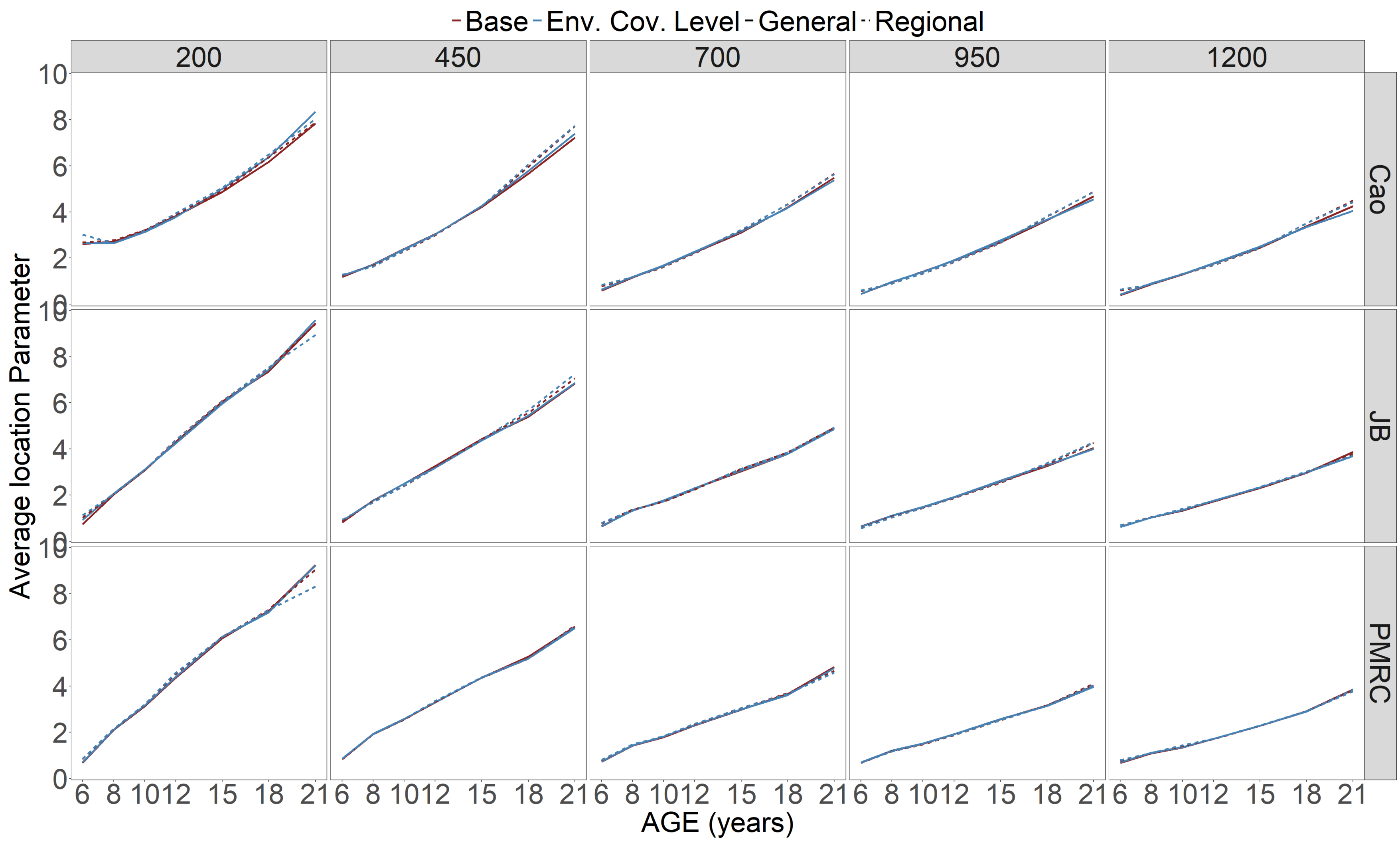

Figure 3.62: Average Weibull location parameter based on three percentile models, under two modeling approaches: (i) the base model (without environmental co-variables), and (ii) the adapted model (accounting for environmental co-variables), conducted for the general and regional modeling level across seven ages and five planting densities. The solid line represents general level, and the dashed line represents regional level.

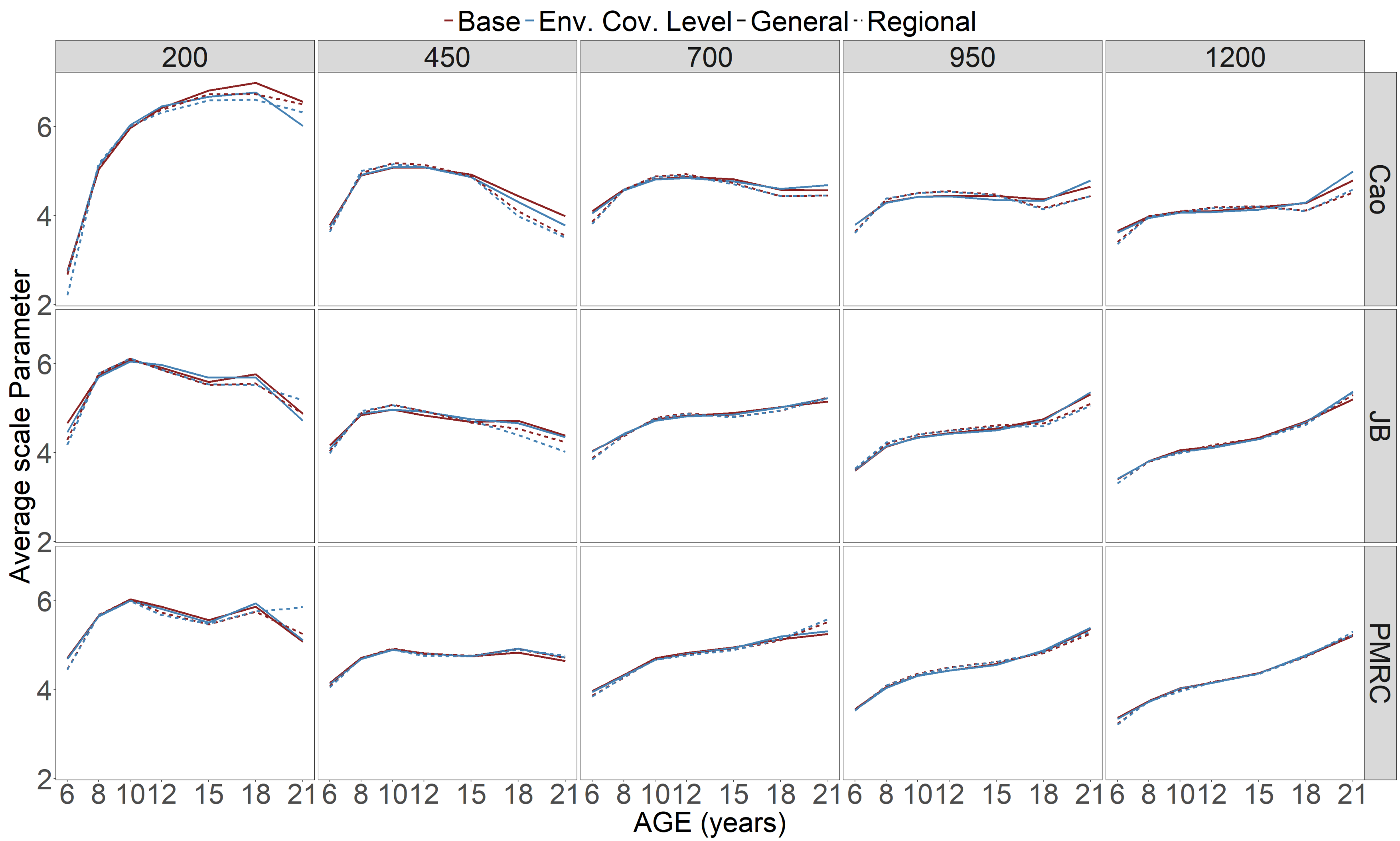

Figure 3.63: Average Weibull scale parameter based on three percentile models, under two modeling approaches: (i) the base model (without environmental co-variables), and (ii) the adapted model (accounting for environmental co-variables), conducted general and regional modeling level across seven ages and five planting densities. The solid line represents general level, and the dashed line represents regional level.

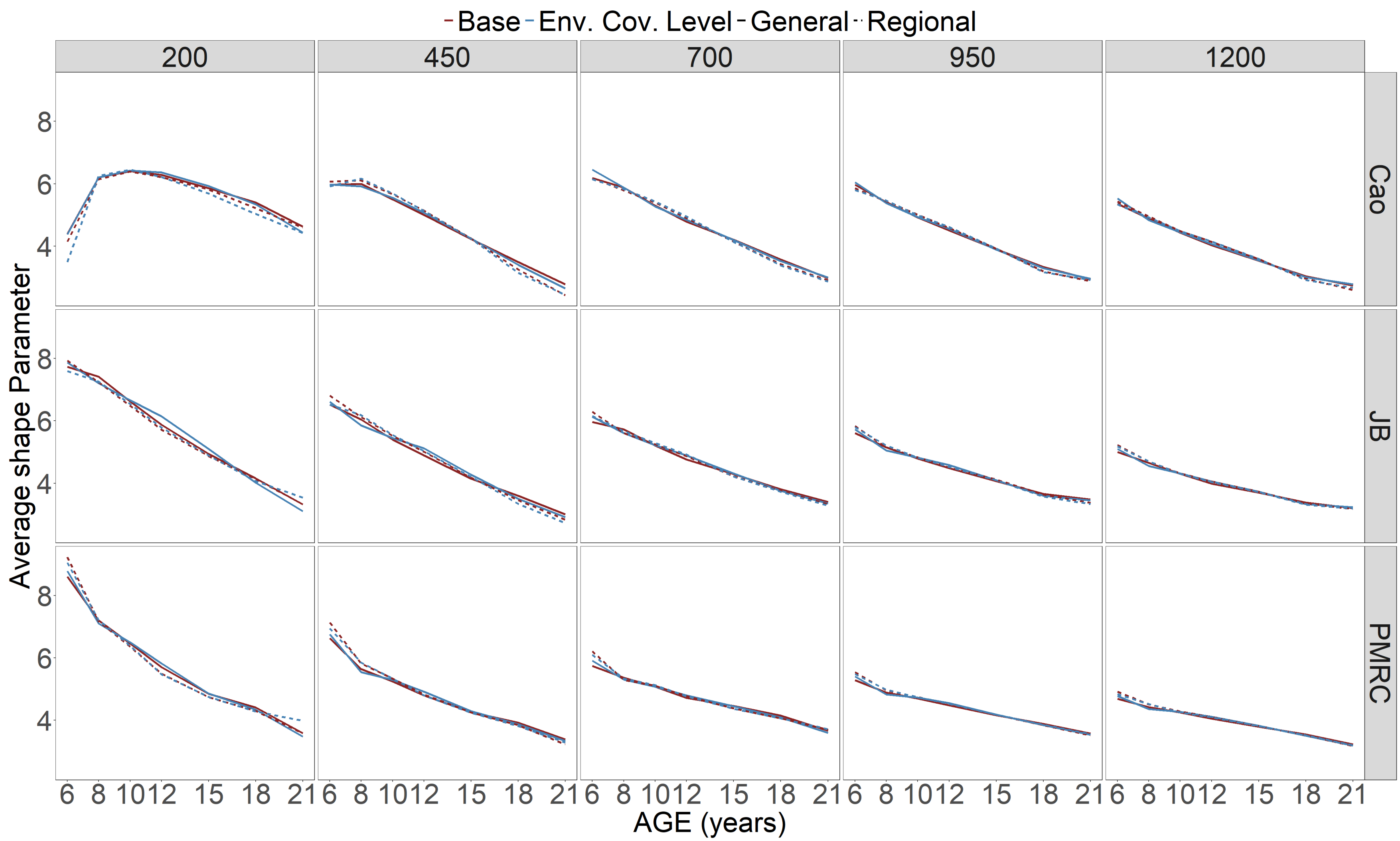

Figure 3.64: Average Weibull shape parameter based on three percentile models, under two modeling approaches: (i) the base model (without environmental co-variables), and (ii) the adapted model (accounting for environmental co-variables), conducted general and regional modeling level across seven ages and five planting densities. The solid line represents general level, and the dashed line represents regional level.

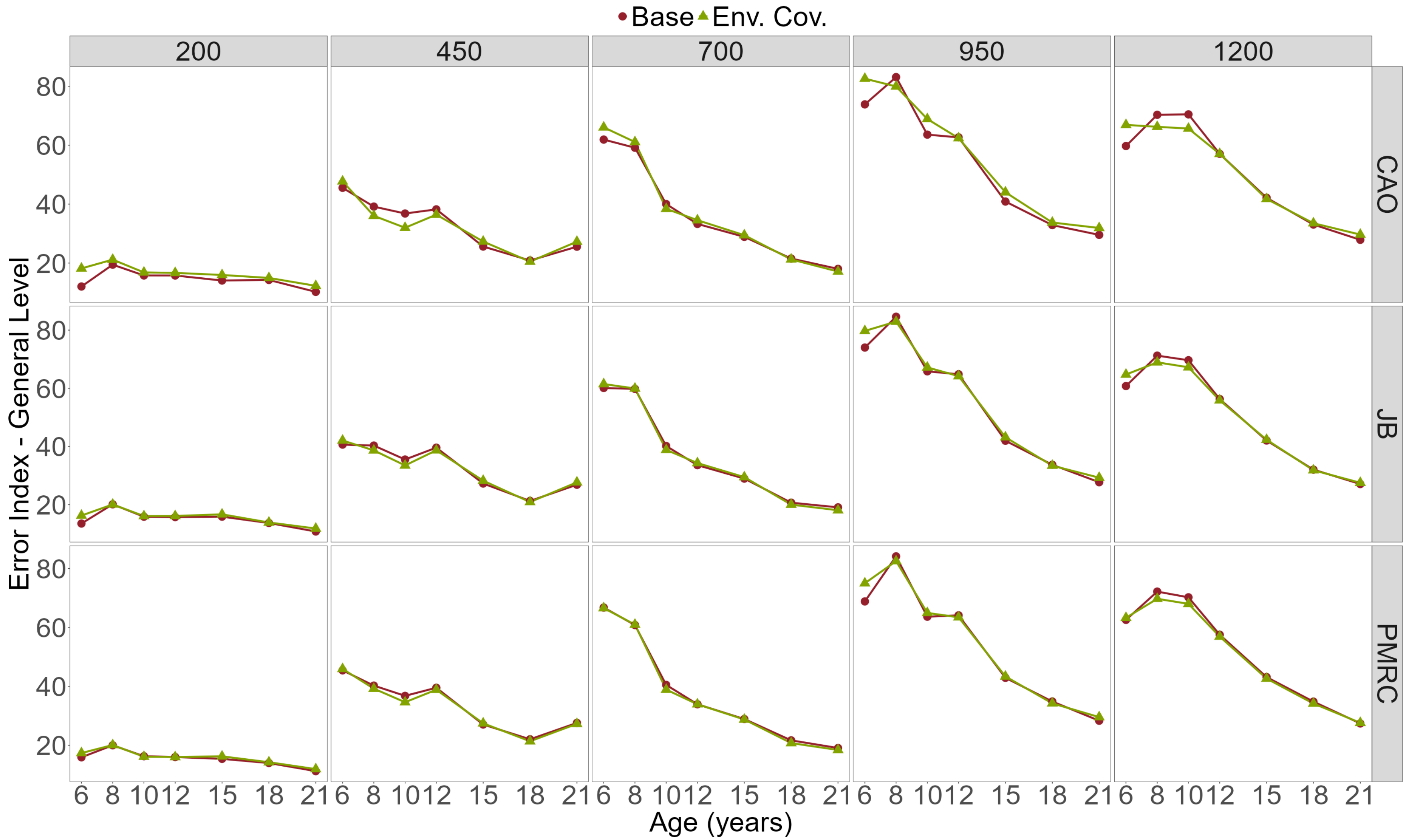

Figure 3.65: Comparison of the Error Index calculated using absolute observed TPA, estimated TPA based on the Weibull cumulative density function (CDF), under two modeling approaches: (i) the base model (without environmental co-variables) and (ii) the extended model (including environmental co-variables), BA_i for each diameter class, and plot BA from the observed dataset. The Weibull CDF was derived from the corresponding probability density function (PDF), which in turn was estimated using three different percentile regressions, conducted for the general modeling level, across all age and five planting densities.

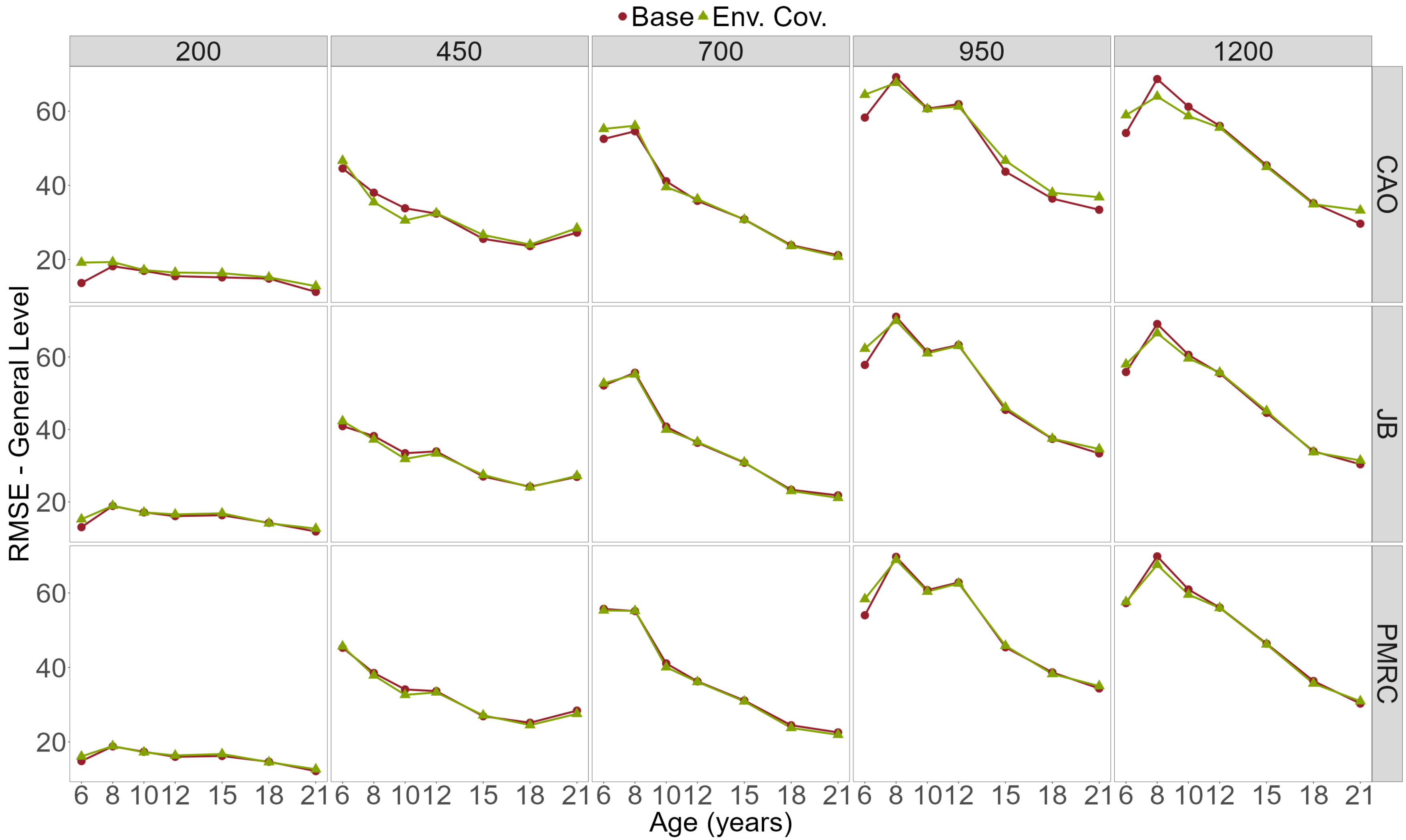

Figure 3.66: Comparison of the RMSE calculated using absolute observed TPA, estimated TPA based on the Weibull cumulative density function (CDF), under two modeling approaches: (i) the base model (without environmental co-variables) and (ii) the extended model (including environmental co-variables). The Weibull CDF was derived from the corresponding probability density function (PDF), which in turn was estimated using three different percentile regressions, conducted for the general modeling level, across all age and five planting densities.

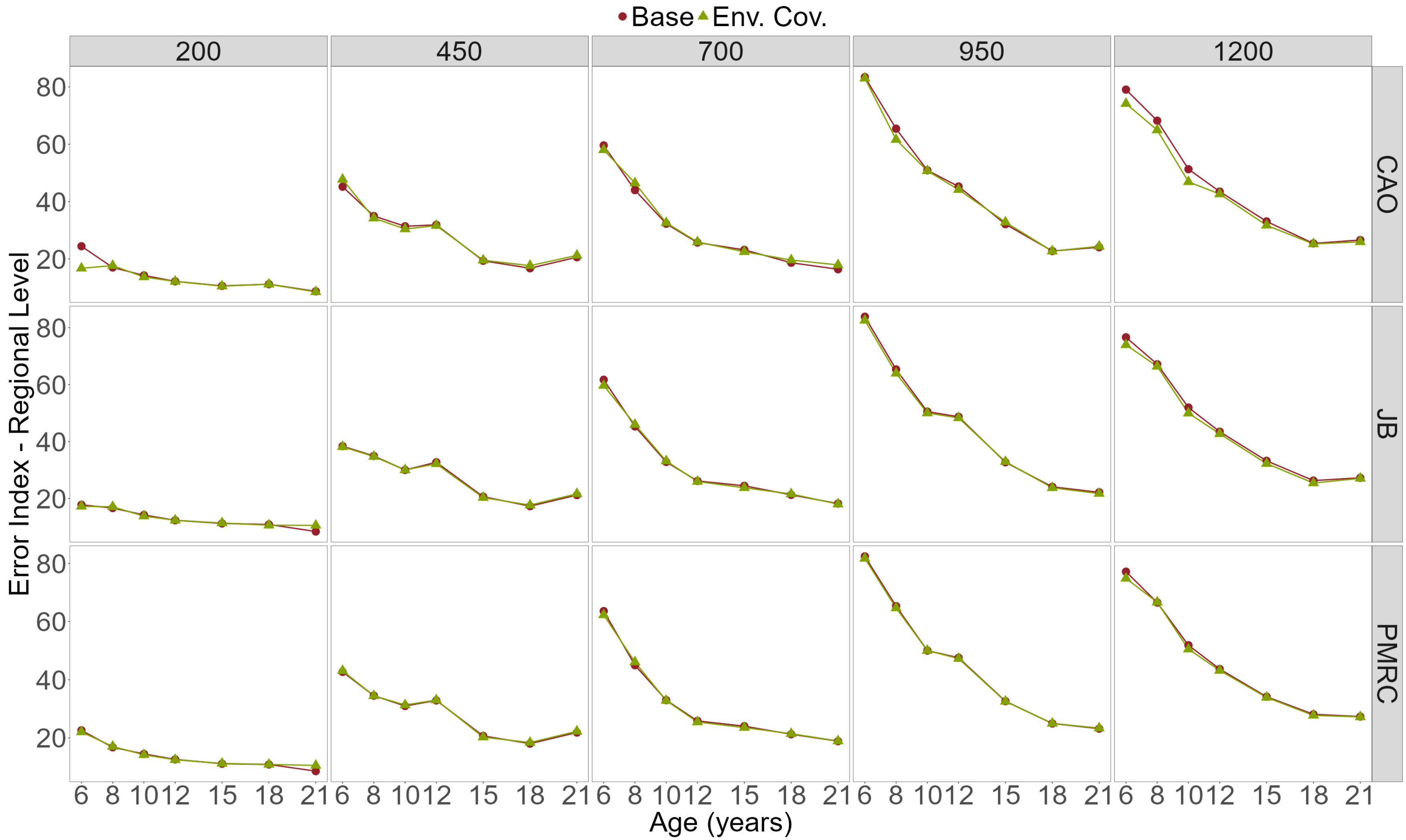

Figure 3.67: Comparison of the Error Index calculated using absolute observed TPA, estimated TPA based on the Weibull cumulative density function (CDF), under two modeling approaches: (i) the base model (without environmental co-variables) and (ii) the extended model (including environmental co-variables), BA_i for each diameter class, and plot BA from the observed dataset. The Weibull CDF was derived from the corresponding probability density function (PDF), which in turn was estimated using three different percentile regressions, conducted for the regional modeling level, across all age and five planting densities.

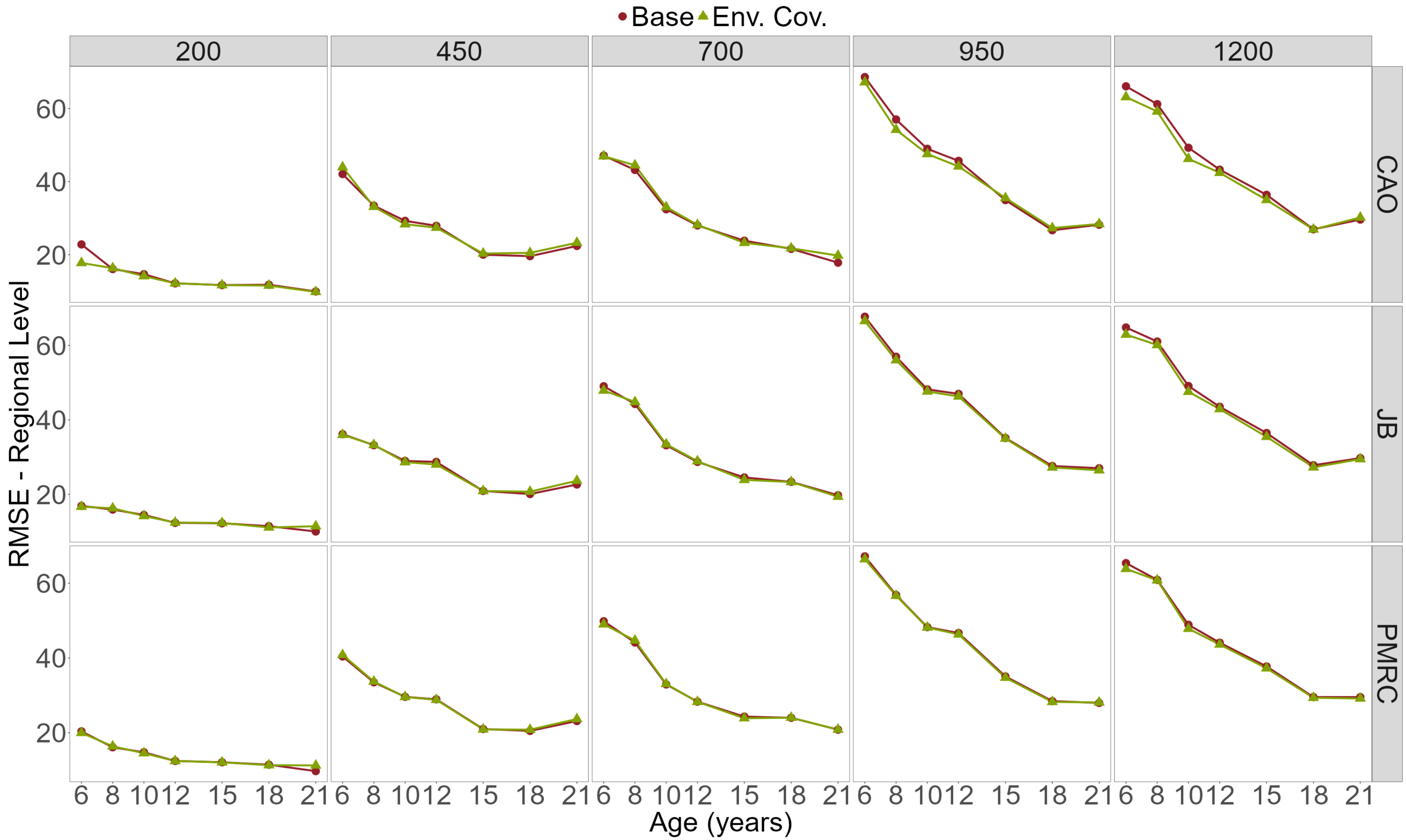

Figure 3.68: Comparison of the RMSE calculated using absolute observed TPA, estimated TPA based on the Weibull cumulative density function (CDF), under two modeling approaches: (i) the base model (without environmental co-variables) and (ii) the extended model (including environmental co-variables). The Weibull CDF was derived from the corresponding probability density function (PDF), which in turn was estimated using three different percentile regressions, conducted for the regional modeling level, across all age and five planting densities.

Chapter 4

Conclusions

Silviculture is the foundation for achieving higher forest productivity and ensuring tree health. Site management practices have a strong influence on site productivity and tree growth. Decisions related to the application of thinning, fertilization, and vegetation control allow for higher production yields and contribute to forest health by reducing mortality caused by self-thinning and controlling pests. Site management decisions are often supported by growth and yield modeling systems. One example is the modeling of diameter distribution, which provides insights into the structure and dynamics of a forest stand. Diameter distribution modeling is an essential technique that provides information about forest structure and supports the development of stand and stock tables, which assist in decision-making for silvicultural management.

Two studies were conducted to evaluate the effects of silvicultural management and environmental co-variables on the diameter distribution of loblolly pine in the Western Gulf physiographic region of the United States, using the Weibull distribution approach. In Chapter II, the effect of fertilization and vegetation control on diameter distribution was validated across five initial planting densities over a seven-year period. This study shows that diameter modeling for loblolly pine plantations in the WGCDS is significantly influenced by management intensity (MAN) and trees per acre (TPA). The Weibull distribution's location parameter was most affected by MAN, while the scale parameter differences were mainly due to mortality. The percentile-based approach proved strongly correlated with DBH, highlighting its reliability for predicting stand structure. Higher fertilization and vegetation control levels under the MAX management regime resulted in greater diameter growth, higher TPA in large diameter classes, and increased basal area at mid-rotation. The MAX regime also achieved lower error index and RMSE values, indicating a better model fit.

Chapter 3 was conducted in two levels to investigate the effect of environmental co-variables in diameter distributions. The first level (i.e. the general level) combined the three regional datasets into a single dataset, and the second level (i.e. the regional level), with the three regional datasets applied separately for the three regions (LCP, UCP, and IF) and the results from the three regions were then combined to compute the three parameter Weibull distribution. The results revealed that accounting for environmental co-variables in diameter distributions, the effects varied with planting density, modeling level, and stand age. Both base models that incorporating common variables (i.e., Age, BA, D_q, and HD) and adapted models that incorporating common variables and environmental co-variables (i.e.; $Temp_{max}$, PPT, and WD) provided reliable percentile predictions; however, the adapted models showed clearer improvements at medium and high planting densities, particularly in younger stands. This reflects the stronger influence of environmental factors—such as precipitation, temperature, and water deficit—on tree growth and competition under denser stand conditions. Cao's (CAO) model was most responsive to environmental co-variables showing strong effects in D_{25} percentile estimation. The Jiang and Brooks (JB) and PMRC (PMRC) models also demonstrated improvements, mainly in predicting D_0 diameter percentile at the regional level. Among the three models, Cao's adapted model exhibited the greatest sensitivity to environmental co-variables. The inclusion of these co-variables increased the estimated values of the location parameter at early ages compared to the Weibull PDF estimated without environmental co-variables, while producing lower shape parameter values at older ages. This pattern suggests a shift toward larger diameter classes as stands mature. The JB adapted model showed moderate effects, mainly on the location and shape parameters at low to medium planting densities (PLTPA), whereas the PMRC adapted model exhibited smaller but consistent effects, particularly in young stands and at lower densities. For the regional level, incorporating environmental co-variables improved parameter estimation across all models—especially during early stand development and at medium planting densities—enhancing the fit of the Weibull distribution and providing forest managers with more reliable information for decision-making.

Appendix A

Table of coefficients estimatation for D_0, D_{25}, D_{50}, D_{95} percentiles regression accounting for enviromental co-varibales for all three adapated model it regional level

Table A.1: Coefficients estimates from the D_0 percentile regression accounting for maximum temperate co-variable, M4 for IF region.

	Estimate	Std. Error	t value	$Pr(>\|t\|)$
(Intercept)	-19.2250	7.8461	-2.4503	0.0158
$\ln D_q$	1.9769	0.5200	3.8015	0.0002
lnAGE	0.1791	0.3222	0.5560	0.5793
HD	0.4453	0.5155	0.8639	0.3894
PLTPA450	0.1758	0.1416	1.2414	0.2170
PLTPA700	0.2524	0.2047	1.2332	0.2200
PLTPA950	0.0917	0.2492	0.3678	0.7137
PLTPA1200	0.1823	0.2843	0.6413	0.5226
$Temp_{max}$	0.2387	0.1058	2.2555	0.0260

Table A.2: Coefficients estimates from the D_{25} percentile regression accounting for maximum temperate co-variable, M4 for IF region.

	Estimate	Std. Error	t value	$Pr(>\|t\|)$
(Intercept)	1.3545	0.6764	2.0026	0.0475
$\ln D_{50}$	1.0888	0.0329	33.0759	0.0000
lnAGE	-0.0484	0.0214	-2.2608	0.0256
PLTPA450	0.0130	0.0107	1.2151	0.2268
PLTPA700	0.0128	0.0137	0.9340	0.3522
PLTPA950	-0.0205	0.0163	-1.2548	0.2120
PLTPA1200	-0.0130	0.0197	-0.6587	0.5114
$Temp_{max}$	-0.0203	0.0091	-2.2271	0.0279

Table A.3: Coefficients estimates from the D_{50} percentile regression accounting for water deficit co-variable, M4 for IF region.

	Estimate	Std. Error	t value	Pr(> $\|t\|$)
(Intercept)	0.0681	0.0150	4.5518	0.0000
$\ln D_q$	0.9700	0.0065	149.8329	0.0000
PLTPA450	-0.0049	0.0046	-1.0687	0.2874
PLTPA700	-0.0108	0.0049	-2.2032	0.0295
PLTPA950	-0.0082	0.0052	-1.5814	0.1165
PLTPA1200	-0.0205	0.0056	-3.6529	0.0004
WD	0.0101	0.0102	0.9946	0.3220

Table A.4: Coefficients estimates from the D_{95} percentile regression accounting for precipitation co-variable, M4 for IF region.

	Estimate	Std. Error	t value	Pr(> $\|t\|$)
(Intercept)	0.0722	0.0768	0.9400	0.3492
$\ln D_{50}$	0.9571	0.0399	24.0061	0.0000
lnAGE	-0.0144	0.0229	-0.6308	0.5294
HD	-0.0940	0.0356	-2.6390	0.0095
PLTPA450	0.0040	0.0128	0.3133	0.7546
PLTPA700	0.0172	0.0170	1.0116	0.3138
PLTPA950	0.0360	0.0200	1.7989	0.0746
PLTPA1200	0.0552	0.0231	2.3886	0.0185
PPT	-0.0332	0.0152	-2.1807	0.0312

Table A.5: Coefficients estimates from the D_0 percentile regression accounting for maximum temperate co-variable, M5 for IF region.

	Estimate	Std. Error	t value	Pr(> $\|t\|$)
(Intercept)	-16.3593	7.6297	-2.1442	0.0341
RS	0.2318	1.1684	0.1984	0.8431
lnTPA	-0.7825	0.3299	-2.3720	0.0194
lnHD	0.7962	0.4896	1.6264	0.1066
AGE	-0.5866	3.1688	-0.1851	0.8535
PLTPA450	0.3649	0.1935	1.8856	0.0619
PLTPA700	0.4653	0.2786	1.6700	0.0976
PLTPA950	0.3923	0.3608	1.0871	0.2792
PLTPA1200	0.4960	0.4012	1.2362	0.2189
$Temp_{max}$	0.2583	0.1042	2.4787	0.0146

Table A.6: Coefficients estimates from the D_{25} percentile regression accounting for maximum temperate co-variable, M5 for IF region.

	Estimate	Std. Error	t value	$Pr(>\|t\|)$
(Intercept)	4.1435	0.9884	4.1922	0.0001
RS	-1.6352	0.1876	-8.7142	0.0000
lnTPA	-0.3898	0.0528	-7.3846	0.0000
lnHD	0.2019	0.0782	2.5822	0.0111
AGE	-0.2230	0.5144	-0.4335	0.6655
PLTPA450	-0.1232	0.0312	-3.9461	0.0001
PLTPA700	-0.1977	0.0449	-4.4052	0.0000
PLTPA950	-0.2431	0.0581	-4.1866	0.0001
PLTPA1200	-0.2867	0.0646	-4.4407	0.0000
$Temp_{max}$	-0.0006	0.0123	-0.0458	0.9636

Table A.7: Coefficients estimates from the D_{50} percentile regression accounting for water deficit co-variable, M5 for IF region.

	Estimate	Std. Error	t value	$Pr(>\|t\|)$
(Intercept)	2.9692	0.5069	5.8577	0.0000
RS	-1.2269	0.1573	-7.7989	0.0000
lnTPA	-0.2864	0.0453	-6.3196	0.0000
lnHD	0.3363	0.0647	5.1984	0.0000
AGE	-0.0844	0.4403	-0.1916	0.8484
PLTPA450	-0.1482	0.0271	-5.4776	0.0000
PLTPA700	-0.2327	0.0389	-5.9899	0.0000
PLTPA950	-0.2592	0.0503	-5.1513	0.0000
PLTPA1200	-0.3107	0.0562	-5.5279	0.0000
WD	-0.0072	0.0259	-0.2782	0.7814

Table A.8: Coefficients estimates from the D_{95} percentile regression accounting for precipitation co-variable, M5 for IF region.

	Estimate	Std. Error	t value	$Pr(>\|t\|)$
(Intercept)	2.6767	0.6299	4.2495	0.0000
RS	-0.9790	0.1926	-5.0828	0.0000
lnTPA	-0.2915	0.0541	-5.3905	0.0000
lnHD	0.4833	0.0797	6.0616	0.0000
AGE	0.4965	0.5371	0.9244	0.3572
PLTPA450	-0.1009	0.0322	-3.1285	0.0022
PLTPA700	-0.1549	0.0462	-3.3506	0.0011
PLTPA950	-0.1497	0.0598	-2.5051	0.0136
PLTPA1200	-0.1711	0.0666	-2.5714	0.0114
PPT	-0.0525	0.0237	-2.2178	0.0285

Table A.9: Coefficients estimates from the D_0 percentile regression accounting for maximum temperate co-variable, M6 for IF region.

	Estimate	Std. Error	t value	Pr(> $\|t\|$)
(Intercept)	-15.1832	7.8043	-1.9455	0.0541
lnBA/TPA	0.8217	0.0552	14.8969	0.0000
PLTPA450	0.1002	0.0808	1.2402	0.2174
PLTPA700	0.1264	0.0858	1.4733	0.1433
PLTPA950	-0.0636	0.0910	-0.6989	0.4860
PLTPA1200	0.0140	0.0978	0.1427	0.8868
$Temp_{max}$	0.2354	0.1047	2.2495	0.0263

Table A.10: Coefficients estimates from the D_{25} percentile regression accounting for maximum temperate co-variable, M6 for IF region.

	Estimate	Std. Error	t value	Pr(> $\|t\|$)
(Intercept)	4.2682	0.6585	6.4819	0.0000
lnBA/TPA	0.4955	0.0050	98.2023	0.0000
PLTPA450	-0.0074	0.0074	-0.9973	0.3207
PLTPA700	-0.0216	0.0079	-2.7439	0.0070
PLTPA950	-0.0583	0.0083	-6.9890	0.0000
PLTPA1200	-0.0711	0.0090	-7.9346	0.0000
$Temp_{max}$	-0.0234	0.0088	-2.6463	0.0092

Table A.11: Coefficients estimates from the D_{50} percentile regression accounting for water deficit co-variable, M6 for IF region.

	Estimate	Std. Error	t value	Pr(> $\|t\|$)
(Intercept)	2.5953	0.0042	622.6917	0.0000
lnBA*TPA	0.4847	0.0034	142.4929	0.0000
PLTPA450	-0.0050	0.0046	-1.0910	0.2775
PLTPA700	-0.0110	0.0049	-2.2194	0.0284
PLTPA950	-0.0085	0.0053	-1.6045	0.1113
PLTPA1200	-0.0208	0.0057	-3.6340	0.0004
WD	0.0118	0.0138	0.8534	0.3952

Table A.12: Coefficients estimates from the D_{95} percentile regression accounting for precipitation co-variable, M6 for IF region.

	Estimate	Std. Error	t value	Pr(> $\|t\|$)
(Intercept)	2.8802	0.0580	49.6469	0.0000
lnBA/TPA	0.5161	0.0048	106.5656	0.0000
PLTPA450	0.0230	0.0067	3.4133	0.0009
PLTPA700	0.0451	0.0072	6.2784	0.0000
PLTPA950	0.0757	0.0077	9.8817	0.0000
PLTPA1200	0.0895	0.0083	10.7978	0.0000
PPT	-0.0266	0.0126	-2.1131	0.0367

Table A.13: Coefficients estimates from the D_0 percentile regression accounting for maximum temperature co-variable, M4 for LCP region.

	Estimate	Std. Error	t value	Pr(> $\|t\|$)
(Intercept)	11.3644	3.6279	3.1325	0.0022
$\ln D_q$	1.2327	0.4715	2.6146	0.0102
lnAGE	0.8469	0.2302	3.6786	0.0004
HD	0.4211	0.4738	0.8887	0.3762
PLTPA450	0.1924	0.1373	1.4012	0.1641
PLTPA700	-0.0474	0.1869	-0.2538	0.8001
PLTPA950	0.1338	0.2349	0.5698	0.5700
PLTPA1200	-0.0645	0.2527	-0.2555	0.7989
$Temp_{max}$	-0.1672	0.0445	-3.7608	0.0003

Table A.14: Coefficients estimates from the D_{25} percentile regression accounting for maximum temperature co-variable, M4 for LCP region.

	Estimate	Std. Error	t value	Pr(> $\|t\|$)
(Intercept)	2.1671	0.5442	3.9822	0.0001
$\ln D_{50}$	0.9643	0.0378	25.4999	0.0000
lnAGE	0.0588	0.0260	2.2620	0.0257
PLTPA450	-0.0207	0.0178	-1.1608	0.2483
PLTPA700	-0.0851	0.0209	-4.0773	0.0001
PLTPA950	-0.0543	0.0245	-2.2138	0.0290
PLTPA1200	-0.1131	0.0258	-4.3790	0.0000
$Temp_{max}$	-0.0298	0.0068	-4.3590	0.0000

Table A.15: Coefficients estimates from the D_{50} percentile regression accounting for water deficit co-variable, M4 for LCP region.

	Estimate	Std. Error	t value	$Pr(>\|t\|)$
(Intercept)	0.0266	0.0248	1.0700	0.2870
$\ln D_q$	0.9895	0.0108	91.6184	0.0000
PLTPA450	-0.0212	0.0080	-2.6370	0.0096
PLTPA700	0.0052	0.0087	0.5994	0.5501
PLTPA950	-0.0200	0.0093	-2.1521	0.0336
PLTPA1200	-0.0217	0.0096	-2.2615	0.0257
WD	-0.0156	0.0105	-1.4883	0.1396

Table A.16: Coefficients estimates from the D_{95} percentile regression accounting for precipitation co-variable, M4 for LCP region.

	Estimate	Std. Error	t value	$Pr(>\|t\|)$
(Intercept)	0.1920	0.1519	1.2636	0.2092
$\ln D_{50}$	0.9933	0.0573	17.3480	0.0000
lnAGE	0.0471	0.0299	1.5761	0.1180
HD	0.0655	0.0603	1.0867	0.2796
PLTPA450	0.0591	0.0197	2.9940	0.0034
PLTPA700	0.0475	0.0240	1.9832	0.0499
PLTPA950	0.0687	0.0306	2.2425	0.0270
PLTPA1200	0.1166	0.0327	3.5616	0.0006
PPT	0.0284	0.0224	1.2647	0.2087

Table A.17: Coefficients estimates from the D_0 percentile regression accounting for maximum temperature co-variable, M5 for LCP region.

	Estimate	Std. Error	t value	$Pr(>\|t\|)$
(Intercept)	11.8621	6.1727	1.9217	0.0574
RS	3.3223	1.8034	1.8423	0.0683
lnTPA	0.1122	0.3028	0.3704	0.7118
lnHD	1.0830	0.5269	2.0557	0.0423
AGE	-10.9834	2.7168	-4.0427	0.0001
PLTPA450	0.1905	0.1549	1.2298	0.2215
PLTPA700	-0.1359	0.2033	-0.6686	0.5052
PLTPA950	-0.0356	0.2549	-0.1398	0.8891
PLTPA1200	-0.2677	0.2750	-0.9735	0.3326
$Temp_{max}$	-0.1951	0.0477	-4.0877	0.0000

Table A.18: Coefficients estimates from the D_{25} percentile regression accounting for maximum temperature co-variable, M5 for LCP region.

	Estimate	Std. Error	t value	Pr(> |t|)
(Intercept)	3.8233	1.1622	3.2897	0.0014
RS	-0.5408	0.3705	-1.4598	0.1473
lnTPA	-0.2622	0.0621	-4.2236	0.0000
lnHD	0.6379	0.1072	5.9522	0.0000
AGE	1.5078	0.5462	2.7603	0.0068
PLTPA450	-0.1021	0.0318	-3.2121	0.0017
PLTPA700	-0.1919	0.0417	-4.5979	0.0000
PLTPA950	-0.2261	0.0523	-4.3232	0.0000
PLTPA1200	-0.2998	0.0564	-5.3133	0.0000
$Temp_{max}$	-0.0351	0.0083	-4.2077	0.0000

Table A.19: Coefficients estimates from the D_{50} percentile regression accounting for water deficit co-variable, M5 for LCP region.

	Estimate	Std. Error	t value	Pr(> |t|)
(Intercept)	1.3358	0.6394	2.0891	0.0391
RS	-0.8906	0.2875	-3.0974	0.0025
lnTPA	-0.2957	0.0486	-6.0816	0.0000
lnHD	0.6394	0.0810	7.8936	0.0000
AGE	2.9491	0.4037	7.3058	0.0000
PLTPA450	-0.1018	0.0253	-4.0192	0.0001
PLTPA700	-0.1296	0.0336	-3.8535	0.0002
PLTPA950	-0.1989	0.0422	-4.7139	0.0000
PLTPA1200	-0.2144	0.0455	-4.7108	0.0000
WD	-0.0132	0.0195	-0.6744	0.5015

Table A.20: Coefficients estimates from the D_{95} percentile regression accounting for precipitation co-variable, M5 for LCP region.

	Estimate	Std. Error	t value	Pr(> |t|)
(Intercept)	0.9541	0.8980	1.0625	0.2904
RS	-0.4152	0.3813	-1.0890	0.2786
lnTPA	-0.2013	0.0657	-3.0655	0.0028
lnHD	0.6134	0.1079	5.6856	0.0000
AGE	1.1606	0.5285	2.1960	0.0303
PLTPA450	-0.0608	0.0345	-1.7632	0.0808
PLTPA700	-0.1195	0.0459	-2.6001	0.0107
PLTPA950	-0.1832	0.0578	-3.1697	0.0020
PLTPA1200	-0.1573	0.0624	-2.5227	0.0131
PPT	0.0327	0.0323	1.0123	0.3137

Table A.21: Coefficients estimates from the D_0 percentile regression accounting for maximum temperature co-variable, M6 for LCP region.

	Estimate	Std. Error	t value	$Pr(>\|t\|)$
(Intercept)	8.7097	3.1659	2.7511	0.0070
lnBA/TPA	0.8750	0.0730	11.9929	0.0000
PLTPA450	0.2678	0.1090	2.4571	0.0156
PLTPA700	0.1435	0.1180	1.2168	0.2263
PLTPA950	0.3849	0.1263	3.0477	0.0029
PLTPA1200	0.2107	0.1299	1.6220	0.1077
$Temp_{max}$	-0.0836	0.0404	-2.0677	0.0411

Table A.22: Coefficients estimates from the D_{25} percentile regression accounting for maximum temperature co-variable, M6 for LCP region.

	Estimate	Std. Error	t value	$Pr(>\|t\|)$
(Intercept)	3.9677	0.3596	11.0345	0.0000
lnBA/TPA	0.5129	0.0102	50.3980	0.0000
PLTPA450	-0.0284	0.0152	-1.8626	0.0652
PLTPA700	-0.0545	0.0165	-3.3070	0.0013
PLTPA950	-0.0398	0.0176	-2.2572	0.0260
PLTPA1200	-0.0971	0.0181	-5.3487	0.0000
$Temp_{max}$	-0.0186	0.0046	-4.0396	0.0001

Table A.23: Coefficients estimates from the D_{50} percentile regression accounting for water deficit co-variable, M6 for LCP region.

	Estimate	Std. Error	t value	$Pr(>\|t\|)$
(Intercept)	2.6019	0.0084	310.6356	0.0000
lnBA/TPA	0.4920	0.0054	90.8108	0.0000
PLTPA450	-0.0221	0.0080	-2.7563	0.0069
PLTPA700	0.0033	0.0087	0.3755	0.7080
PLTPA950	-0.0226	0.0093	-2.4259	0.0169
PLTPA1200	-0.0245	0.0096	-2.5524	0.0121
WD	-0.0131	0.0101	-1.2964	0.1976

Table A.24: Coefficients estimates from the D_{95} percentile regression accounting for precipitation co-variable, M6 for LCP region.

	Estimate	Std. Error	t value	Pr(> $|t|$)
(Intercept)	2.7363	0.0685	39.9613	0.0000
lnBA/TPA	0.4800	0.0076	63.2144	0.0000
PLTPA450	0.0315	0.0114	2.7615	0.0068
PLTPA700	0.0456	0.0123	3.7044	0.0003
PLTPA950	0.0392	0.0132	2.9703	0.0037
PLTPA1200	0.0848	0.0136	6.2509	0.0000
PPT	0.0074	0.0130	0.5732	0.5677

Table A.25: Coefficients estimates from the D_0 percentile regression accounting for maximum temperature co-variable, M4 for UCP region.

	Estimate	Std. Error	t value	Pr(> $|t|$)
(Intercept)	0.3041	0.7750	0.3924	0.6951
$\ln D_q$	0.3538	0.3205	1.1041	0.2707
lnAGE	0.1763	0.1898	0.9287	0.3540
HD	-0.7935	0.2648	-2.9968	0.0030
PLTPA450	-0.2311	0.0913	-2.5307	0.0120
PLTPA700	-0.4449	0.1275	-3.4892	0.0006
PLTPA950	-0.5543	0.1517	-3.6534	0.0003
PLTPA1200	-0.5758	0.1721	-3.3463	0.0010
$Temp_{max}$	-0.0369	0.0112	-3.2955	0.0011

Table A.26: Coefficients estimates from the D_{25} percentile regression accounting for maximum temperature co-variable, M4 for UCP region.

	Estimate	Std. Error	t value	Pr(> $|t|$)
(Intercept)	-0.1394	0.1099	-1.2683	0.2059
$\ln D_{50}$	1.0984	0.0363	30.2809	0.0000
lnAGE	-0.0450	0.0226	-1.9951	0.0472
PLTPA450	0.0117	0.0129	0.9115	0.3630
PLTPA700	-0.0080	0.0158	-0.5053	0.6138
PLTPA950	-0.0149	0.0190	-0.7848	0.4334
PLTPA1200	-0.0050	0.0213	-0.2362	0.8135
$Temp_{max}$	-0.0007	0.0014	-0.5232	0.6013

Table A.27: Coefficients estimates from the D_{50} percentile regression accounting for water deficit co-variable, M4 for UCP region.

	Estimate	Std. Error	t value	Pr(> |t|)
(Intercept)	0.0504	0.0108	4.6873	0.0000
lnD_q	0.9805	0.0047	208.4000	0.0000
PLTPA450	-0.0154	0.0036	-4.2561	0.0000
PLTPA700	-0.0088	0.0038	-2.3501	0.0196
PLTPA950	-0.0165	0.0039	-4.2214	0.0000
PLTPA1200	-0.0257	0.0041	-6.2930	0.0000
WD	-0.0124	0.0039	-3.1608	0.0018

Table A.28: Coefficients estimates from the D_{95} percentile regression accounting for precipitation co-variable, M4 for UCP region.

	Estimate	Std. Error	t value	Pr(> |t|)
(Intercept)	-0.0097	0.0474	-0.2036	0.8389
lnD_{50}	0.8711	0.0341	25.5410	0.0000
lnAGE	0.0565	0.0231	2.4468	0.0151
HD	-0.0303	0.0253	-1.1988	0.2318
PLTPA450	0.0277	0.0114	2.4236	0.0161
PLTPA700	0.0129	0.0146	0.8840	0.3776
PLTPA950	0.0228	0.0173	1.3198	0.1882
PLTPA1200	0.0391	0.0196	1.9938	0.0473
PPT	0.0402	0.0064	6.2479	0.0000

Table A.29: Coefficients estimates from the D_0 percentile regression accounting for maximum temperature co-variable, M5 for UCP region.

	Estimate	Std. Error	t value	Pr(> |t|)
(Intercept)	-2.5789	1.7006	-1.5165	0.1308
RS	1.5915	0.6819	2.3340	0.0204
lnTPA	0.0466	0.1471	0.3168	0.7517
lnHD	1.6466	0.2526	6.5184	0.0000
AGE	0.7127	1.7077	0.4174	0.6768
PLTPA450	-0.1759	0.0922	-1.9076	0.0577
PLTPA700	-0.3837	0.1267	-3.0275	0.0027
PLTPA950	-0.4835	0.1507	-3.2081	0.0015
PLTPA1200	-0.5146	0.1706	-3.0171	0.0028
$Temp_{max}$	-0.0372	0.0113	-3.2976	0.0011

Table A.30: Coefficients estimates from the D_{25} percentile regression accounting for maximum temperature co-variable, M5 for UCP region.

	Estimate	Std. Error	t value	$Pr(>\|t\|)$
(Intercept)	4.0526	0.3710	10.9224	0.0000
RS	-1.3364	0.1489	-8.9721	0.0000
lnTPA	-0.2807	0.0315	-8.9173	0.0000
lnHD	0.1762	0.0543	3.2467	0.0013
AGE	-1.4290	0.3712	-3.8502	0.0002
PLTPA450	-0.1790	0.0198	-9.0226	0.0000
PLTPA700	-0.2912	0.0271	-10.7574	0.0000
PLTPA950	-0.3595	0.0321	-11.1912	0.0000
PLTPA1200	-0.3994	0.0363	-11.0050	0.0000
$Temp_{max}$	-0.0065	0.0020	-3.2501	0.0013

Table A.31: Coefficients estimates from the D_{50} percentile regression accounting for water deficit co-variable, M5 for UCP region.

	Estimate	Std. Error	t value	$Pr(>\|t\|)$
(Intercept)	4.6233	0.2756	16.7733	0.0000
RS	-1.4631	0.1108	-13.2068	0.0000
lnTPA	-0.3542	0.0227	-15.6201	0.0000
lnHD	0.0422	0.0396	1.0650	0.2880
AGE	-1.9182	0.2790	-6.8742	0.0000
PLTPA450	-0.1267	0.0145	-8.7577	0.0000
PLTPA700	-0.1841	0.0196	-9.3915	0.0000
PLTPA950	-0.2219	0.0232	-9.5614	0.0000
PLTPA1200	-0.2516	0.0261	-9.6322	0.0000
WD	0.0318	0.0095	3.3609	0.0009

Table A.32: Coefficients estimates from the D_{95} percentile regression accounting for precipitation co-variable, M5 for UCP region.

	Estimate	Std. Error	t value	$Pr(>\|t\|)$
(Intercept)	4.1624	0.2877	14.4667	0.0000
RS	-1.2209	0.1160	-10.5218	0.0000
lnTPA	-0.3206	0.0235	-13.6484	0.0000
lnHD	0.0663	0.0425	1.5581	0.1206
AGE	-2.3735	0.2954	-8.0343	0.0000
PLTPA450	-0.0689	0.0151	-4.5751	0.0000
PLTPA700	-0.1259	0.0203	-6.1974	0.0000
PLTPA950	-0.1446	0.0240	-6.0215	0.0000
PLTPA1200	-0.1510	0.0270	-5.5880	0.0000
PPT	0.0637	0.0084	7.6002	0.0000

Table A.33: Coefficients estimates from the D_0 percentile regression accounting for maximum temperature co-variable, M6 for UCP region.

	Estimate	Std. Error	t value	$Pr(>\|t\|)$
(Intercept)	2.8750	0.7409	3.8805	0.0001
lnBA/TPA	0.8368	0.0409	20.4700	0.0000
PLTPA450	0.0559	0.0640	0.8740	0.3830
PLTPA700	0.0245	0.0661	0.3699	0.7118
PLTPA950	0.0246	0.0687	0.3585	0.7203
PLTPA1200	0.0934	0.0716	1.3033	0.1937
$Temp_{max}$	-0.0068	0.0096	-0.7013	0.4838

Table A.34: Coefficients estimates from the D_{25} percentile regression accounting for maximum temperature co-variable, M6 for UCP region.

	Estimate	Std. Error	t value	$Pr(>\|t\|)$
(Intercept)	2.5247	0.0872	28.9692	0.0000
lnBA/TPA	0.5029	0.0058	86.7670	0.0000
PLTPA450	-0.0206	0.0091	-2.2638	0.0245
PLTPA700	-0.0430	0.0094	-4.5806	0.0000
PLTPA950	-0.0653	0.0098	-6.6869	0.0000
PLTPA1200	-0.0699	0.0102	-6.8748	0.0000
$Temp_{max}$	0.0001	0.0011	0.0606	0.9517

Table A.35: Coefficients estimates from the D_{50} percentile regression accounting for water deficit co-variable, M6 for UCP region.

	Estimate	Std. Error	t value	$Pr(>\|t\|)$
(Intercept)	2.6030	0.0031	843.3646	0.0000
lnBA/TPA	0.4887	0.0024	205.9182	0.0000
PLTPA450	-0.0157	0.0036	-4.3300	0.0000
PLTPA700	-0.0100	0.0038	-2.6486	0.0086
PLTPA950	-0.0179	0.0039	-4.5527	0.0000
PLTPA1200	-0.0272	0.0041	-6.6484	0.0000
WD	-0.0050	0.0044	-1.1184	0.2645

Table A.36: Coefficients estimates from the D_{95} percentile regression accounting for precipitation co-variable, M6 for UCP region.

	Estimate	Std. Error	t value	Pr(> $\|t\|$)
(Intercept)	2.6350	0.0251	105.1091	0.0000
lnBA/TPA	0.4933	0.0051	96.6574	0.0000
PLTPA450	0.0439	0.0078	5.5982	0.0000
PLTPA700	0.0528	0.0081	6.4951	0.0000
PLTPA950	0.0681	0.0085	8.0431	0.0000
PLTPA1200	0.0850	0.0088	9.6170	0.0000
PPT	0.0242	0.0050	4.8266	0.0000

Appendix B

Chapter 3 - Diameter Distribution Figures

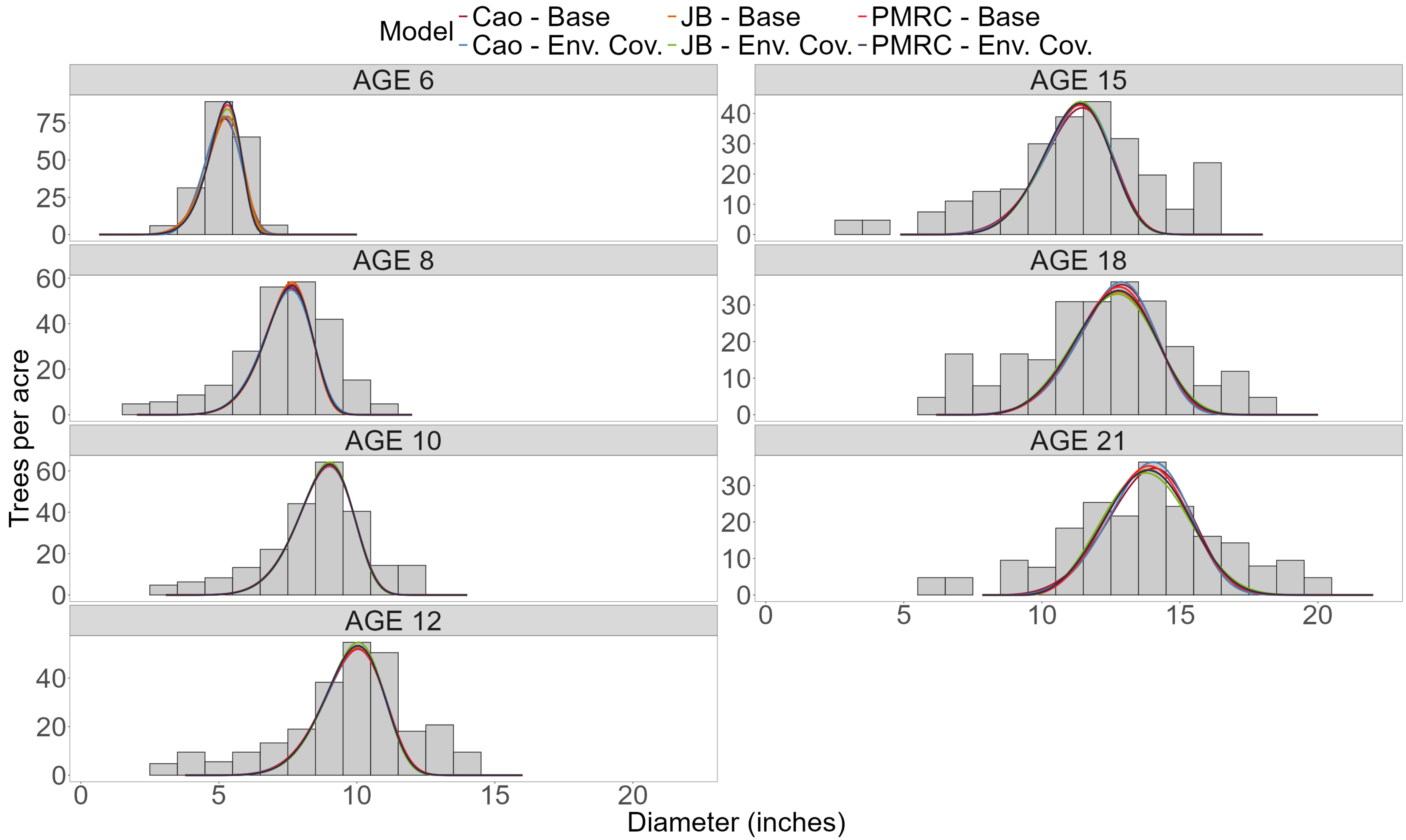

Figure B.1: Diameter distribution of loblolly pine plantations in the Western Gulf physiographic region, modeled using the three-parameter Weibull distribution under two approaches: (i) the base model (without environmental co-variables) and (ii) the adapted model (accounting for environmental co-variables). The analysis was conducted at the general modeling level across seven ages with an initial planting density of 200 trees per acre.

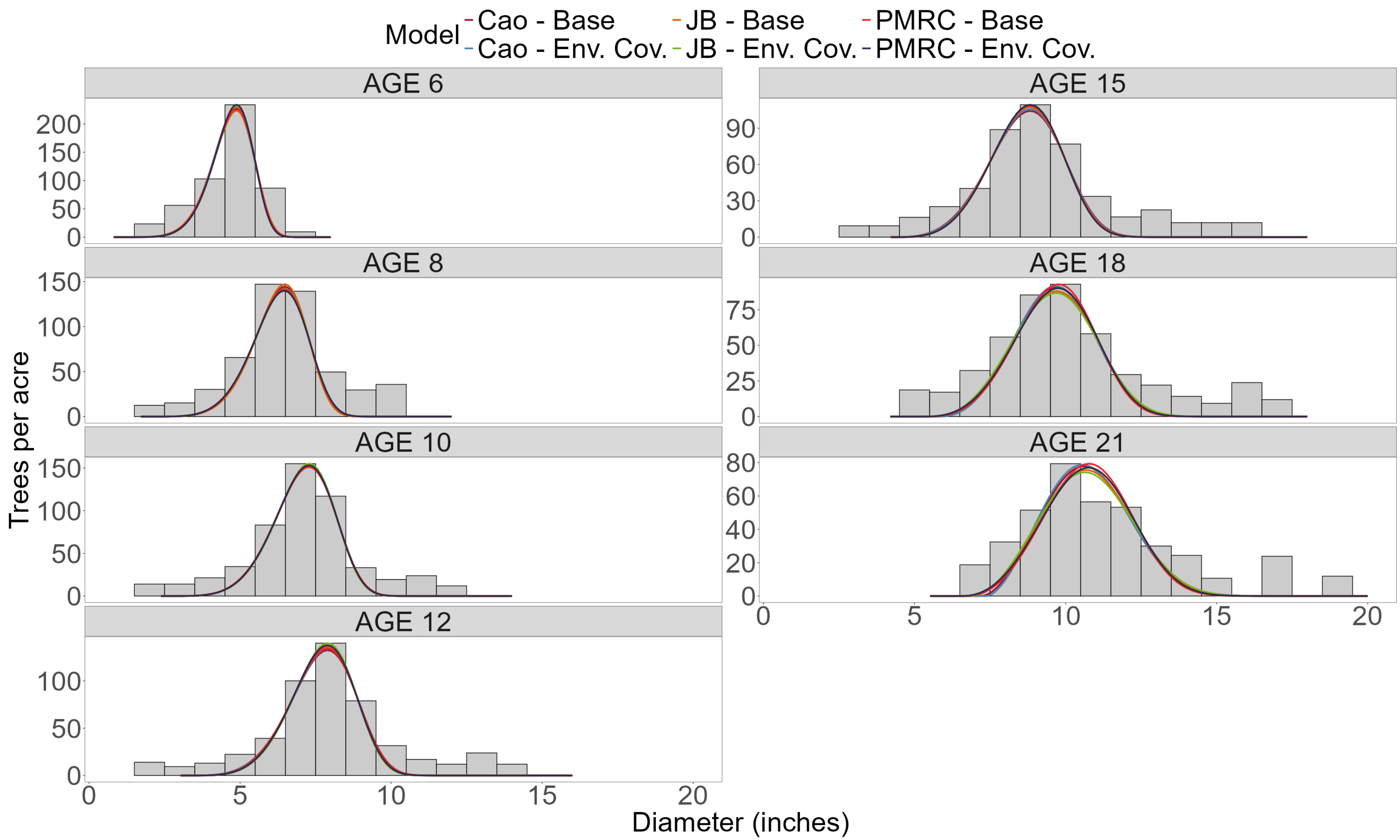

Figure B.2: Diameter distribution of loblolly pine plantations in the Western Gulf physiographic region, modeled using the three-parameter Weibull distribution under two approaches: (i) the base model (without environmental co-variables) and (ii) the adapted model (accounting for environmental co-variables). The analysis was conducted at the general modeling level across seven ages with an initial planting density of 450 trees per acre.

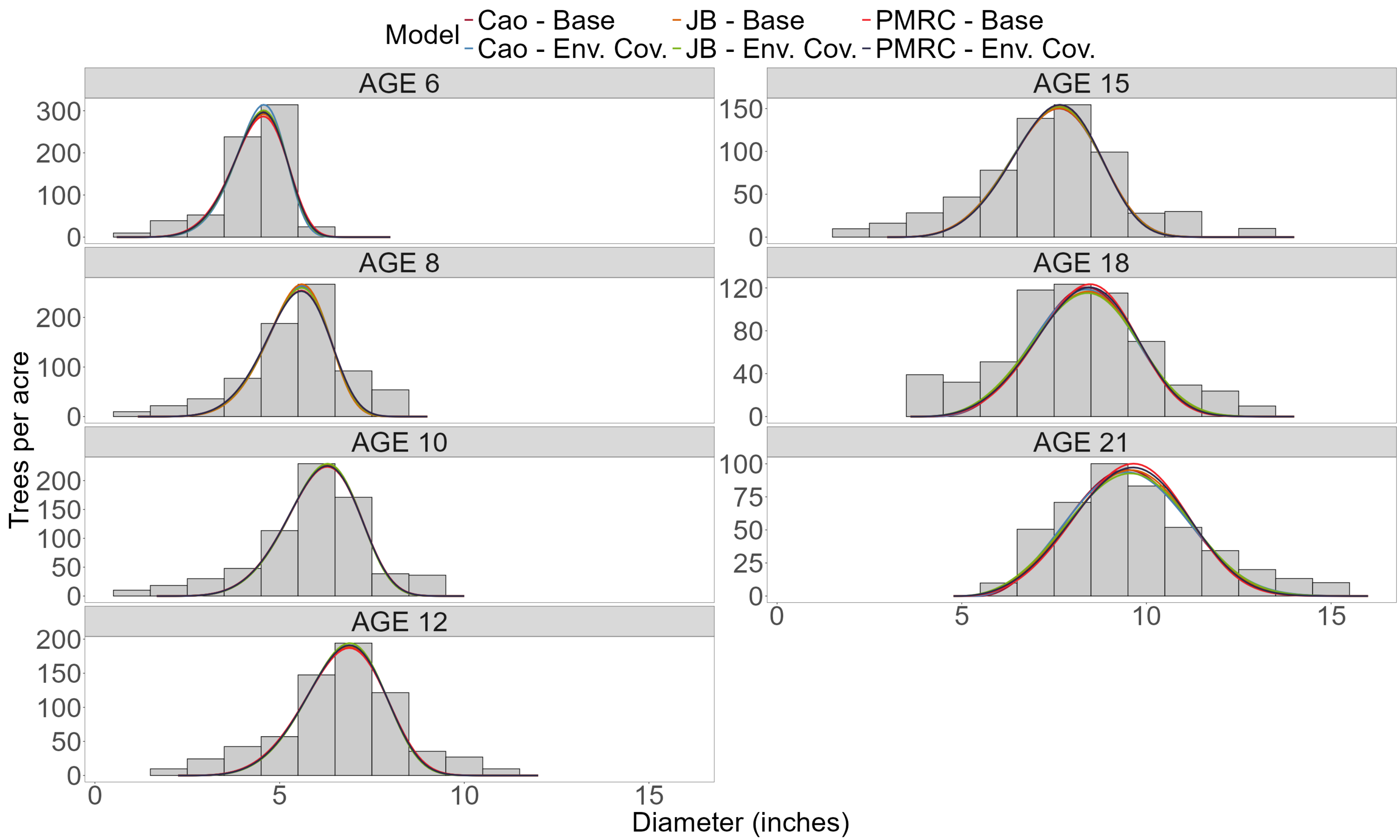

Figure B.3: Diameter distribution of loblolly pine plantations in the Western Gulf physiographic region, modeled using the three-parameter Weibull distribution under two approaches: (i) the base model (without environmental co-variables) and (ii) the adapted model (accounting for environmental co-variables). The analysis was conducted at the general modeling level across seven ages with an initial planting density of 700 trees per acre.

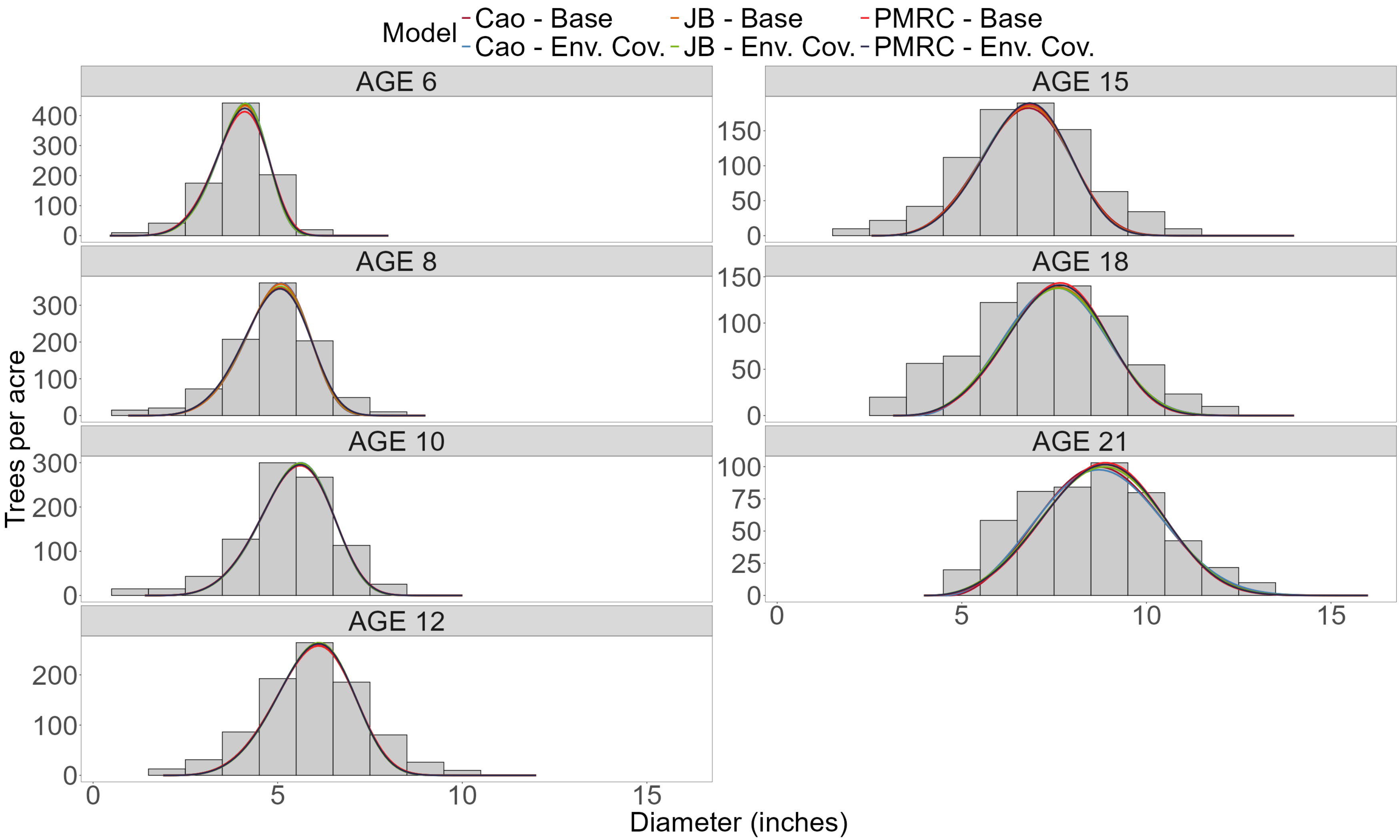

Figure B.4: Diameter distribution of loblolly pine plantations in the Western Gulf physiographic region, modeled using the three-parameter Weibull distribution under two approaches: (i) the base model (without environmental co-variables) and (ii) the adapted model (accounting for environmental co-variables). The analysis was conducted at the general modeling level across seven ages with an initial planting density of 950 trees per acre.

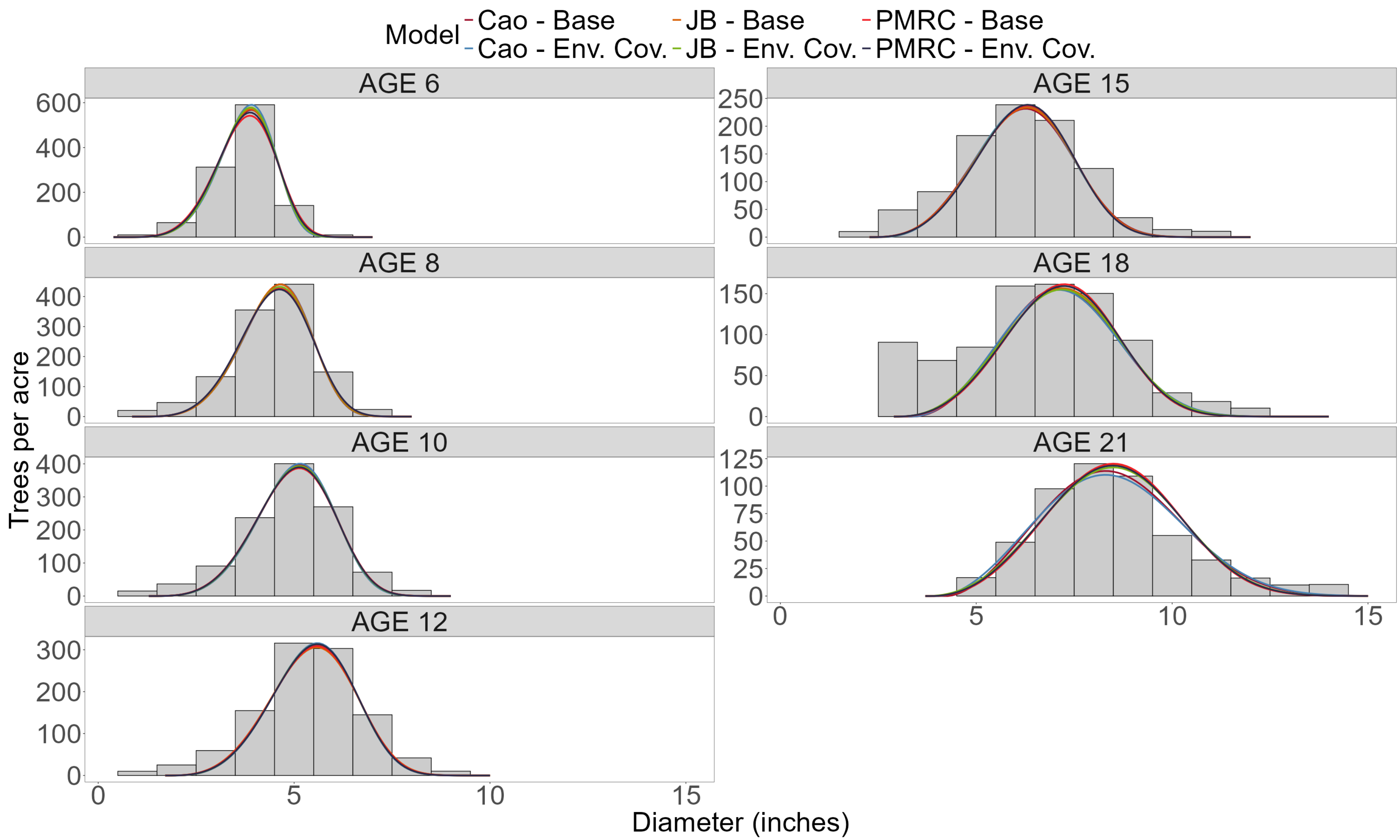

Figure B.5: Diameter distribution of loblolly pine plantations in the Western Gulf physiographic region, modeled using the three-parameter Weibull distribution under two approaches: (i) the base model (without environmental co-variables) and (ii) the adapted model (accounting for environmental co-variables). The analysis was conducted at the general modeling level across seven ages with an initial planting density of 1200 trees per acre.

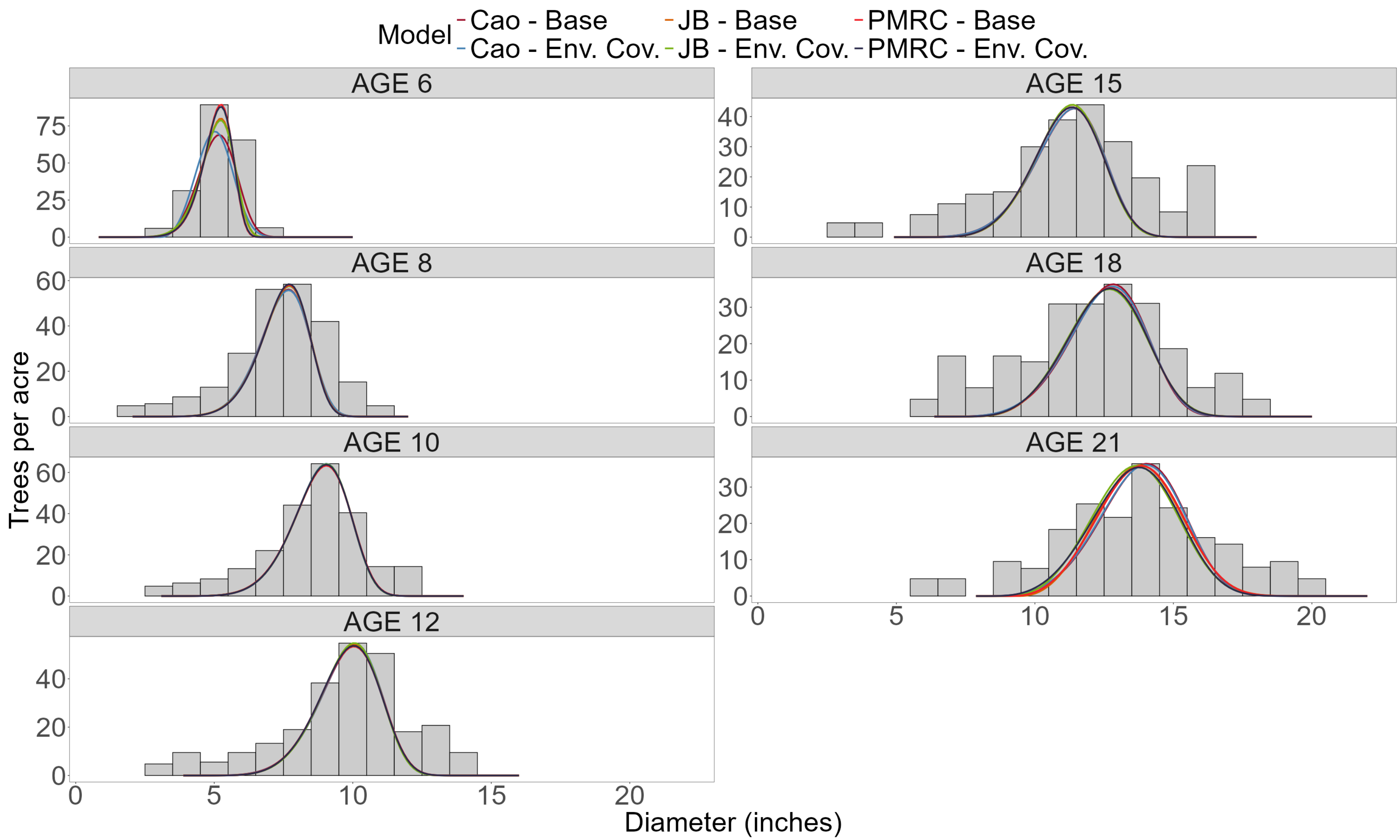

Figure B.6: Diameter distribution of loblolly pine plantations in the Western Gulf physiographic region, modeled using the three-parameter Weibull distribution under two approaches: (i) the base model (without environmental co-variables) and (ii) the adapted model (accounting for environmental co-variables). The analysis was conducted at the regional modeling level across seven ages with an initial planting density of 200 trees per acre.

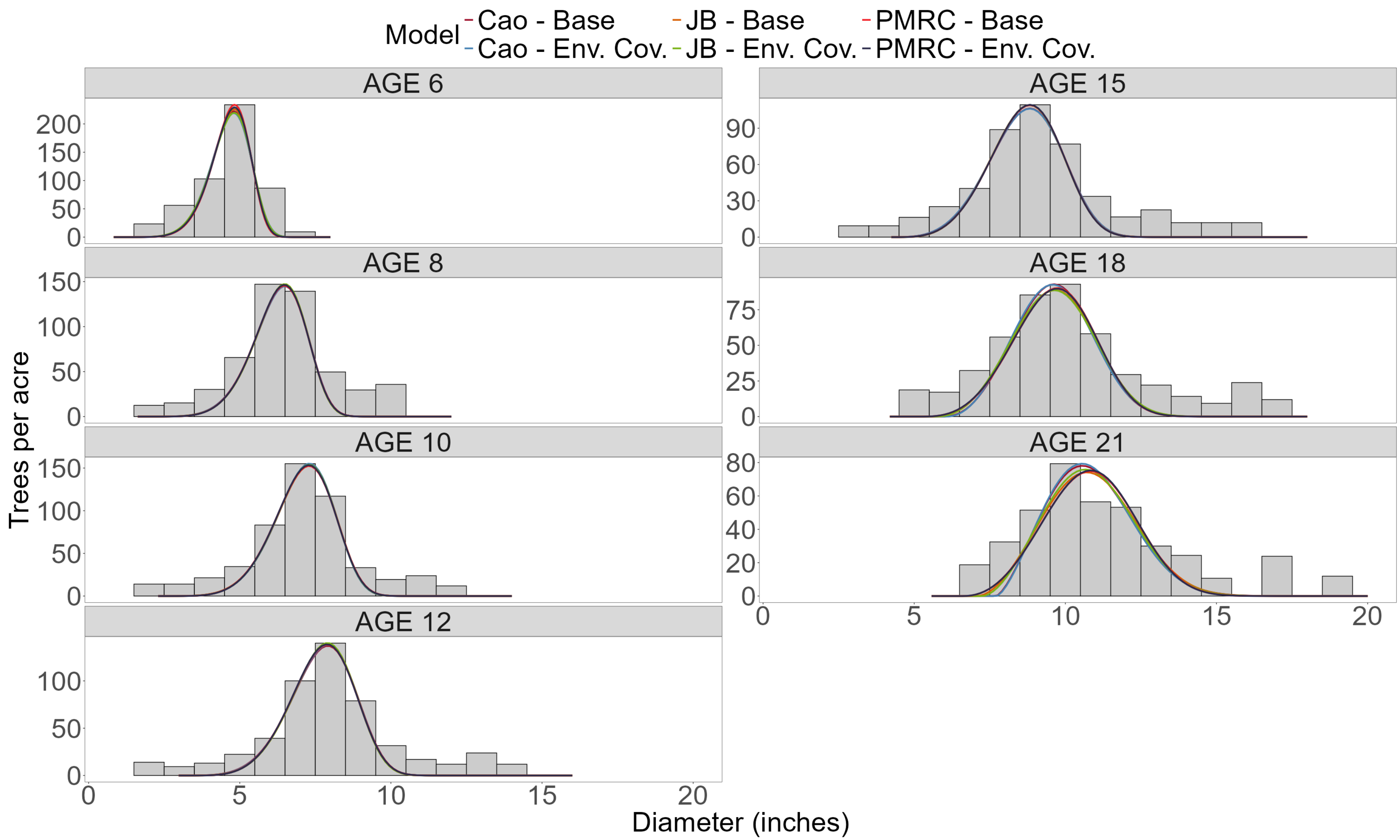

Figure B.7: Diameter distribution of loblolly pine plantations in the Western Gulf physiographic region, modeled using the three-parameter Weibull distribution under two approaches: (i) the base model (without environmental co-variables) and (ii) the adapted model (accounting for environmental co-variables). The analysis was conducted at the regional modeling level across seven ages with an initial planting density of 450 trees per acre.

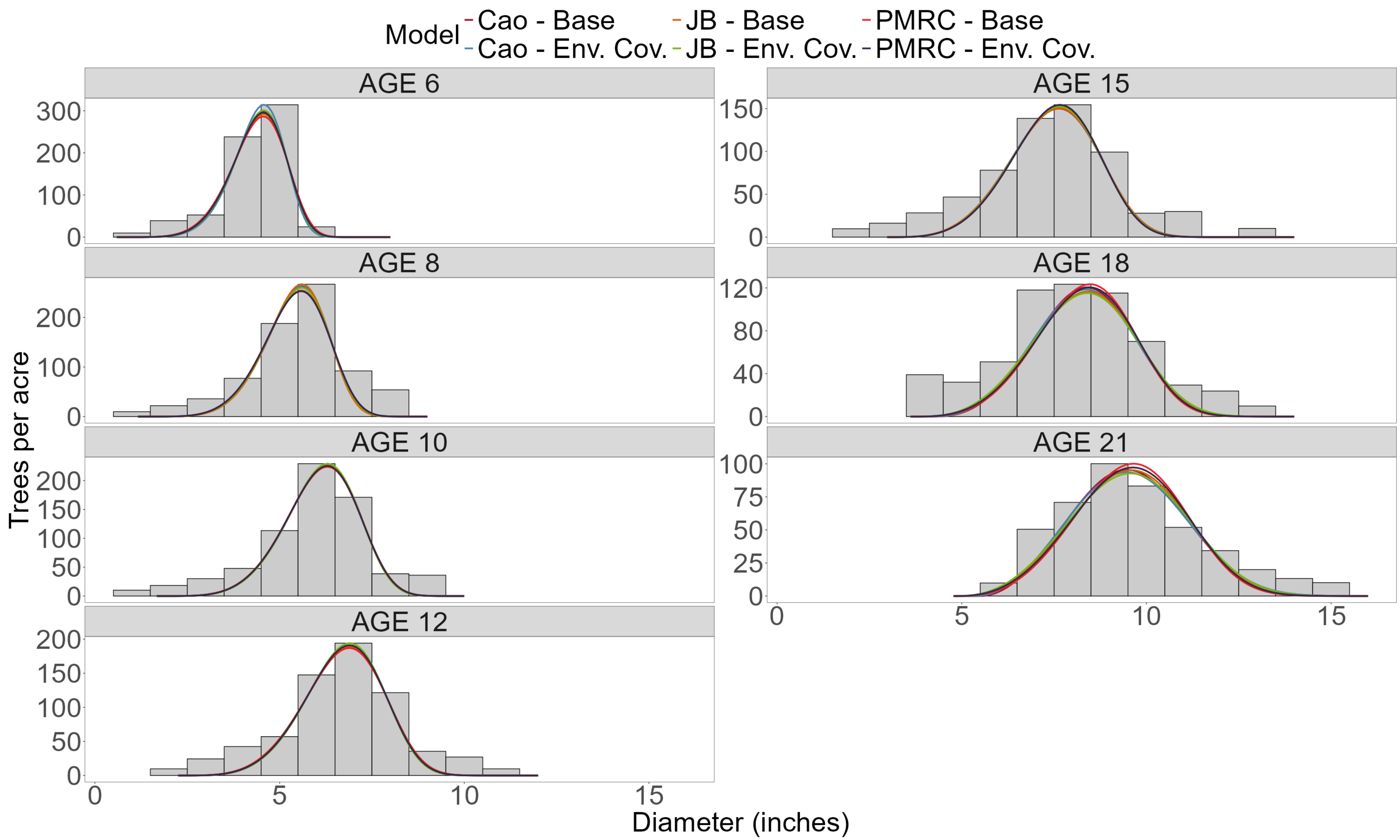

Figure B.8: Diameter distribution of loblolly pine plantations in the Western Gulf physiographic region, modeled using the three-parameter Weibull distribution under two approaches: (i) the base model (without environmental co-variables) and (ii) the adapted model (accounting for environmental co-variables). The analysis was conducted at the regional modeling level across seven ages with an initial planting density of 700 trees per acre.

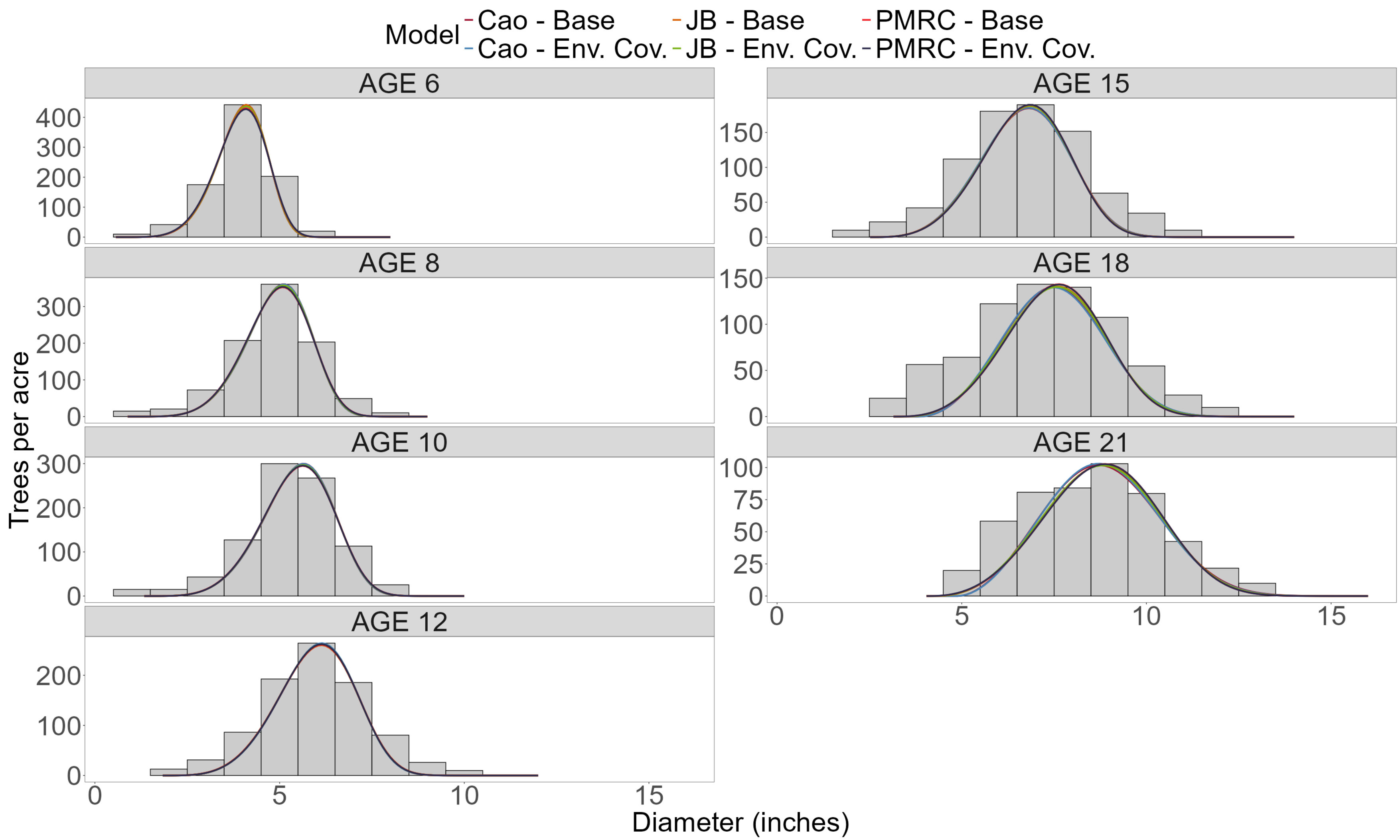

Figure B.9: Diameter distribution of loblolly pine plantations in the Western Gulf physiographic region, modeled using the three-parameter Weibull distribution under two approaches: (i) the base model (without environmental co-variables) and (ii) the adapted model (accounting for environmental co-variables). The analysis was conducted at the regional modeling level across seven ages with an initial planting density of 950 trees per acre.

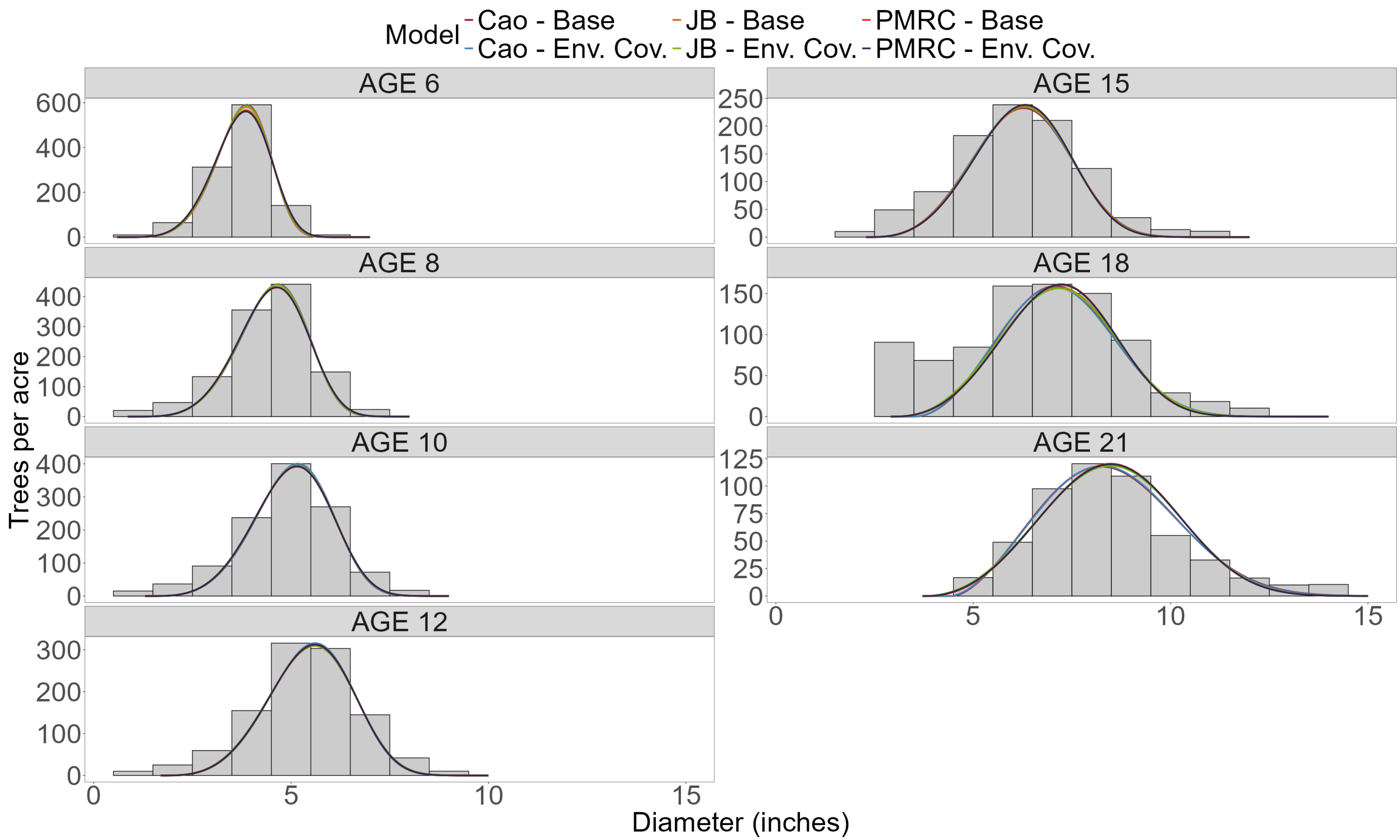

Figure B.10: Diameter distribution of loblolly pine plantations in the Western Gulf physiographic region, modeled using the three-parameter Weibull distribution under two approaches: (i) the base model (without environmental co-variables) and (ii) the adapted model (accounting for environmental co-variables). The analysis was conducted at the regional modeling level across seven ages with an initial planting density of 1200 trees per acre.